
SEDIMENT/DEBRIS BULKING FACTORS AND POST-FIRE HYDROLOGY FOR VENTURA COUNTY

DRAFT REPORT



May 2011

Prepared for:
Ventura County
Watershed Protection District



Prepared by:
WEST Consultants, Inc.
San Diego, California



Sediment/Debris Bulking Factors and Post-fire Hydrology
for Ventura County
Draft Report – May 2011

Contract No. AE09-G20
Task Order No. PW09-171
WEST Project No. COUN002-003

Prepared for:



Ventura County Watershed Protection District
800 South Victoria Avenue
Ventura, CA 93009

Contact: Mark Bandurraga, P.E.

Prepared by:



WEST Consultants, Inc.
11440 W. Bernardo Court, Suite 360
San Diego, CA 92127

A. Jake Gusman, P.E.
WEST Project Manager



EXECUTIVE SUMMARY

Increasing the clear-water discharge to account for a high concentration of sediment in the flow is known as bulking, and its potential depends on the type of sediment-laden flow expected in a watershed. Based on sediment concentration, sediment/water flow ranges from normal streamflow (with conventional suspended load and bedload) to hyperconcentrated flow to mud and debris flows.

Study Purpose and Approach (Chapter 1)

The Ventura County Watershed Protection District (VCWPD) currently uses a bulking method for burned watersheds that is based on a simplification of the Los Angeles County regression curves. The method is intended for mud and debris flows from areas subject to fires and subsequent erosion during design rain events. As such, the method may predict overly conservative bulking factors for the design of bridges, culverts, and other infrastructure. The purpose of this study was to perform flow-bulking factor research and analysis and to provide policy recommendations of how to apply these findings to design studies.

Erosion and Sedimentation (Chapter 2)

Sedimentary rock types and tectonic activity (i.e., movement of the Earth's crust) are prevalent in the western Transverse Ranges found in Ventura County. Debris flows, mud flows, and mass movement are very important, with large amounts of sediment being produced from small, steep watersheds that experience significant geologic and geomorphic activity.

Sediment/Debris Bulking (Chapter 3)

Bulking has been defined as increasing the clear-water discharge to account for high concentrations of sediment in the flow. Mud and debris flows, which can significantly increase the volume of flow transported from a watershed, most often occur in mountainous areas subject to wildfires with subsequent soil erosion, and in arid regions near alluvial fans and other zones of geomorphic and geologic activity. In areas prone to high sediment and debris concentrations, the use of a bulking factor (BF) can help provide for adequately-sized facilities.

The behavior of flood flows can vary significantly, depending on the concentration of sediment/debris in the mixture. Combinations of sediment and water flow can be classified based on: (1) the triggering mechanism, (2) sediment concentration, or (3) rheological and kinematic behavior. Four types of sediment/water flow are often defined—normal streamflow (or water flood), hyperconcentrated flow, debris/mud flows, and landslides. It is important to note that these types of flow are on a continuum, and the boundaries between them are not sharp. In addition, a single debris event may produce different flow types at different times during the event and at different locations along the watercourse.

Modeling Sediment-laden Flows (Chapter 4)

Fluid properties and sediment-transport characteristics change for hyperconcentrated flow as large volumes of sediment can be transported throughout the water column, and the mixture no longer behaves strictly as a Newtonian fluid. The properties of a hyperconcentrated flow are typically between those of a Newtonian and non-Newtonian fluid. Nevertheless, basic hydraulic and

sediment transport equations and models are generally accepted in the range of hyperconcentrated flow. A debris or mud flow acts as a non-Newtonian fluid, and basic hydraulic and sediment transport equations do not apply. If detailed modeling of debris/mud flows is required, a model with specific debris flow capabilities, such as FLO-2D, should be used rather than standard hydraulic models, such as HEC-RAS (River Analysis System).

It is common practice, however, for flows with bulking factors up to 2.0 to be used with HEC-RAS or other standard hydraulic models. The extent to which the use of HEC-RAS for debris/mud flow events may underestimate (or overestimate) flood elevations or flow velocities versus a model such as FLO-2D is not known, and would be an important area for further research. In general, debris flows can move much faster than normal floods in steep channel reaches and much slower than floods in reaches with a low gradient. In addition, debris flows can drastically alter the geometry of channels through scour as well as deposition. Research on the downstream limit of debris/mud flows has suggested that the primary control of the run-out length is channel slope.

While the limit of debris/mud flows was estimated in the research at slopes ranging from 3 to 14 percent, hyperconcentrated flow can continue beyond the debris flow run-out location. However, no studies were found to describe the downstream limit of hyperconcentrated flows. Three drainage networks—Adams Barranca, Hopper Canyon, and Pole Creek—were chosen in this study to examine the limits of hyperconcentrated flow in Ventura County. Based on map data and available aerial photos, the limit of the 1-percent average channel slope was identified as a potential lower limit of hyperconcentrated flow, but further research is recommended before the method is incorporated into any bulking policy.

Agency Bulking Methods (Chapter 5)

Sediment/debris bulking factors and procedures used by southern California counties (Los Angeles, Ventura, San Bernardino, Riverside, Orange, and San Diego), the Los Angeles District of the U.S. Army Corps of Engineers, Federal Emergency Management Agency (FEMA), and the Interagency Burned Area Emergency Response (BAER) Team were reviewed.

Sediment Analysis and Revised BF Curve (Chapter 6)

A number of different analyses were performed to determine the most appropriate bulking factors for Ventura County watersheds, including (1) evaluating sediment sampling data for five stations in the County and estimating the maximum bulking factor and range of values for each; (2) computing the sediment transport capacity for selected reaches in five watersheds and the corresponding peak bulking factor; and (3) comparing the bulking factor calculated using the current VCWPD bulking factor curve to those computed directly based on SCOTSED debris yields and flow hydrographs for several Ventura County watersheds. The results of the three analyses are summarized below:

(1) Estimated bulking factors based on suspended-sediment data range from 1.01 (Ventura River) and 1.04 (Santa Clara River at Montalvo). One could argue that bulking is not required when modeling a large mainstem river using a standard hydraulic model such as HEC-RAS. However, a conservative bulking factor up to 1.1 (10 percent bulking) could be used, if desired (this value includes both suspended sediment and bedload). Note that this bulking factor would not apply if the peak discharge was computed based on streamgage data. With streamgage data, published gage heights and peak discharges already include flow bulking and can be considered bulked, as well as flood frequency results using these data.

(2) A flow versus sediment transport capacity relation was developed for each of the five reaches using the Yang sediment transport function and the 10- and 100-year flood events. Based on the analysis, the computed BF ranged between 1.03 and 1.15 with the exception of the Aliso Canyon, which had a peak bulking factor of 1.58 for the 100-year event. These results did not show a significant difference between the 10- and the 100-year bulking factors for the same reaches.

(3) Computed peak bulking factors for Ventura County watersheds were compared to values from the current VCWPD bulking factor curve as well as the Riverside and Los Angeles County curves. The current Ventura County curve gives a much higher bulking factor than the other two counties. Proposed revised bulking factor curves for Ventura County were developed based on these results, with separate curves based on fire factor and watershed area ($\leq 3 \text{ mi}^2$ and $> 3 \text{ mi}^2$).

Concrete Channels and Bedload (Chapter 7)

Concrete channel roughness (i.e., Manning's n values) should be increased from standard reference values ranging between 0.013 and 0.017 for a channel carrying little or no sediment compared to a concrete channel carrying significant bedload. Based on a literature review, including a review of a model developed for the concrete-lined section of Pole Creek, a Manning's n value of 0.02 appears to be reasonable for concrete channels affected by bedload. In the case of Pole Creek, roughness was increased from 0.015 to 0.02.

Fines and Bulking (Chapter 8)

The impact of wash load on bulking, the inclusion of fine sediment in the VCWPD debris yield method, and the applicability of soil loss equations (USLE, RUSLE, MUSLE) were analyzed. Wash load is generally defined as fine sediment, usually silt and clay less than 0.0625 mm in diameter, that travels in suspension and is not found in significant quantities in the bed.

The USLE and its other forms (RUSLE, MUSLE) provide sediment yield estimates based on sheet and rill erosion (i.e., wash load), and do not include sediment from other potential forms of erosion, such as gully erosion, channel bed and bank erosion, and mass movement. The USLE and similar soil loss methods based on soil loss data from agricultural fields have not proved to be useful in southern California. The MUSLE has given some reasonable results in the western U.S.; however, it would still have limited applicability to the watersheds within the Transverse Ranges of Ventura County. Therefore, the use of MUSLE or other soil loss equations in addition to the VCWPD's debris yield method is not recommended.

Woody Debris (Chapter 9)

This chapter summarizes design guidelines used by local, state, and Federal agencies to account for woody debris accumulation at bridge piers, describes recent research on estimating pier debris, and provides design recommendations for adjusting safety factors used to increase bridge pier widths due to the added woody-debris load. This includes the application of woody pier debris for recently burned watersheds. The general practice used by other agencies is to increase the pier width by two feet on each side to account for the debris accumulation, as well as applying good engineering judgment and practical experience.

A review of the literature showed that most agencies typically use the practice of increasing the pier width by two feet on each side to account for debris. This is a general guideline, and pier debris should be applied on a case-by-case basis for locations where large woody debris has been observed

or expected from the watershed. In addition, bridge design in areas susceptible to wildfires requires additional safety factor adjustments to account for the potential increase volume of woody debris to a stream. Recommendations for Ventura County are based on a recent study by Lagasse et al. (2010) for watershed areas where woody debris is a known issue. The study provides improved guidance compared to current practices in predicting the size and geometry of debris accumulation on bridge piers. However, the procedure requires detailed inputs, and in areas of the County where reliable field data are not available, the general design practice of increasing the pier width by two feet on each side to account for potential woody debris should be followed.

Agency Post-fire Hydrologic Methods (Chapter 10)

Fire can modify watershed hydrologic processes in a number of ways, including changes to evapotranspiration, interception, infiltration, surface and sub-surface soil moisture storage, and surface and sub-surface flow paths. Decreased watershed lag times (and higher peak flows) are caused by loss of vegetation, litter, and duff and resulting lowering of overland, rill and channel flow friction coefficients. In addition to increased sediment bulking, these changes can also include increased clear-water runoff. Post-fire hydrology methods used by the FEMA, Los Angeles County, and Ventura County are described below.

FEMA recommends post-burn adjustment factors for 5- to 100-year design storms between 1.00 for unburned to very low burn areas and 2.62 for high burn area. Estimated sediment bulking factors are then applied to the adjusted peak discharges.

Los Angeles County uses a burn policy based on statistical analysis of historical fire data. The County uses an adjusted burned runoff coefficient in the Modified Rational Method (MRM) based on a 50-year recurrence interval fire factor. The fire factor is then applied to the smaller subareas being studied when using the MRM.

Ventura County uses the following methods to compute design hydrology of an unburned watershed:

- Modified Rational Method, implemented in the VCRat Program
- HSPF (Hydrologic Simulation Program - Fortran, by the U.S. EPA)
- U.S. Army Corps of Engineers' HEC-HMS (Hydrologic Modeling System)
- Flood Frequency Analysis using HEC-SSP (Statistical Software Package) and Bulletin 17B

The County hydrology manual, however, does not provide specific procedures for increasing the unburned clear-water runoff after a burn. Until additional hydrologic studies are performed by the VCWPD, the pre-burn discharge should be increased using an adjustment factor similar to the fire factor applied to the MRM described in the Los Angeles County method. This adjustment factor is termed the "Burn Severity Factor" or BSF.

Burn Severity Factors (Chapter 11)

Burn severity is a term used to describe the magnitude of fire effects on vegetation and soil. There are four general categories used to describe burn severity, including unburned/very low burn, low burn, moderate burn, and high burn. In order to simulate the effect of the burn on hydrologic function, each burn severity class is assigned a "burn severity factor" or BSF based on burn severity

maps and data obtained from the U.S. Geological Survey (USGS). The maps were obtained for 21 fires in Ventura County that have occurred since 1984.

Using average weighted percentages and computed burn severity factors, a percent burn for design was selected, and a weighted BSF of 1.5 was computed. This BSF is recommended for emergency projects (i.e., projects 6 months or less after a burn) where burn severity maps are not available. For a design project (assuming approximately 4.5 years after a burn), a BSF of 1.1 should be applied. These burn severity factors can be directly applied to Ventura County VCRat and HEC-HMS hydrologic model results, or results from regional regression equations using gage data to increase post-fire peaks and hydrographs.

Fire Factor Probability Analysis (Chapter 12)

A joint probability analysis was performed using fire history data from ten watersheds within the County. The purpose of the analysis was to determine the probability of having a 10-year or 50-year storm or larger after the watershed has been recently burned, and to recommend a design burn and bulked condition policy for VCWPD based on the results. The new policy would be applicable to design storm hydrographs for future facility projects. The analysis focused on fire events between 1970 and 2010 because the frequency of fires has been higher in the past 40 years for the majority of County watersheds.

For each watershed, a weighted FF was calculated based on the burned and unburned areas existing during each year. Areas affected by more than one fire within the 7.5-year recovery period were accounted for in the analysis.

Results of the analysis show that the joint probability of a 10-year peak discharge or greater and a design FF of 20 or greater occurring in the same year ranges from 1.2% (*recurrence interval of 82 years*) to 3.8% (*recurrence interval of 27 years*). The analysis also shows that the risk of having a 50-year storm or greater occurs with a $FF \geq 20$ during the 50-year design life ranges from 11 to 31 percent. This range is comparable to the 40% risk of having a 100-year storm during the 50-year design life.

Although seven of the ten watersheds analyzed appear to be subjected to more frequent burns in the last 40 years (1970 to 2010) compared to the record from 1929 to 1969, results from the probability analysis suggest that the current VCWPD policy of using a FF of 20 is still reasonable for these watersheds, and watersheds where SCOTSED computations are required. Study watersheds in Ventura County Zone 1 are considered to have the highest potential fire hazard based on CAL FIRE map data, even though they have been less affected by recent fires and fire factor probabilities are lower. As a result, the design FF should not be lowered for watersheds in this area.

Summary of Recommendations (Chapter 13)

Post-burn hydrology policies developed during the course of this study are summarized in a flowchart provided in Chapter 13. The flowchart can be used as a guide in selecting the BSF and computing the post-burn peak runoff. Post-burn hydrology recommendations are also summarized below:

1. *Emergency projects* intended to mitigate the effects of fire after a recent burn. The 10-year design event would be used, along with a BSF based on burn severity maps and a design condition post-burn. If a burn severity map is not available, a BSF of 1.5 should be used.

2. *Critical infrastructure projects* (hospitals, schools, etc.) downstream of undeveloped areas subject to frequent burns. A watershed is considered to be subject to frequent burns if the VCWPD weighted average fire factor has exceeded the design FF of 20 in more than 10% of the years since 1969. The design condition would be the same as the detention basin criteria i.e., the project is designed for 4.5 years after a total burn of the watershed. This corresponds to a BSF of 1.1.
3. *Projects downstream from known high sediment-producing watersheds* subject to frequent burns, and where damage has occurred due to excessive sedimentation and associated flooding in the past. The design condition would be 4.5 years after total burn of the watershed (BSF = 1.1).

Once the post-fire peak flow is computed, the value is applied to one of the four hydrology models or methods (i.e., VCRat, HEC-HMS, HSPF, or flood frequency analysis). A summary of the application of these methods is provided below:

VCRat (Modified Rational Method): We recommend an approach for immediate implementation and another to supersede it at a later date once additional studies have been completed by the VCWPD.

Recommended Approach (Interim). To compute Q_{burn} , the BSF should be applied directly to the unburned MRM peak flow (Q_u) and hydrograph: $Q_{\text{burn}} = \text{BSF} \times Q_u$

Recommended Approach (Future). To compute Q_{burn} , the runoff coefficient (C) and time of concentration (T_c) should be adjusted for post-burn conditions. To provide a procedure for adjusting the T_c in response to burned conditions, a new set of overland flow curves from the VCWPD is required. In addition, the T_c calculator and VCRat programs would have to be reprogrammed to provide the option of developing T_c 's and calculating peaks and hydrographs for burned conditions. Finally site-specific studies would have to be performed to quantify and confirm the increases in peaks associated with the proposed increases in C coefficients and decreases in T_c .

Hydrologic Simulation Program - Fortran (HSPF): Post-burn adjustments should be made directly to the model parameters instead of applying the BSF to model results.

Hydrologic Modeling System (HEC-HMS): We recommended one approach for immediate implementation and another to supersede it at a later date once additional studies have been completed by the VCWPD.

Recommended Approach (Interim). To compute Q_{burn} , the BSF should be applied directly to the unburned HEC-HMS peak flows and hydrographs: $Q_{\text{burn}} = \text{BSF} \times Q_u$

Recommended Approach (Future). To compute Q_{burn} , post-burn adjustments should be made directly to the model parameters instead of applying the BSF to model results. The VCWPD should perform hydrology studies to create a post-fire S-graph for design, and to determine what additional model parameters should be adjusted to account for the loss of vegetation cover and reduced infiltration.

Flood Frequency Analysis: The recommended approach varies based on whether it is an emergency project or other design project that requires the computation of Q_{burn} .

Emergency projects. Multiply the BSF directly to the peak flow estimate to compute Q_{burn} . The approach for emergency projects is somewhat conservative because the recorded peak discharges already include the effect of historic fires to some extent. However, the BSF should still be applied to reflect burn conditions soon after a fire.

Other projects – Shorter gage record. If the period of record is shorter (e.g., less than 20 years), then the BSF should be multiplied directly to the peak flow estimate to compute Q_{burn} .

Other projects – Longer gage record. If there is a long period of record for the stream gage (e.g., 20 years or more), then the recorded peak discharges should include the effect of historic fires in the watershed. Therefore, an adjustment for Q_{burn} is not required for design.

Figure 13-2 and Figure 13-3 are flowcharts designed to aid in the estimation of a bulking factor. Once the bulking factor has been computed, the design discharge can be computed as follows:

$$Q_{design} = Q_{burn} * \text{Bulking Factor}$$

Provided in an appendix are example applications demonstrating how the BSF and bulking factor are computed for a design and emergency post-fire projects.

TABLE OF CONTENTS

1	INTRODUCTION.....	1-1
1.1	Study Purpose.....	1-1
1.2	Study Approach.....	1-1
1.3	Data Sources.....	1-1
1.4	Acknowledgments	1-2
PART I. SEDIMENT/DEBRIS BULKING		
2	EROSION AND SEDIMENTATION.....	2-1
2.1	Types of Erosion	2-1
2.1.1	Sheet and Rill Erosion.....	2-1
2.1.2	Gully Erosion	2-1
2.1.3	Channel Bed and Bank Erosion	2-1
2.1.4	Mass Wasting.....	2-1
2.2	Spatial Scales.....	2-1
2.3	Debris Flow Potential	2-3
2.3.1	Geology	2-3
2.3.2	Debris Hazard Areas	2-3
2.3.3	Soil Slips and Debris Flows.....	2-3
2.3.4	Alluvial Fans	2-4
2.3.5	Antecedent Rainfall	2-5
2.3.6	Wildfire and Debris Flows	2-5
3	SEDIMENT/DEBRIS AND BULKING.....	3-1
3.1	Bulking Factor Equations.....	3-1
3.2	Sediment/Water Flow Classifications.....	3-2
3.2.1	Normal Streamflow (Water Flood).....	3-2
3.2.2	Hyperconcentrated Flow	3-5
3.2.3	Debris Flows	3-6
3.2.4	Mud Flows	3-7
3.2.5	Landslides.....	3-7
3.3	Flow Behavior	3-7
3.3.1	Newtonian vs. Non-Newtonian Flow	3-7
3.3.2	Sediment Type and Concentration.....	3-8
4	MODELING OF SEDIMENT-LADEN FLOWS	4-1

4.1	Introduction.....	4-1
4.1.1	Hyperconcentrated Flow	4-1
4.1.2	Debris and Mud Flows	4-1
4.2	Modeling Concerns – Hyperconcentrated Flow	4-1
4.2.1	Non-constant Viscosity and Density	4-2
4.2.2	Other Approaches	4-2
4.3	HEC-RAS Adjustments for Hyperconcentrated Flow	4-3
4.3.1	Expansion/Contraction Coefficients.....	4-3
4.3.2	Manning’s <i>n</i> Coefficients	4-4
4.3.3	Limitations	4-5
4.4	Bulked Flow Modeling Comparison – FLO-2D vs. HEC-RAS.....	4-5
4.4.1	Previous Studies	4-5
4.4.2	Differences in 1-D vs. 2-D Modeling.....	4-5
4.4.3	FLO-2D Advantages/Disadvantages	4-6
4.4.4	FLO-2D Application.....	4-6
4.5	Downstream Limit of Debris and Hyperconcentrated Flows	4-7
4.5.1	Debris/Mud Flow Runout	4-7
4.5.2	Limit of Hyperconcentrated Flow.....	4-10
5	AGENCY BULKING METHODS.....	5-1
5.1	Los Angeles County	5-1
5.1.1	Debris Design Events	5-1
5.1.2	Peak Bulking Factor Curves.....	5-1
5.1.3	Converting Debris Yield to Bulking Factor.....	5-4
5.2	Ventura County – Current Bulking Method.....	5-4
5.3	Riverside County.....	5-7
5.4	San Bernardino County.....	5-8
5.5	Orange County.....	5-8
5.6	San Diego County.....	5-8
5.7	U.S. Army Corps of Engineers – Los Angeles District Method	5-8
5.7.1	Debris Yield Equations.....	5-8
5.7.2	Fire Factor.....	5-9
5.7.3	Adjustment and Transposition Factor.....	5-10
5.8	FEMA Post-burn Bulking (2003b).....	5-10

5.9	Interagency BAER Team.....	5-11
5.10	Advantages and Disadvantages of Methods.....	5-12
6	SEDIMENT ANALYSIS AND REVISED BF CURVE	6-1
6.1	Sediment Gage Data Evaluation	6-1
6.2	Streamflow Gages and Flow Bulking.....	6-3
6.3	Sediment Transport Capacity Analysis.....	6-3
6.3.1	Sediment Transport Capacity Results.....	6-3
6.3.2	Limitations of Analysis.....	6-4
6.4	Computed Bulking Factor Comparison	6-5
6.5	Proposed Bulking Factor Curves.....	6-10
PART II. ADDITIONAL BULKING TOPICS		
7	CONCRETE CHANNELS AND BEDLOAD.....	7-1
7.1	Purpose of Investigation.....	7-1
7.2	Previous Studies	7-1
7.2.1	Copeland et al. (2000).....	7-1
7.2.2	Corte Madera Creek – January 1982 Flood	7-3
7.2.3	Standard Manning’s <i>n</i> Reference – Chow (1959).....	7-3
7.2.4	Equivalent Channel Roughness	7-3
7.2.5	Pole Creek FIS Model.....	7-4
7.3	Flows Affected by Increased Manning’s <i>n</i>	7-4
7.3.1	Computed vs. Permissible Velocity and Shear Stress.....	7-4
7.4	Recommendations	7-6
8	FINES AND BULKING	8-1
8.1	Wash Load	8-1
8.2	Scott Method and Fines.....	8-2
8.2.1	Basin Trap Efficiency.....	8-2
8.2.2	Scott and Williams (1978).....	8-2
8.3	USLE/RUSLE/MUSLE and Bulking.....	8-3
8.3.1	USLE and RUSLE.....	8-3
8.3.2	MUSLE	8-3
8.3.3	Applicability to Bulking	8-4
9	WOODY DEBRIS	9-1

9.1	Agency Methods	9-1
9.2	Pier Debris – Size and Configuration	9-2
9.2.1	Diehl (1997)	9-2
9.2.2	Lagasse et al. (2010)	9-3
9.3	Woody Debris Contribution	9-5
9.3.1	Ventura County Vegetation.....	9-5
9.3.2	Post-fire Woody Debris.....	9-9
9.4	Pier Debris Control Structures	9-10
9.5	Woody Debris Summary	9-11
PART III. POST-FIRE HYDROLOGY		
10	AGENCY POST-FIRE HYDROLOGIC METHODS	10-1
10.1	Fire Effects on Hydrology.....	10-1
10.2	FEMA Post-burn Hydrology (2003b)	10-2
10.3	Los Angeles County	10-3
10.4	Ventura County.....	10-5
10.4.1	Modified Rational Method (VCRat Program)	10-5
10.4.2	HSPF (Hydrologic Simulation Program – Fortran)	10-5
10.4.3	HEC-HMS (Hydrologic Modeling System)	10-8
10.4.4	Flood Frequency Analysis	10-9
11	BURN SEVERITY FACTORS	11-1
11.1	Burn Severity Maps.....	11-1
11.2	Proposed Burn Severity Factors	11-1
11.3	Ventura County Fires and Design BSF	11-3
11.4	Application of BSF and Q_{burn}	11-3
11.4.1	Design Application of Q_{burn}	11-3
11.4.2	Critical Infrastructure	11-1
12	FIRE FACTOR PROBABILITY ANALYSIS.....	12-1
12.1	Background.....	12-1
12.2	Fire Factor Probability Analysis (1970-2010)	12-5
12.3	Summary and Recommendations.....	12-11
PART IV. POLICY RECOMMENDATIONS		
13	SUMMARY OF RECOMMENDATIONS	13-1

13.1	Post-fire Hydrology.....	13-1
13.1.1	Design Application of Q_{burn}	13-1
13.1.2	VCRat (Modified Rational Method).....	13-1
13.1.3	HSPF Modeling.....	13-3
13.1.4	HEC-HMS Modeling.....	13-3
13.1.5	Flood Frequency Analysis	13-4
13.2	Sediment/Debris Bulking Factor.....	13-4
13.2.1	Purpose and Limitations.....	13-4
13.3	Combined Q_{burn} and Bulking Factor.....	13-9
13.4	Example Application.....	13-9
13.5	Additional Bulking Recommendations.....	13-9
13.5.1	Alluvial Fans and Bulking.....	13-9
13.5.2	Sediment Transport Modeling and Bulking.....	13-10
13.5.3	Woody Debris	13-10
14	REFERENCES	14-1

LIST OF TABLES

Table 3-1. Flow Classification by Various Researchers (adapted from Bradley & McCutcheon, 1986)	3-4
Table 3-2. Classifications of Flows by Sediment Concentration (modified from O’Brien, 1986)....	3-4
Table 4-1. Computed Expansion/Contraction Coefficients for Bulked Flows	4-3
Table 4-2. Computed Manning’s <i>n</i> for Bulked Flows – Pole Creek Example (Turbulent Flow)	4-4
Table 4-3. Channel Slopes resulting in Debris Flow Runout.....	4-8
Table 4-4. Computed Distance from Slope Failure to Limit of 1% Channel Slope.....	4-10
Table 5-1. Post-fire Bulking Factors used for 2003 Southern California Fires (FEMA, 2003b)	5-11
Table 5-2. Agency Bulking Method Advantages and Disadvantages.....	5-12
Table 6-1. Selected USGS Sediment Sampling Stations in Ventura County and Computed Bulking Factors.....	6-1
Table 6-2. Sediment Transport Capacity Results – 10-year Flood Event.	6-4
Table 6-3. Sediment Transport Capacity Results – 100-year Flood Event.	6-4
Table 6-4. Watersheds Used in Fire Factor Analysis (see Figure 6-3 for map locations)	6-6
Table 6-5. Bulking Factor Comparison for FF = 20	6-8
Table 6-6. Bulking Factor Comparison for FF = 88	6-9
Table 6-7. Conservative Bulking Factors (Optional).....	6-10
Table 7-1. Concrete-lined and Gravel Bottom Channel Roughness Values (Chow, 1959).....	7-3
Table 7-2. Pole Creek – HEC-RAS Channel Velocity and Shear Stress	7-5
Table 7-3. Permissible Velocity and Shear Stress for Channel Materials (adapted from Fischenich, 2001)	7-6
Table 8-1. Sediment Type by Transport, Source, and Sampling Method (adapted from Diplas et al., 2008)	8-1
Table 8-2. Example Debris Basin Trap Efficiencies (data from Scott and Williams, 1978).....	8-2
Table 9-1. Summary of Agency Guidelines for Woody Debris on Bridge Piers.....	9-2
Table 10-1. Post-Burn CN values from Studies of the 2000 Cerro Grande Fire, New Mexico (FEMA, 2003b)	10-2
Table 10-2. Post-Burn Adjustment Factors (FEMA, 2003b).....	10-3
Table 10-3. Computed Pre- and Post-fire Discharges – Santa Clara River Basin (Los Angeles County, 2003)	10-4
Table 11-1. Proposed Burn Severity Factors.....	11-1
Table 11-2. Proposed Burn Severity Factors vs. Years since Burn	11-2
Table 11-3. Ventura County Fires (1984 to 1989) – Area and Percent Burned.....	11-4

Table 11-4. Ventura County Fires (1990 to 1999) –Area and Percent Burned.....	11-4
Table 11-5. Ventura County Fires (2000 to 2008) –Area and Percent Burned.....	11-4
Table 11-6. Proposed Burn Severity Factor for Emergency Projects (6 months post-burn).....	11-5
Table 12-1. Watersheds used in Fire Factor Analysis.....	12-1
Table 12-2. Joint Probability of $FF \geq 20$ and 10-year Storm Event – Fire History 1929 to 2010.	12-3
Table 12-3. Probability of 50-year Event and $FF \geq 20$ during 50-year Design Life –1929 to 2010.....	12-4
Table 12-4. Number of Fires and Years with $FF \geq 20$: 1929 to 1969 and 1970 to 2010.....	12-4
Table 12-5. Joint Probability of a $FF \geq 10$ and a 10-year Storm Event – Fire History 1970 to 2010.....	12-7
Table 12-6. Joint Probability of a $FF \geq 10$ and a 50-year Storm Event – Fire History 1970 to 2010.....	12-7
Table 12-7. Joint Probability of a $FF \geq 15$ and a 10-year Storm Event – Fire History 1970 to 2010.....	12-8
Table 12-8. Joint Probability of a $FF \geq 15$ and a 50-year Storm Event – Fire History 1970 to 2010.....	12-8
Table 12-9. Joint Probability of a $FF \geq 20$ and a 10-year Storm Event – Fire History 1970 to 2010.....	12-9
Table 12-10. Joint Probability of a $FF \geq 20$ and a 50-year Storm Event – Fire History 1970 to 2010.....	12-9
Table 12-11. Joint Probability of a $FF \geq 30$ and a 10-year Storm Event – Fire History 1970 to 2010.....	12-10
Table 12-12. Joint Probability of a $FF \geq 30$ and a 50-year Storm Event – Fire History 1970 to 2010.....	12-10
Table 12-13. Probability of 10-year or 50-year Event with a $FF \geq$ Selected Values during a 50-year Design Life – Fire History 1970 to 2010.....	12-12
Table 12-14. Fire Hazard Class Percentages for VCWPD Zones (based on CAL FIRE data)....	12-13
Table 12-15. Fire Hazard Class Percentages for Study Watersheds (based on CAL FIRE data).	12-13
Table 13-1. HSPF Parameters and Post-burn Adjustment.....	13-3

LIST OF FIGURES

Figure 2-1. Idealized Watershed and Alluvial Channel with Erosion/Sedimentation (HEC, 1995)	2-2
Figure 2-2. Likelihood of Soil Slips vs. Slope Angle (USGS, 1997)	2-4
Figure 3-1. Sediment Concentration vs. Bulking Factor (Maricopa County, 2003).....	3-3
Figure 3-2. Normal Streamflow with Sediment Transport (USGS, 2005a)	3-5
Figure 3-3. Hyperconcentrated Flow – 40% Sediment (USGS, 2005a).	3-6
Figure 3-4. Debris Flow – 65% Sediment (USGS, 2005a)	3-6
Figure 3-5. Shear Stress vs. Shear Rate (modified from O’Brien, 2006)	3-8
Figure 4-1. Stream Order Classification Example (USGS, 1997).....	4-9
Figure 4-2. Debris-flow Occurrence and Movement (Stock and Dietrich, 2006).....	4-9
Figure 4-3. Adams Barranca – Potential Limit of Hyperconcentrated Flow	4-11
Figure 4-4. Hopper Canyon – Potential Limit of Hyperconcentrated Flow	4-12
Figure 4-5. Pole Creek – Potential Limit of Hyperconcentrated Flow.....	4-12
Figure 5-1. Debris Production Rates for the Santa Clara River Basin (Los Angeles County, 2006a).....	5-2
Figure 5-2. Peak Bulking Factors for the Santa Clara River Basin (Los Angeles County, 2006a)	5-3
Figure 5-3. VCWPD Bulking Factor Curve (VCWPD, 2010a)	5-5
Figure 5-4. Ventura County Fire Factors vs. Years after Burn	5-6
Figure 5-5. Riverside County and Ventura County Bulking Factor Curves.....	5-7
Figure 5-6. Fire Factor Curve for Watersheds 0.2 to 3.0 mi ² (USACE, 2000a)	5-9
Figure 5-7. Fire Factor Curves for Watersheds 3.0 to 200 mi ² (USACE, 2000a).....	5-10
Figure 6-1. Bulking Factor vs. Average Daily Flow – Santa Clara River at Montalvo	6-2
Figure 6-2. Bulked and Unbulked Hydrographs – Adams Barranca	6-6
Figure 6-3. Watersheds used in Bulking Factor Evaluation (with VCWPD Zones)	6-7
Figure 6-4. Current Bulking Factor Curve for Ventura County vs. Recommended Curves (FF = 20).....	6-11
Figure 6-5. Current Bulking Factor Curve for Ventura County vs. Recommended Curves (FF = 88).....	6-12
Figure 6-6. Current Local County (Ventura, Los Angeles, and Riverside) Bulking Factor Curves vs. Recommended Curves (FF = 20).....	6-13
Figure 7-1. Bedload Roughness vs. Gravel Concentration (Copeland et al., 2000)	7-2
Figure 7-2. Schematic of a Concrete-lined Channel with Significant Sediment Load (MEI, 2008) ..	7-4
Figure 9-1. Woody Debris Blocking the Waterway Opening of the Bridge (Lyn et al., 2003).....	9-1

Figure 9-2. Woody Debris Accumulation and Bridge Failure (FHWA, 2005) 9-1

Figure 9-3. Rectangular Shaped Woody Debris Representation (Lagasse et al., 2010) 9-4

Figure 9-4. Southern California Vegetation Communities (University of California, 2010) 9-6

Figure 9-5. Ventura County Cover Type Percentages..... 9-7

Figure 9-6. Map of the Ventura County Cover Types 9-8

Figure 9-7. Bendix and Cowell (2010) Study Location Map (including Wolf Fire perimeter) 9-9

Figure 9-8. Example of Elongated Pier Nose 9-10

Figure 10-1. Sespe Creek Watershed within Santa Clara River Watershed (AQUA TERRA, 2010) 10-6

Figure 10-2. 100-year Burn and Pre-burn Design Hydrographs for Sespe Creek (AQUA TERRA, 2010)..... 10-7

Figure 11-1. Proposed Burn Severity Factors vs. Years since Burn..... 11-2

Figure 11-2. Proposed Burn Severity Factor for Design vs. Years since Burn 11-5

Figure 12-1. Ventura County Watersheds and Basin Zone Map used in the Fire Factor Analysis 12-2

Figure 12-2. Weighted Fire Factor vs. Fire Year (between 1970 to 2010) – Zone 1..... 12-5

Figure 12-3. Weighted Fire Factor vs. Fire Year (between 1970 to 2010) – Zone 2..... 12-6

Figure 12-4. Weighted Fire Factor vs. Fire Year (between 1970 to 2010) – Zone 3..... 12-6

Figure 13-1. Post-fire Hydrology Flowchart..... 13-2

Figure 13-2. Bulking Factor Flowchart – Part 1 of 2 13-5

Figure 13-3. Bulking Factor Flowchart – Part 2 of 2 13-6

Figure 13-4. Recommended Bulking Factor Curves – Design Projects (FF = 20)..... 13-7

Figure 13-5. Recommended Bulking Factor Curves – Emergency Projects (FF = 88) 13-8

LIST OF APPENDICES

Appendix A. Derivation of Equivalent HEC-RAS Parameters for Modeling of Bulked Flows

Appendix B. Burn Severity Classes and Burn Severity Maps

Appendix C. Example Application – Burn Severity and Bulking Factors

LIST OF ACRONYMS AND ABBREVIATIONS

ASCE	American Society of Civil Engineers
A-T	Adjustment and Transposition
BAER	Burned Area Emergency Response
BF	Bulking Factor
BARC	Burned Area Reflectance Classification
BSF	Burn Severity Factor
CN	Curve Number
cy	Cubic yards
DA	Drainage Area
DDE	Design Debris Event
DEM	Digital Elevation Model
DPA	Debris Potential Area
ER	Elongation Ratio
FEMA	Federal Emergency Management Agency
FF	Fire Factor
FHWA	Federal Highway Administration
FIS	Flood Insurance Study
GIS	Geographic Information Systems
HEC-HMS	Hydrologic Engineering Center's Hydrologic Modeling System
HEC-RAS	Hydrologic Engineering Center's River Analysis System
HEC-SSP	Hydrologic Engineering Center's Statistical Software Package
HSPF	Hydrologic Simulation Program - Fortran
MEI	Mussetter Engineering, Inc.
MRM	Modified Rational Method
MTBS	Monitoring Trends in Burn Severity
MUSLE	Modified Universal Soil Loss Equation

LIST OF ACRONYMS AND ABBREVIATIONS (Cont.)

NCHRP	National Cooperative Highway Research Program
NRCS	Natural Resources Conservation Service
ppm	Parts per million
RR	Relief ratio
RUSLE	Revised Universal Soil Loss Equation
sq. mi.	Square miles
USACE	U.S. Army Corps of Engineers
USBR	U.S. Bureau of Reclamation
USDA	U.S. Department of Agriculture
USGS	U.S. Geological Survey
USLE	Universal Soil Loss Equation
VCRat	Ventura County Modified Rational Method Model
VCWPD	Ventura County Watershed Protection District

LIST OF EQUATION SYMBOLS

A	Area of watershed
a	Bulking constant
a_d^*	Effective pier width
B_{up}	Width of the channel upstream of the bridge
C_{burn}	Adjusted burned soil runoff coefficient
C_{bulked}	Adjusted expansion/contraction coefficient
C_{gravel}	Concentration of coarse material
C_u	Undeveloped runoff coefficient
C_v	Sediment concentration in percent volume
C_w	Sediment concentration by weight
D	Design storm sediment/debris production rate
D_y	Unit debris yield
I	Rainfall intensity
K	Soil-erodibility factor (<i>USLE equation</i>)
K	Ratio of burned to unburned infiltration rates (<i>Los Angeles County equation</i>)
K	Dimensionless rainfall factor (<i>SCOTSED equation</i>)
K_d	Debris coefficient
L	Slope-length factor (<i>USLE equation</i>)
L	Length of debris upstream from a pier face (<i>equivalent pier width equation</i>)
L_d	Design log length
n	Bulking constant
n	Manning's roughness coefficient
n_c	Composite or equivalent coefficient of roughness
n_i	Coefficient of roughness for individual subsections
P	Wetted perimeter of the channel (<i>equal velocity method</i>)
P	Erosion control practice factor (<i>USLE equation</i>)

LIST OF EQUATION SYMBOLS (Cont.)

q	Bulked flow per linear foot width of channel
Q	Area of watershed
Q_B	Bulked peak discharge
Q_{burn}	Post-fire peak discharge (same as $Q_{\text{post-fire}}$)
Q_{design}	Design discharge
$Q_{\text{pre-burn}}$	Pre-burn peak flow (same as Q_U)
Q_s	Volumetric sediment discharge
Q_w	Clear-water discharge
R	Rainfall and runoff factor
Re	Reynolds number
S	Slope-steepness factor
T	Thickness
T_c	Time of Concentration
V	Storm runoff volume
V	Flow velocity
V_s	Sediment yield
W	Width of the debris
y	Depth of flow in the channel

Greek Symbols

γ	Specific weight of water
γ_s	Specific weight of sediment
μ	Dynamic viscosity (absolute fluid viscosity)
ρ	Fluid density
τ	Shear stress
ν	Kinetic viscosity

1 INTRODUCTION

1.1 Study Purpose

Increasing water discharge to account for a high concentration of sediment in the flow is known as bulking, and its magnitude depends on the type of sediment-laden flow expected in a watershed. Based on sediment concentration, sediment/water flow ranges from normal streamflow (with conventional suspended load and bedload) at low concentrations to hyperconcentrated flow (mud floods) to mud mixed debris flows.

The Ventura County Watershed Protection District (VCWPD) currently uses a bulking method for burned watersheds that is based on a simplification of the Los Angeles County sediment bulking curves. The method is intended for mud and debris flows from areas subject to fires and subsequent erosion during design rain events. As such, the method may predict overly conservative bulking factors for the design of bridges, culverts, and other infrastructure. The purpose of this study was to perform flow bulking factor research and analysis and to provide policy recommendations of how to apply these findings to design projects. In addition, the increase in post-burn clear-water flows has been analyzed and recommendations have been made.

1.2 Study Approach

The bulking factor study was completed in multiple phases:

- Phase I included research of bulking methods with initial recommendations regarding a revised methodology for Ventura County.
- Phase II included an analysis of post-fire hydrologic impacts, wood debris factors, and the hydraulic modeling of bulked flows.
- Phase III included revising the bulking curve presented in Phase I, and providing detailed policy recommendations for computing bulking factors and post-burn hydrology that can be used by the VCWPD and their consultants.

Specific tasks completed during Phase III included estimating hyperconcentrated flow limits, performing a joint-probability analysis of having large storm events after recent fires in a watershed, developing the use of burn severity factors, creating a post-burn hydrology flowchart, and updating/expanding the bulking factor flowchart.

Results from all three phases of the study have been combined to create a single, unified report.

1.3 Data Sources

Pertinent manuals and other publications from local, state, and Federal agencies were obtained and reviewed, including those from:

- Ventura County
- Los Angeles County
- Riverside County
- San Bernardino County
- San Diego County
- Albuquerque Metropolitan Arroyo Flood Control Authority
- U.S. Army Corps of Engineers (USACE)
- U.S. Geological Survey (USGS)
- Federal Emergency Management Agency (FEMA)
- Natural Resources Conservation Service (NRCS)
- U.S. Bureau of Reclamation (USBR)
- American Society of Civil Engineers (ASCE) Conference Proceedings
- ASCE Journal of Hydraulic Engineering and other relevant peer-reviewed journals
- Federal Inter-Agency Sedimentation Conference Proceedings

1.4 Acknowledgments

WEST Consultants, Inc. (WEST) performed this study for the Ventura County Watershed Protection District under Contract No. AE11-G20, Work Order No. PW11-083 (for Phase III). Mark Bandurraga, P.E., served as District project manager for the study, providing valuable data and direction. Important study comments were also provided by Sergio Vargas, P.E., Bruce Rindahl, P.E., Zia Hosseinipour, P.E., Scott Holder, P.E., and Vincent Su, P.E.

Jake Gusman, P.E., served as WEST project manager. The study team included Vicki Tripolitis, Brent Travis, Ph.D., P.E., Darren Bertrand, John (Jack) Humphrey, Ph.D., P.E., Daniela Todesco, P.E., Kayson Shurtz (woody debris factors), Sam Powvall, and Candi Johnston. Martin Teal, P.E., P.H., and Dr. Jeffrey Bradley, P.E., provided study review and oversight.

PART I. SEDIMENT/DEBRIS BULKING

2 EROSION AND SEDIMENTATION

This section describes the general types and spatial scales of erosion, followed by the erosion/sedimentation processes observed in Ventura County watersheds.

2.1 Types of Erosion

Important erosion processes may be roughly grouped into four categories: sheet and rill erosion, gully erosion, channel bed and bank erosion, and mass wasting.

2.1.1 Sheet and Rill Erosion

Sheet (interrill) and rill erosion are caused by raindrop impact and runoff on the earth's surface. For non-agricultural watersheds, rills are transient channels that would not persist through long-term or seasonal land-forming processes (HEC, 1995). Topography (slope and aspect), soil type, vegetation, and land use all have a significant influence on sheet and rill erosion.

2.1.2 Gully Erosion

A gully is defined by Harvey et al. (1985) as a relatively-deep eroding channel that has recently formed where no well-defined channel previously existed. A gully may form rapidly and may be associated with recent changes in the watershed (e.g., land use) or hydrologic conditions. For relatively small drainage areas, gully erosion can produce very large sediment loads; however, for basins exceeding 10 square miles, the contribution of gully erosion to total sediment yield may be small (HEC, 1995).

2.1.3 Channel Bed and Bank Erosion

While the erosion of channel bed and banks is not a major source of sediment for relatively stable channels, it can have a dominant role in the active alluvial channels found in southern California.

2.1.4 Mass Wasting

Mass movement (wasting) of rock, debris, or earth can take the form of falls, slides, or flows. The impact of mass wasting on sediment production from the watershed can be very significant for some watersheds. The amount of sediment that can enter the stream channels will depend on the hydrologic and geologic conditions, as well as the location of mass wasting relative to the drainage system.

2.2 Spatial Scales

Lane et al. (1997) describes three spatial scales on which to consider erosion and sedimentation: (1) the plot and hillslope scale; (2) subwatershed scale; and, (3) watershed scale.

Plot and Hillslope Scale (up to ~2 acres): Overland flow processes dominate and sediment yield is most affected by topography, vegetative canopy cover, surface ground cover (rock, gravel, litter, and plant basal area) and rainfall amount and intensity. For hydraulic design of bridges and culverts, the

plot and hillslope scale would typically not be of direct concern. Instead, the subwatershed or watershed scales would govern in determining sediment yield and bulking factors.

Subwatershed Scale (~2 acres up to ~4 mi²): Hillslope processes remain important, but factors more important to sediment yield are spatial variability of rainfall, geologic parent material and soil interactions, channel erosion and sedimentation processes, and vegetation type. Typical sediment yield equations and methods are most applicable at the subwatershed scale.

Watershed Scale (greater than ~4 mi²): Sediment yield is typically controlled by partial watershed coverage of rainfall, transmission losses in alluvial stream channels, runoff rates and amounts, and sediment transport capacity. Processes at the hillslope and subwatershed scale remain important, but are subordinate to those at the watershed scale. At the watershed scale, the principal stream channels are ephemeral, with broad sand and gravel beds, in which sediment supply is generally abundant and non-limiting. Figure 2-1 shows the erosion and deposition zones of an idealized watershed in plan and profile views.

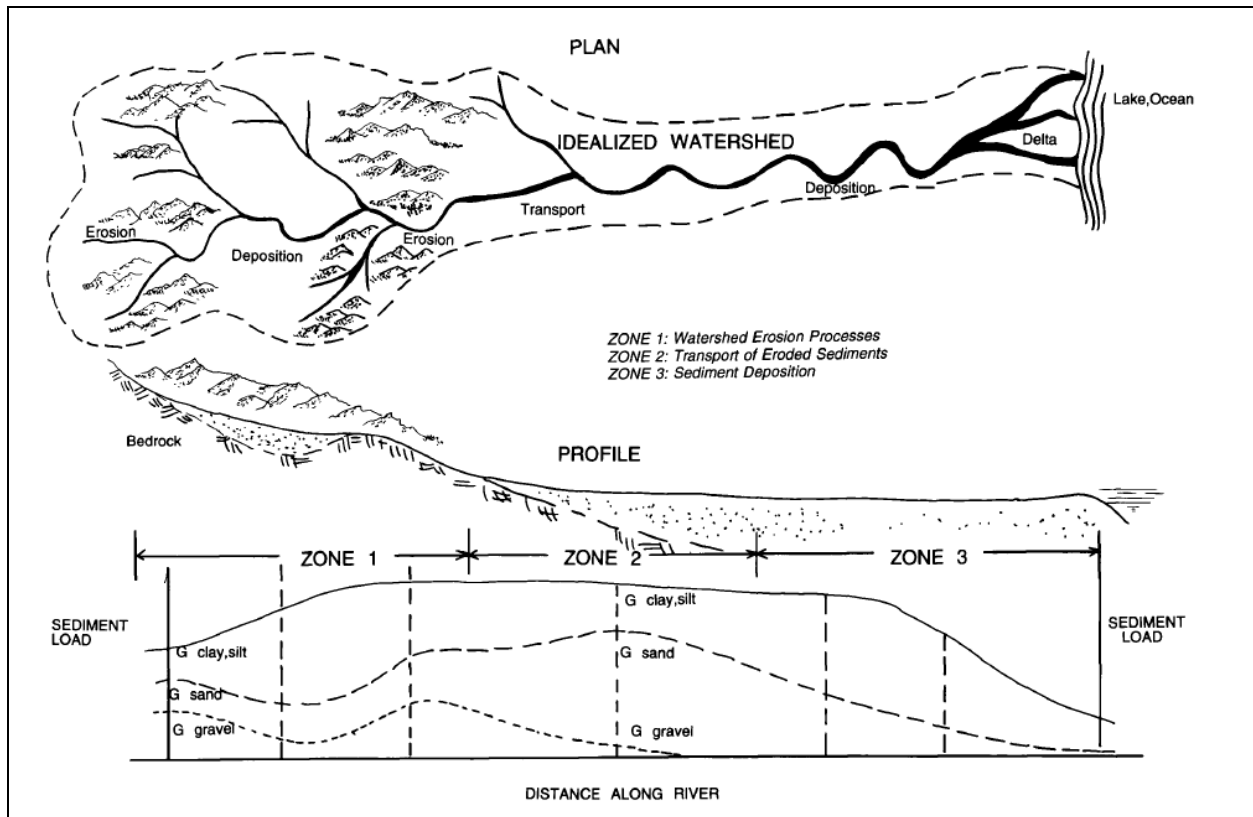


Figure 2-1. Idealized Watershed and Alluvial Channel with Erosion/Sedimentation (HEC, 1995)

2.3 Debris Flow Potential

2.3.1 Geology

Sedimentary rock types and tectonic activity (i.e., movement of the Earth's crust) are prevalent in the western Transverse Ranges, a group of mountain ranges that are oriented from east to west through Ventura County. Debris flows, mud flows, and mass movement are very important, with large amounts of sediment being produced from small, steep watersheds that experience significant geologic and geomorphic activity.

Scott and Williams (1978) performed an extensive study of erosion and sedimentation for Ventura and Los Angeles Counties. Watersheds studied included those in the western Transverse Ranges of Ventura County and in the eastern Transverse Ranges of Los Angeles County. The study found that erosion rates generally decrease from north to south in Ventura County, with the highest rates occurring within the drainage areas of the Ventura River basin along the western side of the county and the lowest rates found in drainage areas of the Calleguas Creek basin to the south. Because of its large size, erosion rates generally vary significantly within the Santa Clara River basin; however, drainage areas studied by Scott and Williams (1978) were generally found to have intermediate sediment production rates.

2.3.2 Debris Hazard Areas

Locations that have a high potential for debris-flow hazards include (USGS, 1997):

- At or near the foot of a steep slope, especially slopes of 26 degrees (1V:2H) or steeper.
- At or near the junctions of ravines with canyons.
- Near the upper points of alluvial fans.
- Within alluvial fans.

Mass movement (wasting) of rock, debris, or earth can take the form of falls, slides, or flows. The impact of mass wasting on sediment production from the watershed can be very significant. The amount of sediment that can enter the stream channels will depend on the hydrologic and geologic conditions, as well as the location of mass wasting relative to the drainage system. Mass wasting events are the primary source of bulked flows.

The availability of sediment in the channel plays an important role in whether hyperconcentrated and/or debris flows are produced. If a major storm event occurs after an earlier debris-producing event, there may not be adequate debris built up to result in another debris event.

2.3.3 Soil Slips and Debris Flows

Debris flows often begin with soil slips, which tend to form on steep slopes. Flowing mud and rocks will accelerate downslope until the steepness of the slope has decreased, where the flow slows and stops, depositing mud, rock, and vegetation (USGS, 1997). Figure 2-2 shows the likelihood of soil slips versus slope angle. Soil slips are the most common, and are most likely to accelerate, at slopes of 26 degrees (2H:1V) or steeper. Soil slips are also common on slopes between 18 degrees (3H:1V) and 26 degrees; however, the potential for acceleration down the slope is much less than for steeper slopes.

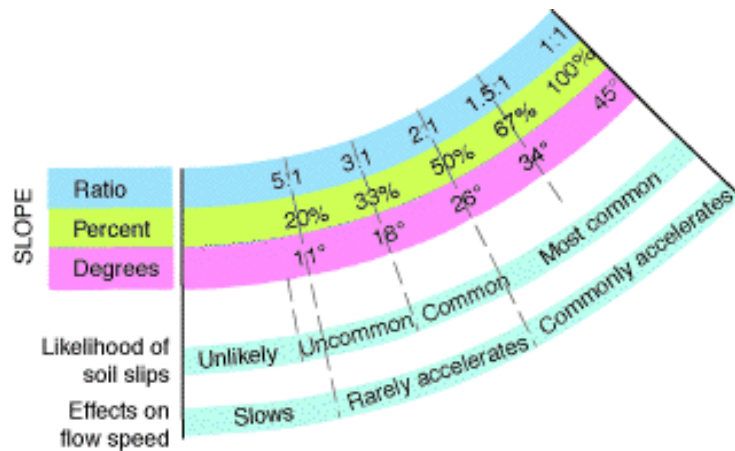


Figure 2-2. Likelihood of Soil Slips vs. Slope Angle (USGS, 1997)

Locations where relatively flat terrain, such as the floodplain of a narrow canyon, adjoins a steep slope, such as a canyon wall or a steep mountain front, are most likely to be exposed to debris flows from small, steep drainage channels. The size of the debris flow increases with a longer slope, and the speed of a debris flow increases with steeper slopes.

The USGS (1997) found that for areas underlain by sedimentary rocks and fractured basement rocks, essentially all of the debris flows were generated on hillsides with slopes of 26 degrees (2H:1V) or steeper. Such conditions are found in the Transverse Ranges.

2.3.4 Alluvial Fans

An alluvial fan has been defined as a “sedimentary deposit located at a topographic break, such as the base of a mountain front, escarpment, or valley side, that is composed of fluvial and/or debris flow sediments and which has the shape of a fan either fully or partially extended” (National Research Council, 1996). An alluvial fan is essentially a depositional area, where the sediment-carrying capacity of the stream or wash is reduced by a greatly increased flow area and/or flatter slope. On an alluvial fan, flow paths are uncertain and ever changing – they may diverge and then rejoin downstream due to debris flows, water flows, or a mixture of the two. The sediment content of a flow through an alluvial fan may vary from negligible to more than 50 percent sediment and debris (FHWA, 2002).

A great deal of research has been devoted to analyzing alluvial fans, and detailed discussion of this topic is beyond the scope of the current study. Instead, the purpose of this section is to provide a brief introduction to alluvial fans in the context of selecting an appropriate sediment/debris bulking factor. More comprehensive references should be consulted for a detailed treatment of alluvial fans, including those from the Federal Emergency Management Agency (FEMA) and the U.S. Army Corps of Engineers (USACE):

- *Guidelines and Specifications for Flood Hazard Mapping Partners*, Appendix G: Guidance for Alluvial Fan Flooding Analyses and Mapping (FEMA, 2003a)
- *Guidelines of Risk and Uncertainty Analysis in Water Resources Planning* (USACE, 1992)

- *Alluvial Fans in California – Identification, Evaluation, and Classification* (USACE, 2000b)
- California Alluvial Fan Task Force (2010) (<http://aftf.csusb.edu/>)

2.3.5 Antecedent Rainfall

The USGS (1997) compared historic rainfall records and times of debris flows for southern California to determine how much rainfall is needed to trigger debris flows and what kinds of storms most often trigger them. For unburned areas of chaparral, sage, or annual vegetation cover, the slope typically had received at least 10 inches of total seasonal rainfall prior to a significant storm event. For recently burned areas, which have many more debris flows than unburned areas, no prior rainfall was required for debris flows to occur. This is because a hydrophobic layer in the soil can be created by intense fires. This is a layer that repels water and increases runoff, increasing the likelihood of debris flows.

2.3.6 Wildfire and Debris Flows

Post-fire debris flows generally are triggered by one of two processes: surface erosion caused by rainfall runoff, and landslides caused by infiltration of rainfall into the ground. Runoff-dominated processes are by far the most common because fires typically reduce the infiltration capacity of soils, which increases runoff and erosion (USGS, 2005b). The focus of this section is on debris flow impacts due to wildfires, although some discussion also applies to increased water runoff after a fire. Post-fire hydrologic impacts, and agency methods of determining clear water (without the bulking effect of sediments) runoff are presented in Chapter 10.

In forested areas, the major factor influencing runoff and erosion from burned hillslopes is the amount of disturbance to the material that protects the underlying mineral soil. The unburned forest floor consists of a litter layer (leaves, needles, fine twigs, etc.) and a duff layer (partially decomposed remnants of the material from the litter layer). These layers absorb rainfall, provide water storage, and obstruct the flow of water on hillslopes. The combustion process converts these layers into ash and charcoal particles, which seal soil pores and decrease the infiltration rate, thereby increasing potential runoff and erosion. When the charcoal and ash are removed from the hillslope by post-fire runoff or wind, the soil is left bare and susceptible to increased erosion and runoff (Martin, 2005).

Soil burn severity is a relative measure of change in a watershed that relates to the severity of the effects of the fire on soil hydrologic function (Interagency BAER Team, 2002). Classes of burn severity are high, moderate, low, and unburned. Sediment generated from moderate and high burn severity slopes has the potential to reach channels and be entrained in the stream flow, causing bulked flows during flood events. In general, the denser the pre-fire vegetation and the longer the fire residence time, the more severe the effects of the fire are on soil hydrologic function. This is because fire promotes the formation of water repellent layers at or near the soil surface, and the loss of soil structural stability, both of which result in increased runoff and erosion (Interagency BAER Team, 2002). This water repellency, or hydrophobicity, is generally broken up or washed away within one or two years after a fire (Martin, 2005).

3 SEDIMENT/DEBRIS AND BULKING

Bulking has been defined as increasing the water discharge to account for high concentrations of sediment in the flow (Richardson et al., 2001). Mud and debris flows, which can significantly increase the volume of flow transported from a watershed, most often occur in mountainous areas subject to wildfires with subsequent soil erosion, and in arid regions near alluvial fans and other zones of geomorphic and geologic activity.

For the design of facilities in areas prone to high sediment and debris concentrations, the use of a bulking factor can help provide for more adequately-sized structures. This chapter describes bulking factor equations, sediment/water flow classifications, the downstream extent of sediment-laden flows, flow behavior, and modeling sediment-laden flows.

3.1 Bulking Factor Equations

As described above, bulking is the increase in flow rate due to the inclusion of sediment/debris in the flow. A bulking factor (BF) is generally applied to the peak flow to obtain the total (bulked) peak flow, and serves to introduce a safety factor into the hydraulic design (Hamilton and Fan, 1996).

For an undeveloped watershed where the entire area contributes debris, the bulked peak flow is expressed by:

$$Q_B = Q_w + Q_s \quad (3.1)$$

where Q_B is the bulked peak discharge, Q_w is the peak clear-water discharge, Q_s is the volumetric sediment discharge.

The BF is the ratio of the bulked discharge to the clear-water discharge:

$$BF = (Q_w + Q_s)/Q_w \quad (3.2)$$

Using this BF, the bulked peak discharge may be defined as:

$$Q_B = BF * Q_w \quad (3.3)$$

The BF may be computed based on the concentration of sediment in the flow:

$$BF = \frac{1}{1 - \frac{C_v}{100}} \quad (3.4)$$

where C_v is the sediment concentration in percent volume (sediment volume/total volume).

In the case of a partially-developed watershed or if a debris-control structure reduces the amount of sediment available for transport, the BF can be applied on a proportional basis.

Equation 3.5 provides the conversion between sediment concentration by weight and concentration by volume (O'Brien, 2006):

$$C_v = \frac{C_w \gamma}{\gamma_s - C_w (\gamma_s - \gamma)} \quad (3.5)$$

where:

C_w is the sediment concentration by weight (sediment weight/total weight).

γ is the specific weight of water.

γ_s is the specific weight of the sediment.

Equation 3.6 provides the conversion between sediment concentration in milligrams per liter and concentration by volume (adapted from Garcia et al., 2008):

$$C_v = \left(\frac{\gamma}{\gamma_s} \right) \frac{C_{mg/l}}{(10^6 mg/l)} \quad (3.6)$$

The relationship between bulking factor and sediment concentration (mg/l) is illustrated in Figure 3-1).

3.2 Sediment/Water Flow Classifications

The behavior of flood flows can vary significantly, depending on the concentration of sediment/debris in the mixture. Combinations of sediment and water flow can be classified in different ways, including (1) the triggering mechanism, (2) sediment concentration, or (3) rheology (the study of the deformation and flow of matter) and kinematic behavior. A summary of flow classifications from different researchers is found in Table 3-1.

The classification developed by O'Brien (1986), which is outlined in Table 3-2, is used for the current study. Four types of sediment/water flow are typically defined – normal streamflow (or water flood), hyperconcentrated flow, debris/mud flow, and landslide.

It is important to note that these types of flow are on a continuum, and the boundaries between them are not sharp or well defined. In addition, a single debris event may produce different flow types at different times during the event and at different locations along the watercourse (USGS, 2005a).

3.2.1 Normal Streamflow (Water Flood)

For normal streamflow conditions, the sediment load has a minimal impact on the behavior of the flow, and it can be modeled using standard hydraulic methods for a Newtonian fluid. Turbulent shear stresses control streamflow and sediment transport, the latter taking the form of conventional suspended load and bedload (Bradley, 1986).

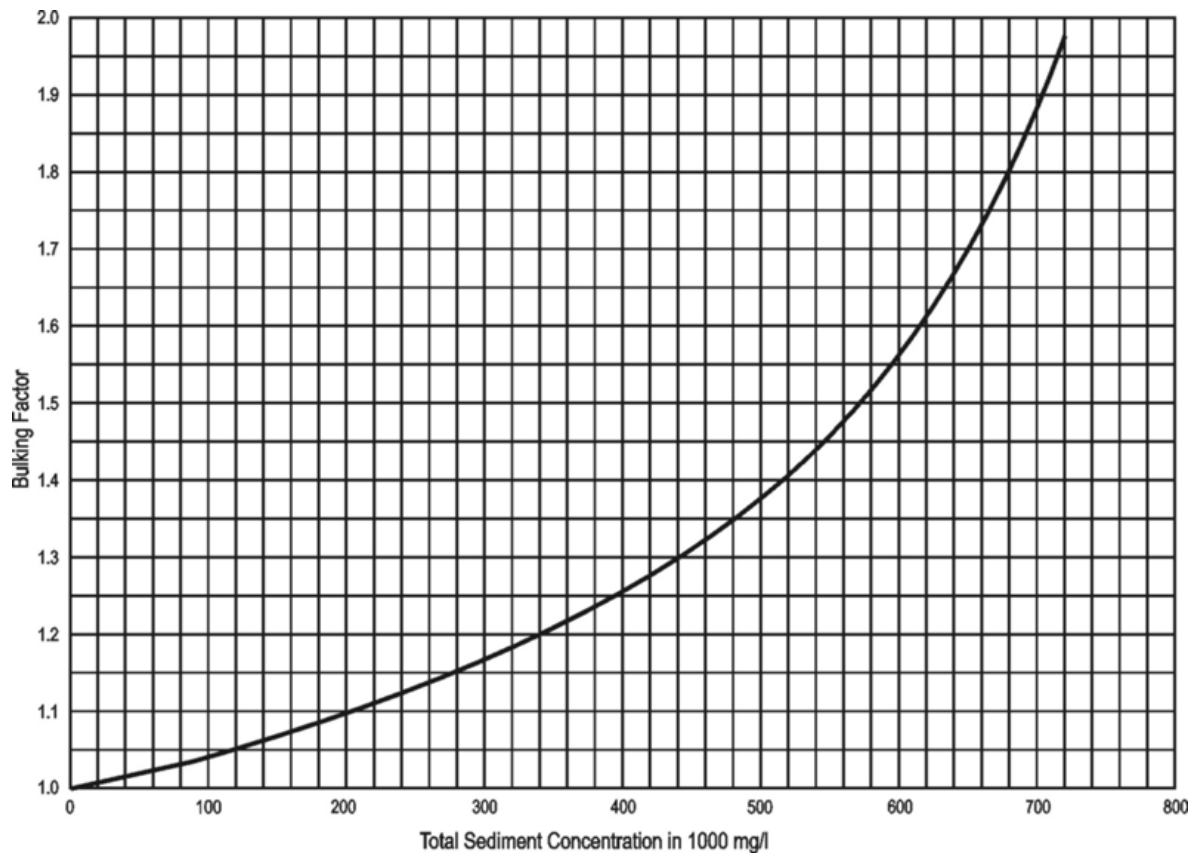


Figure 3-1. Sediment Concentration vs. Bulking Factor (Maricopa County, 2003)

Table 3-1. Flow Classification by Various Researchers (adapted from Bradley & McCutcheon, 1986)

Source	Concentration percent by weight (100% by WT = 1,000,000 ppm)									
	23	40	52	63	72	80	87	93	97	100
	Concentration percent by volume (G. = 2.65)									
Source	10	20	30	40	50	60	70	80	90	100
Beverage and Culbertson (1964)	High	Extreme	Hyperconcentrated			Mud Flow				
Costa (1984)	Water Flood		Hyperconcentrated		Debris Flow					
O'Brien and Julien (1985) using National Research Council (1982)	Water Flood		Mud Flood	Mud Flow	Landslide					
Takahashi (1981)	Fluid Flow		Debris or Grain Flow			Fall, Landslide, Creep, Sturzstrom, Pyroclastic Flow				
Chinese Investigators (Fan And Dou, 1980)	←-----		Debris or Mud Flow-----→					←-----		
Pierson and Costa (1984)	STREAMFLOW			SLURRY FLOW			GRANULAR FLOW			
	Normal: Hyperconcentrated			(Debris Torrent), Debris Mud Flow, Solifluction			Sturzstrom, Debris Avalanche, Earthflow, Soil Creep			

Table 3-2. Classifications of Flows by Sediment Concentration (modified from O'Brien, 1986)

Bulking Factor							
0	1.11	1.25	1.43	1.67	2.00	2.50	> 3.33
Sediment Concentration, % by Weight (100% by WT = 1 x 10 ⁶ ppm)							
0	23	40	52	63	72	80	87 to 100
Sediment Concentration, % by Volume (specific gravity = 2.65)							
0	10	20	30	40	50	60	70 to 100
Normal Streamflow		Hyperconcentrated Flow		Debris Flow/ Mud Flow		Landslide	

A 20-percent sediment concentration by volume is considered by most researchers as the upper limit for normal streamflow (Bradley, 1986). This sediment concentration corresponds to a BF of 1.25; however, a bulking factor is generally not used for streams or washes experiencing normal streamflow and sediment transport.

Although sediment concentrations up to 20 percent by volume are possible for normal streamflow, according to the USGS, normal streamflow typically has less than 5 to 10 percent sediment

concentration (USGS, 2005a). O'Brien (2006) states that river flood sediment bulking rarely exceeds 5 percent by volume, and smaller watersheds and alluvial fans would typically see bulking in the 10 to 15 percent range. Normal streamflow at approximately 5 percent sediment is shown in Figure 3-2.



Figure 3-2. Normal Streamflow with Sediment Transport (USGS, 2005a)

3.2.2 Hyperconcentrated Flow

Hyperconcentrated flow typically has a sediment concentration between 20 and 40 percent by volume. The amount of suspended sediment is large enough to affect the properties of the fluid as well as sediment transport behavior. Large amounts of sand are transported in suspension throughout the water column, although maintaining the sediment loads depends on the velocity and turbulence of the flow (USGS, 2005a). Hyperconcentrated flow occurs in limited conditions, typically within steep channels (O'Brien, 2006). An example hyperconcentrated flow is shown in Figure 3-3.

Hyperconcentrated flow is turbulent with flow resistance dependent on boundary roughness, just like normal streamflow, and it exhibits little or no yield stress (Garcia et al., 2008). The National Research Council (1982) argued that channel resistance for turbulent hyperconcentrated flows can be predicted using normal clear-water methods.

It is important to note that classification by sediment concentration becomes less adequate at higher concentrations because particle size, shape, and interaction become increasingly important (Bradley, 1986). As a result, the transition between hyperconcentrated flow and debris flow varies by researcher, depending on what factors are considered (Garcia et al., 2008).

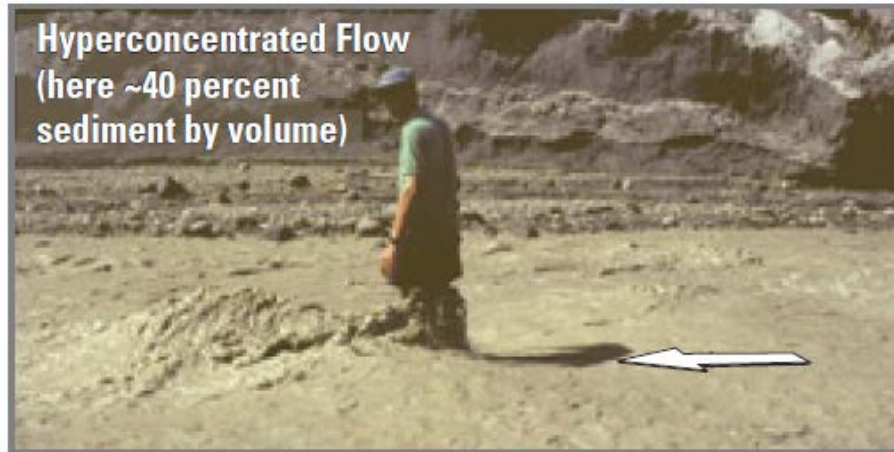


Figure 3-3. Hyperconcentrated Flow – 40% Sediment (USGS, 2005a).

3.2.3 Debris Flows

Debris flows, which contain a high coarse material content including boulders and woody debris, typically have a sediment concentration between 40 and 55 percent by volume, although some researchers use up to 65 percent as the upper limit. The sediment/water mixture is a slurry not unlike wet concrete, and can hold gravel in suspension even when it has slowed or stopped flowing altogether (USGS, 2005a). An example debris flow is shown in Figure 3-4.



Figure 3-4. Debris Flow – 65% Sediment (USGS, 2005a)

Debris flows can achieve high velocities in steep canyons, transporting large boulders and causing catastrophic damage to anything in its path. A debris flow may be slower within low-gradient channels and on alluvial fans; however, they can still quickly fill up channels, divert flow, and destroy vehicles and structures within its path (USGS, 2005a).

As described by O'Brien (2006), during typical debris flow events, clear-water flows arrive first from drainage basin rainfall-runoff. These flows are followed by a surge or "frontal wave" of mud and debris (40 to 50 percent concentration by volume). When the peak water discharge arrives, the average sediment concentration typically drops to the range of 30 to 40 percent by volume. On the falling limb of the hydrograph, surges of higher sediment concentration may occur.

The properties and behavior of debris flows are very different from normal streamflow or hyperconcentrated flow. A key distinction is that the behavior of a debris flow is primarily controlled by the sediment and the composition of the sediment/debris mixture (Krone and Bradley, 1989). The behavior of normal streamflow and even hyperconcentrated flow is controlled by the water rather than the sediment (USGS, 2005a).

Dispersive stresses, which are due to collisions between particles, are dominant in debris flows. Debris flows sometimes occur as a two-phase flow with normal water flow on top of debris slurry (Scott and Williams, 1978).

3.2.4 Mud Flows

Mud flows can be considered a subset of debris flows where greater than 50 percent of the solid material is small (i.e., less than 0.063 mm). High silt and clay concentrations change the flow properties of the matrix, resulting in a fluid with considerable yield strength and viscosity, and the ability to suspend large-sized material in the flow (Garcia et al., 2008). Mud flows commonly occur in watersheds underlain by fine-grained sedimentary rocks and recently burned by wildfire (Scott and Williams, 1978).

3.2.5 Landslides

Sediment-water mixtures with more than 55 percent sediment concentration by volume are generally considered landslides rather than debris flows. Landslides have between 55 and 65 percent concentration by volume, and there may be slow creep prior to a block sliding failure (O'Brien, 2006). Above 65 percent, there is no flow due to the very large solids concentration; instead, failure typically occurs by block sliding alone (O'Brien, 2006).

3.3 Flow Behavior

3.3.1 Newtonian vs. Non-Newtonian Flow

Normal streamflow exhibits “Newtonian” behavior, where shear stress increases linearly with the velocity gradient (strain rate), and the slope of the line is the dynamic viscosity. The viscosity is only dependent on temperature and pressure, and not on the forces acting on the fluid.

$$\tau = \mu \frac{du}{dy} \quad (3.7)$$

Where τ is shear stress, μ is dynamic viscosity, and $\frac{du}{dy}$ is shear rate (i.e., velocity gradient).

A non-Newtonian fluid is one in which the relationship between shear stress and velocity gradient cannot be characterized solely by a single value of viscosity. As the sediment concentration increases, the flow begins to exhibit non-Newtonian behavior with other stresses playing a larger role. Figure 3-5 displays shear stress versus shear rate for different types of fluid, including Newtonian and three non-Newtonian fluids (pseudoplastic, Bingham plastic, and dilatant).

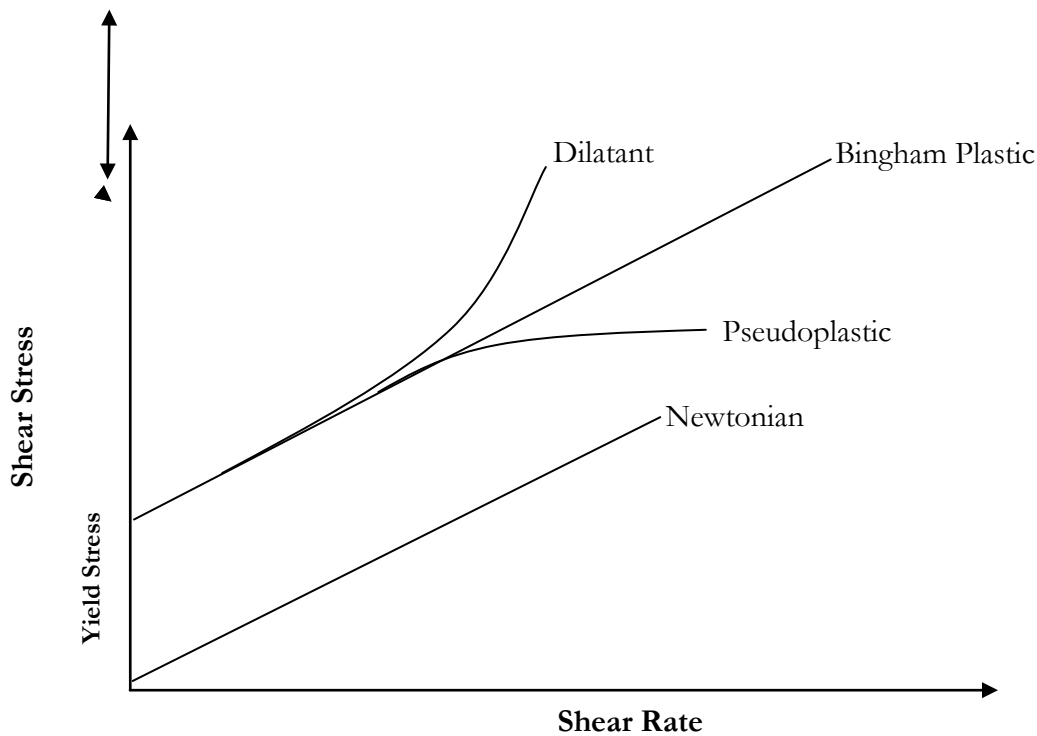


Figure 3-5. Shear Stress vs. Shear Rate (modified from O'Brien, 2006)

3.3.2 Sediment Type and Concentration

The primary mechanism for particle support in the flow is very different between hyperconcentrated flow and a mud flow (Bradley, 1986). For the hyperconcentrated flow, sediment is supported by turbulent stresses in the flow. For the mud flow, cohesive yield stress and viscous shear stress are dominant. In fact, the fall velocity of particles is reduced to near zero in mud flows (Bradley, 1986). A mud flow – which has a large concentration of fine sediment – behaves more like a Bingham plastic (a non-Newtonian fluid) than a Newtonian fluid, with the yield stress and viscosity increasing with clay concentration (Garcia et al., 2008). As illustrated in Figure 3-5, other models of flow behavior include dilatant flow and pseudoplastic flow.

Debris flow and other coarse sediment mixtures exhibit more complex flow behavior, with a dispersive shear stress added due to particle-on-particle interaction (Garcia et al., 2008). This dispersive shear stress increases with the second power of the particle size. A high concentration of non-cohesive particles combined with a low concentration of fines produces more dispersive shear stresses and less viscous shear stresses (O'Brien, 2006). Conversely, dispersive shear stress goes down as viscosity goes up. This is because the more viscous nature of the fluid allows larger particles to be suspended with less collisions occurring between particles.

According to Bradley (1986), the initiation of non-Newtonian flow has been observed for as low as 4 percent concentration by volume with fine, viscous material, and up to 36% for larger material.

4 MODELING OF SEDIMENT-LADEN FLOWS

This chapter deals with the hydraulic modeling of sediment-laden flows, including a modeling overview, a discussion of using the HEC-RAS (River Analysis System) program to model hyperconcentrated flows, a comparison between FLO-2D and HEC-RAS, and the potential downstream limits of debris and hyperconcentrated flows.

4.1 Introduction

4.1.1 Hyperconcentrated Flow

Fluid properties and sediment-transport characteristics change for hyperconcentrated flow as large volumes of sediment can be transported throughout the water column, and the mixture no longer behaves strictly as a Newtonian fluid that has no shear strength. Instead, the properties of a hyperconcentrated flow are typically “between those of a Newtonian and non-Newtonian fluid” (Garcia et al., 2008).

Basic hydraulic and sediment transport equations and models are generally applied to hyperconcentrated flow conditions, although the equations and models were not developed for non-Newtonian fluids. A 40-percent sediment concentration by volume is the approximate upper limit of hyperconcentrated flow, which corresponds to a bulking factor of 1.67 (see Table 3-2).

4.1.2 Debris and Mud Flows

A debris or mud flow acts as a non-Newtonian fluid, and basic hydraulic and sediment transport equations do not apply. If detailed modeling of debris/mud flows is required, a model with specific debris flow capabilities such as FLO-2D should be used rather than standard hydraulic models, such as the USACE one-dimensional HEC-RAS program.

FLO-2D is a two-dimensional hydrodynamic model that can simulate clear water, mud, and debris flooding (O’Brien, 2006). The first version of the model was known as MUDFLOW. FLO-2D is accepted by FEMA for Flood Insurance Studies (FIS) and the USACE considers the model to be “reliable for most alluvial fan problems” (USACE, 2000b).

It is common practice for flows with bulking factors up to 2.0 to be used with HEC-RAS or other standard hydraulic models. However, the extent to which the model is under- or over-estimating flood elevations or flow velocities—compared to a model that can explicitly model debris/mud flows—is not known.

4.2 Modeling Concerns – Hyperconcentrated Flow

One of the main issues with using HEC-RAS to model hyperconcentrated flow is that the hydraulic equations in the program are specific to clear-water flows, and not bulked flow. The model uses these equations to compute sediment transport. In addition, the physical properties of water are hard-coded into the model, and thus cannot be reconfigured to directly account for the different properties of hyperconcentrated (or debris) flows.

4.2.1 Non-constant Viscosity and Density

There is a fundamental issue with any analysis of hyperconcentrated flows using standard hydraulic modeling techniques because these flows are often not characterized by a constant viscosity or even a constant density, even though they may often be described with effective fluid mechanic constants (Whipple, 1997). This issue is exacerbated with burned watersheds because a hyperconcentrated flow can progressively gain or lose material (Gabet and Bookter, 2008). Thus, utilizing a constant density for the flow is only accurate at a particular location and time. For example, O'Brien (2008) reports that the arrival of a debris flow hydrograph usually occurs in three parts: (1) a clear-water wave, followed by (2) a frontal wave of debris (40 to 50% sediment concentration by volume), and finally (3) a peak flow with a reduced concentration of 30 to 40%.

In order to account for rheological differences, bulked flow viscosities have been modeled with a number of non-Newtonian models, including the Bingham plastic, dilatant, pseudoplastic, power-law, linear/power-law, quadratic, and viscoplastic. However, a general model has not been identified to fit all observed bulked viscosities, and cannot account for observed hysteresis, i.e., different transport rates occurring before and after the peak discharge under similar hydraulic conditions (Major and Pierson, 1992).

Unfortunately, the complexity of hyperconcentrated and debris flows does not lend itself simplifying assumptions. For example, with effective viscosities many orders of magnitude greater than water, the corresponding Reynolds number (Re) could fall within the laminar range. However, this is not true for all bulked flows. High velocities (up to 25 ft/sec) and turbulent flows have been observed in the field (O'Brien, 2008). In addition, hyperconcentrated flows do not always follow the “no-slip” condition (where velocities are zero at the boundary) and often contain a “plug” – a dense area of nearly solid material. These two aspects are quite difficult to account for with typical hydraulic modeling (Whipple, 1997).

4.2.2 Other Approaches

The most significant problem with hyperconcentrated flow rheology is that it may simply be the wrong approach. Hungr (2000) argues that actual debris flows are governed by frictional characteristics between the flow and friction front rather than its rheology. Likewise, Iverson and Denlinger (2001) developed a dynamic model based on the Coulomb mixture theory that has provided good results. Iverson (2003) identifies a number of ways that rheology is inconsistent with observed hyperconcentrated flows. Despite these criticisms, simple sediment transport approaches to modeling hyperconcentrated flows have been successful when properly calibrated. For example, Earles et al. (2004) found HEC-RAS to successfully predict sediment outflows from a burned watershed. A thorough review of this ongoing debate is provided in Ancey (2007).

A clear resolution of this debate may not occur for some time. Given the need for adequate modeling of hyperconcentrated flow using readily available modeling tools, it is assumed in the current study that hyperconcentrated flow can be adequately modeled as a fluid. As such, it is desirable to take advantage of the HEC-RAS program, which has become an industry standard for hydraulic modeling. However, application to hyperconcentrated flows requires that the HEC-RAS input coefficients be modified in order to account for the high viscosities and densities relative to water, the properties of which are hard-coded into the program. The adjustment of these input coefficients is described in the next section.

4.3 HEC-RAS Adjustments for Hyperconcentrated Flow

The principle of similitude allows the determination of adjusted coefficients by equating the appropriate non-dimensional parameters. This procedure requires a number of mathematical steps; the specific derivations are shown in Appendix A. The results are described below.

4.3.1 Expansion/Contraction Coefficients

The adjusted expansion/contraction coefficient, C_{bulked} (dimensionless), is given by (Appendix A):

$$C_{bulked} = (\nu / \nu_{bulked})^{2/3} C \quad (4.1)$$

where:

μ = absolute fluid viscosity (lb-sec/ft²)

ρ = fluid density (slugs/ft³)

$\nu = \mu / \rho$ = kinematic viscosity (ft²/sec)

The bulked subscript indicates the bulked flow as opposed to clear water (no subscript).

Table 4-1 shows computed expansion/contraction coefficients for a range of sediment concentrations by volume and corresponding kinematic viscosities. As sediment concentration by volume increases, C_{bulked} decreases, which suggests sediment-laden flows are less affected by expansion/contraction.

Table 4-1. Computed Expansion/Contraction Coefficients for Bulked Flows

Sediment Concentration (% by Volume)	Kinematic Viscosity (ν or ν_{bulked} , ft ² /s)	Expansion/Contraction Coefficient			
		0.1	0.3	0.5	0.7
0 (original value)	0.0000141	0.1	0.3	0.5	0.7
10	0.000067	0.036	0.107	0.178	0.249
20	0.00058	0.008	0.025	0.042	0.059
30	0.0052	0.002	0.006	0.010	0.014
40	0.031	0.0006	0.002	0.003	0.004
50	0.28	0.0001	0.0004	0.0007	0.0009

4.3.2 Manning's n Coefficients

To model hyperconcentrated flow, Manning's n values should be adjusted as follows (Appendix A):

Manning's n (laminar flows, $Re < 500$):

$$n_{bulked} = 0.74 \sqrt{v_{bulked} / q} \quad (\text{English units only}) \quad (4.2)$$

Manning's n (turbulent flows, $Re > 500$):

$$n_{bulked} = \left(\frac{V_{bulked}}{v} \right)^{1/9} n \quad (4.3)$$

where:

V = flow velocity (ft/sec)

y = depth of flow in the channel (ft)

q = is the bulked flow per linear foot width of the channel (ft²/sec)

$Re = 4Vy / v_{bulked} = \text{Reynolds number (dimensionless)}$

To test the use of the Manning's n equation for bulked, turbulent flows, an HEC-RAS hydraulic model for Pole Creek was used as an example. The Reynolds number ranged from approximately 800 to 2,400 (depending on the peak discharge and cross section), which corresponds to the turbulent flow threshold of approximately 500 cfs (using $v_{bulked} = 0.282 \text{ ft}^2/\text{s}$).

Table 4-2 shows computed n_{bulked} values for a range of sediment concentrations by volume. As sediment concentration by volume and clear water Manning's n increase, Manning's n_{bulked} increases, which indicates that higher n values are required to represent sediment-laden flows.

Table 4-2. Computed Manning's n for Bulked Flows – Pole Creek Example (Turbulent Flow)

Sediment Concentration (% by Volume)	Manning's n			
	<i>0.015</i>	<i>0.02</i>	<i>0.025</i>	<i>0.03</i>
0	0.015	0.024	0.030	0.036
10	0.018	0.024	0.030	0.036
20	0.023	0.030	0.038	0.045
30	0.029	0.039	0.048	0.058
40	0.035	0.047	0.059	0.071
50	0.045	0.060	0.075	0.090

4.3.3 Limitations

The equations for adjusting expansion/contraction coefficients and Manning's n values for bulked flow are believed to be applicable to most simple, steady-state applications. However, there are scenarios where the use of HEC-RAS to model hyperconcentrated flows would be expected to be less accurate, including:

- Highly unsteady flow modeling – Note that the laminar n value is inversely related to the flow. This is easily applied to steady state modeling, where there is no change in Q , but may be difficult to implement for unsteady routing. There may be work-around solutions, such as varying the n value by stage, but this would require further investigation.
- Hydraulic paths that include obstacles, such as bridges and weirs – Modeling these elements require empirical equations not easily modified for equivalent hyperconcentrated flows.
- Pressure flow elements, such as culverts and sluice gates – These elements use a number of empirical relations that are not easily modified for equivalent hyperconcentrated flows.
- Erosive channels or deposition zones where the hyperconcentrated flows are expected to significantly gain or lose material, respectively.
- Sediment transport modeling, which utilizes a number of empirical relations not applicable or easily convertible to hyperconcentrated flow modeling.
- Highly non-Newtonian fluids – As noted earlier, hyperconcentrated flows known to be highly non-Newtonian cannot be effectively modeled by HEC-RAS.

In addition, it would be inappropriate to utilize the other optional capabilities of HEC-RAS (e.g., water quality) as these relations are specific to clear-water conveyance.

4.4 Bulked Flow Modeling Comparison – FLO-2D vs. HEC-RAS

The focus of this section is to compare HEC-RAS and FLO-2D in terms of modeling highly bulked flows. FLO-2D is a commercially available quasi-two-dimensional program developed by and available for purchase through FLO-2D Software, Inc. In addition to the dimensionality difference (1-D versus 2-D), FLO-2D is capable of bulked flow modeling whereas HEC-RAS is not (or only indirectly).

4.4.1 Previous Studies

After an extensive literature search and personal communication with Dr. Jim O'Brien (the FLO-2D developer), we found that research directly comparing the modeling of bulked flows with FLO-2D vs. HEC-RAS is virtually non-existent.

4.4.2 Differences in 1-D vs. 2-D Modeling

Before comparing HEC-RAS with FLO-2D for hyperconcentrated flows, the fundamental differences between 1-D and 2-D hydraulic modeling for clear water need to be addressed. In

general, 2-D hydraulic models have at least two potential advantages over 1-D models. First, 2-D models can make more accurate predictions than 1-D models where there are complex flow conditions (Bohorquez and Darby, 2008; Wohl, 1998; and Kidson et al., 2006). Second, there is no need to know (or estimate) the main channel or thalweg location beforehand in a 2-D model, unlike the requirements of a 1-D model (Bohorquez and Darby, 2008).

Potential disadvantages to 2-D modeling as opposed to 1-D modeling include:

- A 3-D topographic surface must be constructed, as opposed to 1-D modeling, which generally requires appropriately spaced cross-section information.
- Roughness parameters, typically determined through 1-D experimentation, need to be adjusted for 2-D applications (Horritt and Bates, 2002).
- Two-dimensional modeling is more complex, leading to more time and expense for model development and calibration, an increased chance of input errors, and longer computing times.

4.4.3 FLO-2D Advantages/Disadvantages

One of the main advantages of FLO-2D is its sophisticated rheology scheme. FLO-2D allows viscosity to be modeled in the form of a flexible quadratic viscous stress relation, which can be used to model a number of different non-Newtonian equations. Put more plainly, the FLO-2D can explicitly model hyperconcentrated/debris flow.

The FLO-2D software program itself has several limitations that must be noted:

- The algorithms employed by the program are not actually 2-D, but instead approximate 2-D space, restricting flow to eight possible directions. As such, convective acceleration is not considered, and the flow follows the path of steepest descent (O'Brien, 2008).
- The model cannot utilize both sediment transport and hyperconcentrated flow modeling simultaneously. Thus, the model cannot perform the progressive bulking or debulking of flows expected through erosive channels (Gabet and Bookter, 2008).

The FLO-2D hyperconcentrated/debris flow accuracy appears to be highly sensitive to the input parameters. A review of numerous case studies found that FLO-2D performed adequately at predicting recorded events (“retrodicting”) only after a rigorous, site-specific calibration had been conducted (Bello et al., 2000; Bertolo and Wieczorek, 2005; and Armento et al., 2008). Only the Lin et al. (2005) study found that FLO-2D performed adequately without requiring calibration. The reliance on calibration may reflect large uncertainties with regard to the watershed properties, which is consistent with the earlier discussion of the inherent rheologic unpredictability and the inability to incorporate inevitable shallow slope failures.

4.4.4 FLO-2D Application

Based on the research, we recommend that FLO-2D be utilized in lieu of HEC-RAS under the following circumstances:

- *Highly unsteady flow modeling.* HEC-RAS cannot be easily utilized to accurately model unsteady hyperconcentrated flows.

- *Highly non-Newtonian fluids.* This is arguably the best reason to use FLO-2D over HEC-RAS, particularly if the specific non-Newtonian aspects of the flow of interest are well known.
- *Highly 2-D flow.* HEC-RAS can only roughly approximate 2-D flow conditions through contraction and expansion coefficients and variation of roughness coefficients. Moreover, the thalweg location must be known beforehand.

The following scenarios cannot be effectively modeled by either HEC-RAS or FLO-2D:

- Routing where progressive bulking or debulking is expected
- Sediment transport modeling for hyperconcentrated flows
- Geomorphological changes
- Highly concentrated bulked flows (landslides, etc.)

4.5 Downstream Limit of Debris and Hyperconcentrated Flows

This section describes research regarding the downstream limit (or runout) of debris/mud flows and hyperconcentrated flow.

4.5.1 Debris/Mud Flow Runout

Research on debris and mud flow runout has found that:

- During major storm events, downstream dilution often leads to less concentrated flow before leaving the mountain front. If channelized, however, large debris flows can travel distances of a mile or more (USGS, 1997).
- Conversely, Scott and Williams (1978) found that the loss of fluidity due to infiltration stopped debris flows within a short distance of mountain fronts.
- Unlike debris flows, mud flows were found to continue “well beyond the mountain fronts” (Scott and Williams, 1978).
- Debris flows will typically stop at channel confluences that result in large changes in debris flow direction and/or gradient (Burnett and Miller, 2007).
- During the large flow events of 1969, coarse fill occurred in downstream reaches of Sespe Creek, a 252 sq. mi. watershed (Scott and Williams, 1978). However, it is not clear whether this was the result of normal sediment transport carrying sediment from upstream, debris-producing drainages, or if hyperconcentrated flow actually extended the entire distance.
- Some empirical methods are available to determine the extent of debris flow events. This has been the focus of numerous statistical studies, including Prochaska et al. (2008).

After applying regression analysis to known events, Prochaska et al. (2008) developed an equation to describe debris flow runout based on watershed and channel slopes and elevation differences. The equation, described in Phase II of the current study, was tested for Adams Barranca, Hopper

Canyon, and Pole Creek. The equation did not provide reasonable results, so it was eliminated from further consideration.

As shown in Table 4-3, the National Research Council (1996) describes approximate downstream limits for debris flows, including coarser- and finer-grained flows. Stock and Dietrich (2003), using contour maps, laser altimetry, and extensive field observations from sites in the western United States (including the San Gabriel Mountains, California Coast Range, King Range, and the Oregon Coast Range), found that debris flows rarely travel below channel slopes of approximately 3 to 10 percent. This research suggests that the primary control on debris flow runout length is channel slope.

Table 4-3. Channel Slopes resulting in Debris Flow Runout

Type of Flow	Approximate Downstream Limit	Source
Coarser-grained debris flows	10 to 14 % slope (6° to 8°)	National Research Council (1996)
Finer-grained debris flows	3.5 to 5.3 % slope (2° to 3°)	National Research Council (1996)
Debris flows	3 to 10% slope (1.7° to 5.7°)	Stock and Dietrich (2003)

Classifying segments of a drainage pattern using a numbering convention is known as “stream order” (USGS, 1997). Stream order can be used to help predict where debris flows are more likely to take place. Whenever two segments of the same order join downstream, the order of the downstream segment is increased by one (e.g., two first-order drainages join together to form a second-order drainage). Figure 3-1 is an example of how the stream order classification system is applied to a drainage network.

Debris flows can typically form on steep slopes and in drainage channels characteristic of first- and second-order streams; it is the base of these steep slopes that will be exposed to small debris flows. The larger second- and third-order streams, which are typically located in and near the mouths of relatively steep, larger ravines can also be vulnerable to large debris-laden flows. Finally, larger drainage basins such as canyons (fourth- and fifth-order drainages), generally have gentler gradients and typically only during intense rainstorms can these larger streams receive increased input from debris flow (USGS, 1997). An example figure showing debris flow occurrence and the movement of material in a watershed is provided in Figure 4-2.

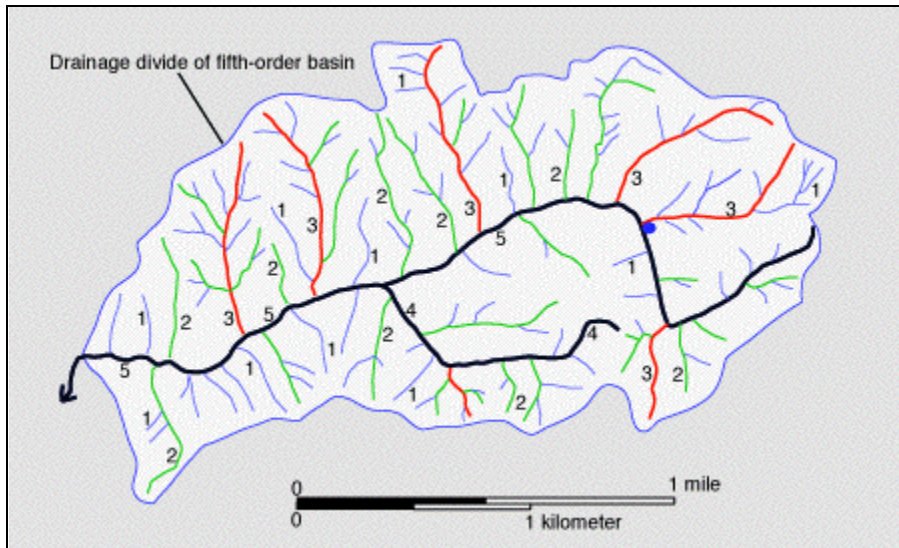


Figure 4-1. Stream Order Classification Example (USGS, 1997)

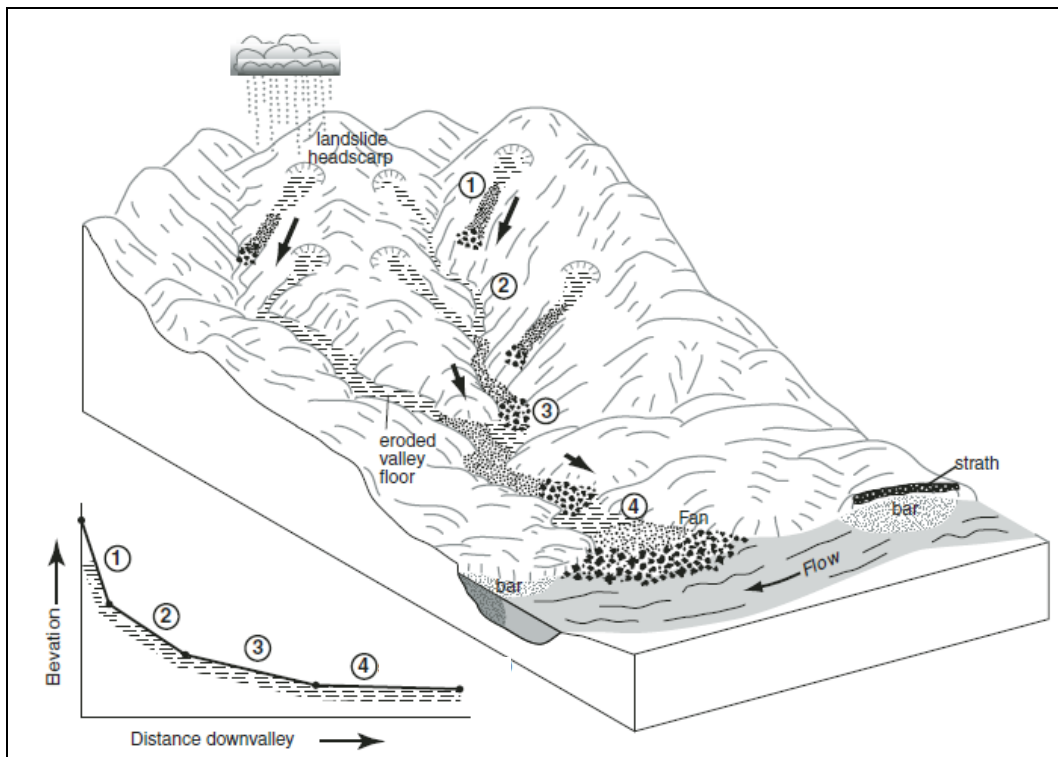


Figure 4-2. Debris-flow Occurrence and Movement (Stock and Dietrich, 2006)

4.5.2 Limit of Hyperconcentrated Flow

While the limit of debris flow was estimated by Stock and Dietrich (2003) at slopes ranging from 3 to 10 percent, hyperconcentrated flow can continue beyond the debris flow runout location. Based on an extensive literature search, no studies were found to describe the downstream limit of hyperconcentrated flows, whereas several studies can be found on the limits of debris flows (as described in the previous section).

Three drainage networks—Adams Barranca, Hopper Canyon, and Pole Creek—were chosen to examine the limits of hyperconcentrated flow in Ventura County. The analysis in ArcGIS used stream centerline and 30-meter resolution Digital Elevation Model (DEM) data from the USGS National Hydrography Dataset, as well as mapping of potential slope failure areas from the California Division of Mines and Geology (GIS layer provided by the VCWPD). Stream segments greater than 0.5, 1, 2, 3, and 4 percent were identified. Based on these data and available aerial photos, the limit of the 1-percent average channel slope was identified as a potential lower limit of hyperconcentrated flow. Figure 4-3, Figure 4-4, and Figure 4-5 illustrate this limit for Adams Barranca, Hopper Canyon, and Pole Creek respectively. Table 4-4 lists distances from the most downstream slope failure near the channel to the downstream limit of the 1-percent average channel slope.

No field investigation was performed for the current study, and we recommend that further research be performed before the 1-percent slope cut-off is incorporated into any bulking recommendations. Nevertheless, the use of the percent-slope approach appears to be a promising approach for estimating the downstream limits of hyperconcentrated flow.

Table 4-4. Computed Distance from Slope Failure to Limit of 1% Channel Slope

Watercourse	Distance from Slope Failure to Limit of 1% Channel Slope
Adams Barranca	14,800 ft (2.8 mi)
Hopper Canyon	5,500 ft (1.0 mi)
Pole Creek	3,600 ft (0.7 mi)

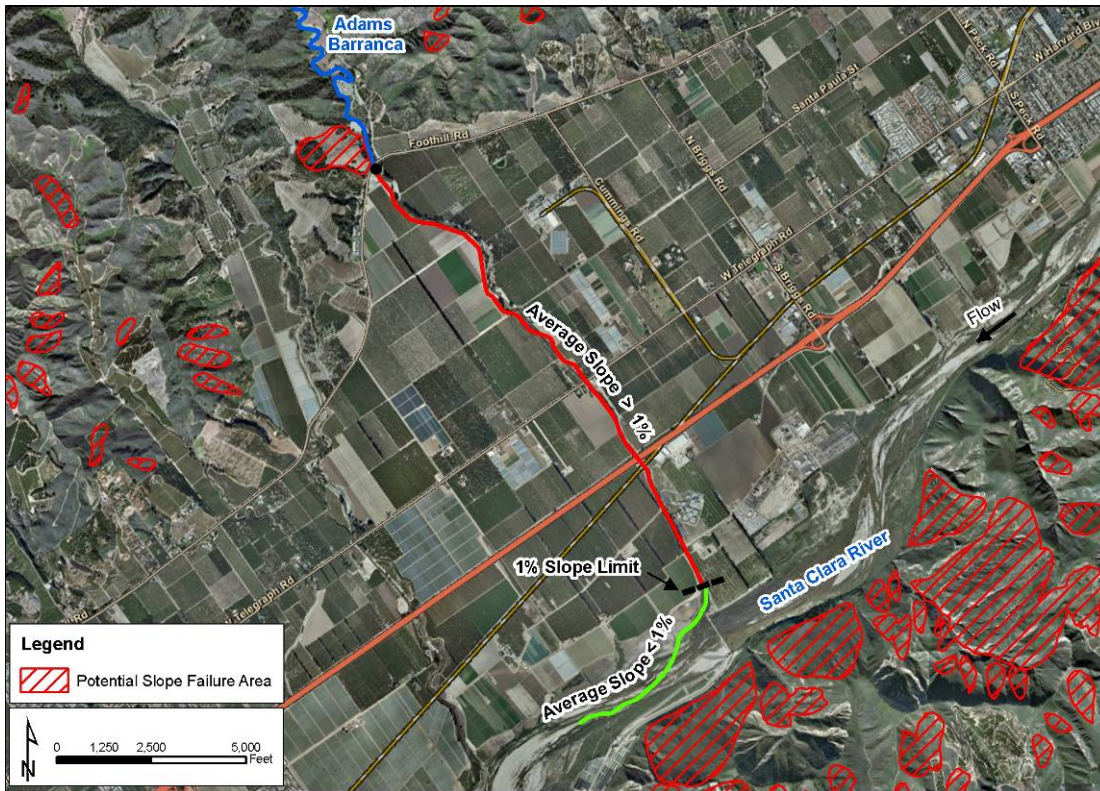


Figure 4-3. Adams Barranca – Potential Limit of Hyperconcentrated Flow

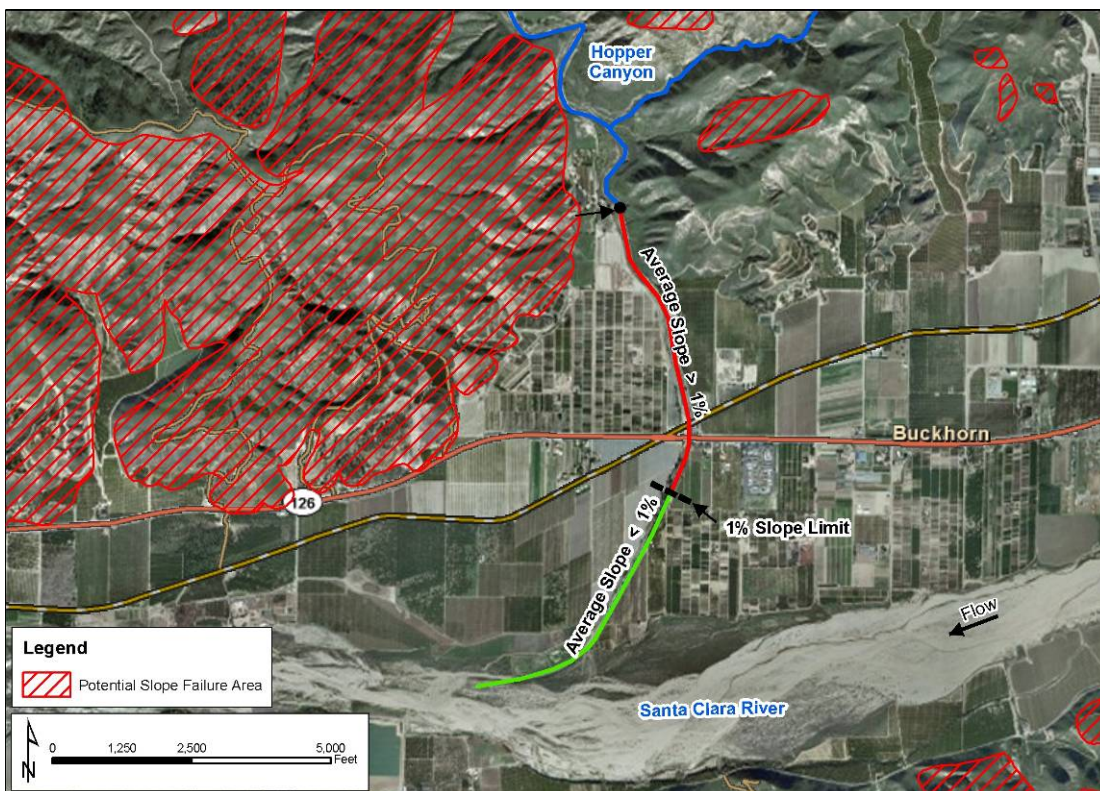


Figure 4-4. Hopper Canyon – Potential Limit of Hyperconcentrated Flow

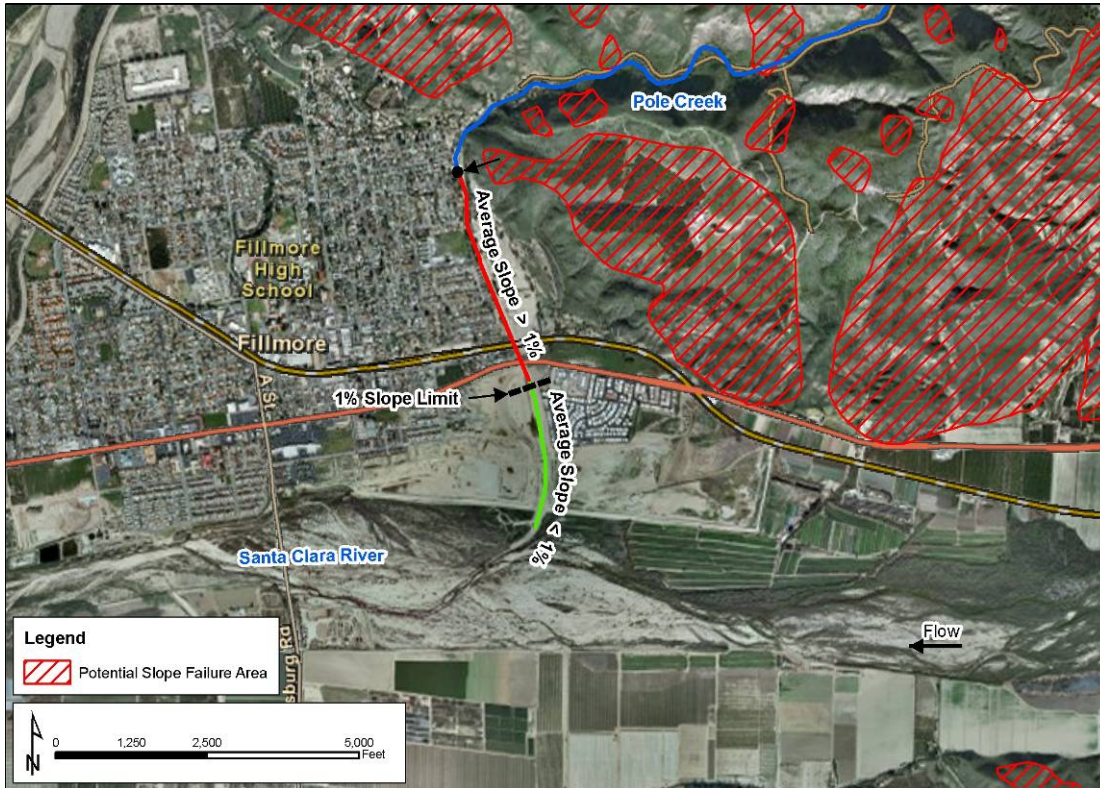


Figure 4-5. Pole Creek – Potential Limit of Hyperconcentrated Flow

5 AGENCY BULKING METHODS

Described below are sediment/debris bulking factors and procedures used by southern California counties (including Los Angeles, Ventura, San Bernardino, Riverside, Orange, and San Diego), the Los Angeles District of the USACE, FEMA, and the Interagency Burned Area Emergency Response (BAER) Team.

5.1 Los Angeles County

The *Los Angeles County Sedimentation Manual* (Los Angeles County, 2006a) divides the county into three overall basins: Los Angeles Basin, Santa Clara River Basin, and Antelope Valley. Sediment production is dependent upon many hydrologic and environmental factors, including rainfall intensity, geology, soil type, vegetative coverage, runoff, and watershed slope. Within each basin, Debris Potential Area (DPA) zones are delineated based on similar hydrologic and environmental conditions, and sediment yield volume production. These DPA zones can be found in Appendix A of the sedimentation manual.

5.1.1 Debris Design Events

The Design Debris Event (DDE) is defined as the quantity of sediment produced by a saturated watershed significantly recovered from a burn (i.e., after four years) as a result of a 50-year, 24-hour rainfall amount. A rate of 120,000 yd³/mi² (74.4 acre-ft/mi²) for the design storm has been established as the DDE for a one square-mile drainage area in the DPA 1 zone. This rate is used in areas of high relief and granitic formations that characterize the San Gabriel Mountains. Other mountain areas in the county have been assigned relatively lower sediment potentials based on historical data and differences in topography, geology, and rainfall. Sediment records indicate that areas less than one square-mile are expected to produce a higher rate of sediment production and areas greater than one square-mile a lower rate. The Santa Clara River Basin has four debris production curves, as shown in Figure 5-1. These curves are for undeveloped watersheds.

5.1.2 Peak Bulking Factor Curves

The Los Angeles County sedimentation manual also provides a series of peak bulking factor curves that show the proportion of the bulked flow rate to burned flow rate during the peak of the flood hydrograph (Los Angeles County, 2006a). The peak bulking factor is estimated using the curves based on the watershed area and the DPA within which the watershed is located. The maximum peak bulking factor ranges from approximately 1.02 (2% bulking) for DPA Zone 11 to 2.0 (100% bulking) for DPA Zone 1. The Los Angeles County procedure specifies a bulking factor for all areas of the county, even where sediment concentrations and the resulting bulking factor are low.

The Santa Clara River Basin has four peak bulking factor curves, as shown in Figure 5-2. Bulking factors for the Santa Clara River Basin range from 1.1 for a large (100 mi²) watershed and a DPA-9 zone, to a value of 1.62 for a very small (0.1 mi²) drainage area and a DPA-3 zone. Curves for the Los Angeles Basin and Antelope Valley are not shown here, but are provided in Appendix B of the sedimentation manual (Los Angeles County, 2006a).

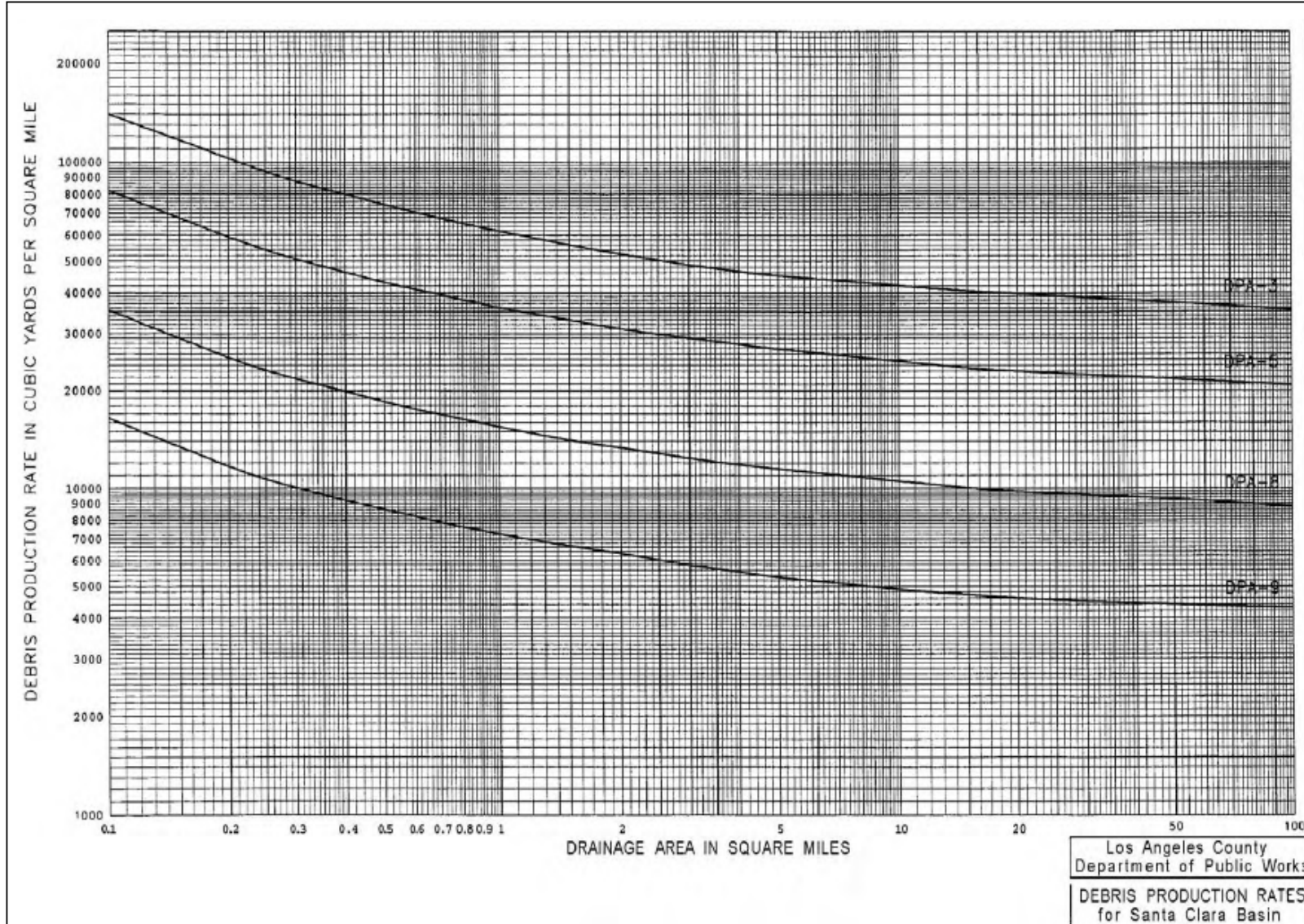


Figure 5-1. Debris Production Rates for the Santa Clara River Basin (Los Angeles County, 2006a)

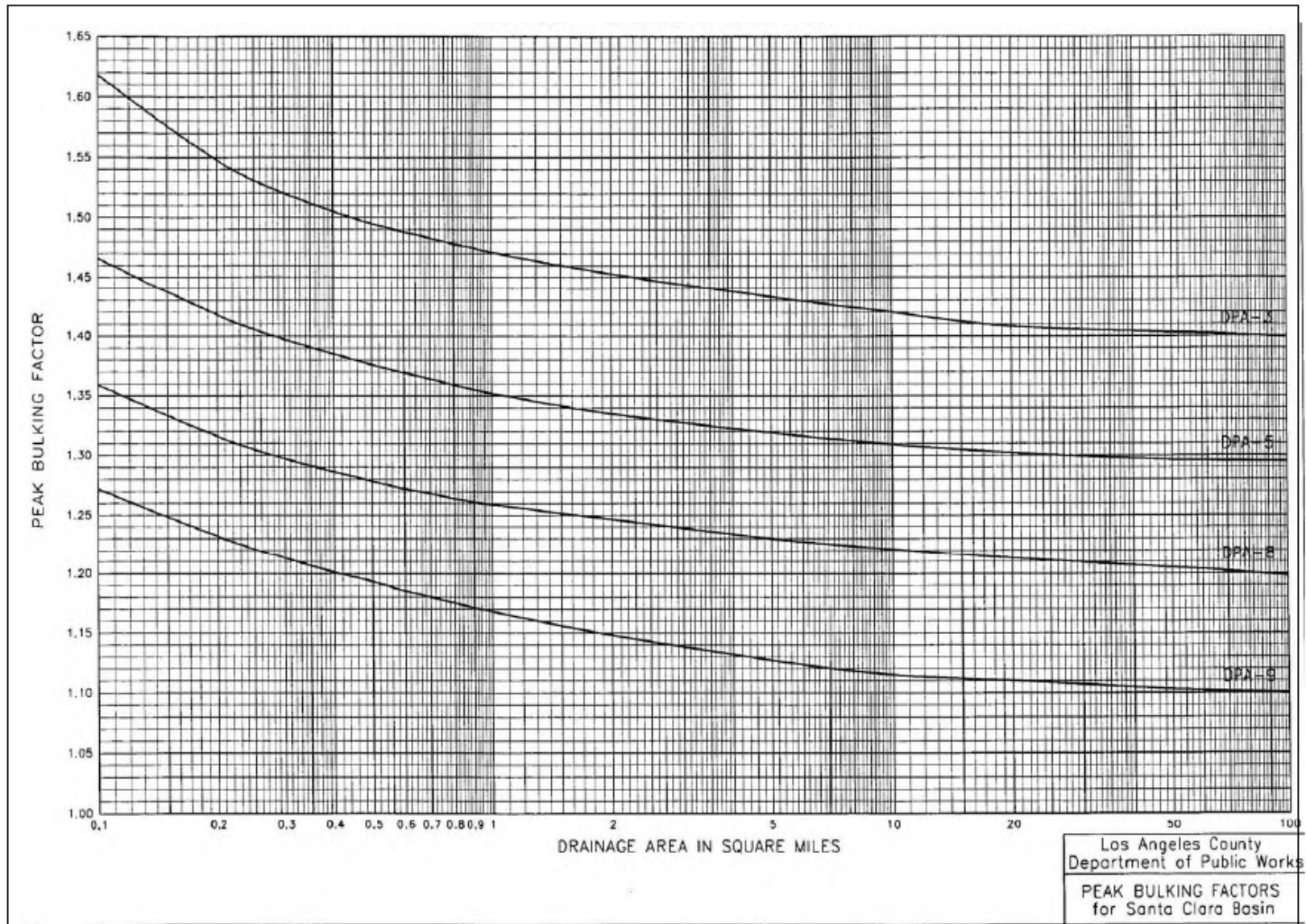


Figure 5-2. Peak Bulking Factors for the Santa Clara River Basin (Los Angeles County, 2006a)

In addition to the sediment production curves, a series of equations have been developed for Los Angeles County basins. These equations can also be found in the sedimentation manual (Los Angeles County, 2006a). The equations are used to calculate weighted bulking factors based on the percentage of development in the watershed, watersheds with multiple debris production zones, and the presence of debris control structures.

5.1.3 Converting Debris Yield to Bulking Factor

To convert the estimated debris yield (i.e., debris volume) to a bulking factor requires that the clear-water hydrograph be computed using a rainfall-runoff model. To distribute the total debris volume throughout the flow hydrograph, the following equation may be used:

$$Q_s = a Q_w^n \quad (5.1)$$

where Q_s is the sediment discharge (cfs), Q_w is the clear-water discharge (cfs), and a and n are bulking constants (fixed throughout the hydrograph). This equation is used in the sedimentation manual (Los Angeles County, 2006a) when using bulked flows in sediment transport studies.

According to Vanoni (2006), the value of n is between 2 and 3 for most sand-bed streams. Combining Equation 5.1 with 3.2 yields:

$$BF = \frac{Q_w + Q_s}{Q_w} = 1 + a Q_w^{n-1} \quad (5.2)$$

The coefficient a is determined by numerical integration of the squared 100-year hydrograph ordinates as follows:

$$a = \frac{V_s}{\sum (\Delta t * Q_w^n)} \quad (5.3)$$

where V_s is the total sediment yield and Δt is the computational time interval from the hydrologic model.

It should be noted that this method assumes that the peak sediment hydrograph outflow will occur at the same time as the peak storm hydrograph, although in reality there can be a significant lag time between peak storm outflow and peak sediment outflow (Bradley, 1986). Moreover, numerous peak sediment outflows can occur from the same storm event, each with different concentrations (Whipple, 1992). Although the method is based on simplifying assumptions, an alternative approach to distributing the sediment discharge—especially one that is also suited to practical application—was not found.

5.2 Ventura County – Current Bulking Method

The VCWPD currently uses a bulking method for burned watersheds based on a simplification of the Los Angeles County sediment production and bulking factor curves. The Ventura County bulking factor curve is shown as Figure 5-3. Bulking factors range from approximately 1.43 at 4,000 yd^3/mi^2 to 1.87 at 92,000 yd^3/mi^2 .

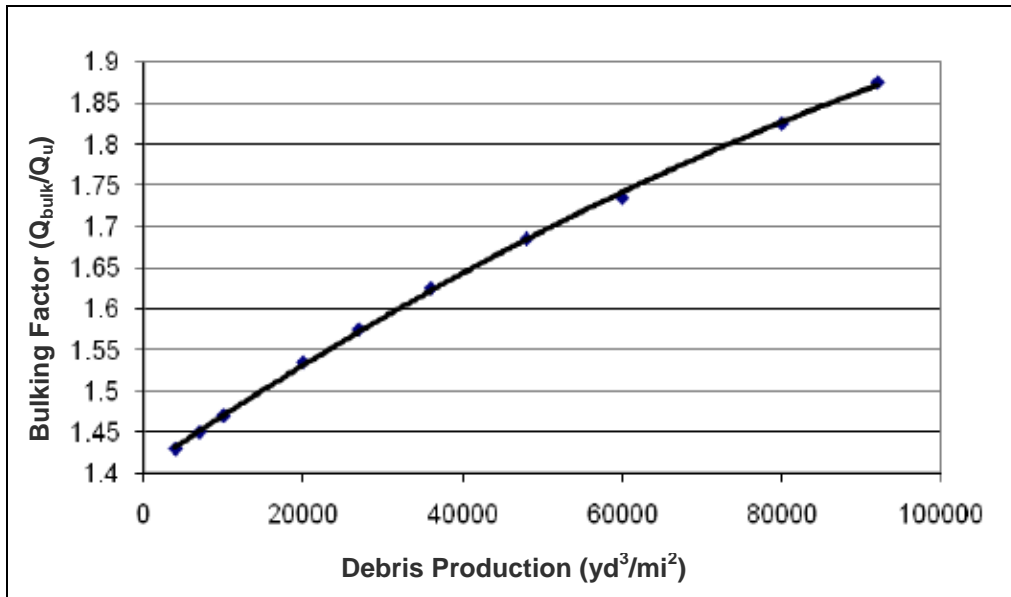


Figure 5-3. VCWPD Bulking Factor Curve (VCWPD, 2010a)

The curve is embedded in the VCWPD's SCOTSED program, which estimates debris production for design events using the Scott and Williams (1978) regression equation. The equation uses several parameters that affect the production rate, including drainage areas, 1- and 10-day rainfall, slope failure area contribution, fire factor, and watershed area, and is presented in Equation 5-4 (VCWPD, 2005):

$$SY = 17.54(A)^{0.828} * (ER)^{1.382} * (FF)^{0.251} * (SF)^{0.375} * (K)^{0.840} \quad (5.4)$$

where:

SY = Sediment yield (yd³)

A = Area of the watershed (mi²)

ER = Elongation ratio – a ratio produced by dividing the diameter of a circle with an area equal to that of the watershed by the maximum watershed length measured in a straight line parallel to the main channel (ft²/ft).

FF = Fire factor – the percentage of non-recovery of vegetative cover in the burned watershed.

SF = Slope failure – watershed area prone to slipping divided by the drainage area, (acres/mi²).

K = Dimensionless rainfall factor – Varies for different storm frequencies and is the product of the square of the 1-day precipitation value and the 10-day precipitation value for a given storm frequency in inches.

Currently, the VCWPD assumes that the increase in clear-water runoff after a fire is included in the bulking factor from SCOTSED, although the exact history of the curve is unknown. The bulked flow factor has not been used in design hydrology consistently by the VCWPD. Two cases where the bulking factor was used in design hydrology are for watersheds with known high sediment production leading to downstream flooding, including Pole Creek in the City of Fillmore and the Fresno Canyon tributary to the Ventura River.

The fire factor (FF) represents the condition of a watershed after a burn or the percentage of non-recovery of vegetative cover in a burned watershed. The Ventura County FF is a weighted value based on the percentage of area burned and the time since the last fire. A plot of the Ventura County FF is presented in Figure 5-4.

Using the figure, a FF of 88 represents six months after a burn (after one wet season) and logarithmically decreases to 1.0 after eight wet seasons or about 7.5 years after the burn. The maximum value of 100, representing the watershed immediately after a fire, is rarely used in design. This is primarily because Ventura County fires usually occur in late summer and early fall, and thus it is typically assumed that soon after a fire some rainfall will occur, leading to some immediate regrowth after a fire. For permanent detention basin design, the VCWPD requires facilities be designed to hold 125% of the sediment from a 100-year design storm occurring 4.5 years (five wet seasons) after a burn, which corresponds to a FF of 20. Chapter 12 provides a detailed analysis of the design FF.

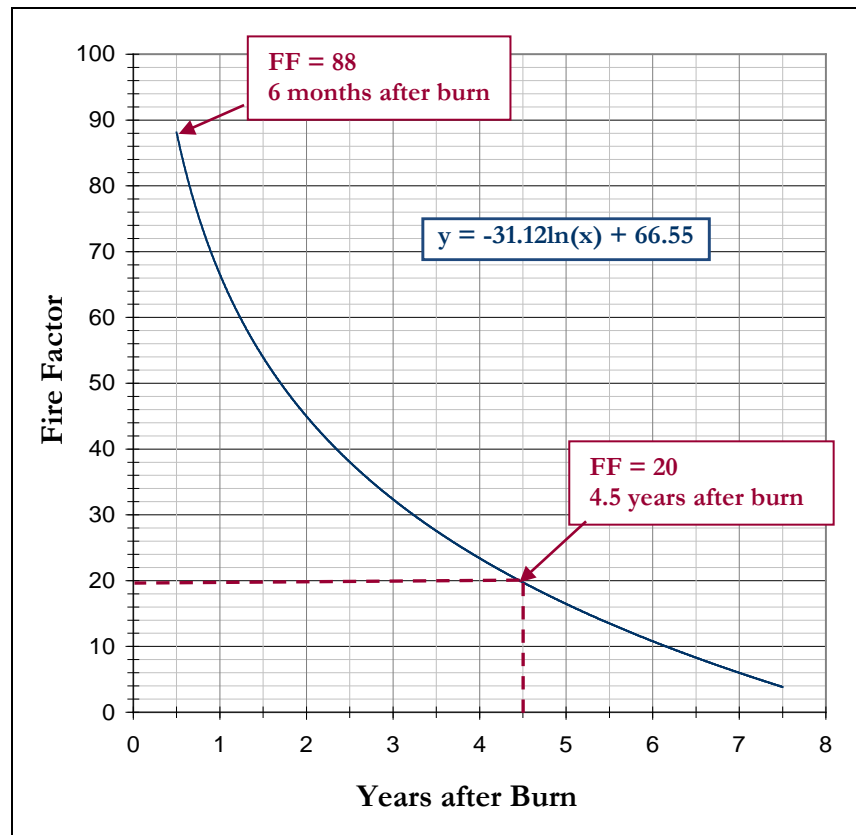


Figure 5-4. Ventura County Fire Factors vs. Years after Burn

5.3 Riverside County

The bulking factor in Riverside County is determined by estimating sediment/debris yield for a single event and comparing it to the largest expected sediment yield for a one square-mile watershed based on Los Angeles County procedures. The 120,000 yd³/mi² (74.4 acre-ft/mi²) sediment yield, which is based on the debris production curve for Los Angeles County DPA Zone 1, is assumed to correspond to the largest expected bulking factor of 2.0. As described in the *Riverside County Hydrology Manual* (Riverside County, 1978), the peak bulking rate is computed as follows:

$$BF = 1 + \frac{D}{120,000} \tag{5.5}$$

where *BF* is the bulking factor and *D* is the design storm sediment/debris production rate for the study watershed (yd³/mi²).

A comparison of the Riverside County bulking factor curve versus the current Ventura County bulking factor curve is provided as Figure 5-5. This figure shows that the Ventura County curve gives a higher bulking factor than the Riverside County curve, especially for lower debris production rates. For example, the bulking factor at 10,000 yd³/mi² is approximately 1.47 for Ventura County vs. 1.08 for Riverside County; using the Ventura County curve rather than the Riverside County curve would result in a nearly 40 percent larger bulked discharge for design purposes. The two bulking factors (47% vs. 8%) also represent the difference between a debris flow (40 to 55%) and normal streamflow (0 to 20%).

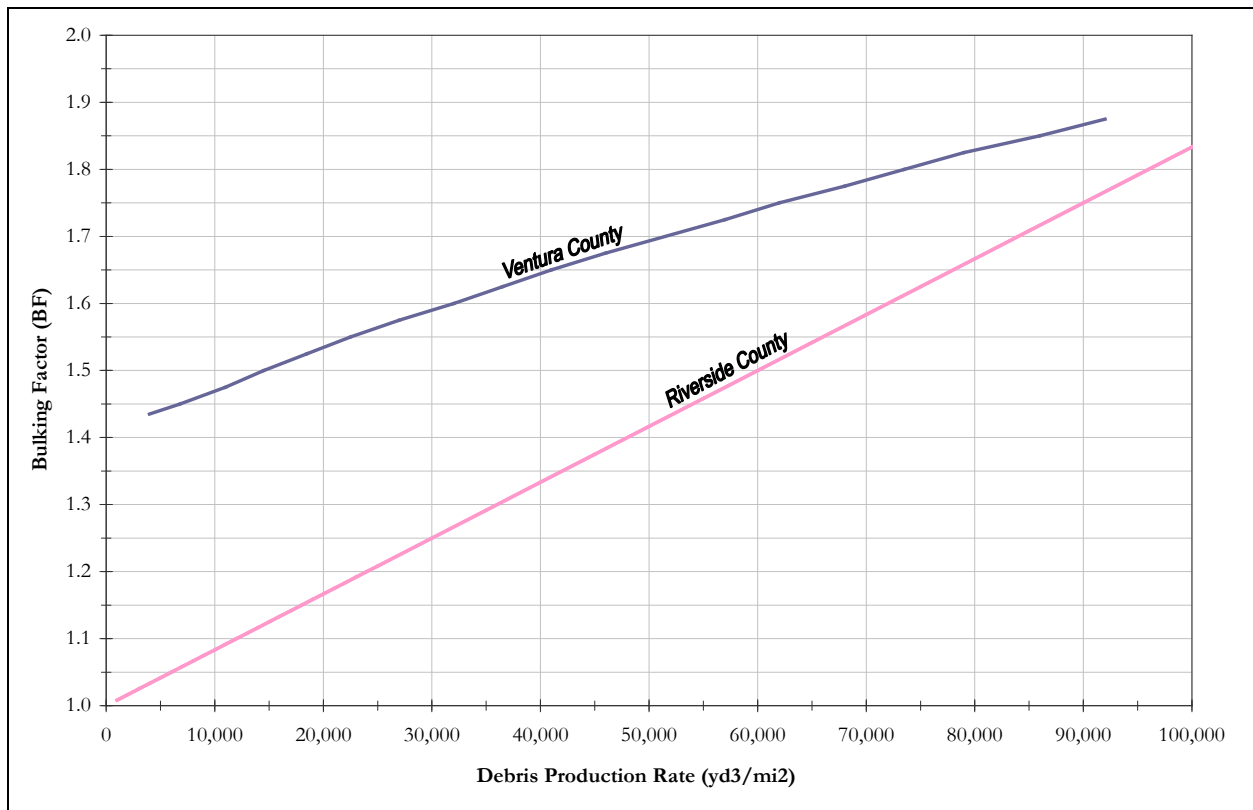


Figure 5-5. Riverside County and Ventura County Bulking Factor Curves

5.4 San Bernardino County

Some jurisdictions use a set value for bulking without conducting a detailed analysis for an individual watershed. The San Bernardino Flood Control District specifies a set bulking factor of 2 (i.e., 100% bulking) for any project where bulking of flows is anticipated. A bulking factor of 2 is equivalent to 50-percent sediment concentration by volume, which is in the upper concentration range for debris flows (40 to 55 percent concentration by volume). Above approximately 55 percent concentration by volume would generally be considered a landslide rather than a debris flow (see Table 3-2).

5.5 Orange County

Orange County does not have a specific method for bulking. Instead, a general freeboard (2 feet in most cases) must be added to computed flood elevations in order to account for bulking as well as variations in Manning's n , stage-discharge relationship, velocity, sedimentation, and air entrainment (Orange County, 2000).

5.6 San Diego County

San Diego County does not have a set method for bulking, although a value between 1.5 and 2.0 has been selected on previous projects (Jim Zhou, personal communication, January 6, 2008). According to Mr. Zhou, the need for a standard bulking method has been acknowledged and may be included in a future update to the San Diego County Hydrology Manual.

5.7 U.S. Army Corps of Engineers – Los Angeles District Method

The Los Angeles District method (USACE, 2000a) was developed to estimate unit sediment/debris yield values for “n-year” flood events for the design and analysis of debris-catching structures in coastal Southern California watersheds, considering the coincident frequency of wildfire and flood magnitude.

The method is applicable to watersheds with an area of 0.1 to 200 mi², and for watersheds with a high proportion of their total area in steep, mountainous terrain. The best results will be obtained for watersheds that have undergone significant antecedent rainfall. In most cases, this antecedent rainfall condition will be satisfied when the watershed has received at least two inches of prior rainfall in approximately 48 hours.

5.7.1 Debris Yield Equations

The Los Angeles District method specifies several equations to estimate unit debris yield depending on the size of the watershed. These equations were developed by multiple regression analysis on sediment/debris data. As an example, for watersheds from 3 mi² to 10 mi² in area, the following predictive equation is used:

$$\log Dy = 0.85 \log Q + 0.53 \log RR + 0.04 \log A + 0.22FF \quad (5.6)$$

where:

D_y is the unit debris yield (yd^3/mi^2).

RR is the relief ratio (ft/mi) – difference in elevation between highest and lowest points on the longest watercourse divided by the length of the longest watercourse.

A is the drainage area (acres).

FF is the non-dimensional fire factor.

Q is the unit peak runoff (cfs/mi^2).

5.7.2 Fire Factor

The non-dimensional FF accounts for an increase in debris yield due to fire in the watershed. This factor varies between 3.0 and 6.5, with a higher factor indicating a more recent fire and higher debris yield. The lowest FF of 3.0 represents a small watershed (basin area $< 3.0 \text{ mi}^2$) without fire for 10 years, as well as 15 years without fire in a relatively large watershed (basin area $\geq 3.0 \text{ mi}^2$). Desert watersheds that have minimal wildfire potential are also assigned a FF equal to 3.0. The Los Angeles District method includes a graph of the fire factor with drainage area and years after fire. The fire factor curves for the Los Angeles District method are presented in Figure 5-6 and Figure 5-7. The curves were graphed on log-log paper to show years since a complete burn versus fire factor (Figure 5-6) and years since a complete burn versus the drainage area (Figure 5-7).

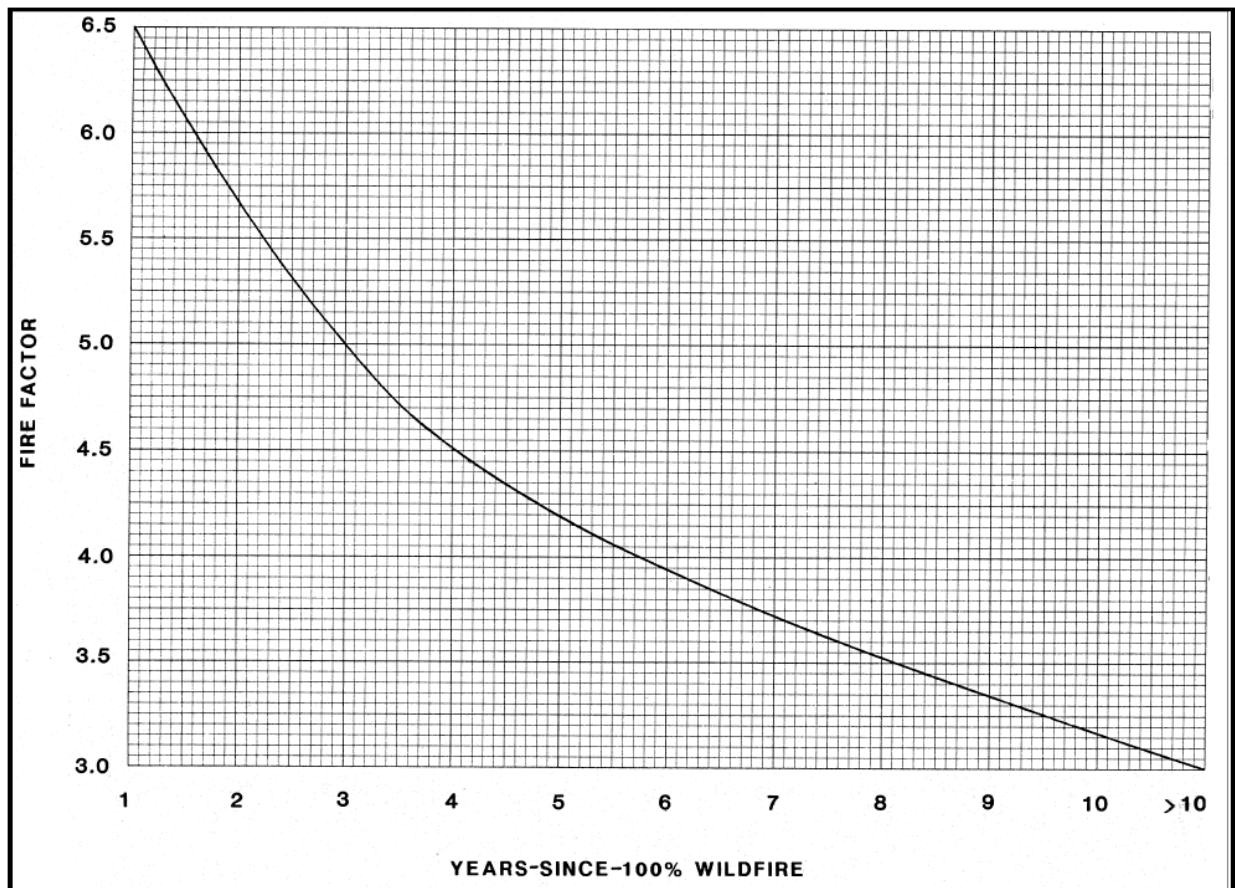


Figure 5-6. Fire Factor Curve for Watersheds 0.2 to 3.0 mi^2 (USACE, 2000a)

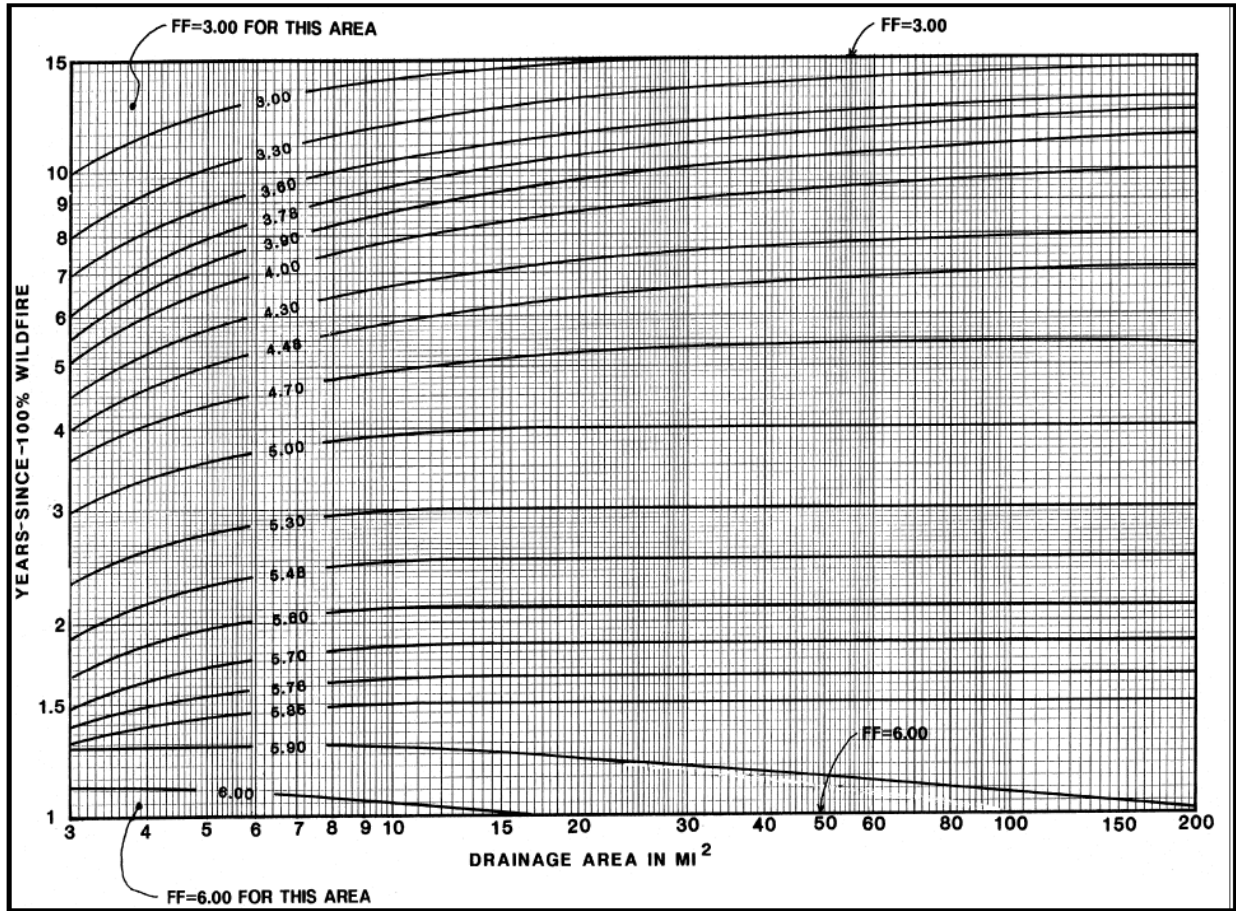


Figure 5-7. Fire Factor Curves for Watersheds 3.0 to 200 mi² (USACE, 2000a)

5.7.3 Adjustment and Transposition Factor

An Adjustment and Transposition (A-T) factor is applied to debris yield estimates to transpose the debris yield from the San Gabriel Mountains (from which the data were taken to develop the regression equations) to the study watershed. Areas with less debris yield potential than the San Gabriel Mountains would have A-T factors less than 1.0. Four techniques are available to estimate this factor, depending on the level of data available (see USACE, 2000a).

Outside of the area from which the data were collected and used to develop the method (San Gabriel Mountains), the A-T factor must be carefully applied. Using this method for watersheds with a high percentage of alluvial fan or valley fill areas may result in yield estimates higher than would actually be produced by the watershed.

5.8 FEMA Post-burn Bulking (2003b)

As part of FEMA's effort to assess the 2003 post-fire flood hazards, a number of flooding sources throughout San Diego, San Bernardino, Riverside, Ventura, and Los Angeles Counties were identified for analysis. Based upon past experience and engineering judgment, FEMA (2003b) used the bulking factors shown in Table 5-1 for their rapid post-fire assessment. The maximum bulking

factor is 1.5. Two key points from this table are (1) bulking factor decreases as the drainage area increases, and (2) bulking factor decreases as the recurrence interval increases (from a 5-year to 100-year recurrence interval, in this case).

Table 5-1. Post-fire Bulking Factors used for 2003 Southern California Fires (FEMA, 2003b)

Area (mi ²)	Sediment Bulking Factor	
	5-yr Storm Event	100-yr Storm Event
0-3	1.5	1.4
3-10	1.3	1.2
Above 10	1.2	1.1

The factors decrease for the 100-year storm due to the fact that the high volume of runoff at this storm level is thought to dilute the sediment and result in a smaller bulking factor. The recommended increase in bulking due to both factors in their study is given by the following equation:

$$Q_{\text{final peak}} = Q_{\text{pre-burn}} \times \text{Clear-water Adjustment Factor} \times \text{Bulking Adjustment Factor} \quad (5.7)$$

Therefore, the 100-year peak discharge can increase by a factor of 3.8 to 2.9 for small to large watersheds subject to severe burns.

5.9 Interagency BAER Team

In their post-fire assessment of the Pines Fire, the Interagency Burned Area Emergency Response (BAER) Team (2002) describes their method for determining the bulked discharge.

The bulked discharge, Q_B , is defined as:

$$Q_B = Q_{\text{pre-fire}} + Q_{\text{pre-fire}}(\% \text{HighBurn} * 0.7 + \% \text{ModerateBurn} * 0.5 + \% \text{LowBurn} * 0.2) \quad (5.8)$$

where $Q_{\text{pre-fire}}$ is the peak discharge before the burn, %HighBurn is the percentage of the watershed with high soil burn severity, %ModerateBurn is the percentage of the watershed with moderate soil burn severity, and %LowBurn is the percentage of the watershed with low soil burn severity, all entered as fractions in the equation above (e.g., 0.25 instead of 25%). Note: These three soil burn severity percentages may not necessarily add up to 1 (or 100%) because a portion of the watershed may have been left unburned. Conversion of Equation 6.8 to a bulking factor yields:

$$BF = 1 + \% \text{HighBurn} * 0.7 + \% \text{ModerateBurn} * 0.5 + \% \text{LowBurn} * 0.2 \quad (5.9)$$

The maximum bulking factor that can be obtained using this equation is 1.7, which occurs when the entire watershed has a high soil burn severity. Equation 6.9 may have less application for design purposes because it is intended for use immediately after a fire occurs.

5.10 Advantages and Disadvantages of Methods

The advantages and disadvantages of the agency bulking methods are summarized in Table 5-2

Table 5-2. Agency Bulking Method Advantages and Disadvantages

Agency	Advantages (for Ventura County)	Disadvantages (for Ventura County)
Los Angeles County	Detailed method that enables watershed-specific analysis	Maps, parameters tailored for Los Angeles County
Ventura County	Simplified method for computing BF (after debris production rate is computed)	May be overly conservative for design of infrastructure
Riverside County	Simplified method for computing BF (after debris production rate is computed)	May not be conservative enough for Ventura County
San Bernardino County	Default method is simple (use BF = 2) and requires no estimation of debris production	May be overly conservative for design of infrastructure Every debris-producing watershed is treated the same BF = 2 represents debris flow conditions that are beyond what should be modeled with a standard hydraulic model such as HEC-RAS
Orange County		Sediment/debris bulking is not treated separately; general freeboard is used instead
San Diego County		No consistent methodology
Corps of Engineers, Los Angeles District	Based on comprehensive study	Uncertainty in applying outside of San Gabriel Mountains
FEMA Post-fire Assessment	Very easy to use for post-fire conditions (emergency-type analysis)	Not intended for design projects
Interagency BAER (Burned Area Emergency Response) Team	Easy to use for post-fire conditions (if detailed burn maps are available)	Not intended for design projects

6 SEDIMENT ANALYSIS AND REVISED BF CURVE

A number of different analyses were performed to determine the most appropriate bulking factors for Ventura County watersheds, including:

- (1) Evaluating sediment sampling data for five recording stations in the County and estimating the maximum bulking factor and range of values for each station and all stations combined.
- (2) Calculating the sediment transport capacity for selected stream reaches and the corresponding peak bulking factor.
- (3) Comparing bulking factors calculated using the current VCWPD bulking factor curve (Figure 5-3) to those computed directly based on SCOTSED debris yields and flow hydrographs for several Ventura County watersheds.

6.1 Sediment Gage Data Evaluation

WEST selected five suspended sediment and USGS flow sampling stations in Ventura County with a sufficient length of daily records (minimum ten years) in order to estimate bulking factors for the period of record. The five stations are listed in Table 6-1. Because both the flow and sediment data are average daily values, peak values are not included in the records.

As shown in Table 6-1, estimated maximum bulking factors for the stations range from 1.01 (for the Ventura River) to 1.04 (for the Santa Clara River at Montalvo) for recorded flow values up to approximately a 10-year event. Figure 6-1 presents the calculated bulking factor versus average daily flow for the Santa Clara River at Montalvo.

Table 6-1. Selected USGS Sediment Sampling Stations in Ventura County and Computed Bulking Factors

VCWPD Zone	USGS Station Number	Station Name	Basin Area (mi ²)	Start Date	End Date	Maximum Bulking Factor
1	11118500	Ventura River Near Ventura	188	1-Oct-68	30-Sep-86*	1.01
2	11108500	Santa Clara River A Los Angeles-Ventura CO Line	625	1-Oct-68	30-Sep-78	1.02
2	11114000	Santa Clara River at Montalvo	1594	1-Oct-67	30-Sep-85*	1.04
3	11105850	Arroyo Simi Near Simi	70.6	1-Oct-68	30-Sep-78	1.02
3	11106550	Calleguas Creek Above Camarillo State Hospital	248	1-Oct-68	30-Sep-78	1.02

*Record is not continuous.

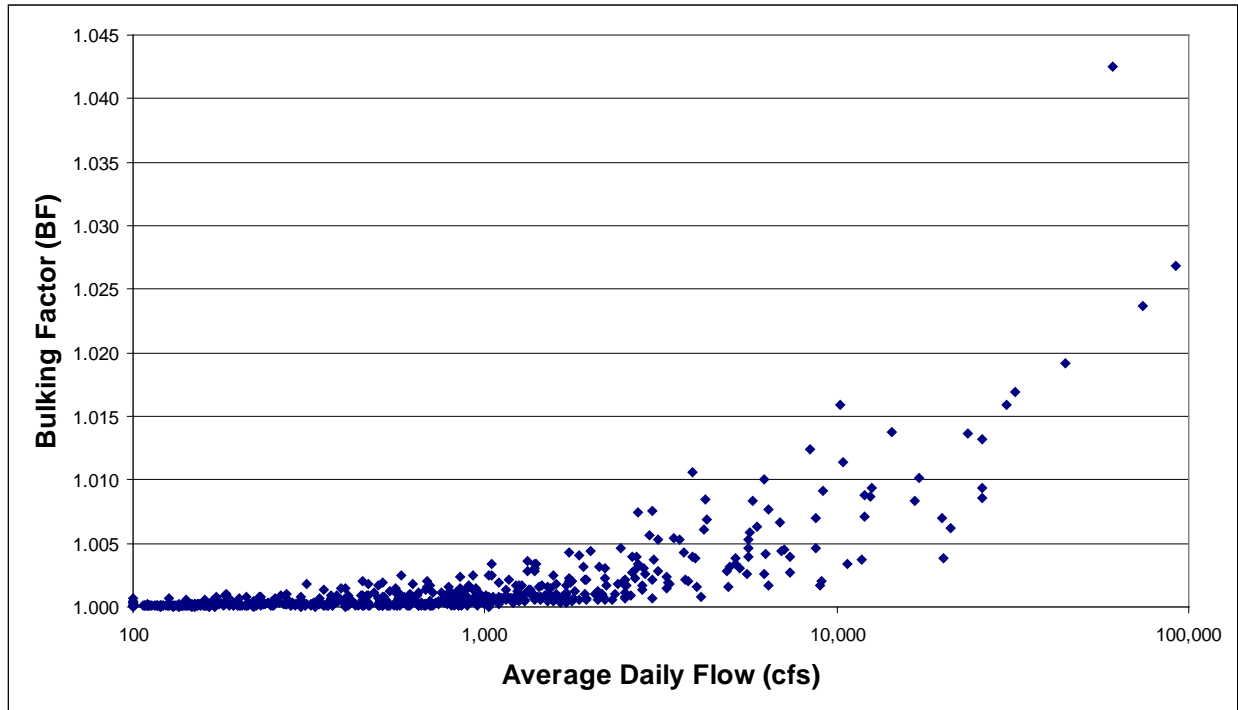


Figure 6-1. Bulking Factor vs. Average Daily Flow – Santa Clara River at Montalvo

The computed bulking factors are expected to be approximately 1 to 5 percent less by volume compared to the actual channel flood sediment bulking. This is primarily due to problems with the suspended sediment data collected at the five USGS stations. The data collected at the stations include virtually the entire wash load and a portion of the bed-material load (MacArthur et al., 2008). The problem with this is that suspended-sediment data does not include bedload. In order to separate the bedload from the data, this must be measured. However, bedload is a challenge to measure in the field. Even where a bedload sampler has been used, there may be a portion of the total sediment load that cannot be collected by either the suspended sediment or the bedload samplers for several reasons, including small particles passing through the bedload sampler, and/or particles too large to enter the bedload nozzle. Therefore, data from suspended sediment and bed-material load samplers may not equal the sum of the bed material plus wash load (Diplas et al., 2008). For these reasons, the computed values may be an underestimate of the actual sediment bulking. Even if the bulking results in Table 6-1 are a few percent too low, they are still consistent with the findings of O’Brien (2006), who noted that river flood sediment bulking rarely exceeds 5 percent by volume.

One could argue that bulking is not required when performing hydraulic modeling of a large mainstem river using a model such as HEC-RAS. This is because the small sediment concentration does not necessarily need to be accounted for if the sediment interaction with the river bed is not being modeled (which it would not be in a fixed bed, standard hydraulic model in HEC-RAS). However, a bulking factor up to 1.1 (which includes suspended and bedload) could be used, if desired. Note that this bulking factor would not apply if the peak discharge was computed based on streamflow gage data, as discussed below.

6.2 Streamflow Gages and Flow Bulking

According to Charles Parrett, hydrologist at the USGS California Water Science Center, streamflow discharge data collected and published by the USGS represent the flow of the “complete sediment-water mixture,” and USGS makes “no attempt to distinguish the sediment mass from the water mass” when calculating the stream discharge (personal communication, November 21, 2008). Mr. Parrett described USGS streamgage data reporting under debris-flow conditions and the effects on bulking, as follows:

... for some peak-flow events, the mixture may be so heavily sediment-laden that the hydraulic characteristics of water flow are no longer applicable. In those “debris-flow” situations, we do not publish a streamflow peak discharge, but will publish a gage height when available. Sometimes it is difficult to distinguish a debris flow from a heavily sediment-laden water flow, and we may publish a streamflow peak in our *Annual Data Report* with a remark that the event may have been a debris flow. In any case, our published peak discharges are presumed to be water flows that may be significantly bulked by sediment, and results of flood frequency-analyses computed using our data also can be considered to be “bulked” as well.

It should be noted that significant debris-laden flow occurring upstream of a stream gage may damage or destroy the gage, and these events may not be in the data record. However, most published gage heights and peak discharges can be assumed to already include flow bulking.

6.3 Sediment Transport Capacity Analysis

The sediment transport potential for five different watersheds (including Adams Barranca, Fox Barranca, Warring Canyon, Aliso Canyon/Ellsworth Barranca, and Hopper Canyon) was evaluated for both the 10-year and the 100-year peak flows using the sediment transport capacity option in the HEC-RAS hydraulic model.

6.3.1 Sediment Transport Capacity Results

Prior to the current study, WEST developed HEC-RAS models of the streams contributing to the Adams, Fox, and Warring debris basins for the *Ventura County Debris Basins Sedimentation Analysis* project (WEST, 2007). The VCWPD provided debris yield, peak flows, peak hydrographs, and sediment gradation curves, as well as hydraulic models of Aliso Canyon and Hopper Creek.

For each stream, WEST selected a reach in the upstream portion of the model and developed a flow versus sediment transport capacity relation for flow values up to the maximum peak flow using the Yang sediment transport function. This function was deemed the most appropriate considering the streambed composition (sand and gravel). WEST assigned each flow value in the 10-year and 100-yr flow hydrograph the corresponding sediment transport capacity and calculated the incremental sediment load for each time step, obtaining the total sediment transport potential for the selected storm event by summing the intermediate sediment loads. The bulking factor for each time step was obtained by dividing the incremental sediment load by the incremental flow volume. The maximum bulking factor for each stream and each storm event, the total potential sediment yield and the sediment yields for burned and unburned conditions estimated by the VCWPD’s debris production program SCOTSED (see Section 5.2) are presented in Table 6-2 and Table 6-3.

With the exception of Aliso Canyon, for which the 100-year computed peak bulking factor based on sediment transport capacity is 1.58, all the other bulking factors estimates are between 1.03 and 1.15. The results do not show a significant difference between the 10-year and the 100-year bulking factors for the same reaches.

Table 6-2. Sediment Transport Capacity Results – 10-year Flood Event.

Basin	Sediment Yield SCOTSED <i>Unburned</i>	Sediment Yield SCOTSED <i>Burned</i>	Computed Potential Load	Computed Peak BF	Velocity Range
	(yd ³)	(yd ³)	(yd ³)		(ft/s)
Adams Barranca	33,932	70,608	64,374	1.04	7.7 to 11.2
Aliso Canyon	101,558	147,306	238,617	1.15	7.6 to 11.0
Fox Barranca	1,405	29,227	17,116	1.03	7.2 to 11.7
Hopper Canyon	131,563	353,982	95,680	1.03	9.2 to 11.1
Warring Canyon	8,949	18,621	22,941	1.10	6.4 to 8.0

Table 6-3. Sediment Transport Capacity Results – 100-year Flood Event.

Basin	Sediment Yield SCOTSED <i>Unburned</i>	Sediment Yield SCOTSED <i>Burned</i>	Computed Potential Load	Computed Peak BF	Velocity Range
	(yd ³)	(yd ³)	(yd ³)		(ft/s)
Adams Barranca	99,913	207,904	130,753	1.04	9.0 to 12.5
Aliso Canyon	302,364	438,568	2,153,911	1.58	10.6 to 14.8
Fox Barranca	43,283	90,065	50,252	1.04	6.8 to 13.6
Hopper Canyon	435,958	1,172,980	346,487	1.03	14.4 to 19.1
Warring Canyon	26,535	55,215	48,746	1.10	8.5 to 11.0

The Aliso Canyon results in Table 6-3 are believed to be higher because the Aliso reach experiences deeper flow than similar reaches that were analyzed. Because shear stress increases with flow depth, Aliso Canyon has a greater capacity to transport sediment based on the standard sediment transport equations.

6.3.2 Limitations of Analysis

While the bulking factors computed based on sediment transport seem to indicate that these channels cannot transport the SCOTSED computed debris production, the bulking factor results have to be used with significant caution for a number of reasons. First, and most importantly, the sediment transport equations were generally not developed to handle hyperconcentrated, let alone

debris, flows. As streamflow becomes more concentrated with increasing sediment content, viscous and dispersive stress effects dominate, which constitute a very different phenomenon than the processes of suspended and bed sediment load in conventional sediment transport (O'Brien, 2006). Therefore, different sets of equations more accurately simulate mud or debris flow events and great caution must be used when applying the "clear water" sediment transport equations to debris or hyperconcentrated flow events.

In addition, all sediment transport functions were developed under different conditions and are valid within a certain range of input values, which include sediment size and concentration, channel depth, flow velocity, energy gradient, channel width, and water temperature (Waterways Experiment Station, 1998; USACE, 2010). For example, the Yang transport equation applies to an average channel velocity between 0.8 ft/s and 6.4 ft/s (USACE, 2010). The computed flow velocities for the channels studied are above the maximum limits of applicability.

6.4 Computed Bulking Factor Comparison

Bulking factors for eight Ventura County watersheds (Table 6-4) were computed using the following two methods:

- (1) VCWPD bulking factor curve included in the SCOTSED program
- (2) Vanoni (2006) method used by Los Angeles County to distribute the SCOTSED computed debris yield throughout the flow hydrograph (see Section 5.1.3).

Bulked and unbulked flow hydrograph results using exponent (n) values of 2 and 3 were compared as shown in Figure 6-2. From the comparison, an n value of 3 was selected for the current study analysis for a more conservative design (i.e., a higher bulking factor).

Comparisons of the computed bulking factors for a 100% burned basin 6 months after a fire ($FF = 88$) and 4.5 years after a fire ($FF = 20$) are provided in Table 6-5 and Table 6-6, respectively. These bulking factors were computed for the 10-, 50-, and 100-year return periods. For the most part, the peak bulking factors from the current VCWPD bulking factor curve are notably higher than the revised bulking factors computed based on the debris yield distributed through the flow hydrograph.

For example, SCOTSED computed a $BF = 1.47$ for Adams Barranca using the 10-year return interval and a $FF = 20$, while the peak computed BF using the SCOTSED sediment yield value and flow hydrograph is 1.12. This may support the assumption that the current Ventura County curve includes not only sediment bulking, but also increased post-fire hydrology to some extent.

Presented in the next section are the proposed revised bulking factor curves for Ventura County.

Table 6-4. Watersheds Used in Fire Factor Analysis (see Figure 6-3 for map locations)

Zone	Watershed	Drainage Area (mi ²)
1	Fresno Canyon	1.4
2	Adams Barranca	8.4
	Aliso Canyon	14.4
	Hopper Canyon	23.9
	Warring Canyon	1.1
3	Fox Barranca	4.9
	Honda West	1.2
	Santa Rosa Basin	1.6

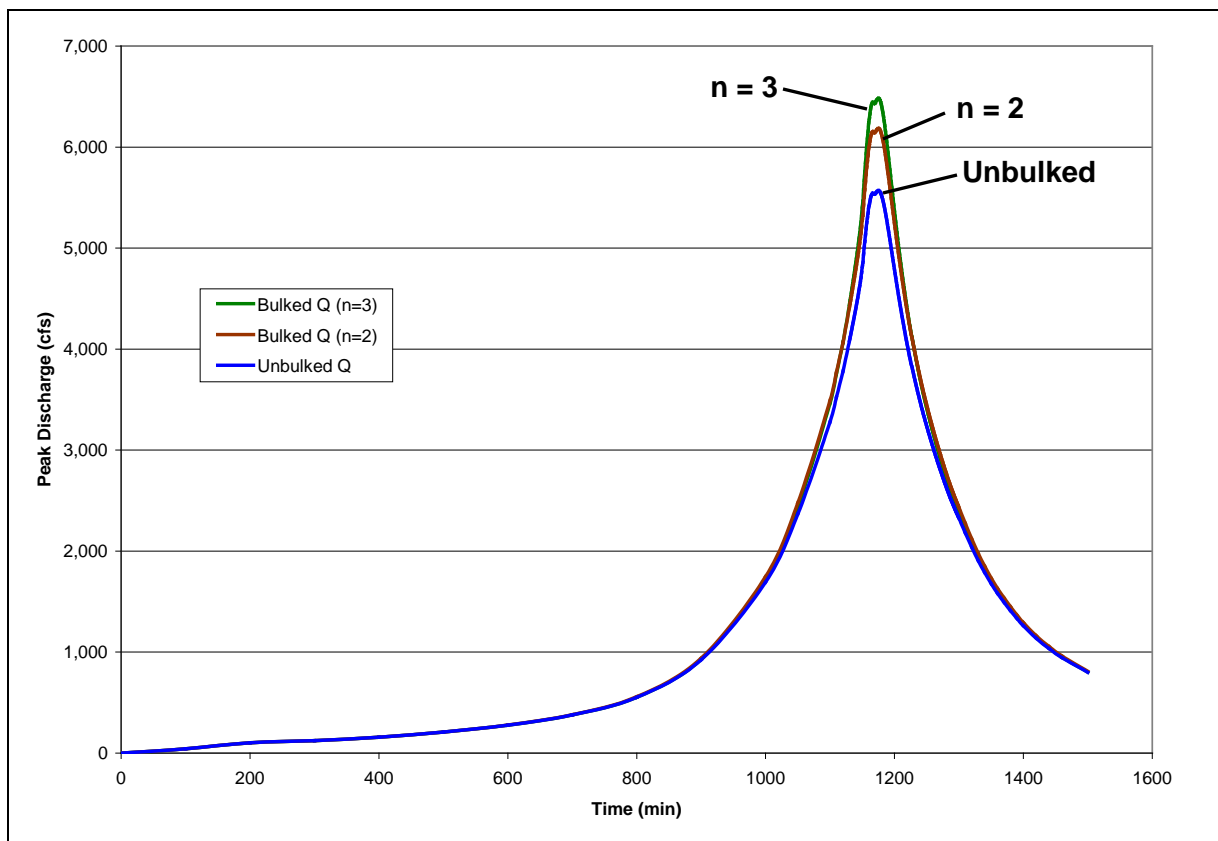


Figure 6-2. Bulked and Unbulked Hydrographs – Adams Barranca

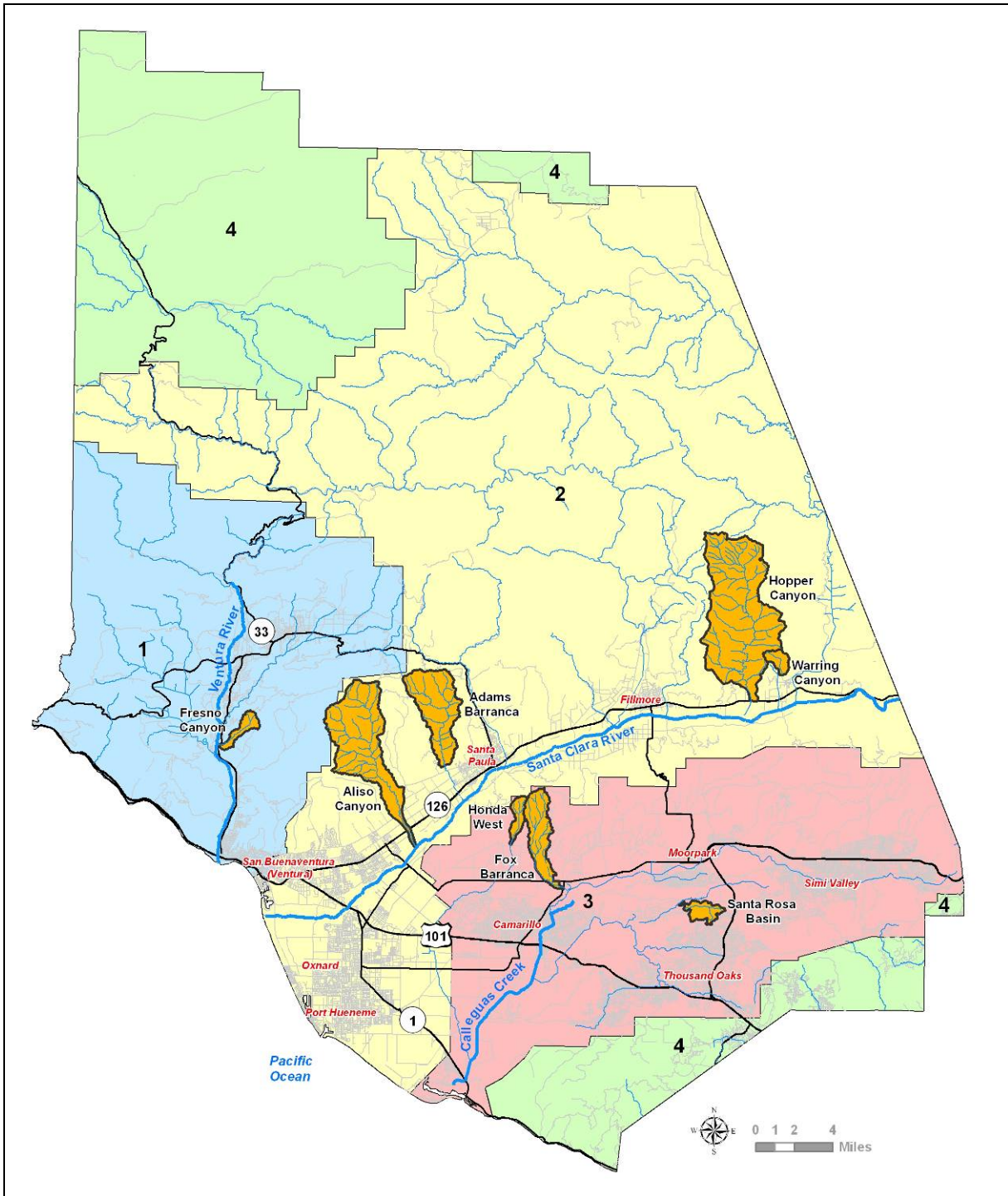


Figure 6-3. Watersheds used in Bulking Factor Evaluation (with VCWPD Zones)

Table 6-5. Bulking Factor Comparison for FF = 20

Basin	Return Interval	Peak Flow	SCOTSED <i>Post-Fire</i>		Peak BF - SCOTSED	Peak BF - Sediment Yield & Flow Hydrograph <i>n</i> = 3
			Sediment Yield	Production Rate		
	(years)	(cfs)	(yd ³)	(yd ³ /mi ²)		
Adams Barranca	10	3,097	71,973	8,644	1.47	1.12
	50	4,593	161,650	19,415	1.53	1.14
	100	5,567	211,923	25,453	1.56	1.17
Aliso Canyon	10	3,287	101,558	8,933	1.47	1.14
	50	9,391	230,810	20,301	1.53	1.12
	100	12,960	302,364	26,595	1.57	1.11
Fox Barranca	10	1,480	29,792	6,118	1.45	1.12
	50	2,318	70,201	14,416	1.5	1.16
	100	2,760	91,806	18,853	1.52	1.16
Fresno Canyon	10	583	11,450	8,365	1.46	1.30
	50	1,166	26,676	19,488	1.53	1.35
	100	1,610	35,255	25,756	1.56	1.34
Honda Barranca	10	581	11,218	9,102	1.47	1.21
	50	874	24,491	19,871	1.53	1.26
	100	1,038	32,031	25,989	1.57	1.29
Hopper Creek	10	4,251	279,057	11,670	1.48	1.17
	50	12,145	654,558	27,373	1.57	1.14
	100	16,796	924,705	38,671	1.63	1.14
Santa Rosa Basin	10	589	3,727	2,355	1.43	1.06
	50	927	7,997	5,053	1.44	1.08
	100	1,234	10,490	6,629	1.45	1.10
Warring Canyon	10	338	8,949	18,981	1.52	1.24
	50	602	20,270	42,994	1.64	1.33
	100	1,217	26,535	56,283	1.7	1.49

Table 6-6. Bulking Factor Comparison for FF = 88

Basin	Return Interval	Peak Flow	SCOTSED <i>Post-Fire</i>		Peak BF - SCOTSED	Peak BF - Sediment Yield & Flow Hydrograph <i>n = 3</i>
	(years)		(cfs)	Sediment Yield		
			(yd ³)	(yd ³ /mi ²)		
Adams Barranca	10	3,097	104,394	12,538	1.49	1.18
	50	4,593	234,468	28,160	1.58	1.21
	100	5,567	307,387	39,918	1.62	1.24
Aliso Canyon	10	3,287	147,306	12,956	1.49	1.21
	50	9,391	334,781	29,446	1.58	1.17
	100	12,960	435,568	38,575	1.63	1.16
Fox Barranca	10	1,480	43,212	8,874	1.47	1.17
	50	2,318	101,824	20,910	1.54	1.24
	100	2,760	133,162	27,345	1.57	1.23
Fresno Canyon	10	583	17,495	13,041	1.49	1.46
	50	1166	40,759	30,383	1.59	1.54
	100	1,610	53,868	40,154	1.64	1.52
Honda Barranca	10	581	16,271	13,202	1.49	1.31
	50	874	35,524	28,823	1.58	1.38
	100	1,038	46,460	37,696	1.63	1.42
Hopper Creek	10	4,251	404,762	16,927	1.51	1.24
	50	12,145	949,412	39,704	1.64	1.20
	100	16,760	1,341,250	56,090	1.72	1.20
Santa Rosa Basin	10	589	5,405	3,416	1.43	1.09
	50	927	11,599	7,329	1.46	1.12
	100	1,234	15,216	9,614	1.47	1.14
Warring Canyon	10	338	27,531	25,550	1.56	1.35
	50	602	62,361	57,874	1.73	1.48
	100	1,217	81,636	75,762	1.81	1.71

6.5 Proposed Bulking Factor Curves

Figure 6-4 and Figure 6-5 show the results of the “distributed” bulking factor versus debris production rate for the eight watersheds with the use of a FF = 20 (design) and FF = 88 (emergency projects), respectively. The current and proposed bulking factor curves are shown, with the bulking factors applicable to undeveloped areas. The proposed curves envelope the data for design purposes.

An evaluation of bulking factor results for the eight study watersheds revealed no clear patterns between the VCWPD zone (1, 2, or 3) and bulking factor. The same is true for the recurrence interval and bulking factor. However, there was a distinct pattern in terms of watershed area and bulking factor. Study watersheds greater than approximately 3 mi² had distinctly lower bulking factors compared to most of the watersheds less than 3 mi². All but one watershed (Santa Rosa) fit well within the basin size criterion.

We recommended providing three options for selecting a bulking factor for a particular project. The first option is to use a conservative bulking factor from those listed in Table 6-7. The benefit of this option is that no SCOTSED computations are required. Conservative bulking factors are based on the highest values on each curve.

The second option is to compute a debris production rate using SCOTSED and use the appropriate curve to determine the bulking factor. The third option is to compute a debris production rate using SCOTSED and distributing the debris volume based on the clear-water hydrograph to determine the bulking factor.

Table 6-7. Conservative Bulking Factors (Optional)

Project	Bulking Factor	
	Drainage Area ≤ 3 mi ²	Drainage Area > 3 mi ²
Design (FF = 20)	1.6	1.2
Emergency (FF = 88)	1.75	1.25

Figure 6-6 provides a comparison of the proposed design curves (FF = 20) with the current Ventura, Riverside, and Los Angeles County curves. The Los Angeles County curves were obtained by combining the bulking factor versus basin area and the bulking factor versus debris production area curves presented in Section 5.1. Figure 6-6 shows that the other county curves are considerably lower than the current Ventura curve. The proposed curve for watersheds less than or equal to 3 mi² matches more closely to the Los Angeles County curve than to the current Ventura County or Riverside County curves. In Phase I of the current study, the Riverside County curve was tentatively recommended based on limited data; however, this is no longer the case based on additional Ventura County data.

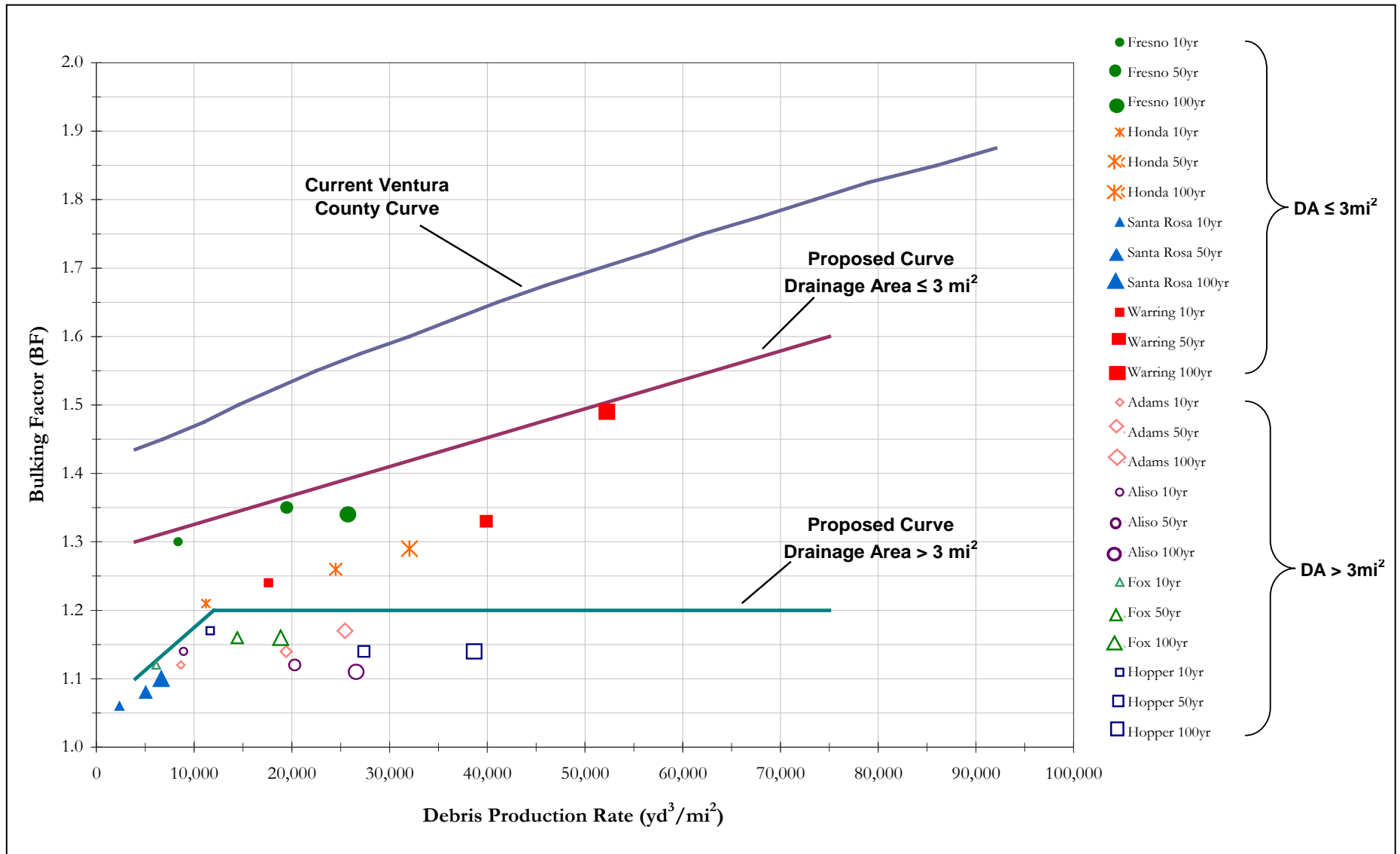


Figure 6-4. Current Bulking Factor Curve for Ventura County vs. Recommended Curves (FF = 20)

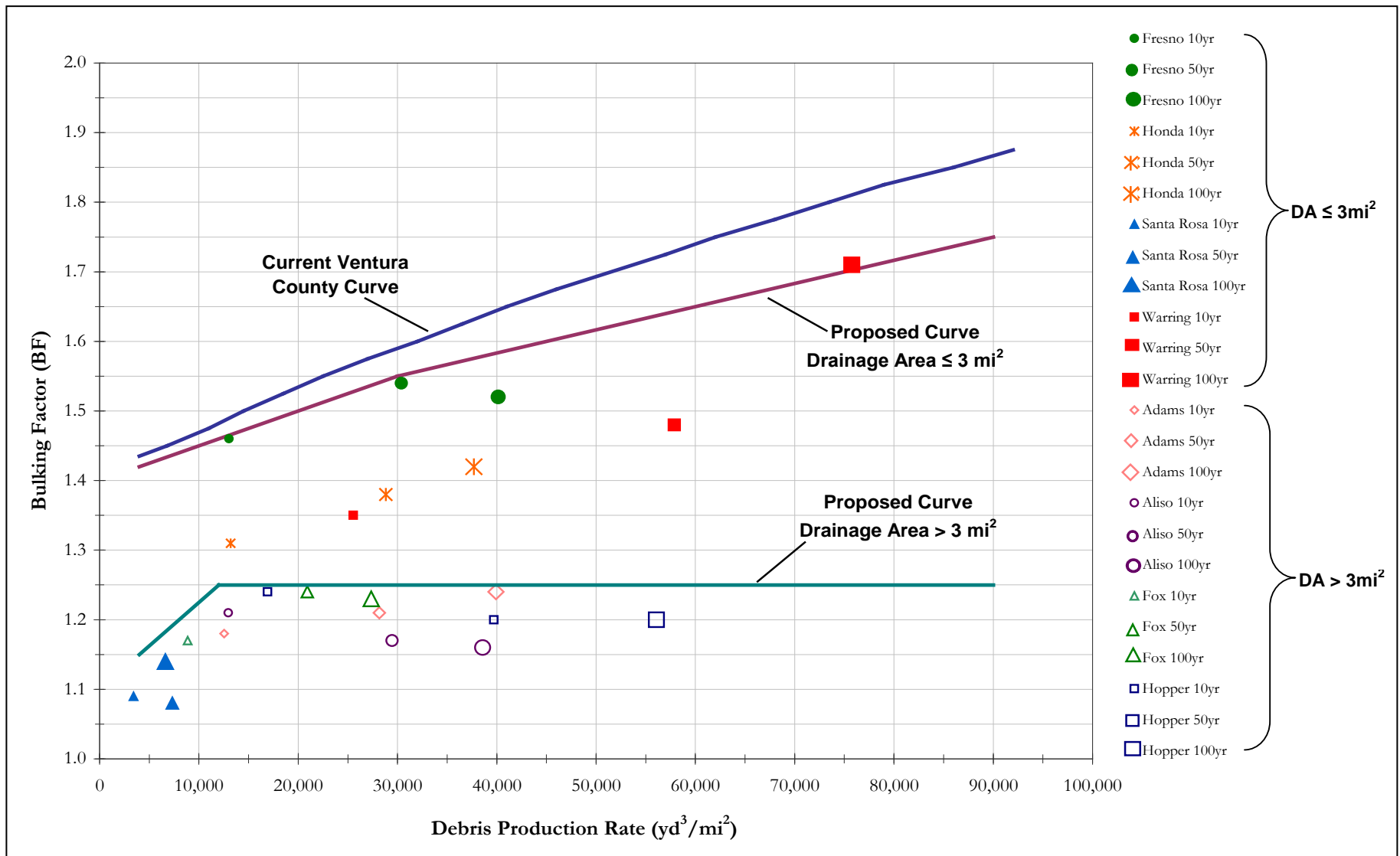


Figure 6-5. Current Bulking Factor Curve for Ventura County vs. Recommended Curves (FF = 88)

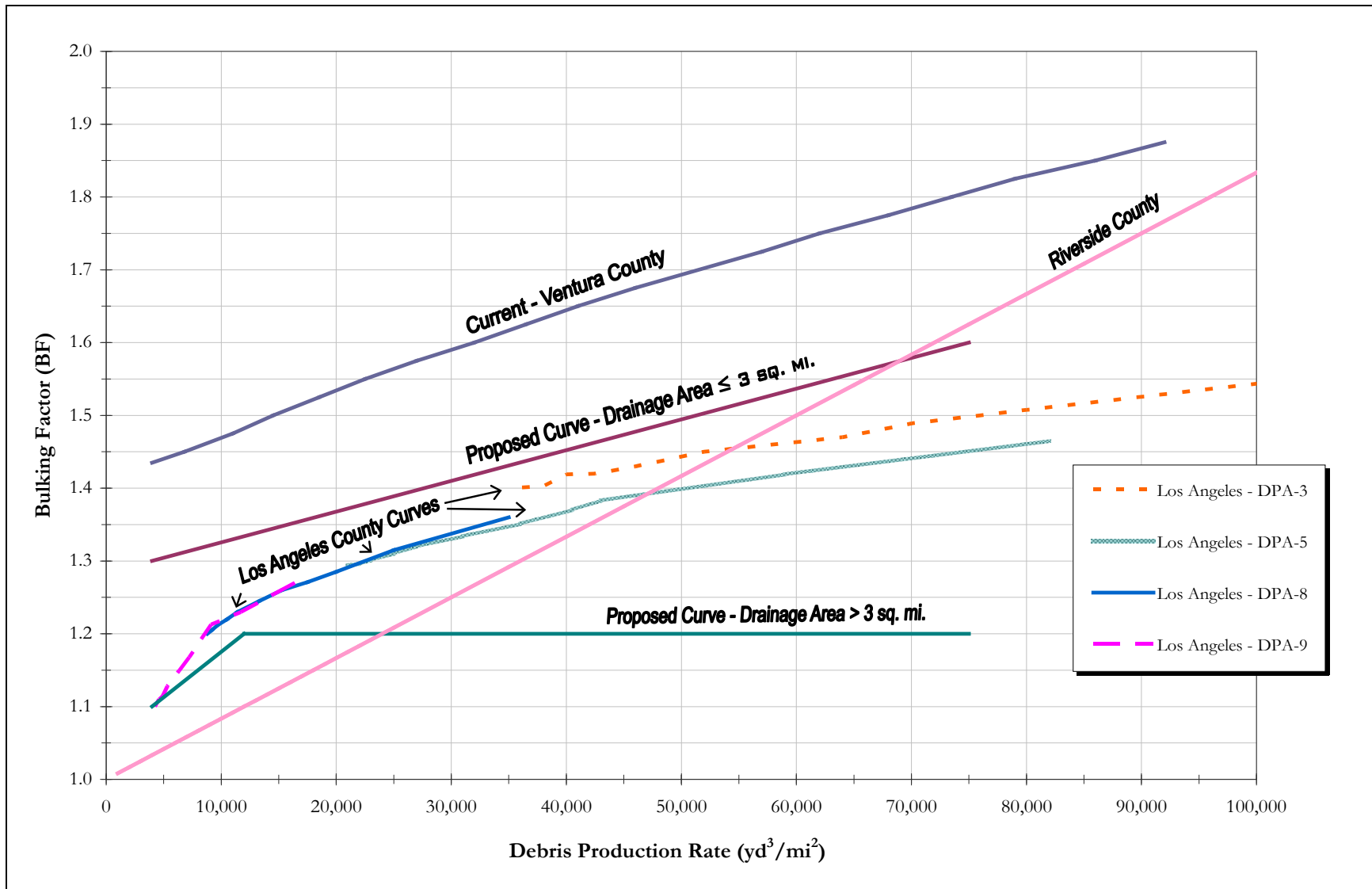


Figure 6-6. Current Local County (Ventura, Los Angeles, and Riverside) Bulking Factor Curves vs. Recommended Curves (FF = 20)

PART II. ADDITIONAL BULKING TOPICS

Concrete Channel and Bedload

Fines and Bulking

Woody Debris

7 CONCRETE CHANNELS AND BEDLOAD

This chapter investigates the question of whether concrete channel roughness (i.e., Manning's n values) should be increased to account for bedload transport (including gravel, cobbles, and boulders) along the channel bottom.

7.1 Purpose of Investigation

The VCWPD requested that this topic to be specifically addressed in the current study because of a previous investigation of the Pole Creek concrete channel, and the need to adjust the Manning's n value to account for the increase in roughness due to bedload along the channel invert. After a technical review of a FLO-2D model developed for the creek, Chang (2003) recommended increasing the channel roughness from 0.015 to 0.020 for the concrete-lined section of the channel to account for sediment loads associated with higher velocity flows. Evidence of heavy bedload through the channel is seen in damage to the concrete lining, which has resulted in exposed and damaged rebar, necessitating frequent repair.

The purpose of this analysis is to review previous studies related to concrete channels and the impact of bedload on Manning's n values and to make recommendations for concrete channels in Ventura County, including Pole Creek.

7.2 Previous Studies

Copeland et al. (2000) cite several researchers, including Swanson and Williams (1988); Williams (1990); and Copeland and Thomas (1989), who have reported cases where hydraulic roughness has increased in concrete channels due to gravel deposition/and or transport. In addition, other researchers have demonstrated that sand moving near the bed increases hydraulic roughness in rivers and flumes (McLean, 1977; Grant and Madsen, 1982; Wiberg and Rubin, 1989 *as cited in* Copeland et al., 2000). The study performed by Copeland et al. (2000) is described below, as well as additional insight from Chow (1959), Mussetter Engineering, Inc. (MEI, 2008), and a recent Flood Insurance Study (FIS) of Pole Creek (FEMA, n.d.).

7.2.1 Copeland et al. (2000)

Copeland et al. (2000) investigated the effect of bedload transport on hydraulic roughness in concrete-lined channels by conducting flume and numerical model investigations for two California streams. One of the streams—Corte Madera Creek in Marin County, California—had an existing concrete-lined flood control channel. The second stream was Mission Creek in Santa Barbara, California, for which a concrete-lined channel was proposed. Neither of the channels included a debris basin upstream, so there was potential for a significant quantity of bedload (primarily gravel, cobbles, and boulders) to be delivered during a flood event. As a result, the effect of bedload transport on the boundary roughness was a concern, especially if the roughness increased to a point at which the flow regime changed from supercritical to subcritical flow.

For Corte Madera Creek, sediment consists of coarse material ranging from 16 mm to 32 mm with varied discharges between 3,500 cfs and 6,900 cfs. The maximum Manning's roughness coefficient

measured for the flume bed was approximately 0.019 (n value adjusted for Corte Madera Creek rather than flume scale) with an equivalent creek discharge of 6,900 cfs and a bedload concentration of 3,000 ppm.

For Mission Creek, three series of flume experiments (A to C) were conducted to determine the increase in bed roughness with increasing bedload concentrations ranging between 200 ppm and 5,000 ppm. Series A represented large cobbles, Series B simulated a uniform grain size (d_{84}), and Series C simulated the gravel portion of the creek bed. The results showed that when the bedload feed rate exceeded the transport capacity of the flume, sediment began to deposit. At this point, bed roughness and bedload concentration began to vary along the length of the flume. The results of the experiment are shown in Figure 7-1.

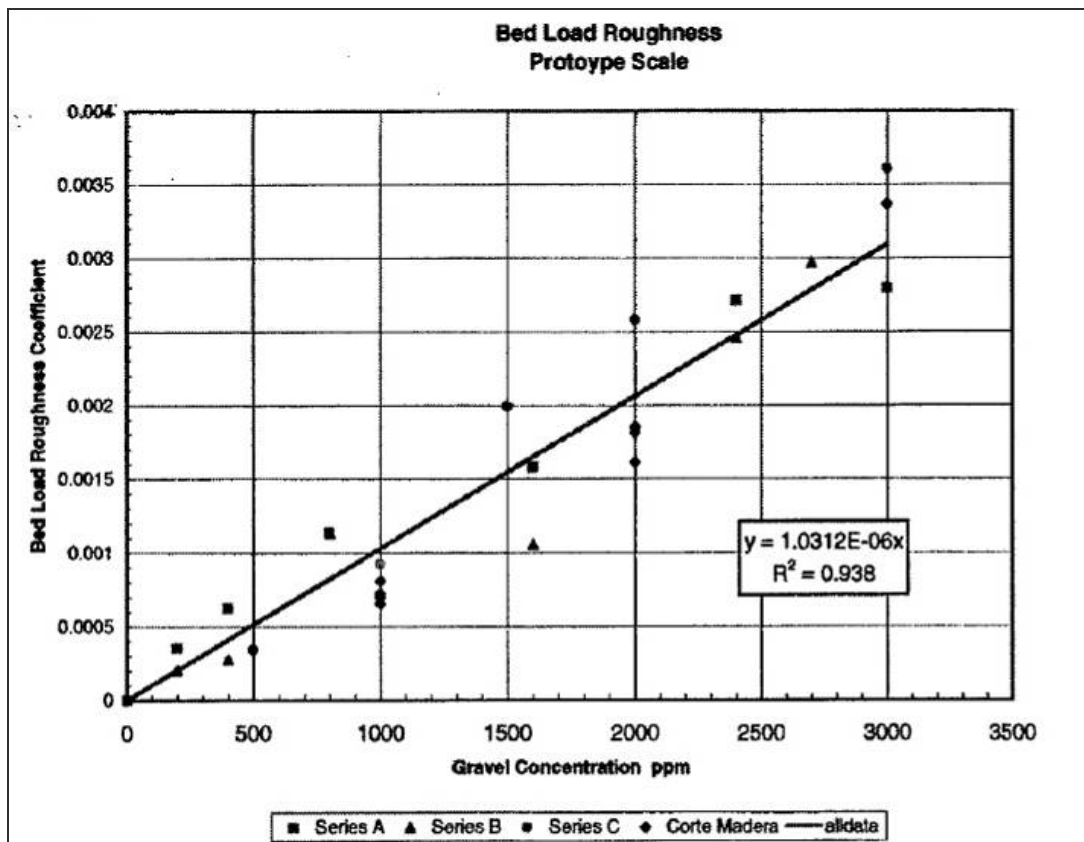


Figure 7-1. Bedload Roughness vs. Gravel Concentration (Copeland et al., 2000)

The maximum Manning's roughness coefficient was approximately 0.0192 at a sediment concentration of 3,000 ppm, which was an increase of 20 percent in roughness compared to a channel clear of sediment (n value of 0.016 in this experiment). The roughness peaked at approximately 0.02 (0.0197) with a feed rate of 3,500 ppm before starting to decrease and eventually stabilizing at about 0.0179 and 0.0178 for bedload feed rates of 4,000 and 5,000 ppm, respectively.

The results for Corte Madera Creek and Mission Creek were combined (Figure 7-1), and linear regression through the data showed that the bedload contribution to the Manning's n value could be determined by the following equation with an R^2 value of 0.938 (Copeland et al., 2000):

$$n_{bedload} = 1.0312 * 10^{-6} C_{gravel} \quad (7.1)$$

where:

C_{gravel} is the concentration of coarse material, including gravel and cobbles.

7.2.2 Corte Madera Creek – January 1982 Flood

In another study of the Corte Madera Creek concrete channel, a comparison of backwater calculations and high-water marks were collected after the major flood of January 1982 (USACE, n.d.). The data showed that the average Manning’s roughness coefficient was between 0.029 and 0.030 in the concrete portion of the channel where deposition of sediment had taken place. Factors contributing to the large roughness value included gravel deposits on the bed, wall roughness due to gravel movement, tubeworm and barnacle deposits on the wall, and channel sinuosity. The concrete channel without sediment was considered to have a roughness value of 0.018.

7.2.3 Standard Manning’s n Reference – Chow (1959)

A standard reference for determining n values (Chow, 1959) provides recommended values for a gravel bottom channel with sides of formed concrete. The recommended range is 0.017 to 0.025, with a normal value of 0.02 (see Table 7-1). Values are also shown in the table for fully concrete-lined channels.

Table 7-1. Concrete-lined and Gravel Bottom Channel Roughness Values (Chow, 1959)

Channel Type	Recommended n -value		
	minimum	normal	maximum
Gravel bottom with sides of formed concrete	0.017	0.02	0.025
Concrete-lined with:			
Trowel finish	0.011	0.013	0.015
Float finish	0.013	0.015	0.016
Unfinished	0.014	0.017	0.020

7.2.4 Equivalent Channel Roughness

In order to account for the increased bed roughness due to sediment, bank and bed roughness can be composited using the equal velocity method to obtain the total roughness for a cross section (Chow, 1959). The method is applied in HEC-RAS for open channel flow as illustrated in Figure 7-2 (MEI, 2008) and described in the equation below:

$$n_c = \left[\frac{\sum_{i=1}^N P_i n_i^{1.5}}{P} \right]^{2/3} \quad (7.2)$$

where:

n_c is the composite or equivalent coefficient of roughness.
 P is the wetted perimeter of the entire main channel.
 P_i is the wetted perimeter of individual subsections across the cross section.
 n_i is coefficient of roughness for individual subsections.

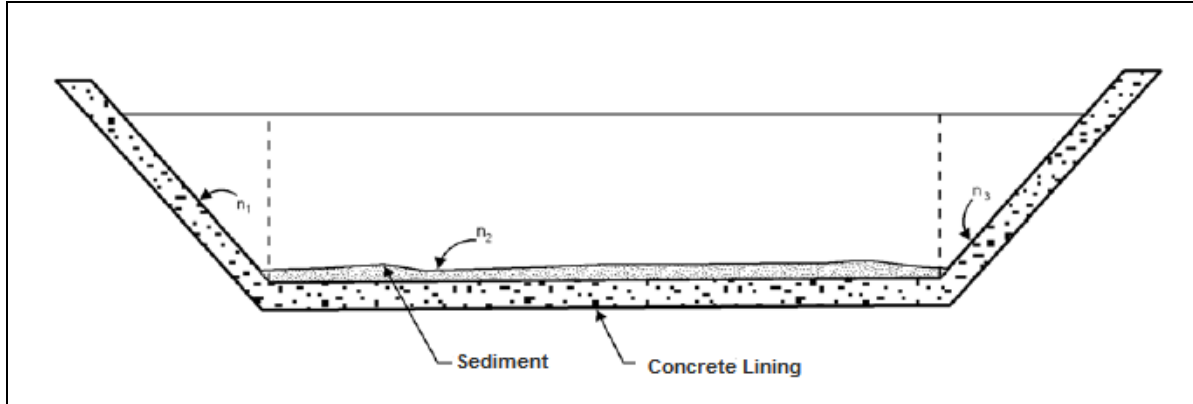


Figure 7-2. Schematic of a Concrete-lined Channel with Significant Sediment Load (MEI, 2008)

7.2.5 Pole Creek FIS Model

A FIS of Pole Creek was recently conducted by FEMA using HEC-RAS. The study model was obtained from the City of Fillmore website (<http://engineering.fillmoreca.com/>) in the “models” directory (no date provided). The study was performed for approximately two miles of the stream, including a rectangular-shaped, concrete-lined segment starting from 300 feet upstream of Union Pacific Railroad to Telegraph Road (approximately 3,300 ft long).

The Manning’s roughness coefficient selected for much of the concrete reach was 0.025, which is higher than the normal range of roughness values for a concrete-lined channel carrying little or no sediment (0.013 to 0.017). It is assumed that the higher value was selected to account for sediment-laden flow originating upstream.

7.3 Flows Affected by Increased Manning’s n

In addition to investigating the appropriate Manning’s n value for a concrete channel affected by bedload, the VCWPD also wanted to determine for which range of Pole Creek flows the increased n value would apply.

7.3.1 Computed vs. Permissible Velocity and Shear Stress

Pole Creek channel velocities and shear stresses were calculated for a range of flows between 200 cfs and 3,000 cfs and a concrete channel roughness of 0.02 (modified from the original 0.025 in the model). The results, which are shown in Table 7-2, were compared with permissible velocities and shear stresses found in the literature (Fischenich, 2001 – Table 7-3) to determine at what flows gravel and cobble movement would be expected within the channel. Significant gravel and cobble movement would be expected with velocities exceeding 5 to 6 ft/s and shear stresses above 1 to 2 lb/ft². These values are consistently seen in the channel for flows of 500 cfs and greater.

Table 7-2. Pole Creek – HEC-RAS Channel Velocity and Shear Stress

Channel Material	River Station (ft)	Q = 200 cfs		Q = 500 cfs		Q = 1,000 cfs		Q = 2,000 cfs		Q = 3,000 cfs	
		Channel Average Velocity (ft/s)	Channel Average Shear Stress (lbs/ft ²)	Channel Average Velocity (ft/s)	Channel Average Shear Stress (lbs/ft ²)	Channel Average Velocity (ft/s)	Channel Average Shear Stress (lbs/ft ²)	Channel Average Velocity (ft/s)	Channel Average Shear Stress (lbs/ft ²)	Channel Average Velocity (ft/s)	Channel Average Shear Stress (lbs/ft ²)
Earthen Channel	10799	5.4	4.2	6.4	5.1	8.3	7.6	11.5	13.5	12.4	15.0
	10615	4.0	2.1	5.3	3.3	6.5	4.3	7.6	5.5	8.5	6.4
	10413	5.5	4.7	7.6	7.6	9.3	10.1	10.4	11.3	11.4	12.6
	9978	3.6	1.7	5.0	2.8	6.3	4.0	7.8	5.5	8.8	6.5
	9450	5.5	4.2	7.2	6.2	8.7	8.1	10.7	10.9	12.3	13.4
	8917	4.3	2.4	5.8	3.9	6.9	5.1	8.8	7.5	10.3	9.6
	8461	3.9	2.3	5.6	3.9	7.1	5.7	8.8	7.7	9.8	9.0
	8187	6.3	6.0	8.5	9.0	10.3	11.8	12.6	15.6	14.0	18.2
Concrete Channel	7844	8.4	0.81	11.6	1.3	14.6	1.9	18.2	2.6	20.5	3.1
	7438	17.4	3.9	21.0	4.6	24.0	5.2	27.2	5.9	29.2	6.3
	6516	9.5	1.0	13.9	1.8	18.5	3.0	24.3	4.6	28.1	5.9
	5914	12.8	2.0	16.2	2.6	19.5	3.3	23.7	4.4	26.5	5.1
	5041	10.4	1.2	15.5	2.4	20.4	3.7	25.6	5.2	28.8	6.2
	4255	4.2	0.16	5.4	0.22	6.5	0.29	6.8	0.31	6.0	0.22
	4232	5.7	0.30	7.7	0.48	9.5	0.66	11.5	0.95	8.1	0.45
	4220	7.3	0.53	9.7	0.80	11.9	1.1	14.4	1.4	15.1	1.6
	4200	11.4	1.6	14.2	2.0	17.0	2.6	20.2	3.2	21.2	3.4
	4182	6.7	0.46	10.8	1.1	13.3	1.5	17.3	2.3	18.6	2.5
	4070	10.7	1.4	13.0	1.7	15.6	2.2	19.2	2.9	20.4	3.1
	3963	9.3	1.0	13.6	1.9	16.7	2.5	20.3	3.3	6.6	0.28
Concrete Channel Summary:	Minimum:	4.2	0.16	5.4	0.22	6.5	0.29	6.8	0.31	6.0	0.22
	Average:	9.5	1.2	12.7	1.7	15.6	2.3	19.1	3.1	19.1	3.2
	Maximum:	17.4	3.9	21.0	4.6	24.0	5.2	27.2	5.9	29.2	6.3

Table 7-3. Permissible Velocity and Shear Stress for Channel Materials (adapted from Fischenich, 2001)

Boundary Category	Boundary Type	Permissible Velocity (ft/s)	Permissible Shear Stress (lb/ft ²)
Soils	Fine colloidal sand	1.5	0.02 – 0.03
	Sandy loam (noncolloidal)	1.75	0.03 – 0.04
	Alluvial silt (noncolloidal)	2.0	0.045 – 0.05
	Silty loam (noncolloidal)	1.75 – 2.25	0.045 – 0.05
	Firm loam	2.5	0.075
	Fine gravels	2.5	0.075
	Stiff clay	3 – 4.5	0.26
	Alluvial silt (colloidal)	3.75	0.26
	Graded loam to cobbles	3.75	0.38
	Graded silts to cobbles	4.0	0.43
	Shales and hardpan	6.0	0.67
Riprap	6-in D ₅₀	5 – 10	2.5
	9-in D ₅₀	7 – 11	3.8
	12-in D ₅₀	10 – 13	5.1
	18-in D ₅₀	12 – 16	7.6
	24-in D ₅₀	14 – 18	10.1
Hard Surfacing	Concrete	> 18	12.5

7.4 Recommendations

Based on the findings discussed in this chapter, a Manning's *n* value of 0.02 appears to be reasonable for concrete channels affected by bedload. In the case of Pole Creek, this increased roughness would apply to flows of approximately 500 cfs or greater.

8 FINES AND BULKING

The impact of wash load on bulking, the inclusion of fine sediment in the VCWPD debris yield method, and the applicability of soil loss equations (USLE, RUSLE, MUSLE) are discussed in this section.

8.1 Wash Load

Wash load is generally defined as fine sediment, usually silt and clay less than 0.0625 mm in diameter, that travels in suspension and is not found in significant quantities in the bed. Table 8-1 illustrates the different sediment types by origin, transport, and sampling method.

Table 8-1. Sediment Type by Transport, Source, and Sampling Method (adapted from Diplas et al., 2008)

Transport Mechanism	Sediment Source	Sampling Method
Suspended Load	Wash Load	Measured Load
	Bed Material Load	
Bed Load		Unmeasured Load

Wash load is primarily controlled by land surface erosion as a function of rainfall, vegetation, and land use. Wash load can contribute to bulking of flows like any other sediment material.

It is important to note that the division of total sediment load into bed-material load and wash load no longer applies once the mixture reaches a hyperconcentrated level. Instead of two relatively distinct components of sediment flow, the hyperconcentrated flow forms a well-integrated mixture.

Fine sediment can affect bedforms and therefore resistance. Gravel beds can be smoothed by sand/silt during high concentrations. For example, the Cowlitz River downstream of Mount St. Helens experienced high silt and fine sand wash load concentrations – the bed forms changed from dunes to a plane bed, lowering the estimated Manning’s n value from 0.03 to 0.018 and resulting in a 3-foot reduction in flow depth (Bradley, 1986). Fine sediment can also affect transport rates by “lubricating” the movement of coarser particles (Curran and Wilcock, 2005).

8.2 Scott Method and Fines

The VCWPD's debris production rate equation – known as the Scott method – is derived from Scott and Williams (1978). Described below is the extent to which the debris production rate includes any fines. The trap efficiency of debris basins is a key part of this discussion.

8.2.1 Basin Trap Efficiency

The trap efficiency of a reservoir or debris basin can be defined as the percentage of the material entering the reservoir (or basin) that remains in the basin. Sedimentation measured from debris basins would not be equal to sediment yield from the watershed when the trap efficiency is below 100 percent. A trap efficiency of 100 percent means that all of the sediment delivered to a basin remains in the basin. A trap efficiency of 0 percent means that all of the sediment delivered to a basin washes through the basin and continues downstream.

Scott and Williams (1978) estimated trap efficiencies for properly designed debris basins with a 1 to 2 mi² contributing watershed and a functioning outlet. As shown in Table 8-2, a majority (60%) of the fines would pass through the debris basin and would not be included in the basin sediment data. Conversely, this indicates that a significant percentage (40%) of the fines would be trapped instead of being flushed downstream and would be recorded in the measured sediment data.

Table 8-2. Example Debris Basin Trap Efficiencies (data from Scott and Williams, 1978)

Material	Trap Efficiency (%) (Material Remains in Debris Basin)	Passed Thru (%) (Materials Washes Thru Debris Basin)
Fines (silt and clay)	40	60
Sand	94	6
Sizes coarser than sand	99	1

It is important to note that the overall trap efficiency for a basin is dependent not only on the trap efficiencies of individual sediment fractions (fines, sand, etc.), but also on what sediment sizes are reaching the basin. For example, if 90 percent of the sediment is sand (with a trap efficiency of 94 percent), and 10 percent is fines (40 percent trap efficiency), then the overall trap efficiency is 89 percent – and fines would not be a significant factor in any measured sediment data. However if 50 percent of the sediment entering the basin is sand and 50 percent is fines, the overall trap efficiency would drop to 67 percent.

8.2.2 Scott and Williams (1978)

The debris production equations developed by Scott and Williams (1978) are based on actual debris basin data, so the debris production rates computed by the equations include the fines trapped in those basins. The degree to which fines are included in the debris basin data and therefore the Scott

and Williams equations is unknown, however, because the data came from numerous debris basins with varying amounts of fines in their watersheds.

If a particular watershed contains a large amount of fines, the computed debris volume using the VCWPD debris yield method may require adjustment if the purpose is sizing a debris basin. This would result in a reduction in volume because more fines from the watershed would wash through the debris basin.

For the purpose of bulking flows, however, the sediment concentration depends on the debris volume and not directly on whether it is composed of fines or coarse sediment. Therefore, the computed debris volume does not have to be reduced based on the percentage of fines in the watershed.

8.3 USLE/RUSLE/MUSLE and Bulking

8.3.1 USLE and RUSLE

The Universal Soil Loss Equation (USLE) was developed based on slope erosion data from agricultural fields, and was developed primarily for conservation planning purposes (Wischmeier and Smith, 1978).

$$A = R K L S C P \tag{8.1}$$

where:

A is the computed soil loss per unit area.

R is the rainfall and runoff factor.

K is the soil-erodibility factor.

L is the Slope-length factor.

S is the slope-steepness factor.

C is the cover and management factor.

P is the erosion control practice factor.

The Revised Universal Soil Loss Equation (RUSLE) has the same general formula as the USLE, but provides new and revised approaches for estimating factors in the equation, and allows for more detailed consideration of farming practices and topography (Renard et al., 1997; Borah et al., 2008).

8.3.2 MUSLE

The MUSLE (Modified USLE; Williams, 1975), which was developed by Williams and Berndt (1977), is an event-specific version of the original Universal Soil Loss Equation (USLE). The MUSLE is provided below (note: equation has been converted to a volumetric sediment yield):

$$Q_s = 0.05816 (V \times Q_w)^{0.56} K L S C P \tag{8.2}$$

where:

Q_s is the single-event sediment yield (acre-ft); converted from short tons based on a bulk density of 0.0375 ton/ft³.

V is the storm runoff volume (acre-ft).

Q_w is the peak water discharge (cfs).

Williams and Berndt (1977) provide guidance regarding how each factor should be computed.

MUSLE provides a methodology that is better suited to western conditions than the USLE (Clark County, 1999).

8.3.3 Applicability to Bulking

The USLE and its other forms (RUSLE, MUSLE) provide sediment yield estimates based on sheet and rill erosion (i.e., wash load), and do not include sediment from other potential forms of erosion, such as gully erosion, channel bed and bank erosion, and mass movement (HEC, 1995).

According to Scott and Williams (1978), the USLE and similar soil loss methods based on soil loss data from agricultural fields have not proved to be useful in southern California. Although the MUSLE has given some reasonable results in the western U.S., the current version has limited applicability to the watersheds within the Transverse Ranges of Ventura County.

In addition, during hyperconcentrated or debris flow events, mass wasting and the movement of sediment collected in the channel would be the primary sources of sediment rather than the sheet and rill erosion computed by soil loss equations. Therefore, the use of MUSLE or other soil loss equations in addition to the VCWPD's debris yield method is not recommended.

9 WOODY DEBRIS

In addition to investigating bulking factors to account for debris composed primarily of a mixed mass of colluvium (i.e., fine sediments, gravel, and boulders), design methods were also reviewed for accommodating woody debris loads (i.e., trees and logs). VCWPD requested that the focus of woody debris flows be on recently burned watersheds, and recommendations for adjusting safety factors used to increase bridge pier widths due to the added load. Woody debris transported downstream by floods can become caught at bridge piers and accumulate into large piles, narrowing or completely blocking the waterway opening (Figure 9-1). The obstructed flow path can increase backwater elevations upstream, increase flow velocity through the narrowed waterway, and modify flow patterns. These changes can lead to increased flood risks, local scour, and even bridge failure (Figure 9-2).

The purpose of this chapter is to summarize the bridge pier woody debris design guidelines used by other agencies, describe recent research on estimating pier debris, and provide recommendations for Ventura County. This includes the application of woody pier debris for recently burned watersheds.



Figure 9-1. Woody Debris Blocking the Waterway Opening of the Bridge (Lyn et al., 2003)



Figure 9-2. Woody Debris Accumulation and Bridge Failure (FHWA, 2005)

9.1 Agency Methods

Table 9-1 summarizes bridge pier woody debris guidelines used by local, state and federal agencies. The general practice is to increase the pier width by two feet on each side to account for the debris accumulation, as well as applying good engineering judgment and practical experience.

Table 9-1. Summary of Agency Guidelines for Woody Debris on Bridge Piers

Agency	Pier Debris Standards/Guidelines
Los Angeles County Department of Public Works	No set standard, but commonly use a 2 ft debris width on each side of bridge piers and, a debris depth (from the water surface) of 6-8 ft.
Riverside County Flood Control and Water Conservation District	No set standard, but commonly use a 2-ft debris width on each side of bridge piers.
San Bernardino County Flood Control District	No set standard. Default to Caltrans recommendations.
Orange County Flood Control District	Four different levels of debris accumulation on bridge piers are used. The most severe case indicates a 3-ft increase to pier widths on each side.
San Diego County Department of Public Works	No set standard. Rely on engineering judgment.
Caltrans	No set standard. Method varies depending on location, but they commonly use a 2-ft debris width on each side of bridge piers.
Arizona Department of Transportation (2010)	Recommend increasing the pier width by a total of 4 ft, and using a 12-ft depth-of-debris blockage from the water surface. When the depth of flow is <12 ft, the depth of debris blockage shall be set equal to the depth of flow.
Federal Highway Administration (FHWA)	Recommended guidelines based on Diehl (1997, refer to Section 9.2.1).
U.S. Forest Service	No set standard.
U.S. Army Corps of Engineers	No set standard.

9.2 Pier Debris – Size and Configuration

The typical pier debris guidelines used by agencies are “rules of thumb” rather than values based on any detailed analysis. In order to develop more robust guidelines, research regarding the expected size and configuration of pier debris was reviewed, including commonly applied research and design guidelines by Diehl (1997) and Lagasse et al. (2010).

9.2.1 Diehl (1997)

Diehl (1997) conducted a study for the FHWA regarding the potential for debris (“drift”) accumulation at a bridge, and the maximum size of the debris accumulation. The concept of a design log length was used to represent a length “above which logs are insufficiently abundant...to produce drift accumulations equal to their length.” The design log length becomes the width of the obstruction for the entire depth of the channel. Diehl recommends estimating the design log length as the smallest of the following three values (FHWA, 2005):

1. Width of the channel upstream for the site.
2. Maximum length of sturdy logs. This is determined by the height and diameter of mature trees on the channel banks that can be delivered to the bridge as floating debris, and capable of withstanding the hydraulic forces when trapped against the piers.
3. Design log length equation (below).

$$L_d = 30 + \left(\frac{B_{up}}{4} \right) \quad (9.1)$$

where:

L_d = design log length (ft)

B_{up} = width of the channel upstream of the bridge (ft)

9.2.2 Lagasse et al. (2010)

Lagasse et al. (2010) recently completed a study regarding the effects of woody debris accumulation at bridge piers. One of the objectives of the study was to develop guidelines for predicting the size and geometry of the debris. The research effort, which is an extension of the work by Diehl (1997), provides a more robust characterization of the potential debris accumulation at a proposed bridge than current practice.

The procedure takes into account the main factors related to debris accumulation including the shape of the debris accumulation (rectangular as shown in Figure 9-3, and triangular), size of the accumulation (length, width and thickness), location (floating, subsurface, or buried), roughness, porosity, and approach velocity. The study presents the following equations to compute equivalent pier width:

$$a_d^* = \frac{K_{d1}(TW)(L/y)^{K_{d2}} + (y - K_{d1}T)a}{y} \quad \text{for } L/y > 1.0 \quad (9.2)$$

and

$$a_d^* = \frac{K_{d1}(TW) + (y - K_{d1}T)a}{y} \quad \text{for } L/y \leq 1.0 \quad (9.3)$$

where:

a_d^* = effective pier width (ft)

W = width of the debris (ft)

T = thickness of the debris (ft)

$K_{d1} = 0.79$ for rectangular debris, and 0.21 for triangular debris (dimensionless)

$K_{d2} = -0.79$ for rectangular debris, and -0.17 for triangular debris (dimensionless)

L = length of debris upstream from a pier face (ft)

a = pier width (without debris) normal to flow (ft)

y = depth of approach flow (ft)

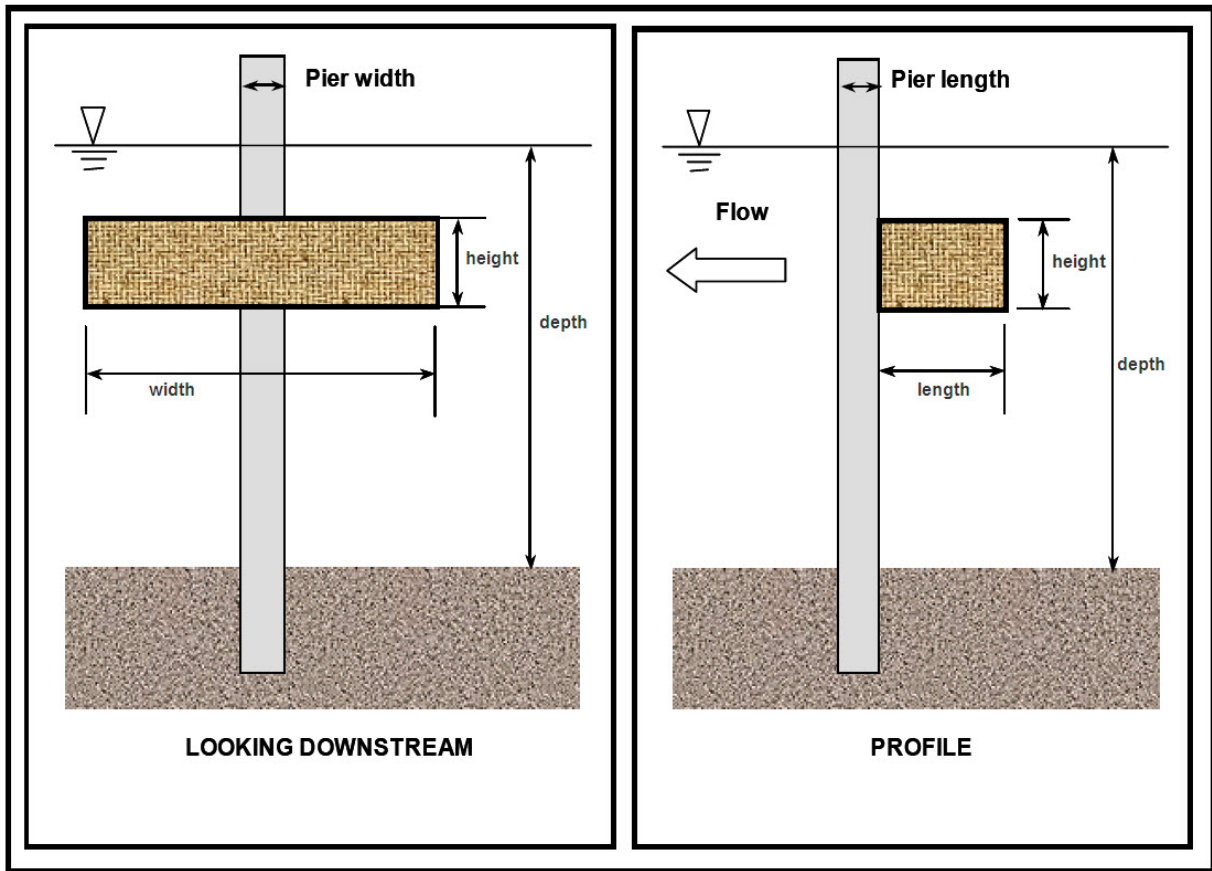


Figure 9-3. Rectangular Shaped Woody Debris Representation (Lagasse et al., 2010)

Based on the woody debris research conducted by Diehl (1997), Lagasse et al. (2010) developed detailed flowcharts for estimating the potential for debris production and delivery from the contributing watershed of a selected bridge and the potential for accumulation on individual bridge elements. Although Lagasse et al. (2010) provide guidelines for predicting the size and geometry of debris accumulations at bridge piers, the methods require a comprehensive and extensive site visit for data collection prior to estimating debris dimensions. For a more detailed description of the guidelines and flowcharts for estimating debris production, accumulation and dimensions please refer to the Transportation Research Board NCHRP Report 653 (Lagasse et al., 2010).

9.3 Woody Debris Contribution

Provided below is a discussion of Ventura County vegetation and potential woody debris contributions, as well as the potential impact of fires on woody debris contribution.

9.3.1 Ventura County Vegetation

The major vegetation communities in Ventura County that could potentially contribute to floating debris include chaparral, coastal scrub, and hardwood and conifer forest, including both riparian corridors and montane forests (Figure 9-4). Chaparral and coastal scrub dominate foothills and mountain slopes of the county, consisting of approximately 51% (combined) of its total area (Figure 9-5 and Figure 9-6). Other dominant vegetation consists of hardwood and conifer forests, which combined make up approximately 28% of the land coverage. These hardwood forests include coast live oak, which is not highly flammable and may not be a significant contributor of woody debris. The montane forests consist primarily of pine and fir trees, occurring at the higher elevations of the mountainous area of the county (from 3,000 to 8,500 ft). The lower elevation species are generally more sensitive to fire than those at higher elevations.

Riparian woody debris contributing to Ventura County streams and rivers can include native coast live oaks, willows, and cottonwoods. However, non-native *Arundo* and *Tamarisk* (commonly known as salt cedar) grow in dense stands in many riparian areas of the county, and have been known to accumulate often on bridge piers, more so than the native community. Areas of riparian vegetation generally occur in narrow canyons or along broad, wooded corridors that follow the creeks and rivers of the county. For chaparral watersheds, woody debris would primarily originate from the riparian vegetated areas along the stream.



Chaparral



Coastal Sage Scrub



Montane Forest



Riparian Corridor

Figure 9-4. Southern California Vegetation Communities (University of California, 2010)

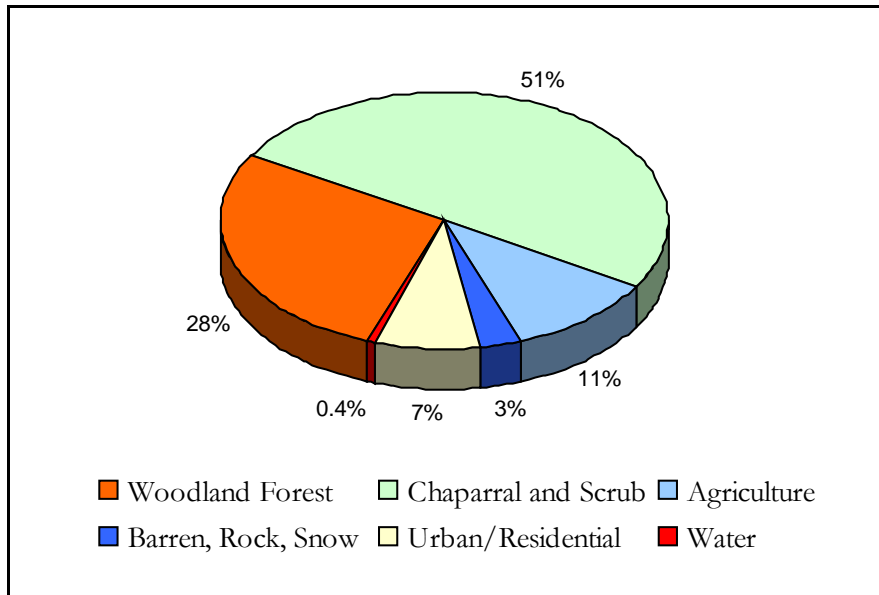


Figure 9-5. Ventura County Cover Type Percentages

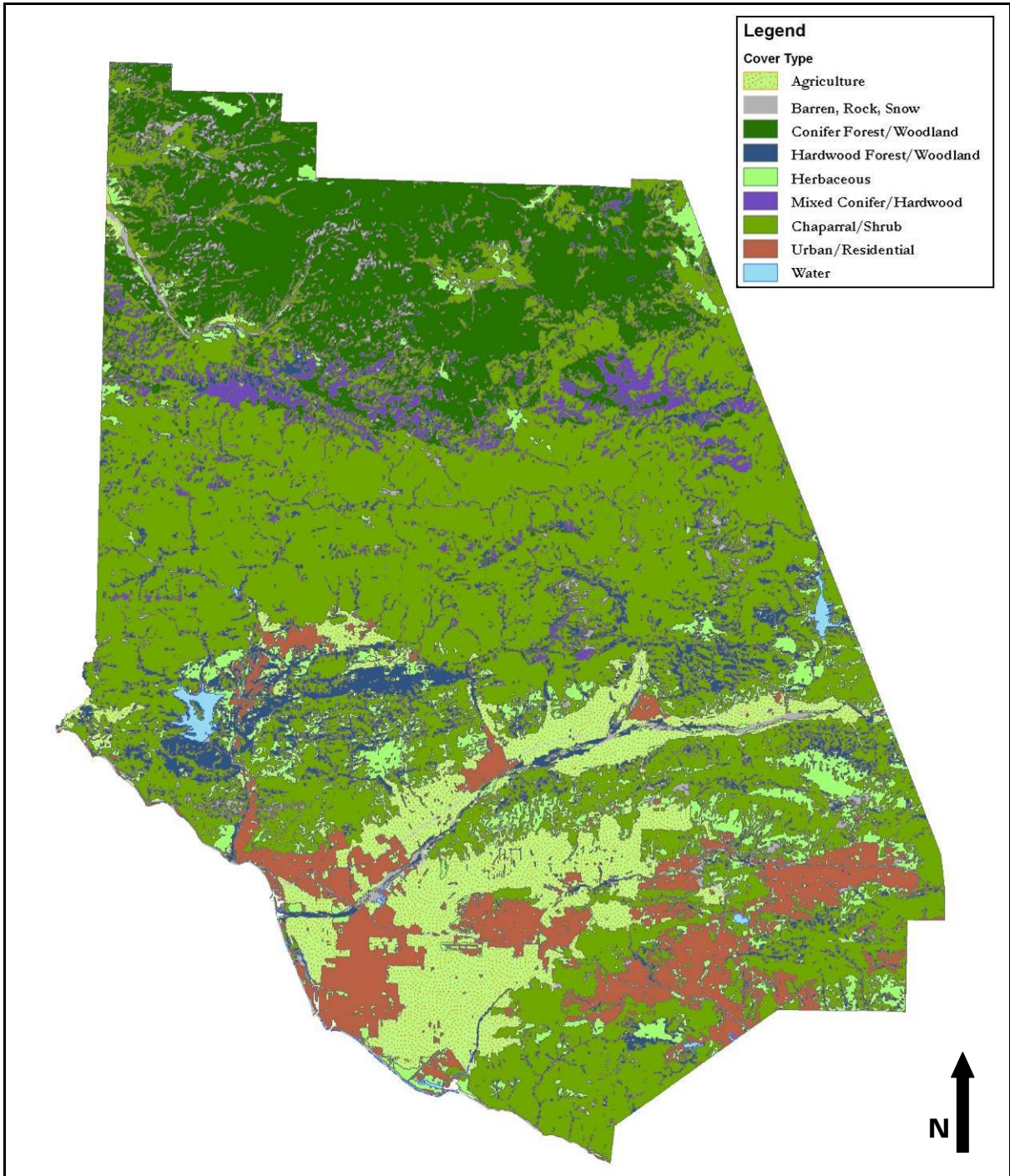


Figure 9-6. Map of the Ventura County Cover Types

9.3.2 Post-fire Woody Debris

An example of post-fire woody debris within Ventura County is from a study conducted by Bendix and Cowell (2010). For the study, data were collected from two small Ventura County streams located within the perimeter of the 2002 Wolf Fire that burned approximately 34 mi² of chaparral in the Los Padres National Forest. The purpose of the study was to investigate the interactions between fire, floods, and supply of woody debris. The two sampled streams, Piedra Blanca Creek and Potrero John Creek, contribute flow to Sespe Creek as shown in Figure 9-7. The watersheds are characterized by steep slopes with pre-fire chaparral cover. For the two streams investigated, the watersheds had high growth of *Alnus rhombifolia* (white alder), *Populus fremontii* (Femont cottonwood), *Quercus agrifolia* (coast live oak), *Quercus dumosa* (scrub oak), and *Salix* sp. (willows) on the valley floor (Bendix and Cowell, 2010).

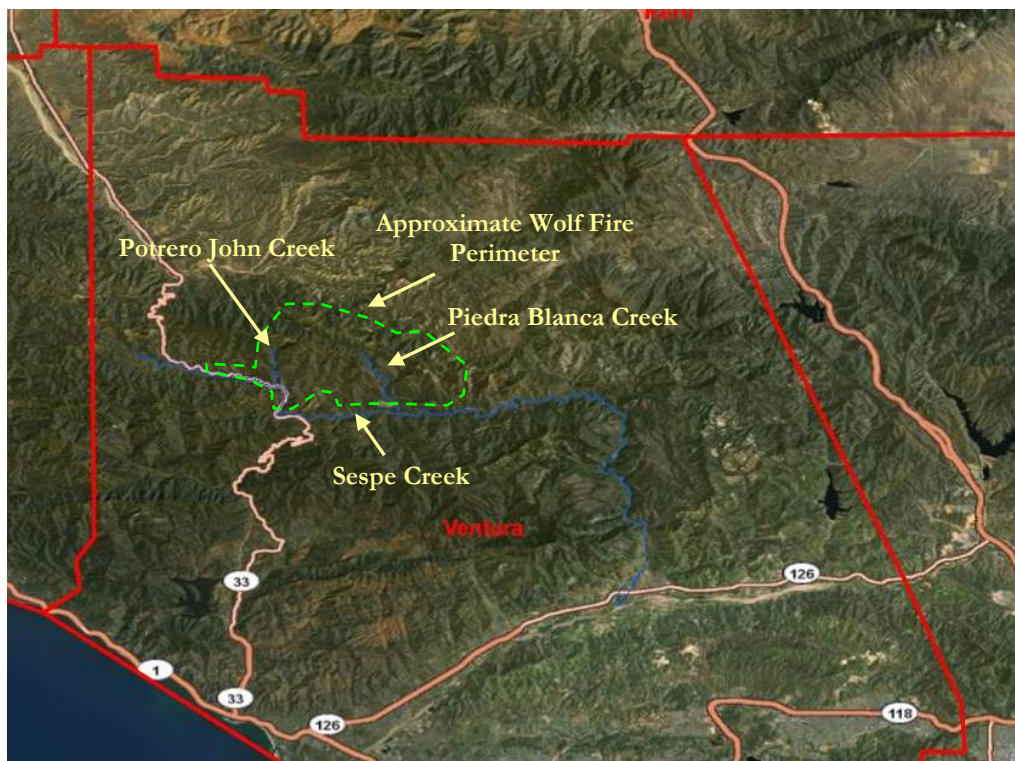


Figure 9-7. Bendix and Cowell (2010) Study Location Map (including Wolf Fire perimeter)

Most woody debris is supplied to a stream channel from the riparian zone after natural mortality, but because wildfire can cause extensive tree mortality, it has the potential to significantly affect the volume of woody debris added to the system. Results from Bendix and Cowell (2010) indicate that species were variable in susceptibility to falling after a fire. Based on these results, Bendix and Cowell (2010) concluded that the variability in species composition (and corresponding fall rates) must be considered in predicting post-disturbance channel inputs of woody debris.

Other researchers (Spies et al., 1988; and Bragg, 2000) have indicated that wildfire can cause multiple, sequential pulses of burnt tree fall, and subsequent debris input to a channel. However, the results of these studies differed in the timing of woody debris recruitment. Spies et al. (1988) suggested that there was a pulse of woody debris post-fire followed by a decline in the recruitment

to levels below those before the fire. On the other hand, Bragg (2000) concluded that there would be a lag of 30 years after the fire before peak debris loadings, because it would take decades for burned snags to actually fall into the channel. The Bendix and Cowell (2010) study results were similar to Spies et al. (1988) in that there was a pulse in burnt woody debris soon after the fire. Of the total burnt trees (94% of the study area), 17% fell within two years. Seventy-five percent of the fallen trees that had experienced significant flood depths had mobilized. This most likely was due to high flood waters potentially knocking multiple burned trees down rather than leaving them to decay and fall individually. Another factor that was shown to have an effect on the variance of tree fall timing and rates was difference in species. For riparian communities with species such as *Alnus rhombifolia* (white alder), relatively rapid debris recruitment following fire might be expected, whereas if *Quercus agrifolia* (coast live oak) dominates, a delay in recruitment on the order of years to decades may occur (Bendix and Cowell, 2010).

9.4 Pier Debris Control Structures

A commonly used method to divert and guide debris through bridge openings are debris fins. Debris fins are thin walls that are built in the stream channel upstream of the bridge parallel with the flow (Figure 9-8). The purpose of the fins is to align large floating debris parallel to flow, enabling it to pass through the bridge opening without incident. Debris fins are also referred to as “pier nose extensions” (FHWA, 2005). Note that with debris fins installed, pier debris would not be expected to accumulate in significant quantities at a bridge, and therefore debris would not need to be added to the piers in a hydraulic model.



Figure 9-8. Example of Elongated Pier Nose

9.5 Woody Debris Summary

A summary of the woody debris findings and recommendations for Ventura County is provided below.

- Rather than having a strict standard, most agencies use a general guideline of increasing the pier width by two feet on each side to account for debris.
- Pier debris should be applied on a case-by-case basis for locations where large woody debris has been observed or expected from the watershed, including areas of the county with montane hardwood and/or conifer forest. For watersheds where chaparral is predominant, woody debris is expected to originate from the riparian corridor along the stream.
- Wildfire can cause extensive tree mortality that in turn can significantly affect the volume of woody debris available to the stream, which can eventually accumulate on a bridge pier.
- The timing of a post-fire increase in woody debris will depend on the species composition. For riparian communities with species such as white alder, relatively rapid debris recruitment might be expected, whereas if coast live oak dominates, a delay in woody debris recruitment on the order of years to decades may occur.
- NCHRP Report 653 (Lagasse et al., 2010) provides improved guidance in predicting the size and geometry of debris accumulation on bridge piers, but requires detailed inputs to use.
- Installation of debris fins to act as an extension of upstream pier nose can help guide woody debris through the bridge openings, eliminating the need to specify pier debris in a hydraulic model.

It is recommended that the results from the Lagasse et al. (2010) study, as described in Section 9.2.2, be followed in Ventura County if woody debris is a known issue and reliable field data are available. Otherwise, Ventura County should use the general design practice of increasing the pier width by two feet on each side to account for potential woody debris.

PART III. POST-FIRE HYDROLOGY

10 AGENCY POST-FIRE HYDROLOGIC METHODS

Fire can modify watershed hydrologic processes in a number of ways. In addition to increased sediment bulking, these changes can also include increased clear-water runoff and decreased watershed lag times between peak precipitation and runoff. The focus of this chapter is the post-fire increase in clear-water runoff and the methods used by governmental agencies to compute the post-fire peak discharge, i.e., Q_{burn} .

An online literature and hydrology manual review of fire methodologies was performed for government agencies in southern California, Arizona, and New Mexico. These areas have similar vegetation and climate as Ventura County. No hydrology manual fire methodologies were found for the counties of San Diego, Riverside, San Bernardino, Santa Barbara, California or Maricopa County, Arizona. However, numerous references were found on the effects of fire on hydrology of forested watersheds. In this chapter, an introduction to fire effects on hydrology is provided, followed by a description of FEMA, Los Angeles County, and Ventura County post-fire hydrologic methods.

10.1 Fire Effects on Hydrology

Fire effects on the hydrology of clear-water runoff include changes to evapotranspiration, interception, infiltration, surface and sub-surface soil moisture storage, and surface and sub-surface flow paths (Neary et al., 2003). Decreased watershed lag times (and higher peak flows) are caused by loss of vegetation, litter, and duff and resulting lowering of overland, rill and channel flow friction coefficients. Fire effects on vegetation, soils, and hydrologic processes are summarized below:

Vegetation

- Reduced groundcover and increased exposure of mineral soil
- Reduced evapotranspiration
- Reduced interception

Soil Properties

- Reduced litter layer and soil organic matter
- Reduced storage capacity of surface organic material
- Increased hydrophobic soil (waxes released from volatilized organic matter move downward in the soil and form a water repellent layer)
- Reduced infiltration (fine sediment and ash sealing)

Hydrology (hill slope)

- Decreased surface roughness
- Increased overland flow/rill flow
- Decreased interflow due to loss of litter/duff layer
- Increased snow accumulation and melt

Hydrology (watershed response)

- Decreased watershed lag time
- Decreased flow path composite roughness (n) values
- Seasonal changes in base flow
- Increased peak flows

10.2 FEMA Post-burn Hydrology (2003b)

Post-burn peak flow adjustment factors for clear water were established in response to the October 2003 fires in California (FEMA, 2003b). Ratios were established between peak discharge estimates computed using the USGS Regional Regression Equations for California and the NRCS Curve Number Method. Post-burn CN values for New Mexico chaparral (Table 10-1) were compared to existing values for southern California chaparral. No variation by hydrologic soil group was provided for the CN data. Adjustment of CN values with a fire factor is a reasonable approach; however, the hydrologic model used should also consider changes in lag time due to burned flow paths.

Table 10-1. Post-Burn CN values from Studies of the 2000 Cerro Grande Fire, New Mexico (FEMA, 2003b)

Burn Intensity	Curve Number (CN)
Low Burn (no hydrophobic soils)	77
Low Burn (hydrophobic soils)	83
Moderate Burn (no hydrophobic)	85
Moderate Burn (hydrophobic soils)	89
High Burn (no hydrophobic)	90
High burn (hydrophobic soils)	95

FEMA recommended post-burn adjustment factors for 5- to 100-year design storms are provided in Table 10-2. Sediment bulking adjustment factors were then applied to the adjusted peak discharges (see Section 5.8).

Table 10-2. Post-Burn Adjustment Factors (FEMA, 2003b)

Burn Condition	Post-fire Adjustment Factor (Burn Severity Factor)
Unburned/ Very Low Burn	1.00
Low Burn	1.76
Moderate Burn	2.20
High Burn	2.62

10.3 Los Angeles County

Los Angeles County (2003) proposed a “Burn Policy Methodology” using statistical analysis of historical fire data to develop a 50-year design fire factor. In a pilot study for the Santa Clara River watershed, they developed burned area statistics for 1911-1996. They proposed that an adjusted burned runoff coefficient be used in the Modified Rational Method (MRM). They also proposed that the burned runoff coefficient be based on a 50-year recurrence interval fire factor index between unburned and completely burned watershed conditions based on the fire history of the watershed.

Results of this analysis were incorporated into the *Los Angeles County Hydrology Manual* (Los Angeles County, 2006b), which provides equations for the adjusted burned soil runoff coefficient and peak runoff from a burned area.

The burned runoff coefficient, used in the MRM, is calculated by:

$$C_{burn} = FF * [(1 - K) * (1 - C_u)] + C_u \quad (10.1)$$

where:

C_{burn} = adjusted burned soil runoff coefficient

FF = fire factor, the effectively burned ratio of watershed area (0 to 1)

K = ratio of burned to unburned infiltration rates, equal to $0.677 * I^{-0.102}$

I = rainfall intensity (in/hr)

C_u = undeveloped runoff coefficient

Los Angeles County defines the fire factor as an index between 0 (natural or unburned) and 1 (completely burned) watershed conditions. Design fire factors are assigned to large regional watersheds in the L.A. County Hydrology Manual, including a fire factor equal to 0.34 for the Santa Clara River Watershed and Antelope Valley. The fire factor is then applied to the smaller subareas being studied when using the Modified Rational Method.

The peak runoff from a burned area is computed by:

$$Q_{burn} = C_{burn} * I * A \quad (10.2)$$

Combining Equation (10.1) with (10.2) yields:

$$Q_{burn} = FF * [(0.677 * I^{-0.102} - 1) * (Q_u - A * I)] + Q_u \quad (10.3)$$

where:

Q_{burn} = peak runoff from burned area (cfs)

A = watershed area (acres)

Q_u = peak runoff from unburned area (cfs)

One of the most important parameters in the Los Angeles County methodology is the ratio of burned to unburned infiltration rates (K), which was developed through double-ring infiltrometer tests of representative undeveloped areas in the county. After test plots were used to obtain pre-burn infiltration rates, they were burned and retested. The resultant data set was used to develop the K parameter discussed above. An example in Los Angeles County (2003) shows peak flow increases for completely burned vs. unburned watershed in the Santa Clara River basin of 16 to 32 percent for a fully burned watershed as shown in Table 10-3.

Table 10-3. Computed Pre- and Post-fire Discharges – Santa Clara River Basin (Los Angeles County, 2003)

Watershed	Area (acres)	COMPUTED 50-YEAR PEAK DISCHARGE (CFS)		
		Unburned	34% Burned	100% Burned
Mint Canyon	16,922	12,400	13,600	14,900
South Fork Santa Clara River	22,638	34,900	36,800	40,400
San Francisquito Canyon	29,979	20,700	22,700	27,400

It should be noted that the results in are computed using an equation that is based on field testing of infiltration rates rather than observed runoff data. Literature references show that the ratio of post-burn to unburned peak discharges can be up to 2 or even higher, depending on the size of the drainage area and the burn severity (e.g., Martin, 2005). As a result, the Los Angeles County results for the Santa Clara River watershed, although consistent with their methodology, may not be conservative enough. The MRM also needs to account for the significantly lower time of concentration for severely burned conditions. A lower time of concentration for burned flow paths increases the rainfall intensity in the formula, and in effect, can increase the apparent MRM C factor to values greater than 1.0.

10.4 Ventura County

The Ventura County Design Hydrology Manual (VCWPD, 2010a) describes four methods used to compute design hydrology of an unburned watershed, which include:

- Modified Rational Method, implemented in the VCRat Program
- HSPF (Hydrologic Simulation Program - Fortran, by the U.S. Environmental Protection Agency)
- U.S. Army Corps of Engineers' HEC-HMS (Hydrologic Modeling System)
- Flood Frequency Analysis Using HEC-SSP (Statistical Software Package) and Bulletin 17B

The hydrology manual does not provide specific procedures for increasing the unburned clear-water runoff (Q_u) after a burn.

Until additional hydrologic studies are performed by the VCWPD, the pre-burn discharge should be increased using an adjustment factor similar to the fire factor applied to the MRM described in the Los Angeles County method in Section 10.3. This adjustment factor is termed the “Burn Severity Factor” or BSF and is described in Chapter 11. The following sections briefly describe the current methods used in Ventura County to obtain pre-burn peak flows and hydrographs and the information required for each method to provide post-burn results.

10.4.1 Modified Rational Method (VCRat Program)

VCRat is a computer program developed to perform MRM computations in Ventura County. The method is applicable for modeling partially- to fully-developed urbanized catchments of up to about 5,000 acres. The VCWPD has created VCRat models for many of the developed areas of the County. Input parameters include the watershed drainage area, rainfall intensity-duration curves, runoff coefficient curves, and time of concentration (T_c).

The BSF can be used to adjust the VCRat unburned peak flows and hydrographs until a more deterministic approach is developed. While adjusted C coefficients can be computed based on the Los Angeles County approach, a procedure to adjust T_c is required for burned conditions. This involves providing a new set of overland flow curves for use in calculating T_c for the burned watershed condition, and the Ventura County T_c calculator and VCRat programs would have to be reprogrammed to allow the option of calculating hydrology for burned conditions. Site specific studies should also be conducted to quantify the increases in peaks associated with the proposed increases in C coefficients and decreases in T_c .

10.4.2 HSPF (Hydrologic Simulation Program – Fortran)

The USEPA's HSPF model is a continuous simulation model that has the ability to model hydrology, as well as erosion and water quality parameters. The model uses rainfall history, temperature and solar radiation, land surface characteristics (such as land use patterns), and land management practices to simulate the processes that occur in a watershed. HSPF models are similar to HEC-HMS models in that they can represent large watersheds (in contrast, VCRat models are typically limited to watersheds less than 5,000 acres).

AQUA TERRA (2009) conducted an analysis of the increase in clear-water runoff due to fires using HSPF. The model was developed to evaluate the post-fire increase in runoff following the 2006 Day Fire that burned approximately one-third of the Sespe Creek watershed. A delineation of the Sespe Creek watershed and its outlet near the City of Fillmore are shown in Figure 10-1.

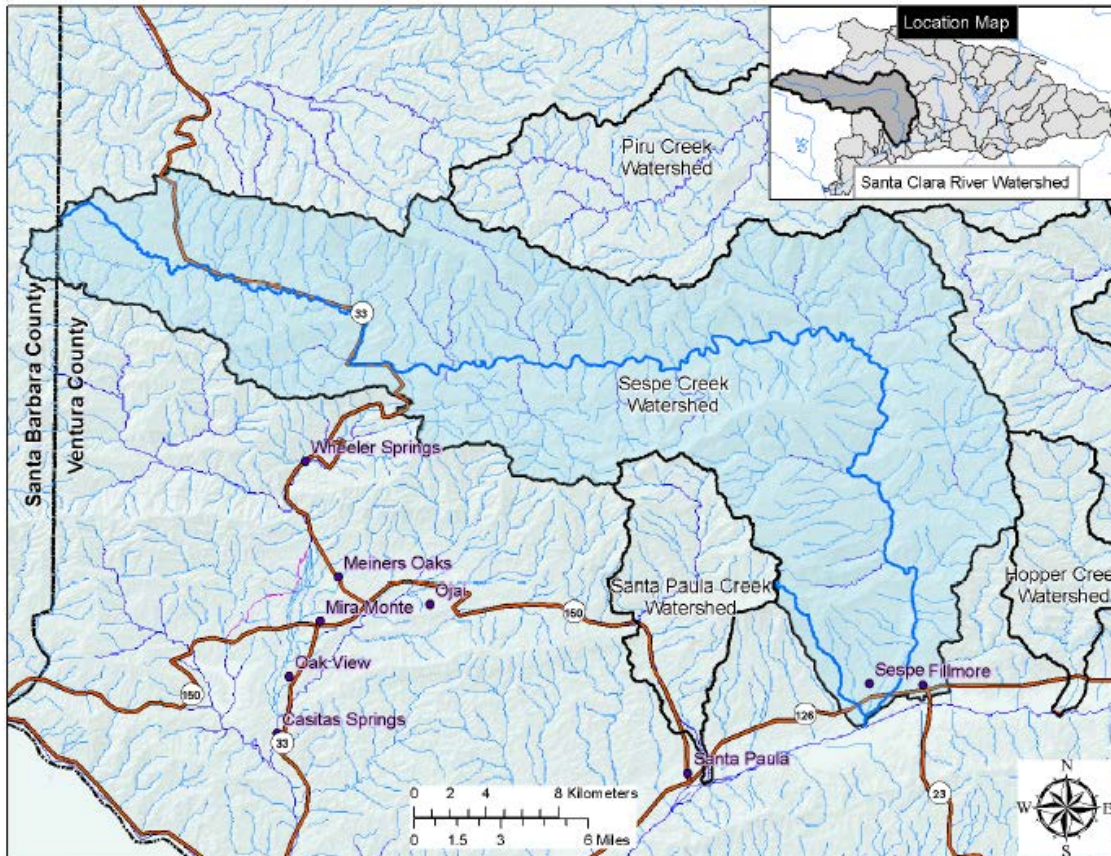


Figure 10-1. Sespe Creek Watershed within Santa Clara River Watershed (AQUA TERRA, 2010)

The HSPF model results show that when model input parameters were varied to reflect burned conditions, the Sespe Creek computed 100-year peak discharge increased from approximately 136,000 cfs to 143,000 cfs, only a 5 percent increase (VCWPD, 2010a; AQUA TERRA, 2010). The impact of the 2006 fire on the 100-year computed hydrograph for Sespe Creek is shown in Figure 10-2. Results of the study showed that the 100-year design storm peak on Sespe Creek increased by about 5 percent when approximately one-third of the watershed was modeled with burned conditions.

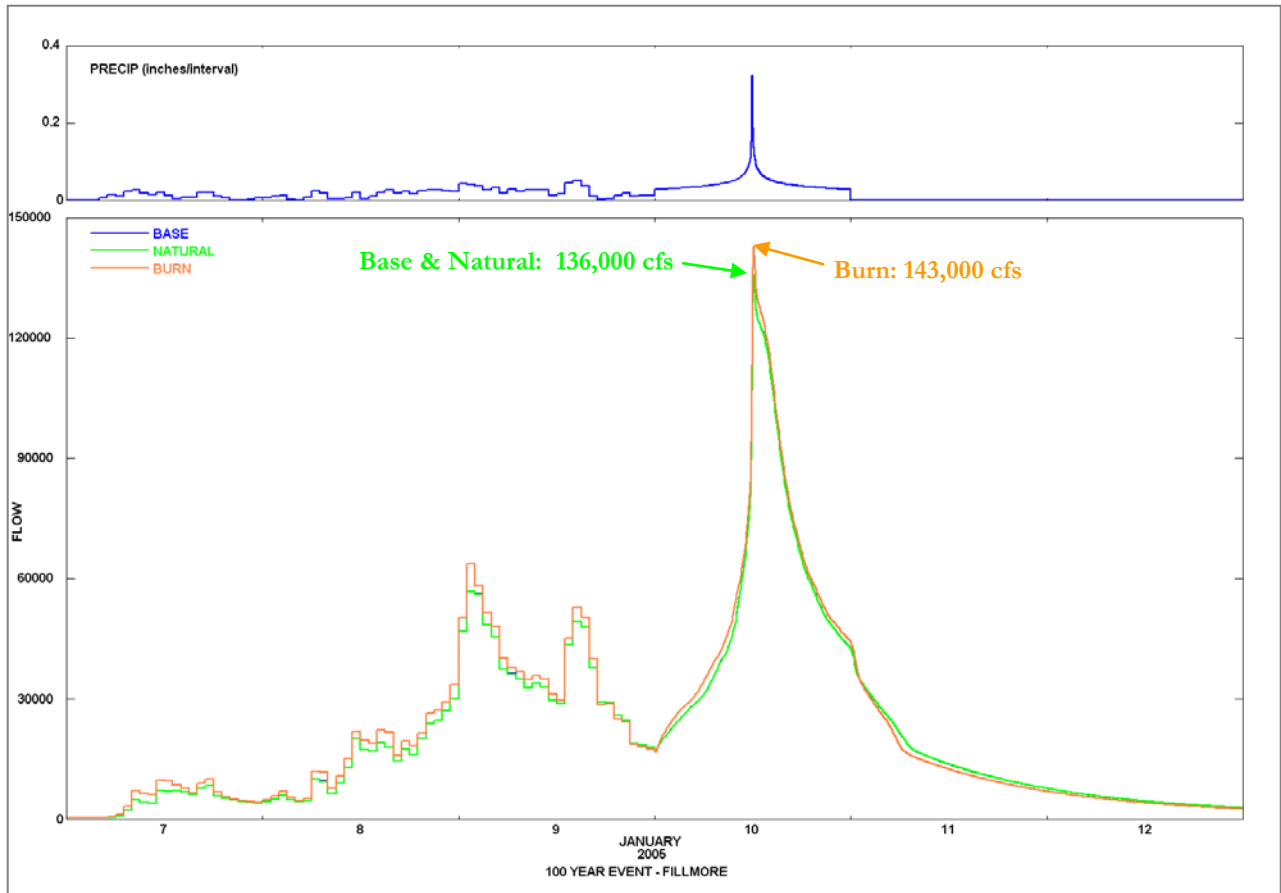


Figure 10-2. 100-year Burn and Pre-burn Design Hydrographs for Sespe Creek (AQUA TERRA, 2010)

For burned conditions, the following hydrologic parameters were adjusted:

- Reduced vegetation and litter interception parameter by 90%
- Reduced infiltration parameters by 35% - based on Los Angeles County methodology
- Reduced the upper zone soil moisture storage parameter and interflow by 50%.
- Reduced the soil evapotranspiration (ET) parameter by 70%
- Reduced riparian ET parameter to zero

No changes were made to the lower zone soil moisture storage parameter on the assumption that the fire impacts would not extend below the surface and upper soil zones.

10.4.3 HEC-HMS (Hydrologic Modeling System)

In Ventura County, the HEC-HMS computer program can be applied to undeveloped, intermediate to large sized watersheds to model flood peaks and volumes. Unit hydrographs and associated S-graphs have been developed by the VCWPD for use with the HEC-HMS model for unburned hydrology conditions, and are described in the design hydrology manual (VCWPD, 2010a). The hydrology manual also describes the use of the Snyder synthetic unit hydrograph, the USACE lag equation, and a uniform and constant loss approach. According to the hydrology manual, in the County HEC-HMS modeling should not be used on developed or mixed- use watersheds, or on watersheds less than 3,200 acres in size.

There has been some research effort over the past decade using HEC-HMS to predict post-fire conditions. For example, McLin et al. (2001) studied the immediate post-fire period using HEC-HMS (and HEC-RAS) to establish floodplain boundaries and guide detention structure construction after the Cerro Grande fire in northern New Mexico. Cydzik and Hogue (2009) investigated the ability of HEC-HMS to simulate pre- and post-fire discharge of a burned watershed in San Bernardino County, California. The primary objective of the San Bernardino study was to simulate immediate post-fire floods and evaluate model performance over several rainy seasons after the fire. The Natural Resources Conservation Service (NRCS) Curve Number (CN) method was selected to simulate the runoff within the HEC-HMS model. Results of the simulation showed that the post-fire curve numbers were significantly higher immediately following the fire, but returned to near pre-fire values by the end of the second year. The initial abstraction values did not return to pre-fire conditions until the end of the third rainy season. Lag time, however, remained significantly lower than the pre-fire values throughout the three-year study period (Cydzik and Hogue, 2009).

Important parameters that could require adjustment, depending on the methods used in HEC-HMS, include the following:

- Reduced evapotranspiration (ET) (zero for high burn)
- Reduced interception and initial losses (zero for high burn)
- Reduced moisture storage capacity of surface organic material (zero for high burn)
- Reduced moisture storage capacity of surface or upper zone soil layer (mineral soil values for high burn)
- Reduced infiltration rates (hydrophobic mineral soil may approach impervious values for high burn)
- Reduced overland flow surface roughness (bare soil *n* value for high burn)
- Reduced surface roughness for rill/gully/channel (non-vegetated channel *n* values for high burn)
- Reduced interflow due to loss of litter/duff layer (near loss of interflow for high burn)
- Reduced watershed lag time (decrease of basin *n* value to 0.03 for high burn)

Until post-burn unit hydrographs and associated S-graphs have been developed for Ventura County, it is recommended that a BSF be applied to the unburned peak discharges and hydrographs. Other parameters may require adjustment, depending on which methods are used in HEC-HMS.

10.4.4 Flood Frequency Analysis

For sites with available streamgage data, a flood frequency analysis can be performed using Bulletin 17B procedures with the HEC-SSP computer program. For discharges computed by a flood frequency analysis of stream gage data, the recommended approach for post-fire adjustment depends on whether it is an emergency project or another project that requires the computation of the post-burn peak flow. For example, an emergency project would use the BSF as a direct multiplier to the peak flow estimate to compute the post-fire peak runoff. However, the approach for emergency projects is somewhat conservative because the recorded peak discharges already include the effect of historic fires to some extent.

For other design projects, if the period of record is sufficient at the stream gage to perform a flood frequency analysis, the recorded peak discharges should include the effect of historic fires in the watershed. Therefore, an adjustment for the post-fire peak discharge is not required for design.

11 BURN SEVERITY FACTORS

Burn severity is a term used to describe the magnitude of fire effects on vegetation and soil. There are four general categories typically used by USGS and others to describe burn severity: unburned/very low burn, low burn, moderate burn, and high burn. In order to simulate the effect of the burn on hydrologic function, each burn severity class has been assigned a “burn severity factor” or BSF. This chapter describes the methods used to determine these factors and how they should be applied to Ventura County projects.

11.1 Burn Severity Maps

Burn severity data were obtained from the USGS Monitoring Trends in Burn Severity (MTBS) Project (<http://mtbs.gov/dataquery/customquery.html>) and were available for most wildfires that have occurred since 1984. These maps were created by the USGS Center for Earth Resources Observation and Science and the USDA Forest Service Remote Sensing Application Center using Landsat7 satellite imagery at 30-meter spatial resolution. The burn severity maps are primarily used to analyze trends in burn severity and to aid in policy making decisions within an affected watershed. Applicable maps for the current study, as well as a detailed description of the burn severity categories, are included in Appendix B.

It should be noted that the MTBS burn severity maps are generally based on an extended assessment of the vegetative conditions and pre-fire vegetation density, and can vary from maps made during an immediate assessment (typically within 7 days of fire containment) of burned soil to create the Burned Area Reflectance Classification (BARC) maps used to help rapid response crews temporarily stabilize the watershed.

11.2 Proposed Burn Severity Factors

Table 11-1 presents the recommended burn severity factors for each of the burn severity classes, which apply to a condition up to 6 months following a burn. The BSF can be applied to clear-water, pre-burn hydrology peaks and hydrographs prior to applying a sediment/debris bulking factor.

Table 11-1. Proposed Burn Severity Factors

Burn Condition	BSF	Description
Unburned to Very Low Burn	1.0	No fire in eight years or very light burn (<i>Note: Complete watershed recovery of chaparral is normally expected after eight wet seasons</i>).
Low Burn	1.3	Black ash and blackened vegetation 0 to 6 months after burn. Low burn areas recover faster because the surface soil seeds and chaparral roots are largely intact.
Moderate Burn	1.6	Grey ash with most duff, litter and vegetation consumed
High Burn	2.0	White or reddish ash with all vegetation and surface and sub-surface organic material consumed to mineral soil. Formation of hydrophobic soils would be expected. High burn are may take over ten years to recover due to loss of surface seeds and chaparral roots.

Figure 11-1 shows the proposed burn severity factors vs. years since burn for the low, moderate, and high burn severity factors. These factors are summarized in Table 11-2. The BSF decreases at a rate similar to the VCWPD FF curve, both based on watershed recovery after eight wet seasons.

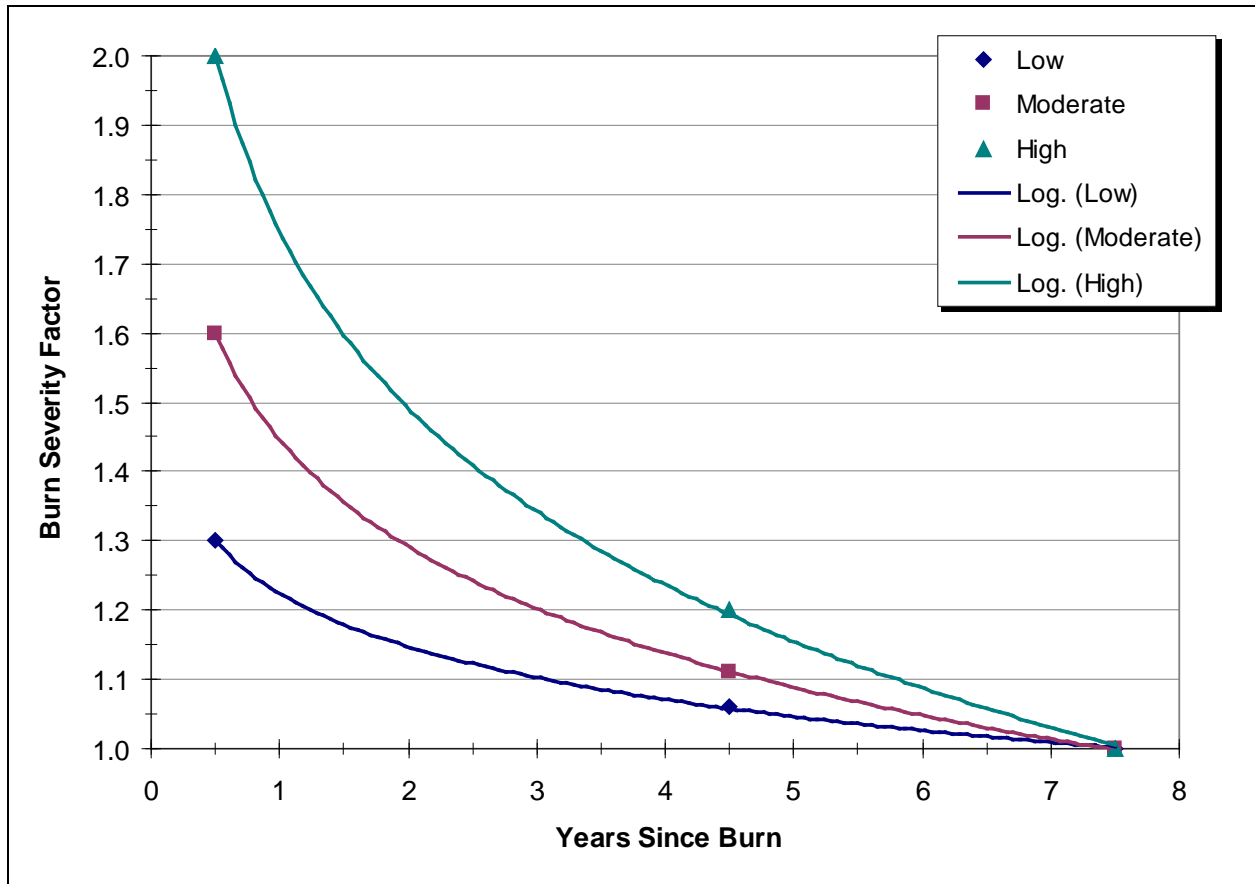


Figure 11-1. Proposed Burn Severity Factors vs. Years since Burn

Table 11-2. Proposed Burn Severity Factors vs. Years since Burn

Years Since Burn	FF	BURN CONDITION		
		Low Burn	Moderate Burn	High Burn
0.5 <i>(after one wet season)</i>	88	1.3	1.6	2.0
4.5 <i>(after five wet seasons)</i>	20	1.06	1.11	1.20
7.5 <i>(after eight wet seasons)</i>	1	1.0	1.0	1.0

For comparison, the FEMA (2003b) approach for emergency post-fire projects described in Section 10.2 recommends using a BSF of 1.0 for unburned/very low burn, 1.76 for low burn, 2.2 for moderate burn and 2.62 for high burn conditions (see Table 10-2). In areas where burn severity maps were not available, FEMA assumed a moderate burn condition of 2.2. The two studies differ in part because the FEMA BSF values are for immediate post-burn conditions, while the current study BSF values are based on conditions up to 6 months after a burn.

11.3 Ventura County Fires and Design BSF

For an emergency post-fire project where a burn severity map is available, the burn severity factors listed in Table 11-2 can be used along with the map to compute a weighted BSF and the resulting post-fire peak discharge (Q_{burn}).

For an emergency project where a burn severity map is not available, the design BSF should be based on typical burn severities from Ventura County fires. This approach is also recommended for non-emergency projects where a BSF based on a single burn severity map is not appropriate. This is because the most recent fire in the watershed may have occurred years ago. Instead, the BSF should be based on a design condition of 4.5 years post-burn and typical Ventura County burn severities.

Typical burn severity data for such projects were obtained for 21 fires in Ventura County that have occurred since 1984 (maps are provided in Appendix B). Table 11-3 to Table 11-5 summarize by decade the area burned, percent burn severity, and weighted BSF for each of the fires used in the analysis. A design BSF of 1.5 was computed for conditions up to 6 months following a burn (i.e., corresponding to a fire factor of 88), and a BSF of 1.1 for conditions 4.5 years after a burn (Figure 11-2).

11.4 Application of BSF and Q_{burn}

Burn severity factors can be directly applied to Ventura County VCRat and HEC-HMS hydrologic model results to increase post-fire peaks and hydrographs.

11.4.1 Design Application of Q_{burn}

We recommend that the post-fire peak discharge (Q_{burn}) be computed in the design of the following projects:

1. *Emergency projects* intended to mitigate the effects of fire after a recent burn. The 10-year design event would be used, along with a BSF based on burn severity maps and a FF = 88, as listed in Table 11-2. If a burn severity map is not available, a BSF of 1.5 should be used.
2. *Critical infrastructure projects* (hospitals, schools, etc.) downstream of undeveloped areas subject to frequent burns. A watershed is considered to be subject to frequent burns if the VCWPD weighted average fire factor has exceeded the design FF of 20 in more than 10% of the years since 1969. The design condition would be the same as the detention basin criteria i.e., the project is designed for 4.5 years after a total burn of the watershed. This corresponds to a BSF of 1.1.

Table 11-3. Ventura County Fires (1984 to 1989) – Area and Percent Burned

Burn Condition	Grimes Fire 1984		Squaw Flat 1984		Box Canyon 1985		Ferndale Fire 1985		Wheeler #2 Fire 1985		Bradley Fire 1986		Keuhner Fire 1988	
	Acres	% Burned	Acres	% Burned	Acres	% Burned	Acres	% Burned	Acres	% Burned	Acres	% Burned	Acres	% Burned
Unburned to Very Low Burn	710	7	2,780	49	562	46	19,614	51	23,956	20	1,481	15	200	5
Low Burn	6,781	62	1,582	28	670	54	14,786	38	24,202	20	8,128	81	3,434	88
Moderate Burn	3,427	31	900	16	2	0	3,665	10	39,011	32	377	4	262	7
High Burn	0	0	423	7	0	0	469	1	33,772	28	0	0	4	0
<i>Weighted BSF:</i>	<i>1.37</i>		<i>1.25</i>		<i>1.16</i>		<i>1.18</i>		<i>1.53</i>		<i>1.27</i>		<i>1.31</i>	

Table 11-4. Ventura County Fires (1990 to 1999) –Area and Percent Burned

Burn Condition	Chatsworth Fire#2 1993		Steckel Fire 1993		Wheel Fire 1993		Aliso Fire 1994		Hopper Fire 1997		Piru Incident Fire 1998	
	Acres	% Burned	Acres	% Burned	Acres	% Burned	Acres	% Burned	Acres	% Burned	Acres	% Burned
Unburned to Very Low Burn	281	14	10,841	43	55	4	1,618	48	6,872	30	2,324	23
Low Burn	1,546	79	12,023	48	326	22	1,203	35	7,666	33	4,802	48
Moderate Burn	119	6	2,040	8	977	67	518	15	5,896	26	2,531	25
High Burn	0	0	88	0	102	7	66	2	2,585	11	379	4
<i>Weighted BSF:</i>	<i>1.28</i>		<i>1.20</i>		<i>1.54</i>		<i>1.22</i>		<i>1.37</i>		<i>1.33</i>	

Table 11-5. Ventura County Fires (2000 to 2008) –Area and Percent Burned

Burn Condition	Adams Canyon 2003		Simi Fire 2003		Piru Fire 2003		Topanga Fire 2005		School Incident Fire 2005		Day Fire 2006		Ranch Fire 2007		Sesnon Fire 2008	
	Acres	% Burned	Acres	% Burned	Acres	% Burned	Acres	% Burned	Acres	% Burned	Acres	% Burned	Acres	% Burned	Acres	% Burned
Unburned to Very Low Burn	286	23	43,283	45	9,380	15	1,568	7	1,717	63	9,602	6	10,430	35	910	6
Low Burn	881	72	33,139	34	7,205	11	5,512	23	786	29	64,835	41	13,600	45	7,096	47
Moderate Burn	54	4	20,502	21	20,095	31	13,328	55	220	8	58,215	36	5,560	18	6,817	45
High Burn	0	0	0	0	27,180	43	3,680	15	17	1	27,053	17	528	2	389	3
<i>Weighted BSF:</i>	<i>1.24</i>		<i>1.23</i>		<i>1.65</i>		<i>1.55</i>		<i>1.14</i>		<i>1.51</i>		<i>1.26</i>		<i>1.43</i>	

Table 11-6. Proposed Burn Severity Factor for Emergency Projects (6 months post-burn)

Burn Condition	Proposed BSF	Average Weighted % Burn	Computed BSF Range	% Burn <i>used for Design</i>	Proposed Weighted BSF <i>for design</i>
Unburned to Very Low Burn	1.0	26	1.14 to 1.65	10	1.5
Low Burn	1.3	45		40	
Moderate Burn	1.6	22		35	
High Burn	2.0	7		15	

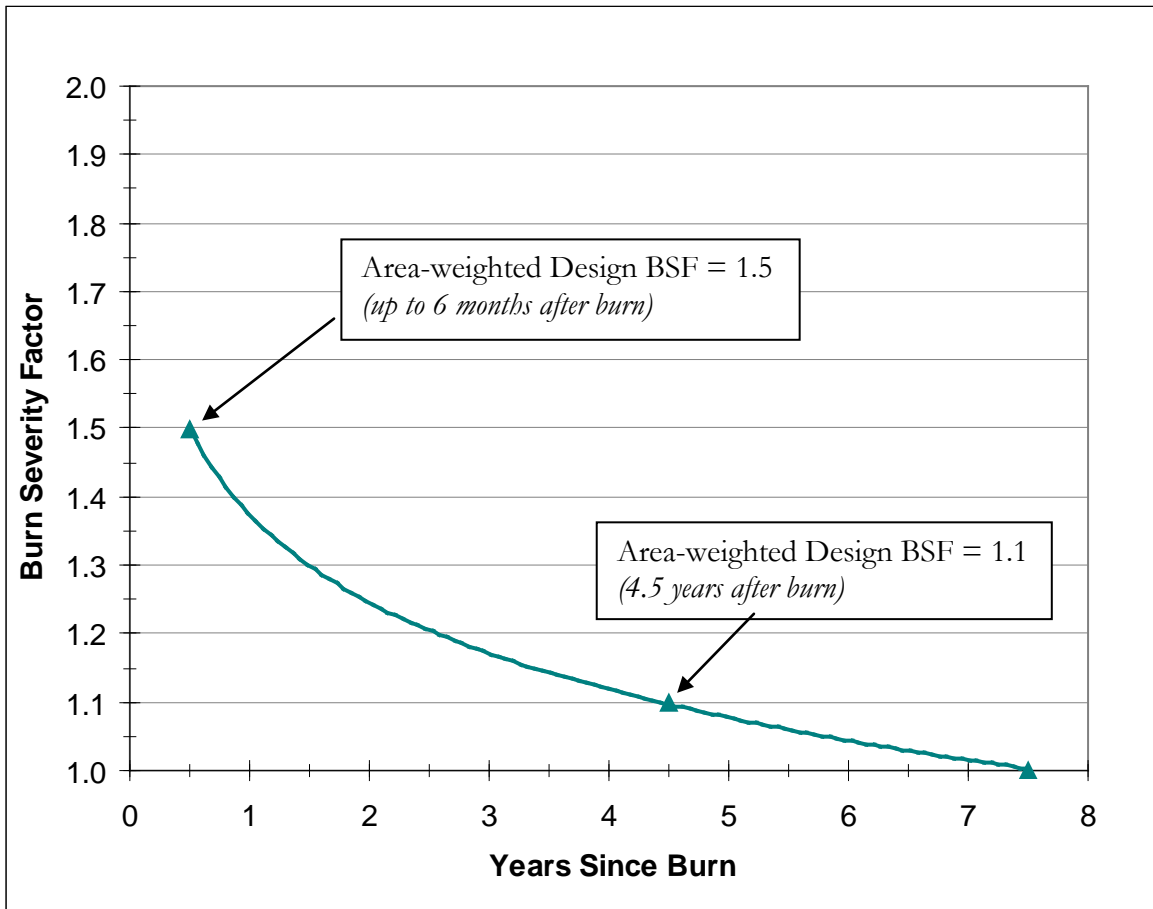


Figure 11-2. Proposed Burn Severity Factor for Design vs. Years since Burn

3. *Projects downstream from known high sediment-producing watersheds* subject to frequent burns, and where damage has occurred due to excessive sedimentation and associated flooding in the past. The design condition would be 4.5 years after total burn of the watershed (BSF = 1.1).

A flowchart for selecting the BSF and computing Q_{burn} is provided in Chapter 13. Post-fire peak flow (Q_{burn}) should be computed prior to applying a sediment/debris bulking factor.

11.4.2 Critical Infrastructure

Critical infrastructure in Ventura County includes facilities deemed important for public safety, emergency response, and/or disaster recovery functions. Most commonly associated with the term “critical infrastructure” are the following facilities (Association of State Floodplain Managers, 2010):

- **Governmental Facilities:** Essential for the delivery of critical services and crisis management, including data and communication centers, key government complexes, etc.
- **Essential Facilities:** Those that are vital to health and welfare of entire populations, including hospitals and other medical facilities, retirement homes, police and fire departments, emergency operations centers, prisons, evacuation shelters, and schools, etc.
- **Transportation Systems:** Those systems, and the supporting infrastructure, necessary for transport of people and resources (including airports, highways, railways, and waterways) during major disasters, including flood events up to the 500-year flood.
- **Lifeline Utility Systems:** Those vital to public health and safety, including potable water, wastewater, oil, natural gas, electric power, communication systems, etc.
- **High Potential Loss Facilities:** Failure or disruption of operations may have significant physical, social, environmental, and/or economic impact to neighboring communities, including nuclear power plants, high-hazard dams, urban levees, and military installations.
- **Hazardous Material Facilities:** Involved in the production, storage, and/or transport of corrosives, explosives, flammable materials, radioactive materials, toxins, etc.

12 FIRE FACTOR PROBABILITY ANALYSIS

A joint probability analysis was performed using fire history data from several watersheds within Ventura County. The purpose of the analysis was to determine the probability of having a 10-year or 50-year storm or larger after the watershed has been recently burned, and to evaluate a design burn and bulked condition policy for VCWPD based on the results. The new policy would be applicable to design storm hydrographs for future facility projects. This chapter describes the fire factor (FF) probability analysis, while the resulting policy recommendations are made in Chapter 13.

12.1 Background

Data used in the analysis were provided by the VCWPD, including fire history (1929 to 2010) and weighted fire factors. Ten watersheds, located within VCWPD Zones 1, 2, and 3, were analyzed. These watersheds are listed in Table 12-1 and shown in Figure 12-1.

Table 12-1. Watersheds used in Fire Factor Analysis

Zone	Watershed	Drainage Area (mi ²)	General Location
1	Cañada Larga	19.2	SE of Ojai; NW of Santa Paula
	Matilija North Fork	16.1	Ojai
	Stewart Canyon	1.9	Ojai
2	Adams Barranca	8.4	Santa Paula
	Aliso Canyon	14.4	Santa Paula
	Hopper Canyon	23.9	Fillmore (near Piru)
	Pole Creek	8.6	Fillmore
3	Coyote Canyon	7.0	Moorpark
	Gabbert Canyon	3.8	Moorpark
	White Oak Creek	6.9	Simi Valley

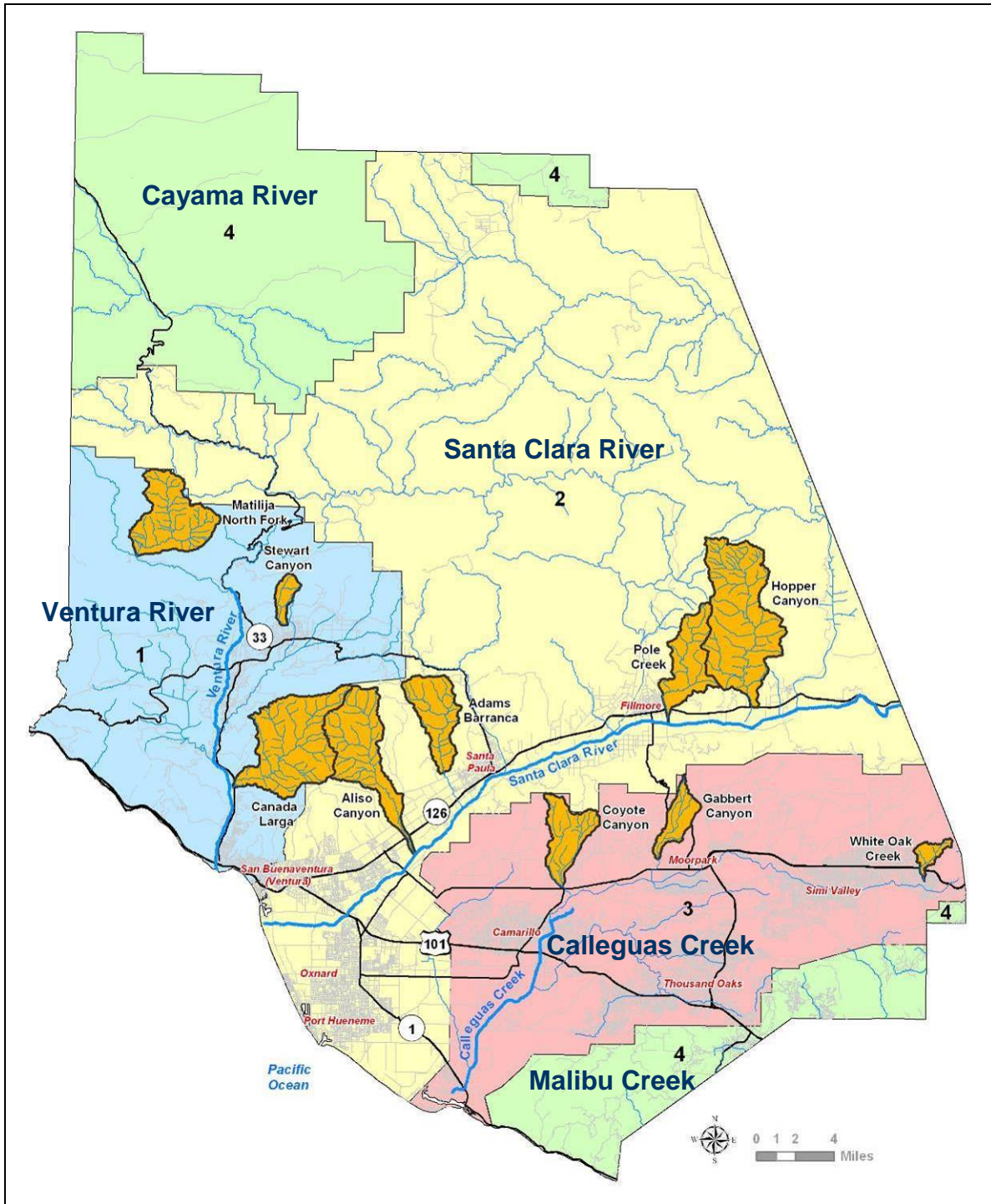


Figure 12-1. Ventura County Watersheds and Basin Zone Map used in the Fire Factor Analysis

The VCWPD currently uses a weighted FF of 20 to estimate the sediment delivery for detention basin design. A FF of 20 represents a general watershed condition 4.5 years post-burn (see Section 5.2). The appropriateness of this design factor was originally evaluated based on the entire recorded fire history, from 1929 to the 2010 (VCWPD, 2010b). The results show that the joint probability of a 10-year storm or greater and a design FF of 20 or greater occurring in the same year ranges from 1.1% (recurrence interval of 90 years) for Stewart Canyon to 2.0% (recurrence interval of 51 years) for White Oak Creek (Table 12-2).

Based on the scope of the current study, joint probability was computed based on the assumption of independence between the peak discharge and fire factor. However, it is important to note that fire and large flow events are not strictly independent because the probability of having a relatively high fire factor in one year is predetermined if there is a high FF in the previous year. Also, a high FF may lead to a higher than normal peak discharge due to post-fire hydrologic impacts. As a result, the computed probabilities presented in this section would tend to be on the low side, i.e., actual probabilities would be somewhat higher.

The probability of having the two independent events (peak discharge and design FF) occur in the same year is the product of their individual probabilities:

$$\text{Prob}(\geq \text{peak Q and } \geq \text{design FF}) = \text{Prob}(\geq \text{peak Q}) * \text{Prob}(\geq \text{design FF}) \quad (12.1)$$

Table 12-2. Joint Probability of FF ≥ 20 and 10-year Storm Event – Fire History 1929 to 2010

Zone	Watershed	FF ≥ 20		Joint Probability FF ≥ 20 & 10-year or greater event	
		Exceedance Probability	Recurrence Interval (yrs)	Exceedance Probability	Recurrence Interval (yrs)
1	Cañada Larga	13%	8	1.3%	80
	Matilija North Fork	15%	7	1.5%	67
	Stewart Canyon	11%	9	1.1%	90
2	Adams Barranca	15%	7	1.5%	68
	Aliso Canyon	16%	6	1.6%	62
	Hopper Canyon	14%	7	1.4%	73
	Pole Creek	18%	6	1.8%	57
3	Coyote Canyon	12%	8	1.2%	81
	Gabbert Canyon	19%	5	1.9%	54
	White Oak Creek	20%	5	2.0%	51

The risk of having a 50-year design event or greater with a FF ≥ 20 during the 50-year design life of a detention facility ranges from 11% to 18% (Table 12-3). This range is less than (but generally comparable to) the 40% risk of having a 100-year storm during the 50-year design life. However, these results are based on historical data with fairly infrequent fire occurrences prior to 1970. Data available after 1970 show that fires are generally occurring more frequently compared to previous years, so the probability of having a high FF may also be increasing. For this reason, the current design FF of 20 was re-evaluated using fire events from 1970 to 2010.

As shown in Table 12-4, the largest increase in fire frequency was seen in the Zone 2 watersheds, including Adams Barranca, Aliso Canyon, Hopper Canyon, and Pole Creek, as well as White Oak Creek in Zone 3. Although the majority of the watersheds evaluated had an increased fire frequency, there were three watersheds—Matilija North Fork, Stewart Canyon, and Gabbert Canyon—where the fire frequency in terms of FF was either lower over the more recent period or relatively unchanged.

Table 12-3. Probability of 50-year Event and FF ≥ 20 during 50-year Design Life –1929 to 2010

Zone	Watershed	FF ≥ 20 and Q ≥ 50-year
1	Cañada Larga	12%
	Matilija North Fork	14%
	Stewart Canyon	11%
2	Adams Barranca	14%
	Aliso Canyon	15%
	Hopper Canyon	13%
	Pole Creek	16%
3	Coyote Canyon	12%
	Gabbert Canyon	17%
	White Oak Creek	18%
Ranges:	<i>Minimum</i>	11%
	<i>Average</i>	14%
	<i>Maximum</i>	18%

Table 12-4. Number of Fires and Years with FF ≥ 20: 1929 to 1969 and 1970 to 2010

Zone	Watershed	Fire History 1929 to 1969		Fire History 1970 to 2010	
		Number of Fires (total area burned)	Number of Years FF ≥ 20	Number of Fires (total area burned)	Number of Years FF ≥ 20
1	Cañada Larga	5 (8,251 acres)	3	8 (19,138 acres)	7
	Matilija North Fork	2 (15,040 acres)	7	3 (11,655 acres)	5
	Stewart Canyon	1 (1,217 acres)	4	2 (1,248 acres)	5
2	Adams Barranca	2 (3,228 acres)	2	5 (12,463 acres)	10
	Aliso Canyon	4 (1,631 acres)	0	7 (24,080 acres)	13
	Hopper Canyon	6 (4,880 acres)	0	6 (38,474 acres)	11
	Pole Creek	1 (554 acres)	0	7 (18,472 acres)	14
3	Coyote Canyon	4 (4,936 acres)	3	6 (4,901 acres)	7
	Gabbert Canyon	3 (3,511 acres)	8	3 (4,283 acres)	7
	White Oak Creek	8 (2,724 acres)	1	11 (14,729 acres)	15

12.2 Fire Factor Probability Analysis (1970-2010)

For each watershed, a weighted FF was calculated based on the burned and unburned areas existing during each year between 1970 and 2010. Areas affected by more than one fire within the 7.5-year recovery period were accounted for in the analysis. Figure 12-2 to Figure 12-4 show the computed FF values separated by watershed zone. A fire factor probability analysis was then performed, with results shown in Table 12-5 to Table 12-12. The probability of exceedance for a range of fire factors was analyzed (FF = 10, 15, 20, and 30), as well as the joint probability of that FF occurring in with the 10-year or 50-year peak discharge in any given year. Recurrence intervals associated with the computed probabilities have also been provided.

For the 1970-2010 period, the joint probability of a 10-year peak discharge or greater and a design FF of 20 or greater occurring in the same year ranges from 1.2% (*recurrence interval of 82 years*) for Stewart Canyon to 3.8% (*recurrence interval of 27 years*) for White Oak Creek (Table 12-9).

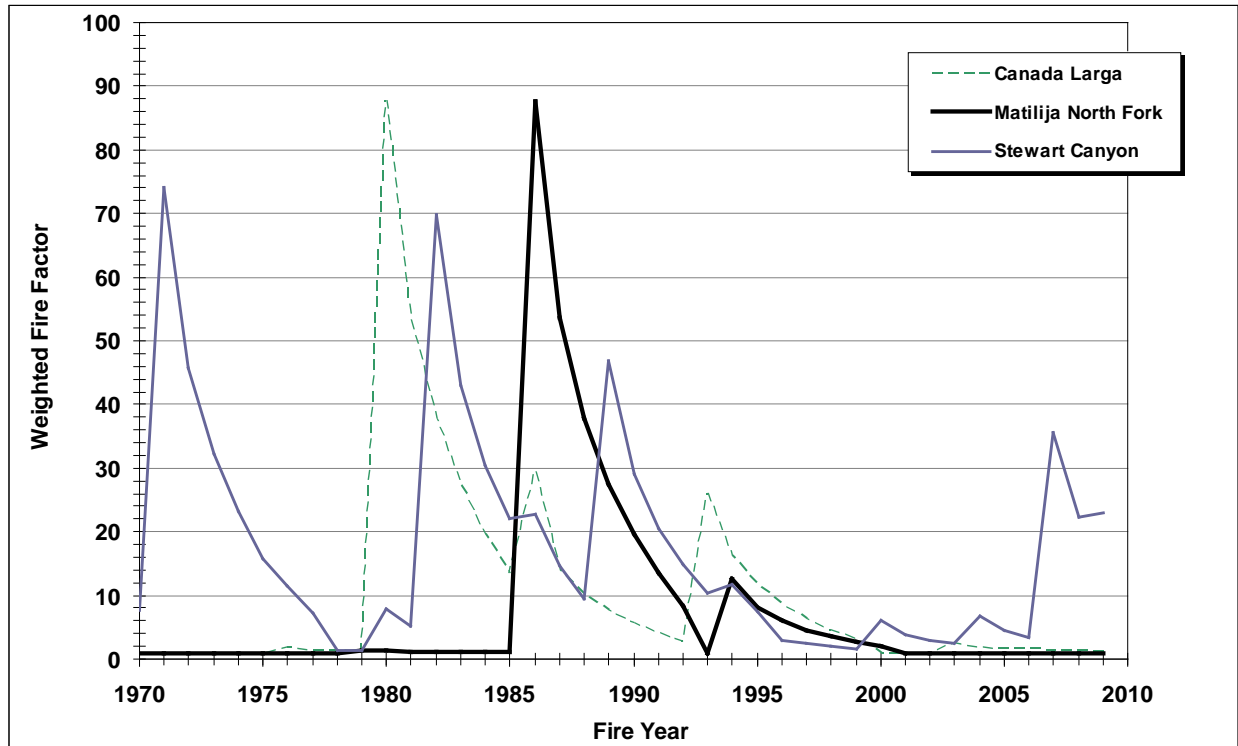


Figure 12-2. Weighted Fire Factor vs. Fire Year (between 1970 to 2010) – Zone 1

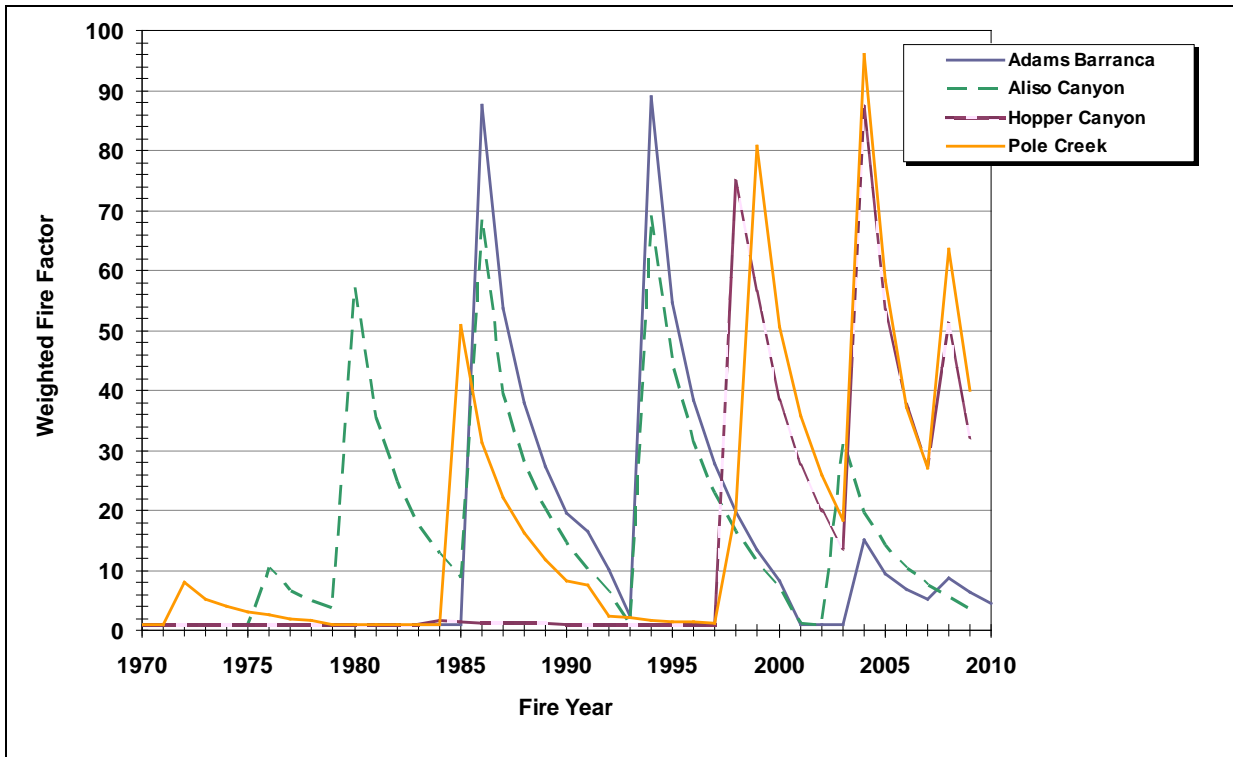


Figure 12-3. Weighted Fire Factor vs. Fire Year (between 1970 to 2010) – Zone 2

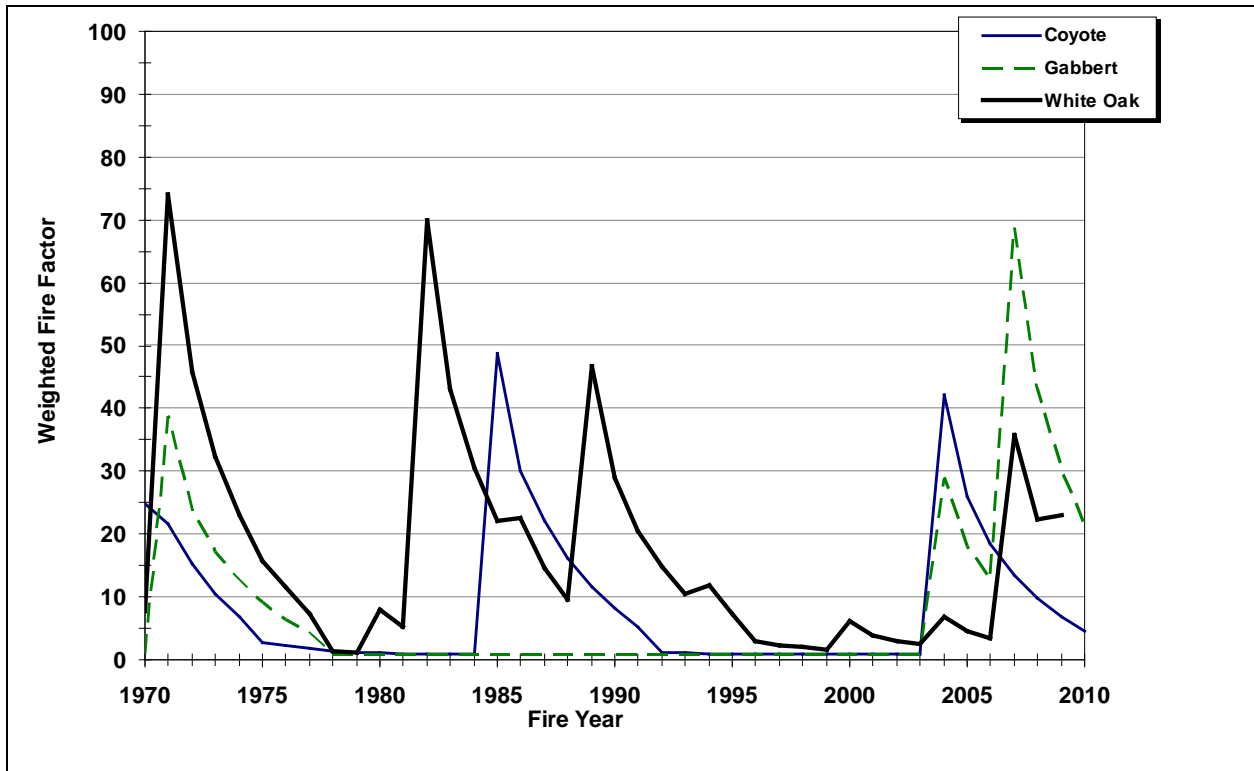


Figure 12-4. Weighted Fire Factor vs. Fire Year (between 1970 to 2010) – Zone 3

Table 12-5. Joint Probability of a **FF ≥ 10** and a **10-year** Storm Event – Fire History 1970 to 2010

Zone	Watershed	FF ≥ 10		Joint Probability <i>FF ≥ 10 & 10-year or greater event</i>	
		Exceedance Probability	Recurrence Interval (yrs)	Exceedance Probability	Recurrence Interval (yrs)
1	Cañada Larga	30%	3	3.0%	33
	Matilija North Fork	18%	6	1.8%	57
	Stewart Canyon	17%	6	1.7%	59
2	Adams Barranca	37%	3	3.7%	27
	Aliso Canyon	56%	2	5.6%	18
	Hopper Canyon	30%	3	3.0%	33
	Pole Creek	43%	2	4.3%	24
3	Coyote Canyon	34%	3	3.4%	29
	Gabbert Canyon	27%	4	2.7%	37
	White Oak Creek	53%	2	5.3%	19

Table 12-6. Joint Probability of a **FF ≥ 10** and a **50-year** Storm Event – Fire History 1970 to 2010

Zone	Watershed	FF ≥ 10		Joint Probability <i>FF ≥ 10 and 50-year or greater event</i>	
		Exceedance Probability	Recurrence Interval (yrs)	Exceedance Probability	Recurrence Interval (yrs)
1	Cañada Larga	30%	3	0.60%	167
	Matilija North Fork	18%	5	0.35%	286
	Stewart Canyon	17%	6	0.34%	293
2	Adams Barranca	37%	3	0.73%	137
	Aliso Canyon	56%	2	1.1%	91
	Hopper Canyon	30%	3	0.60%	167
	Pole Creek	43%	2	0.85%	118
3	Coyote Canyon	34%	3	0.68%	146
	Gabbert Canyon	27%	4	0.54%	186
	White Oak Creek	53%	2	1.1%	95

Table 12-7. Joint Probability of a **FF ≥ 15** and a **10-year** Storm Event – Fire History 1970 to 2010

Zone	Watershed	FF ≥ 15		Joint Probability <i>FF ≥ 15 and 10-year or greater event</i>	
		Exceedance Probability	Recurrence Interval (yrs)	Exceedance Probability	Recurrence Interval (yrs)
1	Cañada Larga	20%	5	2.0%	50
	Matilija North Fork	13%	8	1.3%	80
	Stewart Canyon	15%	7	1.5%	68
2	Adams Barranca	29%	3	2.9%	34
	Aliso Canyon	40%	3	4.0%	25
	Hopper Canyon	28%	4	2.8%	36
	Pole Creek	40%	3	4.0%	25
3	Coyote Canyon	24%	4	2.4%	41
	Gabbert Canyon	22%	5	2.2%	46
	White Oak Creek	45%	2	4.5%	22

Table 12-8. Joint Probability of a **FF ≥ 15** and a **50-year** Storm Event – Fire History 1970 to 2010

Zone	Watershed	FF ≥ 15		Joint Probability <i>FF ≥ 15 and 50-year or greater event</i>	
		Exceedance Probability	Recurrence Interval (yrs)	Exceedance Probability	Recurrence Interval (yrs)
1	Cañada Larga	20%	5	0.40%	250
	Matilija North Fork	13%	8	0.25%	400
	Stewart Canyon	15%	7	0.29%	342
2	Adams Barranca	29%	3	0.59%	171
	Aliso Canyon	40%	3	0.80%	125
	Hopper Canyon	28%	4	0.55%	182
	Pole Creek	40%	3	0.80%	125
3	Coyote Canyon	24%	4	0.49%	205
	Gabbert Canyon	22%	5	0.44%	228
	White Oak Creek	45%	2	0.90%	111

Table 12-9. Joint Probability of a **FF ≥ 20** and a **10-year** Storm Event – Fire History 1970 to 2010

Zone	Watershed	FF ≥ 20		Joint Probability <i>FF ≥ 20 and 10-year or greater event</i>	
		Exceedance Probability	Recurrence Interval (yrs)	Exceedance Probability	Recurrence Interval (yrs)
1	Cañada Larga	18%	6	1.8%	57
	Matilija North Fork	13%	8	1.3%	80
	Stewart Canyon	12%	8	1.2%	82
2	Adams Barranca	24%	4	2.4%	41
	Aliso Canyon	33%	3	3.3%	31
	Hopper Canyon	28%	4	2.8%	36
	Pole Creek	35%	3	3.5%	29
3	Coyote Canyon	17%	6	1.7%	59
	Gabbert Canyon	17%	6	1.7%	59
	White Oak Creek	38%	3	3.8%	27

Table 12-10. Joint Probability of a **FF ≥ 20** and a **50-year** Storm Event – Fire History 1970 to 2010

Zone	Watershed	FF ≥ 20		Joint Probability <i>FF ≥ 20 and 50-year or greater event</i>	
		Exceedance Probability	Recurrence Interval (yrs)	Exceedance Probability	Recurrence Interval (yrs)
1	Cañada Larga	18%	6	0.39%	286
	Matilija North Fork	13%	8	0.25%	400
	Stewart Canyon	12%	8	0.24%	410
2	Adams Barranca	24%	4	0.49%	205
	Aliso Canyon	33%	3	0.65%	154
	Hopper Canyon	28%	4	0.55%	182
	Pole Creek	35%	3	0.70%	143
3	Coyote Canyon	17%	6	0.34%	293
	Gabbert Canyon	17%	6	0.34%	293
	White Oak Creek	38%	3	0.75%	133

Table 12-11. Joint Probability of a **FF ≥ 30** and a **10-year** Storm Event – Fire History 1970 to 2010

Zone	Watershed	FF ≥ 30		Joint Probability <i>FF ≥ 30 and 10-year or greater event</i>	
		Exceedance Probability	Recurrence Interval (yrs)	Exceedance Probability	Recurrence Interval (yrs)
1	Cañada Larga	10%	10	1.0%	100
	Matilija North Fork	8%	13	0.8%	133
	Stewart Canyon	7%	14	0.7%	137
2	Adams Barranca	15%	7	1.5%	68
	Aliso Canyon	20%	5	2.0%	50
	Hopper Canyon	20%	5	2.0%	50
	Pole Creek	25%	4	2.5%	40
3	Coyote Canyon	7%	14	0.7%	137
	Gabbert Canyon	10%	10	1.0%	103
	White Oak Creek	20%	5	2.0%	50

Table 12-12. Joint Probability of a **FF ≥ 30** and a **50-year** Storm Event – Fire History 1970 to 2010

Zone	Watershed	FF ≥ 30		Joint Probability <i>FF ≥ 30 and 50-year or greater event</i>	
		Exceedance Probability	Recurrence Interval (yrs)	Exceedance Probability	Recurrence Interval (yrs)
1	Cañada Larga	10%	10	0.20%	500
	Matilija North Fork	8%	13	0.15%	667
	Stewart Canyon	7%	14	0.15%	683
2	Adams Barranca	15%	7	0.29%	342
	Aliso Canyon	20%	5	0.40%	250
	Hopper Canyon	20%	5	0.40%	250
	Pole Creek	25%	4	0.50%	200
3	Coyote Canyon	7%	14	0.15%	683
	Gabbert Canyon	10%	10	0.20%	513
	White Oak Creek	20%	5	0.40%	250

Table 12-13 presents the risk of having a peak discharge greater than or equal to either the 10-year or 50-year event along with the selected FF during the typical 50-year facility design life. For example, the risk of having a 50-year storm or greater occur with a $FF \geq 20$ during the 50-year design life ranges from 11 to 31 percent. The lowest risk, based on the 1970 to 2010 fire history, is for the Zone 1 watersheds (11 to 16 percent), which is significantly lower than the risk for Zone 2 watersheds (22 to 30 percent) and Zone 3 watersheds (16 to 31 percent).

The results for Zone 1 would indicate that a lower FF (e.g., $FF = 10$) may be more appropriate for design purposes. However, two important questions must be asked for these watersheds:

1. Do these watersheds have certain characteristics that make them less likely to burn, or are other factors involved (e.g., fewer arsonists have targeted the area, but could more affect it in the future)?
2. Does the lower frequency of burn in the past actually make it more likely that fires will occur in the future (due to increased dry fuels available)?

To shed some light on these questions, fire hazard mapping from CAL FIRE was examined. Table 12-14 and Table 12-15 summarize the fire class hazard (Moderate, High, and Very High) percentages for the VCWPD zones and study watersheds. The GIS shape files showing the fire hazard classes were obtained from CAL FIRE. Based on these data, the study watersheds in Zone 1 are considered to have the highest potential fire hazard, even though they have been less affected by recent fires and fire factor probabilities are lower.

12.3 Summary and Recommendations

Results from the probability analysis are summarized below:

- The risk of having the current design FF of 20 or greater in a year with a design storm of 50 years or greater ranges from 11% to 31% (fire years 1970 to 2010) during the 50-year design life (Table 12-13). These values compare well to the risk of 40% that at least one 100-year storm or greater will occur during the 50-year design life of a facility.
- Seven of the ten watersheds analyzed appear to be subjected to more frequent burns in the last 40 years (1970 to 2010) compared to the record from 1929 through 1969. These watersheds include: Zone 1 – Cañada Larga; Zone 2 – Adams Barranca, Aliso Canyon, Hopper Canyon and Pole Creek; Zone 3 – Coyote Canyon and White Oak Creek. However, based on the probability analysis, the current policy of using a FF of 20 is still reasonable for these watersheds.
- Study watersheds in Zone 1 are considered to have the highest potential fire hazard based on CAL FIRE data, even though they have been less affected by recent fires and fire factor probabilities are lower. As a result, we do not recommend that the design FF be lowered for watersheds in this zone.

Given these findings, we recommend that a design FF of 20 still be used for all watersheds where SCOTSED computations are required.

Table 12-13. Probability of 10-year or 50-year Event with a FF \geq Selected Values during a 50-year Design Life – Fire History 1970 to 2010

Zone	Watershed	FF \geq 10 and		FF \geq 15 and		FF \geq 20 and		FF \geq 30 and	
		Q \geq 10-yr	Q \geq 50-yr						
1	Cañada Larga	78%	26%	64%	18%	59%	16%	39%	10%
	Matilija North Fork	59%	16%	47%	12%	47%	12%	31%	7%
	Stewart Canyon	58%	16%	52%	14%	46%	11%	31%	7%
2	Adams Barranca	84%	31%	77%	25%	71%	22%	52%	14%
	Aliso Canyon	94%	42%	87%	33%	81%	28%	64%	18%
	Hopper Canyon	78%	26%	75%	24%	75%	24%	64%	18%
	Pole Creek	89%	35%	87%	33%	83%	30%	72%	22%
3	Coyote Canyon	82%	29%	71%	22%	58%	16%	31%	7%
	Gabbert Canyon	74%	24%	67%	20%	58%	16%	39%	9%
	White Oak Creek	93%	41%	90%	36%	85%	31%	64%	18%
	<i>Minimum</i>	58%	16%	47%	12%	46%	12%	31%	7%
	<i>Average</i>	79%	29%	72%	24%	67%	21%	50%	13%
	<i>Maximum</i>	94%	42%	90%	36%	85%	31%	72%	22%

Table 12-14. Fire Hazard Class Percentages for VCWPD Zones (based on CAL FIRE data)

Zone	Hazard Class		
	Moderate	High	Very High
1	6.9%	13%	75%
2	3.5%	4.8%	77%
3	8.7%	7.3%	55%
4	1.3%	3.1%	91%

Table 12-15. Fire Hazard Class Percentages for Study Watersheds (based on CAL FIRE data)

Zone	Watershed	Hazard Class		
		Moderate	High	Very High
1	Cañada Larga	0.3%	22%	78%
	Matilija North Fork	0%	0%	100%
	Stewart Canyon	0%	0%	100%
2	Adams Barranca	6.4%	8.4%	85%
	Aliso Canyon	9.9%	39%	47%
	Hopper Canyon	0.7%	20%	77%
	Pole Creek	1.9%	38%	60%
3	Coyote Canyon	13%	0%	53%
	Gabbert Canyon	11%	0%	47%
	White Oak Creek	0.2%	0.5%	99%

PART IV. POLICY RECOMMENDATIONS

13 SUMMARY OF RECOMMENDATIONS

The policy recommendations developed during the course of this study are summarized in this chapter. Included are recommendations for post-fire hydrology and sediment/debris bulking factors, as well as additional bulking topics investigated in this study.

13.1 Post-fire Hydrology

A flowchart outlining the recommended post-fire hydrology approach is provided as Figure 13-1 and is described below.

13.1.1 Design Application of Q_{burn}

We recommend that the post-fire clear water peak discharge (Q_{burn}) be computed in the design of the following projects:

1. *Emergency projects* intended to mitigate the effects of fire after a recent burn. The 10-year design event would be used, along with a Burn Severity Factor (BSF) based on burn severity maps and a design condition post-burn. If a burn severity map is not available, a BSF of 1.5 should be used.
2. *Critical infrastructure projects* (hospitals, schools, etc.) downstream of undeveloped areas subject to frequent burns. A watershed is considered to be subject to frequent burns if the weighted average fire factor has exceeded the design FF of 20 in more than 10% of the years since 1969. The design condition would be the same as the detention basin criteria, i.e., the project is designed for 4.5 years after a total burn of the watershed. This corresponds to a BSF of 1.1.
3. *Projects downstream from known high sediment-producing watersheds* subject to frequent burns, and where damage has occurred due to excessive sedimentation and associated flooding in the past. The design condition would be 4.5 years after total burn of the watershed (BSF = 1.1).

Q_{burn} should be computed prior to applying a sediment/debris bulking factor. The proposed computation of Q_{burn} is discussed below.

13.1.2 VCRat (Modified Rational Method)

For the MRM computations using the VCRat program, we recommend one approach for immediate implementation and another to supersede it at a later date once additional studies have been completed by the VCWPD.

Recommended Approach (Interim). To compute Q_{burn} , the BSF should be multiplied directly with the unburned MRM peak flow (Q_u) and hydrograph.

$$Q_{\text{burn}} = \text{BSF} \times Q_u \quad (13.1)$$

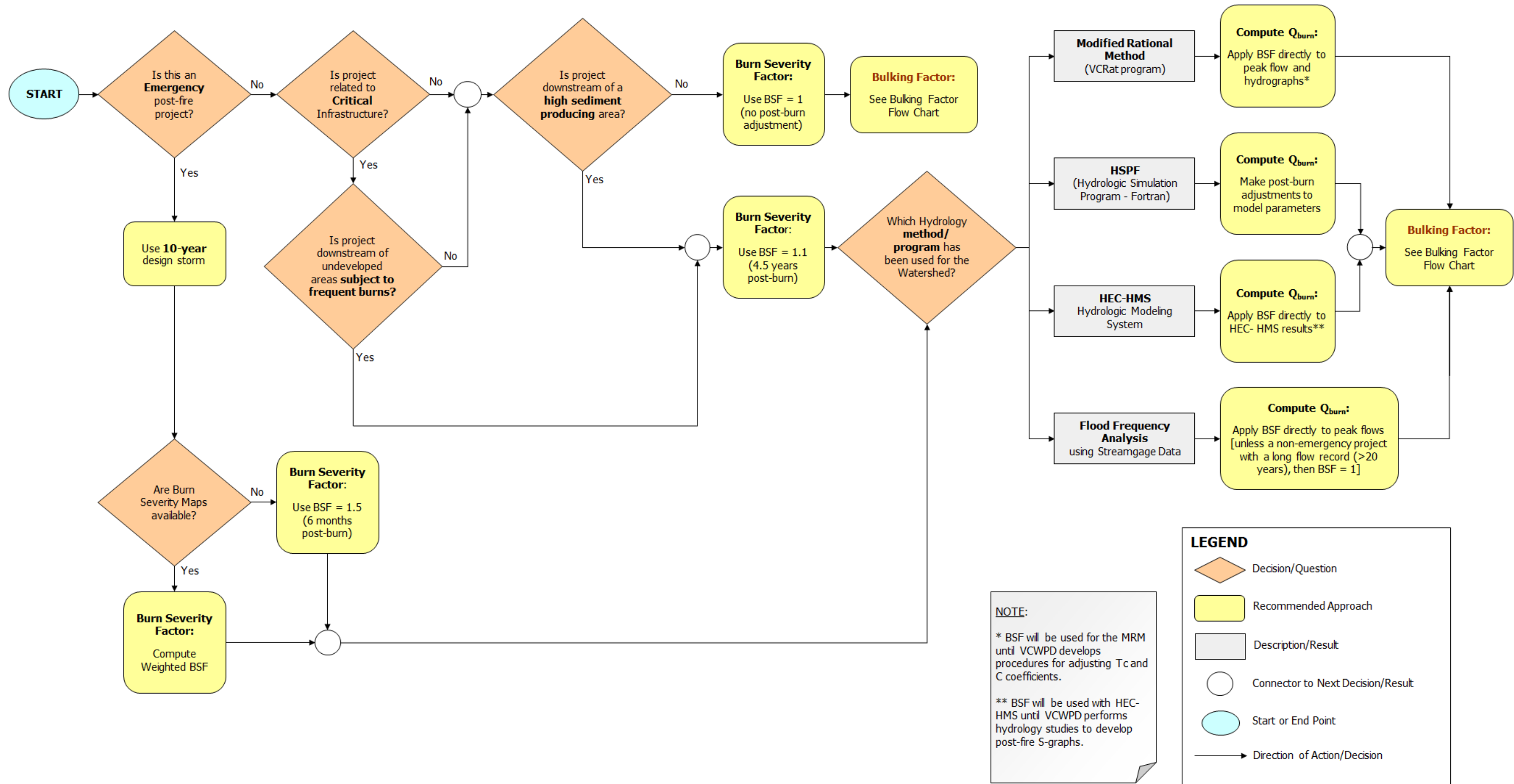


Figure 13-1. Post-fire Hydrology Flowchart

Recommended Approach (Future). To compute Q_{burn} , the runoff coefficient (C) and time of concentration (T_c) should be adjusted for post-burn conditions. To provide a procedure for adjusting the T_c in response to burned conditions, a new set of overland flow curves from the VCWPD is required. In addition, the T_c calculator and VCRat programs would have to be reprogrammed to provide the option of developing T_c 's and calculating peaks and hydrographs for burned conditions. Finally site-specific studies would have to be performed to quantify and confirm the increases in peaks associated with the proposed increases in C coefficients and decreases in T_c .

13.1.3 HSPF Modeling

For HSPF (Hydrologic Simulation Program – Fortran), post-burn adjustments should be made directly to the model parameters instead of applying the BSF to model results. Recommended parameter adjustments are summarized in Table 13-1. These adjustments are based on a recent study of the burned portion of the Sespe Creek watershed (AQUA TERRA, 2009).

Table 13-1. HSPF Parameters and Post-burn Adjustment

HSPF Parameter	Parameter Description	Post-burn Adjustment
CEPSC	Vegetation and litter interception	Reduce by 90%
INFILT	Infiltration	Reduce by 35%
UZSN INTFW	Upper zone soil moisture storage and interflow	Reduce by 50%
LZETP	Soil evapotranspiration	Reduce by 70%
ET	Riparian evapotranspiration	ET = 0
LZSN	Lower zone soil moisture storage parameter	No change

No change was made to the lower zone soil moisture storage parameter (LZSN) on the assumption that the fire impacts would not extend below the surface and upper soil zones.

13.1.4 HEC-HMS Modeling

For HEC-HMS modeling, we recommended one approach for immediate implementation and another to supersede it at a later date once additional studies have been completed by the VCWPD.

Recommended Approach (Interim). To compute Q_{burn} , the BSF should be applied directly to the unburned HEC-HMS peak flows and hydrographs (Equation 13-1).

Recommended Approach (Future). To compute Q_{burn} , post-burn adjustments should be made directly to the model parameters instead of applying the BSF to model results. The VCWPD should perform hydrology studies to create a post-fire S-graph for design, and to determine what additional model parameters should be adjusted to account for the loss of vegetation cover and reduced infiltration.

13.1.5 Flood Frequency Analysis

For discharges computed by a flood frequency analysis of stream gage data, the recommended approach varies based on whether it is an emergency project or other design project that requires the computation of Q_{burn} .

Emergency projects. Multiply the BSF directly with the peak flow estimate to compute Q_{burn} . The approach for emergency projects is somewhat conservative because the recorded peak discharges already include the effect of historic fires to some extent. However, the BSF should still be applied to reflect burn conditions soon after a fire.

Other projects – Short gage record. If the period of record is short (e.g., less than 20 years), then the BSF should be multiplied directly to the peak flow estimate to compute Q_{burn} .

Other projects – Long gage record. If there is a long period of record for the stream gage (e.g., 20 years or more), then the recorded peak discharges should include the effect of historic fires in the watershed. Therefore, an adjustment for Q_{burn} is not required for design.

13.2 Sediment/Debris Bulking Factor

A flowchart outlining the bulking factor selection process is provided as Figure 13-2. Figure 13-4 and Figure 13-5 present the recommended bulking factor curves for Ventura County based on the current study. A bulking factor for a given project will vary as a function of drainage area, location (e.g., on or near an alluvial fan, close to a debris basin, etc.), and type of project.

13.2.1 Purpose and Limitations

For hydraulic design, the main purpose of using a bulking factor is to introduce a safety factor when computing the required bridge/culvert opening or channel dimensions. Unlike the application of Q_{burn} , the sediment/debris bulking factor can be applied on a general basis for all design projects. Selection of a bulking factor is generally based on a combination of watershed data, engineering judgment, and geomorphic experience rather than a computed value based solely on the expected maximum sediment concentration in the flow.

Debris production equations can provide only a rough estimate of the sediment/debris loads that may be experienced in any given watershed. Converting an estimated debris load into a bulking factor can add additional uncertainty. Therefore, a computed bulking factor based on the flowchart provided in Figure 13-2 or any other method must be considered an estimate. Depending on the data available for the watershed (or lack thereof), this bulking factor could be increased by the design engineer and/or the VCWPD.

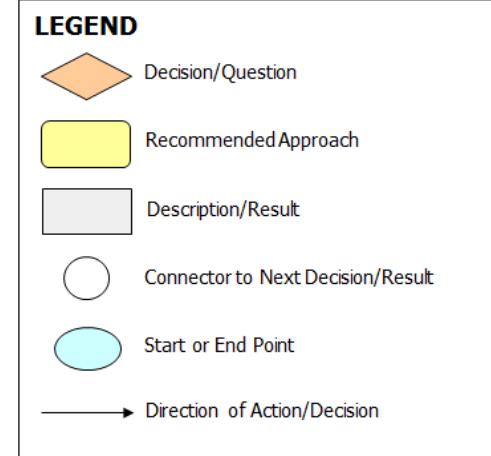
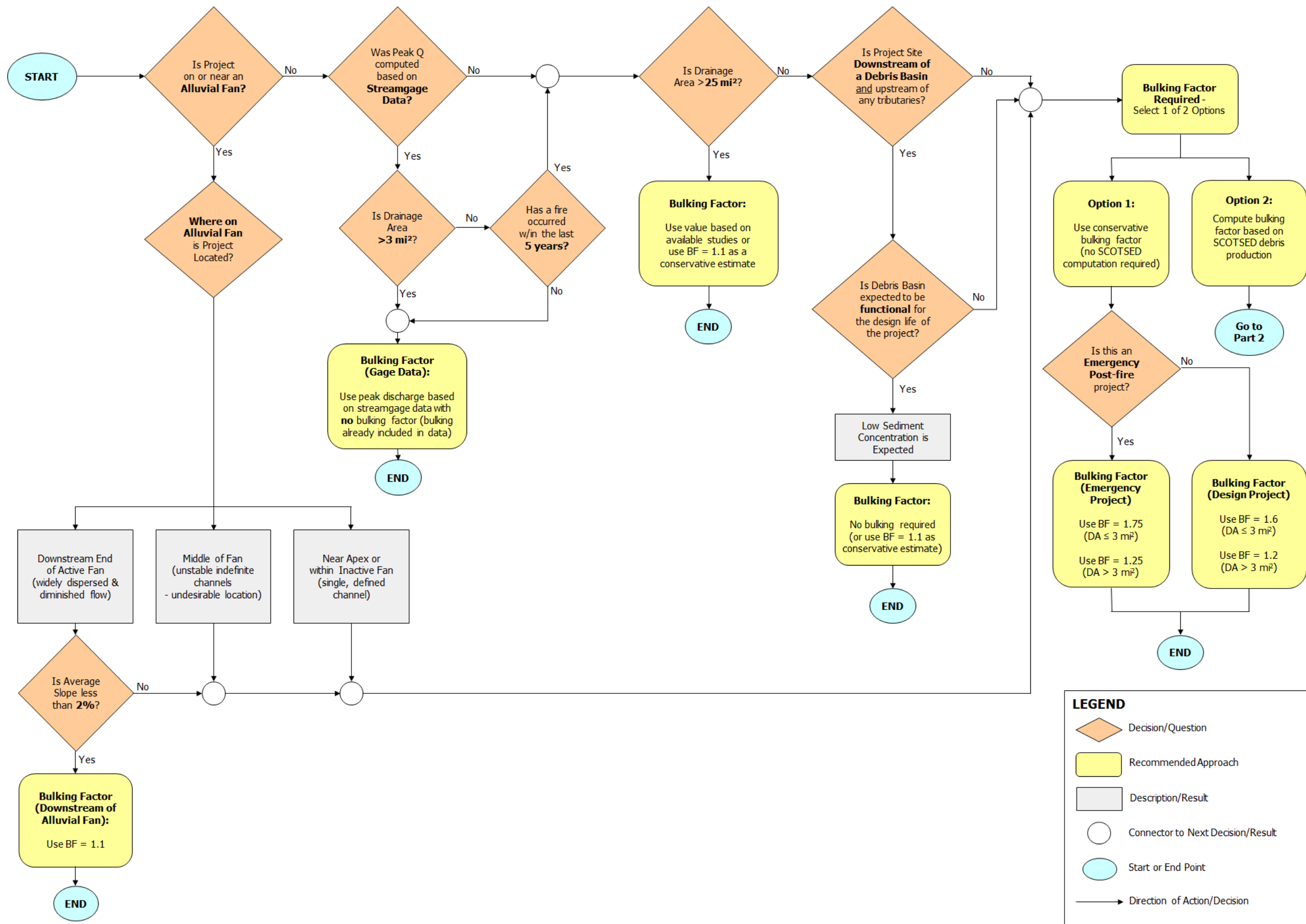


Figure 13-2. Bulking Factor Flowchart – Part 1 of 2

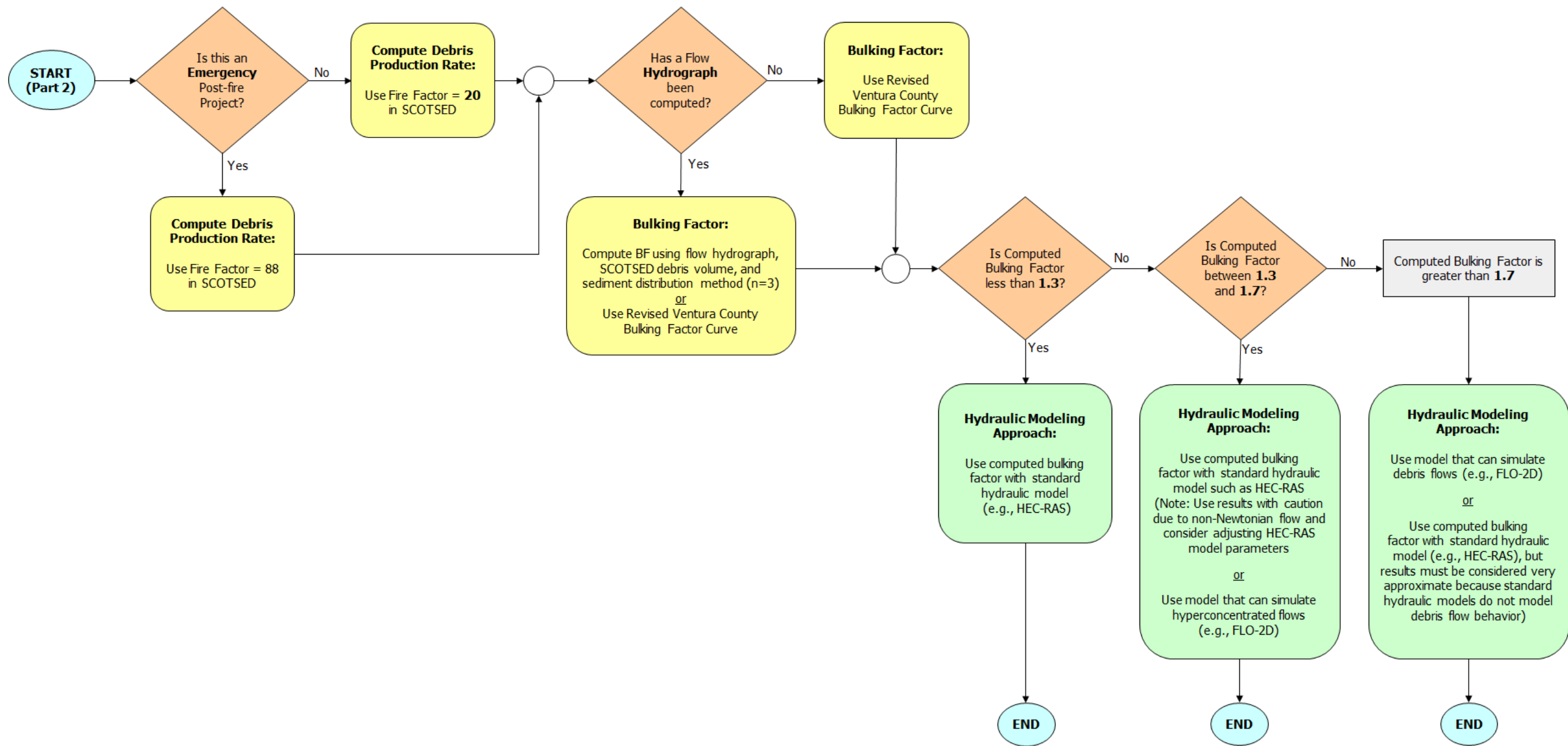


Figure 13-3. Bulking Factor Flowchart – Part 2 of 2

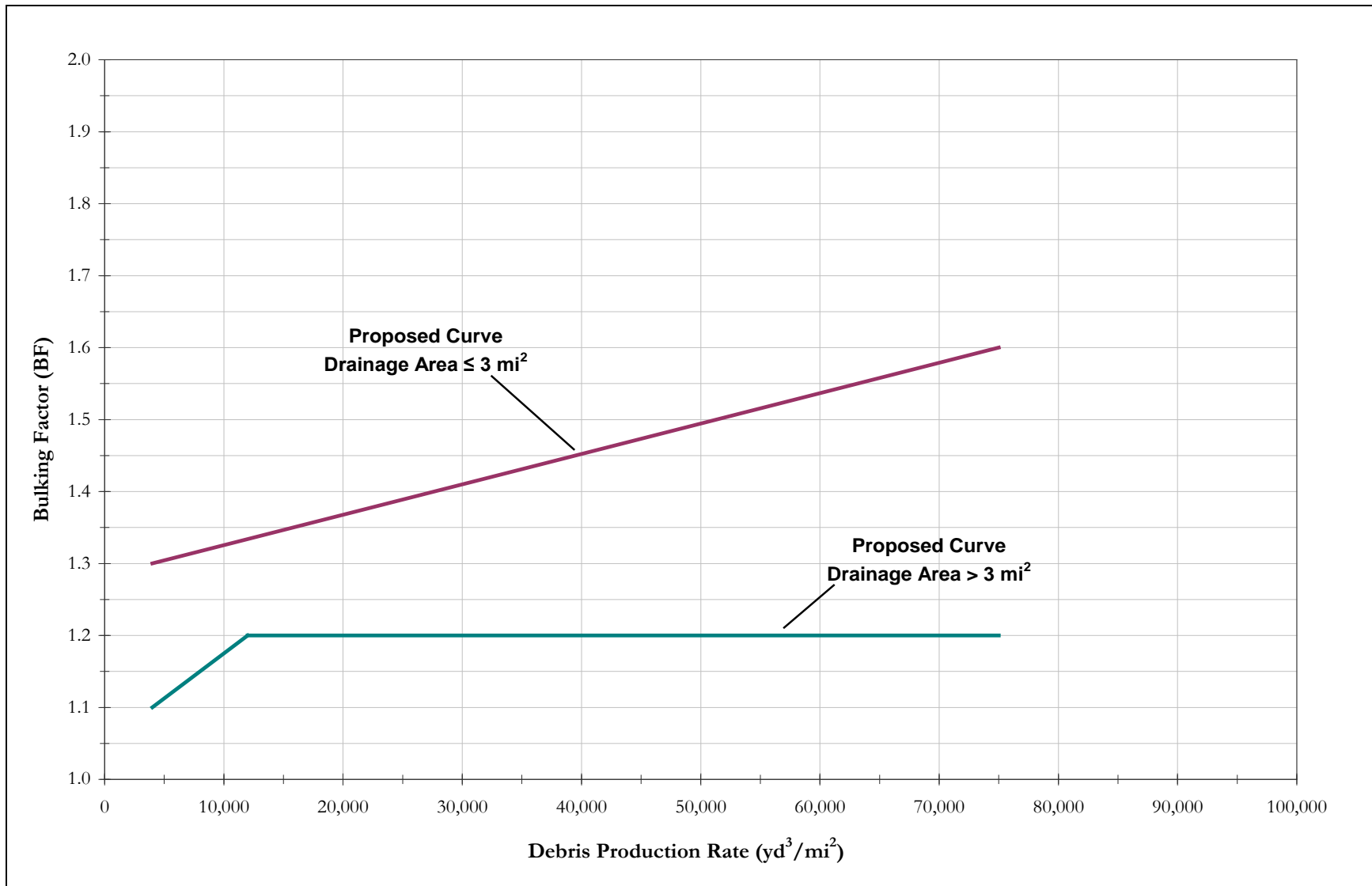


Figure 13-4. Recommended Bulking Factor Curves – Design Projects (FF = 20)

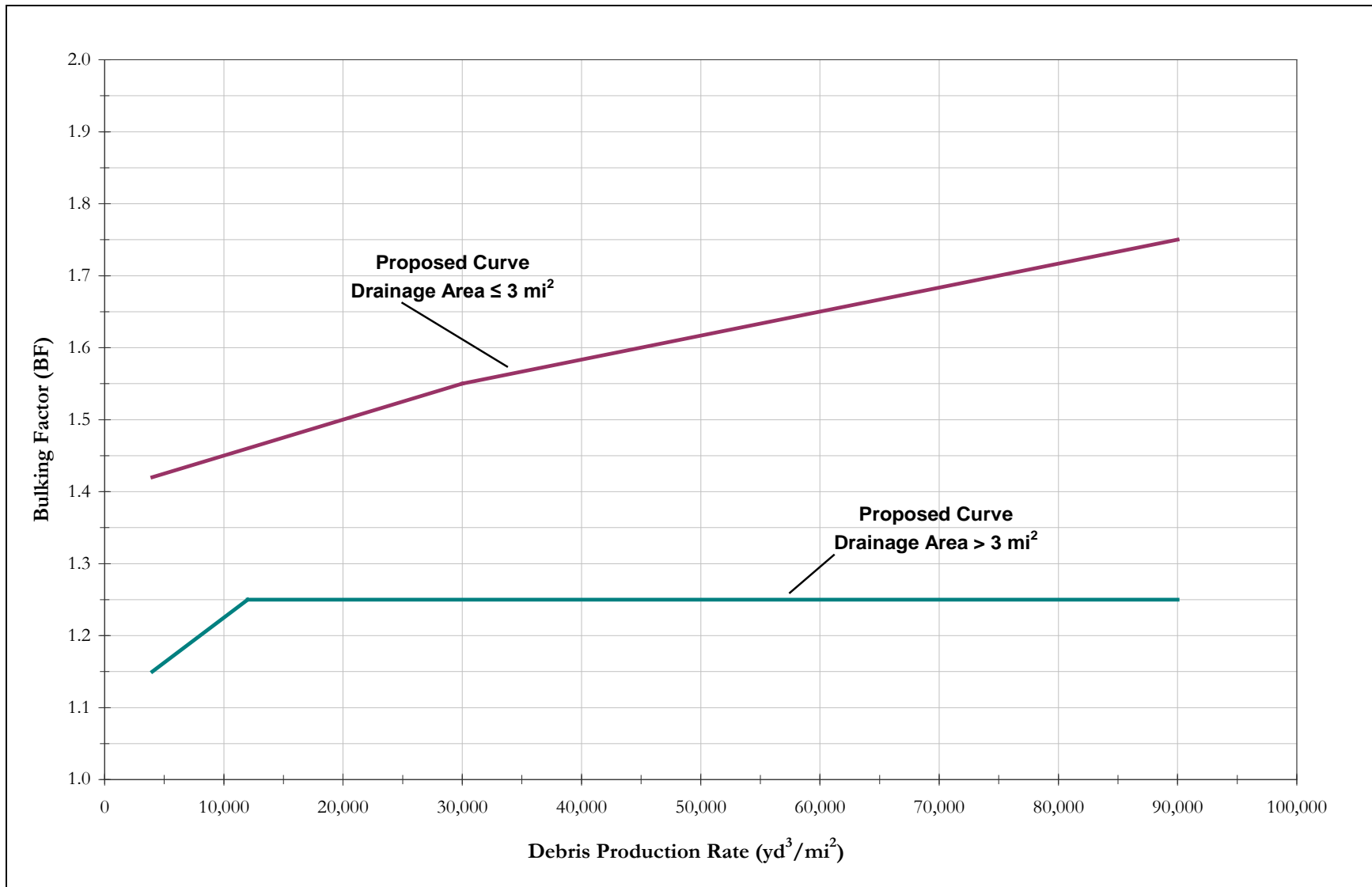


Figure 13-5. Recommended Bulking Factor Curves – Emergency Projects (FF = 88)

13.3 Combined Q_{burn} and Bulking Factor

The design discharge should be computed as follows:

$$Q_{design} = Q_{burn} * \text{Bulking Factor} \quad (13.2)$$

It is expected that the use of Q_{burn} along with a bulking factor would not require an additional factor of safety to make the results even more conservative. Moreover, the selection of conservative hydraulic coefficients and the use of freeboard in facility design include additional safety factors to the project so that it is not necessary to be overly conservative in developing and applying the burn severity and bulking factors.

The maximum potential burned and bulked factor was computed based on the following:

$$FF = 88 \text{ (6 months since burn)}$$

$$\text{High burn: BSF} = 2.0$$

$$\text{Watershed} > 3 \text{ mi}^2 = \text{maximum BF} = 1.25 \text{ (Figure 13-4)}$$

$$\text{Watershed} \leq 3 \text{ mi}^2 = \text{maximum BF} = 1.75 \text{ (Figure 13-4)}$$

Applying these results, the combined burned and bulked factor would not exceed the following:

$$2.0 * 1.25 = \underline{2.5} \quad \text{for basins} > 3 \text{ mi}^2$$

$$2.0 * 1.75 = \underline{3.5} \quad \text{for basins} \leq 3 \text{ mi}^2$$

These values are consistent with what would be expected in Ventura County (Mark Bandurraga, personal communication, September 8, 2010).

13.4 Example Application

Appendix C provides two example applications—one for a design project (critical infrastructure) and one for an emergency post-fire project.

13.5 Additional Bulking Recommendations

Provided below is a summary of bulking recommendations related to alluvial fans, sediment transport modeling, and woody debris.

13.5.1 Alluvial Fans and Bulking

The bulking factor methodology described in this chapter applies to both typical riverine and alluvial fan conditions. The main difference for alluvial fans is in the hydraulic modeling approach rather than the bulking factor. In particular, the need for 2-D modeling should be carefully considered. For a Flood Insurance Study map revision, the engineer must also determine whether the proposed hydraulic model is approved by FEMA for alluvial fans. Which models *should* be acceptable for use on alluvial fans is an area of ongoing debate and will be for the foreseeable future.

13.5.2 Sediment Transport Modeling and Bulking

Sediment transport modeling would typically be performed for the following:

- System-wide sediment instabilities that have been observed or are expected
- Excessive general scour or aggradation affecting a bridge or pipeline crossing, or a levee
- Long-term rather than a short-term sediment concerns
- Normal streamflow with transport with sediment/debris concentrations up to approximately 20 percent

A bulking factor (i.e., a bulked discharge) should not be used with sediment transport models because a sediment load is already specified at the upstream end of the model. Using a bulked discharge would result in “double counting” of the sediment in the incoming flow.

The recommended modeling process where sediment transport modeling is required is outlined below:

1. Perform sediment transport modeling using unbulked flow hydrograph
2. Determine expected long-term bed (or bank) adjustments in sediment transport model
3. Adjust bed (or bank) elevations accordingly in fixed bed hydraulic model
4. Use adjusted fixed bed model with a bulked flow for the design of a bridge, channel, levee, etc.

13.5.3 Woody Debris

Woody debris accumulation at bridge piers was investigated as part of the bulking study. A summary of woody debris findings and recommendations for Ventura County is provided below.

- Rather than having a strict standard, most agencies use a general guideline of increasing the pier width by two feet on each side to account for debris.
- Pier debris should be applied on a case-by-case basis for locations where large woody debris has been observed or expected from the watershed, including areas of the county with montane hardwood and/or conifer forest. For watersheds where chaparral is predominant, woody debris is expected to originate from the riparian corridor.
- Wildfire can cause extensive tree mortality that in turn can significantly affect the volume of woody debris available to the stream, which can eventually accumulate on a bridge pier.
- The timing of a post-fire increase in woody debris will depend on the species composition. For riparian communities with species such as white alder, relatively rapid debris recruitment might be expected, whereas if coast live oak dominates, a delay in woody debris recruitment on the order of years to decades may occur.

- NCHRP Report 653 (Lagasse et al., 2010) provides improved guidance in predicting the size and geometry of debris accumulation on bridge piers, but requires detailed inputs to use.
- Installation of debris fins to act as an extension of upstream pier nose can help guide woody debris through the bridge openings, eliminating the need to specify pier debris in a hydraulic model.

It is recommended that the results from the Lagasse et al. (2010) study, as described in Section 9.2.2, be followed if woody debris is a known issue and reliable field data are available. Otherwise, the general design practice of increasing the pier width by two feet on each side to account for potential woody debris should be used where woody debris is expected.

14 REFERENCES

- Ancey, C. (2007). "Plasticity and geophysical flows: A review," *J. Non-Newtonian Fluid Mech.*, 142, 4-35.
- Alluvial Fan Task Force (2010). *Findings and Recommendations Report [Draft]*, March 2010.
- AQUA TERRA Consultants (2009). *Hydrologic Modeling of the Santa Clara River Watershed with the U.S. EPA Hydrologic Simulation Program – FORTRAN (HSPF)*. Prepared by AQUA TERRA Consultants, Mountain View, CA for the Ventura County Watershed Protection District. July 24, 2009.
- AQUA TERRA Consultants (2010). *Sespe Creek Hydrologic, Hydraulics, and Sedimentation Analysis: Hydrologic Modeling of the Sespe Creek Watershed*. Prepared by AQUA TERRA Consultants, Mountain View, CA for RBF Consulting, Inc., and the Ventura County Watershed Protection District, March 12, 2010.
- Armento, M.C., Genevois, R., and Tecca, P.R. (2008). "Comparison of numerical models of two debris flows in the Cortina d' Ampezzo area, Dolomites, Italy," *Landslides*, 5, 143 – 150.
- Arizona Department of Transportation (2010). *Bridge Design Guidelines, Section 3 – Load and Load Factors*. www.azdot.gov/Highways/bridge/Guidelines/DesignGuidelines/PDF/Section3-LoadAndLoadFactors.pdf (Accessed June 14, 2010).
- Association of State Floodplain Managers (2010). *Critical Facilities and Flood Risk*, Association of State Floodplain Managers, Inc., Madison, WI, November 2010.
- Bello, M. E, O'Brien, J. S., Lopez, J. L., and Garcia-Martinez, R.. (2000). "Simulation of flooding and debris flows in the Cerro Grande River," *Libro de resúmenes Jornadas de Investigación Facultad de Ingeniería*, JIFI 2000, Universidad Central de Venezuela, 531.
- Bendix, J. and Cowell, C.M. (2010). "Fire, Floods and Woody Debris: Interactions Between Biotic and Geomorphic Processes," *Geomorphology*, 116 (2010), 297-304.
- Bertolo, P. and Wieczorek, G. F. (2005). "Calibration of numerical models for small debris flows in Yosemite Valley, California, USA," *Nat. Hazards Earth Syst. Sci.*, 5, 993 – 1001.
- Bohorquez, P. and Darby, S. (2008). "The use of one- and two-dimensional hydraulic modelling to reconstruct a glacial outburst flood in a steep Alpine valley," *J. Hydrol.*, 361, 240 – 261.
- Borah, D.K., Krug, E.C. and Yoder, D. (2008). "Watershed Sediment Yield" in *Sedimentation Engineering – Processes, Measurements, Modeling, and Practice* (ed. Marcelo Garcia). ASCE Manuals and Reports on Engineering Practice No. 110. ASCE, Reston, Virginia.
- Bradley, J.B. (1986). *Hydraulics and Bed Material Transport at High Fine Suspended Sediment Concentrations*, Ph.D. Dissertation, Colorado State University, Fort Collins, Colorado.
- Bradley, J.B., and McCutcheon, S.C. (1987). *Influence of Large Suspended Sediment Concentrations in Rivers*, Sediment Transport in Gravel Bed Rivers, edited by C.R. Thorne, J.C. Bathurst, and R.D. Hey, John Wiley and Sons.
- Bragg, D.C. (2000). "Simulating Catastrophic and Individualistic Large Woody Debris Recruitment for a Small Riparian System," *Ecology*, 81 (5), 1383-1394, as cited in Bendix and Cowell, 2010.

- Burnett, K.M. and Miller, D.J. (2007). “Streamside Policies for Headwater Channels: An Example Considering Debris Flows in the Oregon Coastal Province,” *Forest Science*, 53: 239-253.
- Chow, V.T. (1959). *Open Channel Hydraulics*. McGraw-Hill, Inc.
- Chang, H.H. (2003). *Technical Review of the Study Simulation of the Existing Conditions 100-yr Flood on Pole Creek* by PACE Engineers, Inc., Prepared by Howard H. Chang Consultants - Hydraulic, Hydrologic and Sedimentation Engineering, Rancho Santa Fe, CA, February 2003.
- Clark County (1999). *Hydrologic Criteria and Drainage Design Manual*, Clark County Regional Flood Control District. August 12, 1999.
- Cook, A. and Merwade, V. (2009). “Effect of topographic data, geometric configuration and modeling approach on flood inundation mapping,” *J. Hydrol.*, 377, 131 – 142.
- Copeland, R.R. and Thomas, W.A. (1989). *Corte Madera Creek sedimentation study – Numerical model investigation*, Technical Report HL-89-6, U.S. Army Engineer Waterways Experiment Station, Vicksburg, MS, *as cited in* Copeland et al., 2000.
- Copeland, R. R., McVan, D.C. and Stonestreet, S.E. (2000). *Sedimentation Study and Flume Investigation, Mission Creek, Santa Barbara, California; Corte Madera Creek, Marin County, California*, U.S. Army Engineer Research and Development Center, Vicksburg, Mississippi.
- Curran, J. C. and Wilcock, P. R. (2005). “Effect of Sand Supply on Transport Rates in a Gravel-Bed Channel”, *Journal of Hydraulic Engineering*, 131(11): 961-967.
- Cydzik, K. and Hogue, T.S. (2009). “Modeling Post-fire Response and Recovery using the Hydrologic Engineering Center Hydrologic Modeling System (HEC-HMS),” *Journal of the American Water Resources Association*, 45(3):702-714.
- Diehl, T.H. (1997). *Potential Drift Accumulation at Bridges*, Report FHWA-RD-9728, U.S. Department of Transportation, Federal Highway Administration Research and Development, Turner-Fairbank Highway Research Center, McLean, VA.
- Diplas, P., Kuhnle, R., Gray, J. and Glysson, D. (2008). “Sediment Transport Measurements” in *Sedimentation Engineering – Processes, Measurements, Modeling, and Practice (ed. Marcelo Garcia)*. ASCE Manuals and Reports on Engineering Practice No. 110. ASCE, Reston, Virginia.
- Earles, T. A., Wright, W.R., Brown, C., and Langan, T.E. (2004). “Los Alamos Forest Fire Impact Modeling,” *Journal of the American Water Resources Association (JAWRA)*, 40(2), 371-384.
- FEMA (2003a). *Guidelines and Specifications for Flood Hazard Mapping Partners, Appendix G: Guidance for Alluvial Fan Flooding Analyses and Mapping*, FEMA’s Flood Hazard Mapping Program.
- FEMA (2003b). *The Hydrologic and Hydraulic Methodology used to Estimate Post-Burn Floodplain Hazards*. FEMA-1498-DR-CA.
- FEMA (n.d.). *Flood Insurance Study conducted for Pole Creek in the City of Fillmore*, Ventura County. <http://engineering.fillmoreca.com/> (Accessed May 2010).
- FHWA (2002). *Highway Hydrology*. Hydraulic Design Series No. 2, Second Edition. Publication No. FHWA-NHI-02-001, National Highway Institute, U.S. Department of Transportation, Federal Highway Administration, Washington, D. C., October 2002.

- FHWA (2005). *Debris Control Structures-Evaluations and Countermeasures*. Hydraulic Engineering Circular 9, Third Edition. Publication No. FHWA-IF-04-016, National Highway Institute, U.S. Department of Transportation, Federal Highway Administration, Washington, D. C., October 2005.
- Fischenich, C. F. (2001). *Stability Thresholds for Stream Restoration Materials*. ERDC TN-EMRRP-SR-29 USACE, Vicksburg, MS. May 2001.
- Gabet E.J., and Bookter A. (2008). “A morphometric analysis of gullies scoured by post-fire progressively bulked debris flows in southwest Montana, USA,” *Geomorphology* 96, 298-309.
- Garcia, M., MacArthur, R., French, R., and Miller, J. (2008). “Sedimentation Hazards” in *Sedimentation Engineering – Processes, Measurements, Modeling, and Practice* (ed. Marcelo Garcia). ASCE Manuals and Reports on Engineering Practice No. 110. ASCE, Reston, Virginia.
- Hamilton, D.L. and Fan, S.S. (1996). *Reliability of Sediment Transport Modeling for Shallow Flow on Initially Dry Areas*. Proceedings of the Sixth Federal Interagency Sedimentation Conference, March 10 to 14, 1996, Las Vegas, Nevada.
- Harvey, M.D., Watson, C.C., and Schumm, S.A. (1985). *Gully Erosion*. Technical Note 366. Prepared by Water Engineering and Technology, Inc. (Fort Collins, CO) for Bureau of Reclamation, March 1985.
- Horritt, M.S., and Bates, P.D. (2002). “Evaluation of 1-D and 2-D numerical models for predicting river flood inundation,” *Journal of Hydrology*, 268, 87 – 99.
- Hungerford, R.D. (1996). *Soils: Fire in ecosystem management Notes: Unit II-I*, U.S. Department of Agriculture, Forest Service, National Advanced Technology Center, Marana, AZ. as cited by Parsons, 2003.
- Hungr, O. (2000). “Analysis of debris-flow surges using the theory of uniformly progressive flow,” *Earth Surface Processes and Landforms*, 25, 483–495.
- HEC (1995). *Application of Methods and Models for Prediction of Land Surface Erosion and Yield*. Training Document 36 (TD-36). U.S. Army Corps of Engineers’ Hydrologic Engineering Center (HEC), Davis, California. March 1995.
- Interagency BAER Team (2002). *Pines Fire Burned Area Emergency Stabilization and Rehabilitation Plan*. Julian, California. Interagency Burned Area Emergency Response (BAER) Team BLM, BIA, California DFG, California Parks & Recreation, USFS, County of San Diego, Santa Ysabel and Los Coyotes Reservations, August 26, 2002.
- Iverson, R.M., and Denlinger, R.P. (2001). “Flow of variably fluidized granular masses across three-dimensional terrain: 1. Coulomb mixture theory,” *Journal of Geophysical Research*, 106 (B1), 537-552
- Iverson, R. M. (2003). “The debris-flow rheology myth,” in *Debris-Flow Hazards Mitigation: Mechanics, Prediction and Assessment* (ed. D. Rickenmann & C. L. Chen) pp. 303–314. Millpress.
- Kidson, R.L., Richards, K.S., and Carling, P.A. (2006). “Hydraulic model calibration for extreme floods in bedrock-confined channels: case study from northern Thailand,” *Hydrological Processes*, 20, 329–344.
- Krone, R.B. and Bradley, J.B. (1989). *Hyperconcentrations, Mud and Debris Flows - A Summary*. Proceedings, ASCE International Symposium on Sediment Transport Modeling, New Orleans, Louisiana, August 1989.

- Lagasse, P.F., Clopper, P.E., Zevenbergen, L.W, Spitz, W.J., and Girard, L.G. (2010). *Effects of Debris on Bridge Pier Scour*. Prepared by Ayres Associates, Inc. for the National Cooperative Highway Research Program (NCHRP) Report 653 - Transportation Research Board, Washington, D.C.
- Lane, L.J., Hernandez, M., and Nichols, M. (1997). "Processes controlling sediment yield from watersheds as functions of spatial scale." *Environmental Modelling & Software*, Vol. 12, No. 4, pp. 355-369.
- Lin, M.-L., Wang, K.-L., and Huang, J.-J. (2005). "Debris flow run off simulation and verification – case study of Chen-You-Lan watershed, Taiwan," *Nat. Hazards Earth Syst. Sci.*, 5, 439–445pp.
- Lyn, D., Thomas, C., Yong-Kon, Y., Sinha, R., and Rao, A. (2003). *Debris Accumulation at Bridge Crossings: Laboratory and Field Studies*, Civil Engineering Joint Transportation Research Program, Purdue Libraries.
- Los Angeles County (2003). *Development of Burn Policy Methodology (Santa Clara River Watershed Pilot Project)*. Water Resources Division, Hydrology Section, June 2003.
- Los Angeles County (2006a). *Sedimentation Manual, 2nd Edition*. Los Angeles County Department of Public Works, Water Resources Division, March 2006.
- Los Angeles County (2006b). *Los Angeles County Hydrology Manual*. Los Angeles County Department of Public Works, Water Resources Division.
- MacArthur, R., Neill, C. Hall, B., Galay, V. and Shvidchenko, A. (2008) "Overview of Sedimentation Engineering" in *Sedimentation Engineering – Processes, Measurements, Modeling, and Practice* (ed. Marcelo Garcia). ASCE Manuals and Reports on Engineering Practice No. 110. ASCE, Reston, Virginia.
- Maricopa County (2003). *Drainage Design Manual for Maricopa County, Arizona – Volume I, Hydrology*. Flood Control District of Maricopa County, November 2003 (Draft).
- Major, J.J., and Pierson, T.C. (1992). "Debris flow rheology: experimental analysis of fine-grained slurries," *Water Resources Research*, 28, 841-857.
- Martin, M.G. (2005). *Soil and Watershed Resource Assessment*. Appendix to: *Burned Area Emergency Stabilization Plan – Hackberry Complex*. National Park Service, Mojave National Preserve. Prepared by National-Interagency Burned Area Emergency Response Team, July 5, 2005.
- McLin, S.G., Springer, E.P. and Lane, L.J. (2001). "Predicting floodplain boundary changes following the Cerro Grande wildfire," *Hydrological Processes*, 15(15), in press. 2001.
- MEI (Musetter Engineering, Inc) (2008). *Sediment and Erosion Design Guide*. Prepared for: Southern Sandoval County Arroyo Flood Control Authority, Rio Rancho, NM. Prepared by: MEI, Fort Collins, CO., November 2008.
- National Research Council (1982). *Selecting a Methodology for Delineating Mudslides Hazard Areas for National Flood Insurance Program*. National Academy of Sciences Report by the Advisory Board on the Build Environment, Washington, D.C.
- National Research Council (1996). *Alluvial Fan Flooding*. National Research Council Committee on Alluvial Fan Flooding. Washington, DC: National Academy Press.
- National Wildfire Coordinating Group (2001). *Fire Effects Guide*, NFES #2393, National Interagency Fire Center, Boise, ID as cited by Parsons, 2003.

- Neary, D.G., Gottfried, G.J., and Folliott, P.F. (2003). *Post-Wildfire Watershed Flood Responses*. 22nd International Wildland Fire Ecology and Fire Management Congress.
- O'Brien, J.S. (1986). *Physical Processes, Rheology, and Modeling of Mud Flows*. Ph.D. Dissertation, Colorado State University, Fort Collins, Colorado.
- O'Brien, J.S. (2006). *FLO-2D Users Manual*. Version 2006.01, January 2006. Nutrioso, AZ: FLO-2D Software, Inc.
- O'Brien, J.S. (2008). *FLO-2D Reference Manual*. Version 2009. Nutrioso, AZ: FLO-2D Software, Inc.
- Orange County (2000). *Orange County Flood Control District Design Manual*. County of Orange Public Facilities and Resources Department. November 2000.
- Parsons, A. (2003). *Burned Area Emergency Rehabilitation (BAER) Soil Burn Severity Definitions and Mapping Guidelines – Draft*. USDA Forest Service unpublished document. April 2003. p.12. http://www.fws.gov/fire/ifcc/esr/Remote%20Sensing/soil_burnsev_summary_guide042203.pdf
- Prochaska, A.B., Santi, P.M., Higgins, J.D., and Cannon, S.H. (2008). “Debris-flow runout predictions based on the average channel slope (ACS),” *Engineering Geology*, 98, 29–40.
- Renard, K.G., Foster, G.R., Weesies, G.A., McCool, K.K. and Yoder, D.C. (1997). *Predicting soil erosion by water: A guide to conservation planning with the revised Universal Soil Loss Equation (RUSLE)*, Agriculture Handbook No. 703. USDA, Washington, DC.
- Richardson, E.V., Simons, D.B., and Lagasse, P.F. (2001). *River Engineering for Highway Encroachments – Highways in the River Environment*. Hydraulic Design Series Number 6, Publication No. FHWA NHI 01-004. Prepared for Federal Highway Administration by Ayres Associates, December 2001.
- Riverside County (1978). *Hydrology Manual*. Riverside County Flood Control and Water Conservation District, April 1978.
- Scott, K. and Williams, R. (1978). *Erosion and Sediment Yields in the Transverse Ranges, Southern California*. Geological Survey Professional Paper 1030. Prepared in cooperation with the Ventura County Department of Public Works and the Ojai Resource Conservation District. United States Government Printing Office, Washington, D.C.
- Spies, T.A., Franklin, J.F., and Thomas, T.B. (1988). “Coarse Woody Debris in Douglas-Fir Forests of Western Oregon and Washington,” *Ecology*, 69 (6), 1689-1702, *as cited in* Bendix and Cowell, 2010.
- Stock, J. and Dietrich, W. E. (2003). “Valley incision by debris flows: Evidence of a topographic signature,” *Water Resources Research* 39, 1089.
- Stock, J. D., and Dietrich, W. E. (2006). “Erosion of steepland valleys by debris flows,” *Geological Society of America Bulletin* 118, 1125-1148.
- Swanson, M.L. and Williams, P.B. (1988). *Mission Creek alternative study – Basis of Philip Williams and Associates technical analyses – Specific issues regarding flood protection design*. Philip Williams and Associates, San Francisco, CA., *as cited in* Copeland et al., 2000.

- University of California (2010). *Safe Landscapes Sustainable and Fire-Safe*. University of California Agriculture and Natural Resources. <http://ucanr.org/sites/SAFElandscapes/> (Accessed June 18, 2010).
- USACE (1992). *Guidelines for Risk and Uncertainty Analysis in Water Resources Planning*. Report 92-R-1, Fort Belvoir, Virginia.
- USACE (2000a). *Alluvial Fans in California – Identification, Evaluation, and Classification*. U.S. Army Corps of Engineers, Sacramento District. Prepared at the request of the State of California Department of Water Resources. May 2000.
- USACE (2000b). *Debris Method, Los Angeles District Method for Prediction of Debris Yield*. U.S. Army Corps of Engineers, Los Angeles District. February 1992, updated February 2000.
- USACE (2010). *HEC-RAS River Analysis System – Hydraulic Reference Manual, Version 4.1*. January 2010. U.S. Army Corps of Engineers’ Hydrologic Engineering Center, Davis, CA.
- USACE (n.d.) *Corte Madera Flood Control Project – General Re-evaluation Report Hydrology and Hydraulics Appendix*, Sponsor Marin County Water Conservation and Flood Control District, Authorization Section 201 of the Flood Control. <http://www.co.marin.ca.us/depts/pw/main/cm/cmc.html> (Accessed May 3, 2011).
- USDA Forest Service (1995). *Burned Area Emergency Rehabilitation Handbook*. Forest Service Handbook FSH 2509.13 as cited by Parsons, 2003.
- USGS (1997). “Debris flows and El Niño in southern California landscape,” December 29, 1997.
- USGS (2005a). *Distinguishing between Debris Flows and Floods from Field Evidence in Small Watersheds*. U.S. Geological Survey Fact Sheet 2004-3142.
- USGS (2005b). *Southern California – Wildfires and Debris Flows*. U.S. Geological Survey Fact Sheet 2005-3106.
- Vanoni, V.A., ed. (2006). *Sedimentation Engineering*. Manuals and Reports on Engineering Practice No. 54. American Society of Civil Engineers: Reston, VA.
- VCWPD (2005). *Debris and Detention Basins*. Ventura County Watershed Protection District. September 2005.
- VCWPD (2010a). *Hydrology Manual*. Ventura County Watershed Protection District, Ventura, California. August 2010.
- VCWPD (2010b). *Results of Fire History Analysis – Effect of Design Fire Factor*. Draft Memorandum from Mark Bandurraga to Bruce Rindahl, Planning & Regulatory, Hydrology Section, Ventura County Watershed Protection District, February 23, 2010.
- WEST Consultants, Inc. (2007). *Ventura County Debris Basins Sedimentation Analyses – Final Report*. Prepared for Ventura County Watershed Protection District.
- Whipple, K. X., (1992). “Predicting debris-flow runout and deposition on fans: The importance of the flow hydrograph”, in Walling, D.; Davies, T.; and Hasholt, B., eds., *Erosion, Debris Flow, and Environment in Mountainous Regions: Chengdu, China, Int. Assoc. Hydro. Sci.*, p. 337–345.
- Whipple, K. X., (1997). “Open-channel flow of Bingham fluids: Applications in debris-flow research,” *J. Geol.*, 105, 243– 262.

- Williams, J.R.. (1975). *Sediment-yield prediction with universal equation using runoff energy factor*. p. 244–252. In Present and prospective technology for predicting sediment yield and sources. ARS.S-40, U.S. Gov. Print. Office, Washington, DC.
- Williams, P.B. (1990). *Rethinking flood-control channel design*. Civil Engineering, ASCE, January, 57-59 as cited in Copeland et al., 2000.
- Williams, J.R. and Berndt, H.D. (1977). “Sediment yield prediction based on watershed hydrology,” *Transactions of the ASAE*, pp. 1100-1104.
- Wischmeier, W.H., and Smith, D.D. (1978). *Predicting rainfall-erosion losses: A guide to conservation planning*. Agriculture Handbook #507. USDA, Washington, DC.
- Wohl, E.E., (1998). “Uncertainty in flood estimates associated with roughness coefficient,” *Journal of Hydraulic Engineering*, 124 (2), 219 – 223.

APPENDIX A

DERIVATION OF EQUIVALENT HEC-RAS PARAMETERS FOR MODELING OF BULKED FLOWS

Derivation of Equivalent HEC-RAS Parameters for Modeling of Bulked Flows

The primary differences between bulked flows and normal flows are the viscosity and density, best expressed by the kinematic viscosity ν , (ft²/sec), defined as $\nu = \mu / \rho$, where μ (lb-sec/ft²) is the absolute fluid viscosity and ρ (slugs/ft³) is the fluid density.

Two non-dimensional parameters govern almost all open channel flow equations: The Reynolds number $Re = 4VR_h / \nu$, where V (ft/sec) is the fluid velocity and R_h (ft) the hydraulic radius, is given by $R_h = A / P$, where A is the wetted area (ft²), and P the wetted perimeter (ft). The second is the Froude number $Fr = V / \sqrt{gy_m}$, where g (ft / sec²) is the acceleration due to gravity (32.2 ft/sec²), and y_m (ft) is the hydraulic mean depth, given by $y_m = A / T$, where T (ft) is the top width of flow.

For a wide channel, both R_h and y_m equal y (ft), the depth of flow in the channel. This approximation is utilized here and throughout the remainder of this discussion.

Many of the parameters implemented into HEC-RAS are in the form:

$$H_L = k \frac{V^2}{2g} \quad (A.1)$$

where k is an experimentally determined, non-dimensional coefficient, and H_L (ft) is the headloss. It is possible to express velocity as a direct function of the Reynolds and Froude numbers, simply by multiplying Re and Fr^2 :

$$Re \times Fr^2 = \frac{4Vy}{\nu} \frac{V^2}{gy} = \frac{4}{\nu g} V^3 \quad (A.2)$$

Hence,

$$V^2 = 2^{4/3} g^{2/3} \nu^{2/3} Re^{2/3} Fr^{4/3} \quad (A.3)$$

This H_L to be expressed in terms of the viscosity as

$$H_L = 2^{1/3} g^{-1/3} Re^{2/3} Fr^{4/3} \nu^{2/3} k \quad (A.4)$$

The implicit dependence of k on viscosity is evident in the above equation. Thus, an equivalent parameter k_{bulk} may be developed if

$$k_{bulk} = \left(\nu / \nu_{bulk} \right)^{2/3} k \quad (A.5)$$

Additionally, the following conversion is valid for the expansion and contraction loss coefficient C (dimensionless):

$$C_{bulked} = (v / v_{bulked})^{2/3} C \quad (\text{A.6})$$

Friction losses are somewhat more complicated. In HEC-RAS, the friction loss per linear foot for a wide channel, S_f , is estimated by the Manning's equation, valid for turbulent flow only:

$$S_f = 0.452 y^{-4/3} V^2 n^2, \text{ (turbulent flow)} \quad (\text{A.7})$$

which is specific to English units only. Noting that $y = V^2/g\text{Fr}^2$, equation (A.7) can be expressed

$$S_f = 46.40 V^{-2/3} \text{Fr}^{8/3} n^2 \quad (\text{A.8})$$

Substituting the expression for V as derived in equation (A.3), equation (A.8) becomes

$$S_f = 3.0 g^{10/9} \text{Fr}^{20/9} \text{Re}^{-2/9} v^{-2/9} n^2 \quad (\text{A.9})$$

The implicit dependence on the viscosity is again apparent. The equivalent bulked roughness coefficient (n_{bulked}) is therefore:

$$n_{bulked} = (v_{bulked} / v)^{1/9} n, \text{ (turbulent flow)} \quad (\text{A.10})$$

When the flow becomes laminar ($\text{Re} < 2000$), as is common for bulked flows, the friction loss per linear foot is given by:

$$S_f = \frac{32}{\text{Re}} \frac{V^2}{g y}, \text{ (laminar flow)} \quad (\text{A.11})$$

Laminar flow is not considered in HEC-RAS, and must be approximated by the Manning's equation and then applied directly to the bulked flow simulation. This is found by equating the friction slopes expressed in equations (A.11) and (A.7) and then solving for n_{bulked} :

$$n_{bulked} = 0.74 y^{1/6} \sqrt{v_{bulked} / q_{bulked}}, \text{ (laminar flow)} \quad (\text{A.12})$$

where q_{bulked} (ft^2/sec) is the bulked flow per linear foot width of the channel.

Given the dependence on $y^{1/6}$, the difference between the bulked flow and the flow as modeled in HEC-RAS can no longer be expressed as a simple constant. However, this dependence on $y^{1/6}$ also applies to the well known general dependence that Manning's n has on $y^{1/6}$. In practice, this difference is accounted for by the selection of a representative n value or specifying different n -values at different elevations. As long as that same method is applied here, n_{bulked} is expressed as follows:

$$n_{bulked} = 0.74 \sqrt{v_{bulked} / q} \text{ (account for elevation changes in HEC-RAS)} \quad (\text{A.13})$$

APPENDIX B

BURN SEVERITY CLASSES AND BURN SEVERITY MAPS

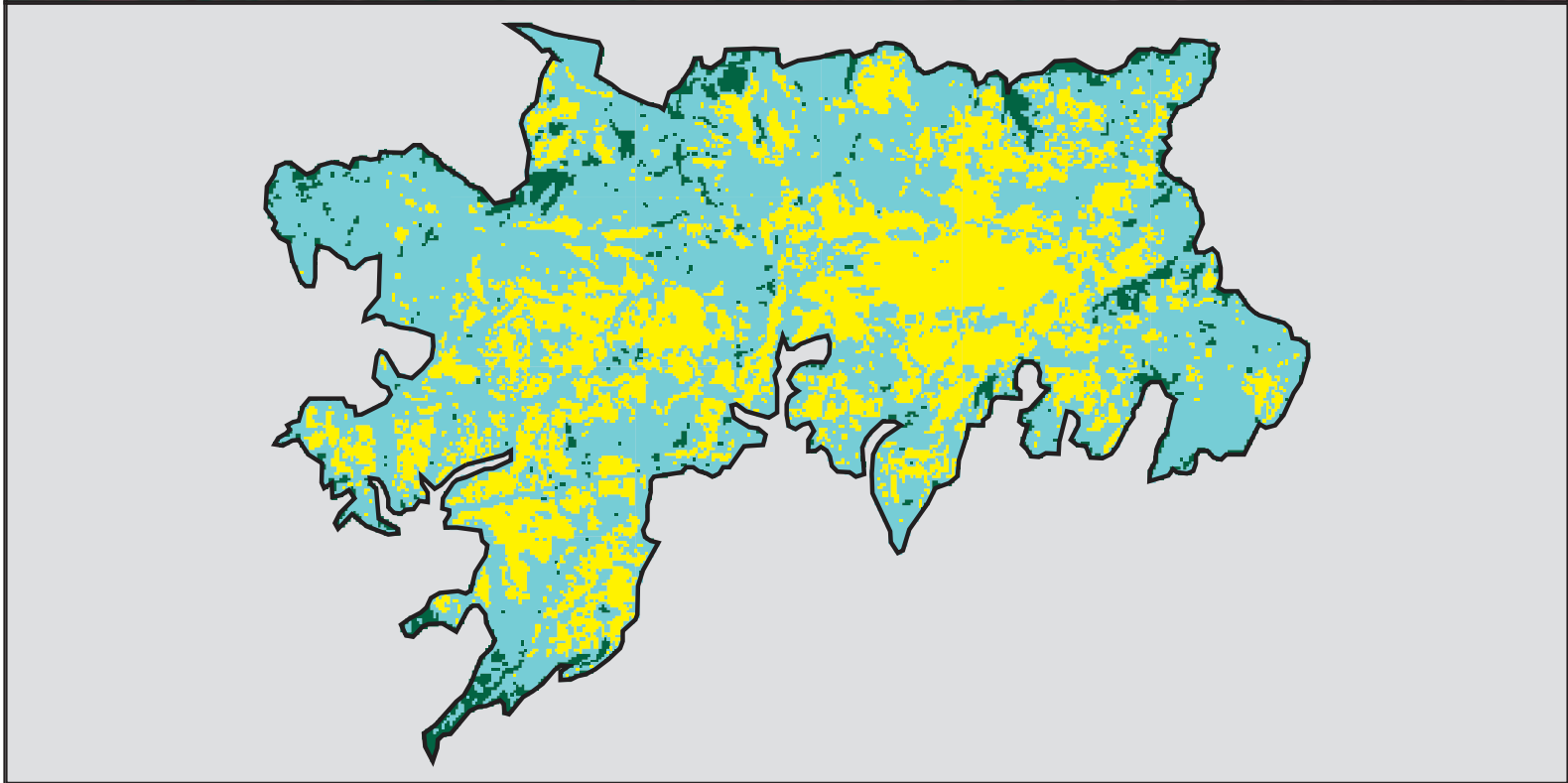
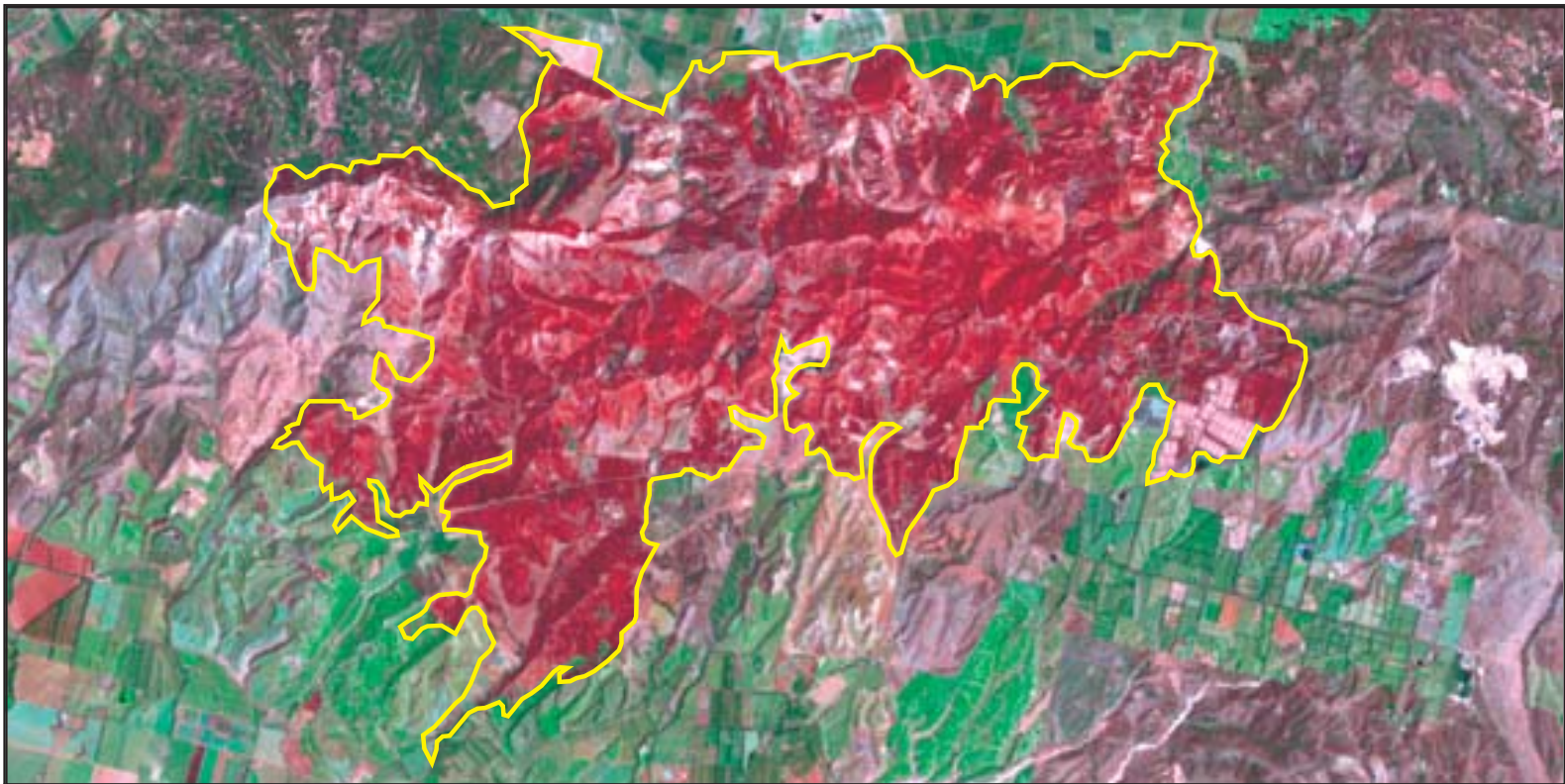
Table B-1. Burn Severity Classes and Descriptions

(adapted from National Wildfire Coordinating Group, 2001; Hungerford, 1996 and USDA Forest Service, 1995 *as cited in* Parsons, 2003)

Burn Severity Condition	Description of Class
Unburned to Very Low Burn	Fire has not entered the area, or has very lightly charred only the litter and fine fuels on the ground such that the degree of severity is so slight that the soil and vegetation are not significantly altered from an unburned condition (typically less than 5 percent burn); soil organic matter, structure, and infiltration unchanged.
Low Burn	Low soil heating or light ground char occurs; mineral soil is not changed; leaf litter may be charred or partially consumed, and the surface of the duff may be lightly charred; original forms of surface materials, such as needle litter or lichens may be visible; very little to no change in runoff response. Indicators include very small diameter (<1/4 inch) foliage and twigs are consumed, some small twigs may remain; generally, foliage may be yellow; the surface is mostly black in a grassland or shrubland ecosystem, but some gray ash may be present; above-ground portions of vegetation may be consumed, but root masses are intact. Change in runoff response is usually slight.
Moderate Burn	Moderate soil heating with moderate ground char; soil structure is usually not altered; decreased infiltration due to fire-induced water repellency may be observed; litter and duff are deeply charred or consumed; shallow light colored ash layer and burned roots and rhizomes are usually present. Indicators include understory foliage, twigs (1/4 to 3/4 inch) are consumed; rotten wood and larger diameter woody debris are deeply charred or partially consumed; on shrubland sites, gray or white ash is present and char can be visible in the upper 1 cm of mineral soil, but the soil is not altered; in forested ecosystems, brown needles or leaves may remain (but not always) on overstory trees—these are important as mulch, and should play a role when identifying treatment candidate sites; increase in runoff response may be moderate to high, depending on degree of fire-caused changes to the pre-fire vegetation community, density of pre-fire vegetation, and presence or absence of mulch potential, sprouting vegetation, etc.
High Burn	High soil heating, or deep ground char occurs; duff is completely consumed; soil structure is often destroyed due to consumption of organic matter; decreased infiltration due to fire induced water repellency is often observed over a significant portion of the area; top layer of mineral soil may be changed in color (but not always) and consistence and the layer below may be blackened from charring of organic matter in the soil; deep, fine ash layer is present, often gray or white; all or most organic matter is removed; essentially all plant parts in the duff layer are consumed; increase in runoff response is usually high. Other indicators include large fuels > 3/4 inch including major stems and trunks are consumed or heavily charred. On a shrub site, shrub stems and root crowns are often consumed. In forested ecosystems, generally no leaves or needles remain on standing trees; high soil burn severity areas are primary treatment candidate sites if there are downstream values at risk.

1984 California: GRIMES FIRE

(CA-VNC-00000000-19840507)



Latitude: 34° 19' 51.9" N
 Longitude: 118° 57' 52.1" W
 Fire Ignition Date: May 7, 1984
 Assessment Type: Initial (SS)
 Pre-Fire Image Date: N/A
 Post-Fire Image Date: June 30, 1984 (Landsat 5)

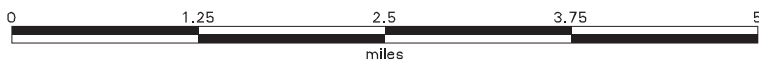


Acreage of Burn Severity

Burn Severity	Acres
Unburned to Low	710
Low	6,781
Moderate	3,427
High	0
Increased Greenness	0
Non-Processing Area Mask *	0
Total	10,918

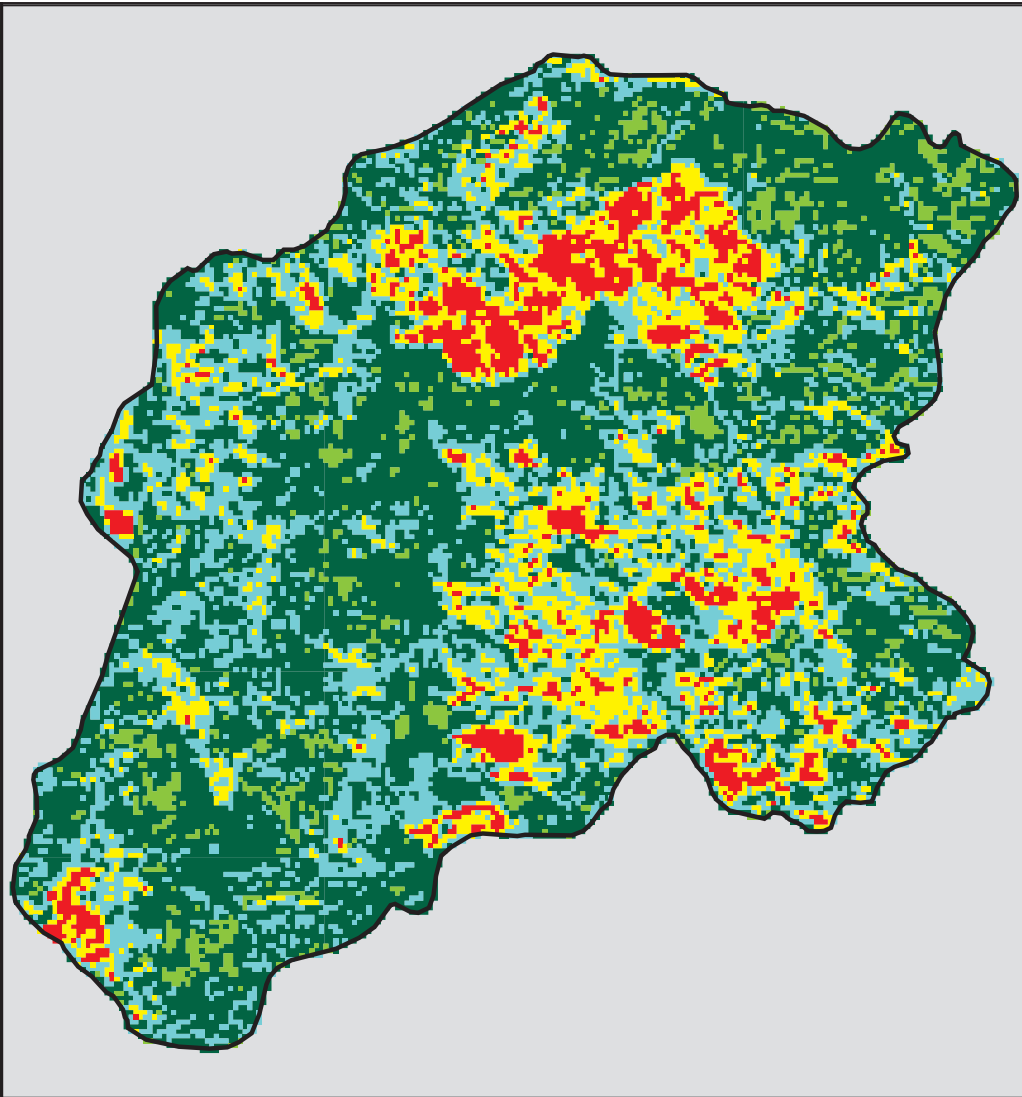
This map portrays fire severity for the fire specified in the map title and summarizes proportions of fire severity classes. These data are produced under the Monitoring Trends in Burn Severity (MTBS) project jointly implemented by the USGS EROS and the USFS RSAC. The MTBS project ascertains the locations of fires based on available fire occurrence information provided by federal and state agencies, and other reliable sources. The MTBS project reserves the right to correct, update or modify geospatial inputs to this map without notification.

* - Areas in either the pre-fire or post-fire reflectance data containing clouds, snow, shadows, smoke, significantly sized water bodies or missing lines of data



1984 California: SQUAW FLAT

(CA-VNC-00000974-19841015)



Latitude: 34° 26' 35.3" N
 Longitude: 118° 53' 43.9" W
 Fire Ignition Date: October 15, 1984
 Assessment Type: Extended
 Pre-Fire Image Date: June 30, 1984 (Landsat 5)
 Post-Fire Image Date: June 17, 1985 (Landsat 5)

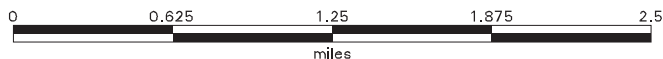


Acreage of Burn Severity

Burn Severity	Acres
Unburned to Low	2,780
Low	1,582
Moderate	900
High	423
Increased Greenness	362
Non-Processing Area Mask *	0
Total	6,047

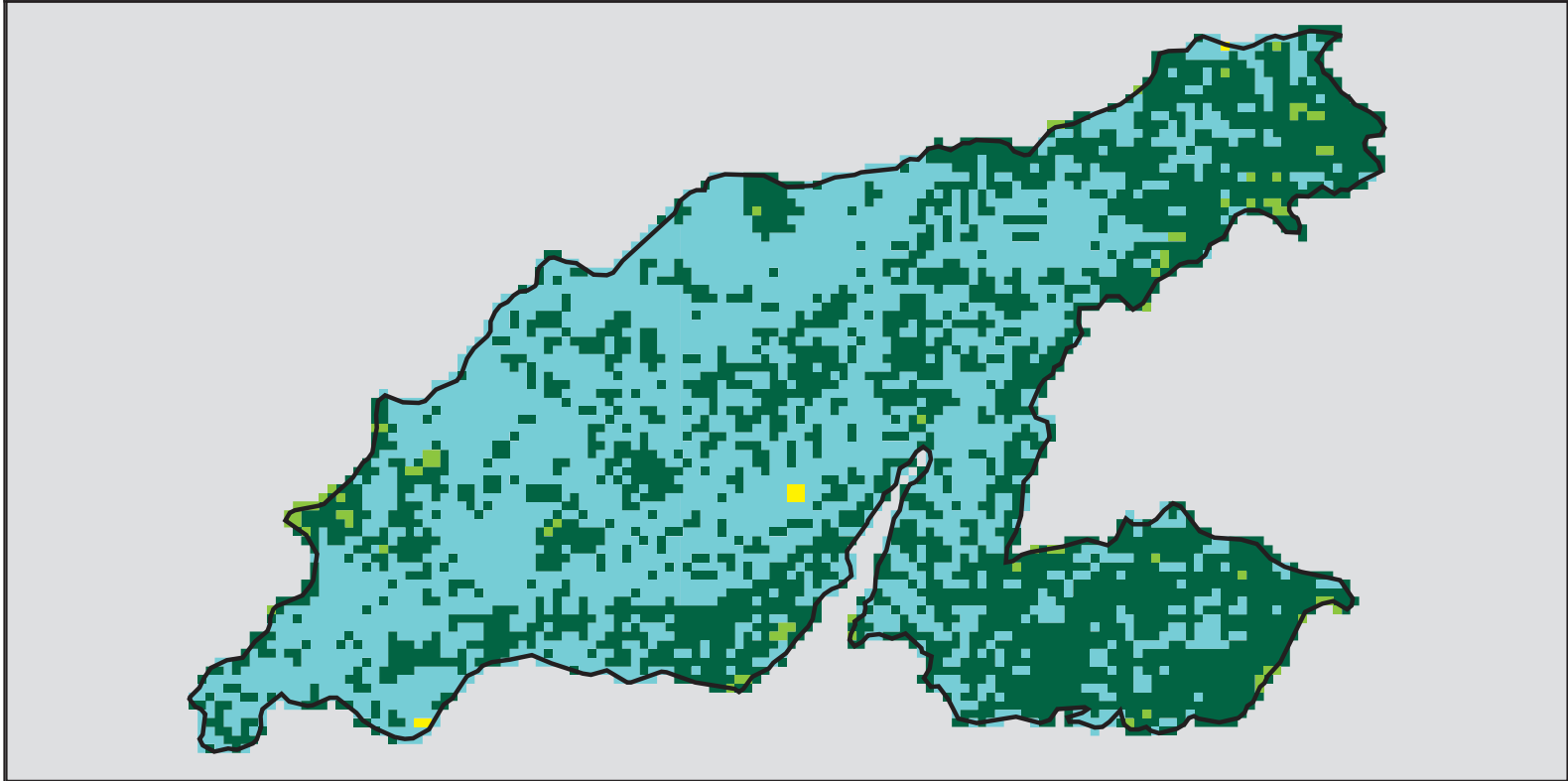
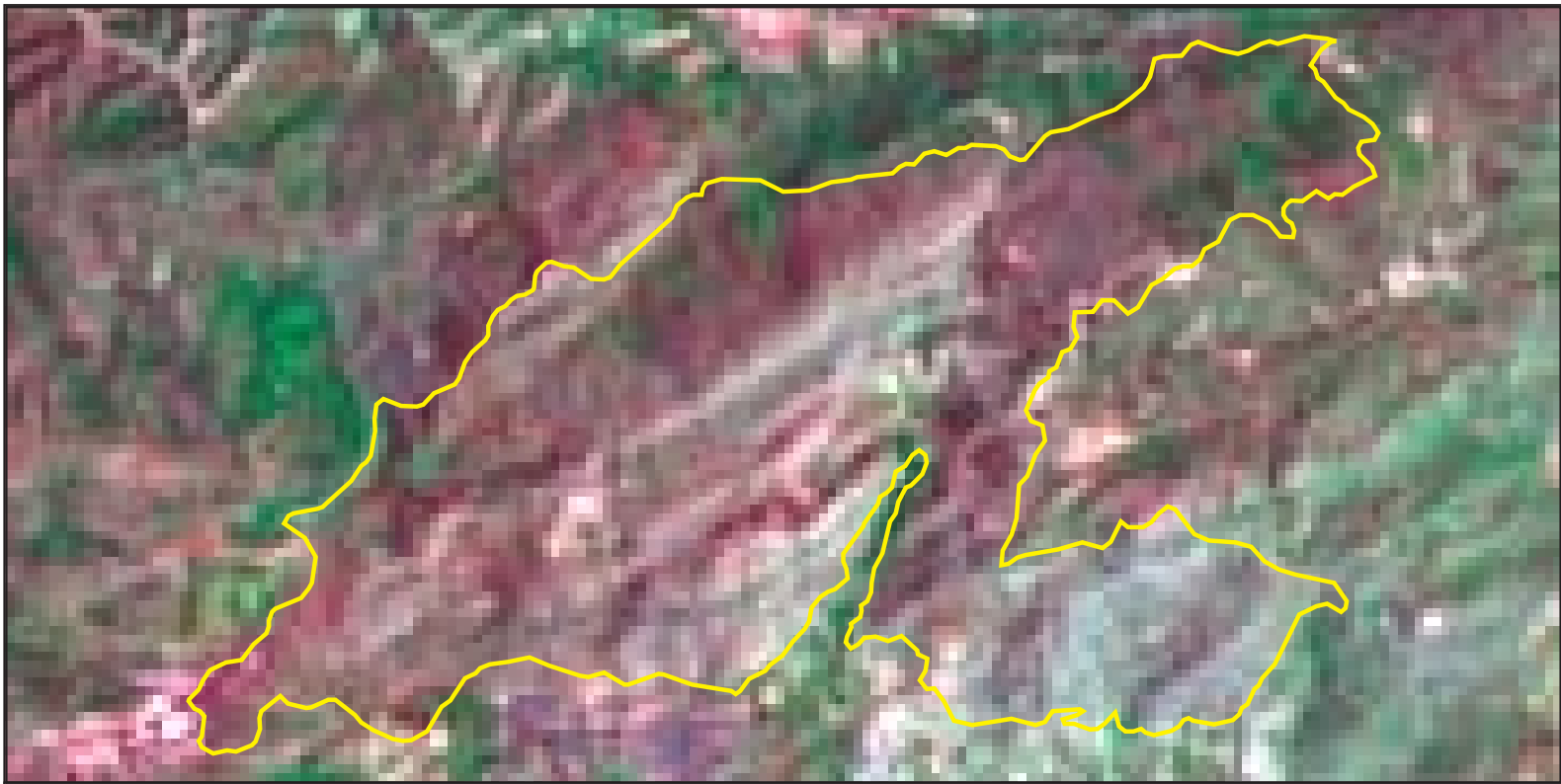
This map portrays fire severity for the fire specified in the map title and summarizes proportions of fire severity classes. These data are produced under the Monitoring Trends in Burn Severity (MTBS) project jointly implemented by the USGS EROS and the USFS RSAC. The MTBS project ascertains the locations of fires based on available fire occurrence information provided by federal and state agencies, and other reliable sources. The MTBS project reserves the right to correct, update or modify geospatial inputs to this map without notification.

* - Areas in either the pre-fire or post-fire reflectance data containing clouds, snow, shadows, smoke, significantly sized water bodies or missing lines of data



1985 California: BOX CANYON (PIONEER) FIRE

(CA-LAC-00000685-19851014)

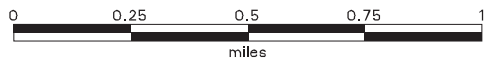


Latitude: 34° 14' 55.1" N
 Longitude: 118° 39' 13.1" W
 Fire Ignition Date: October 14, 1985
 Assessment Type: Extended
 Pre-Fire Image Date: June 17, 1985 (Landsat 5)
 Post-Fire Image Date: June 20, 1986 (Landsat 5)



This map portrays fire severity for the fire specified in the map title and summarizes proportions of fire severity classes. These data are produced under the Monitoring Trends in Burn Severity (MTBS) project jointly implemented by the USGS EROS and the USFS RSAC. The MTBS project ascertains the locations of fires based on available fire occurrence information provided by federal and state agencies, and other reliable sources. The MTBS project reserves the right to correct, update or modify geospatial inputs to this map without notification.

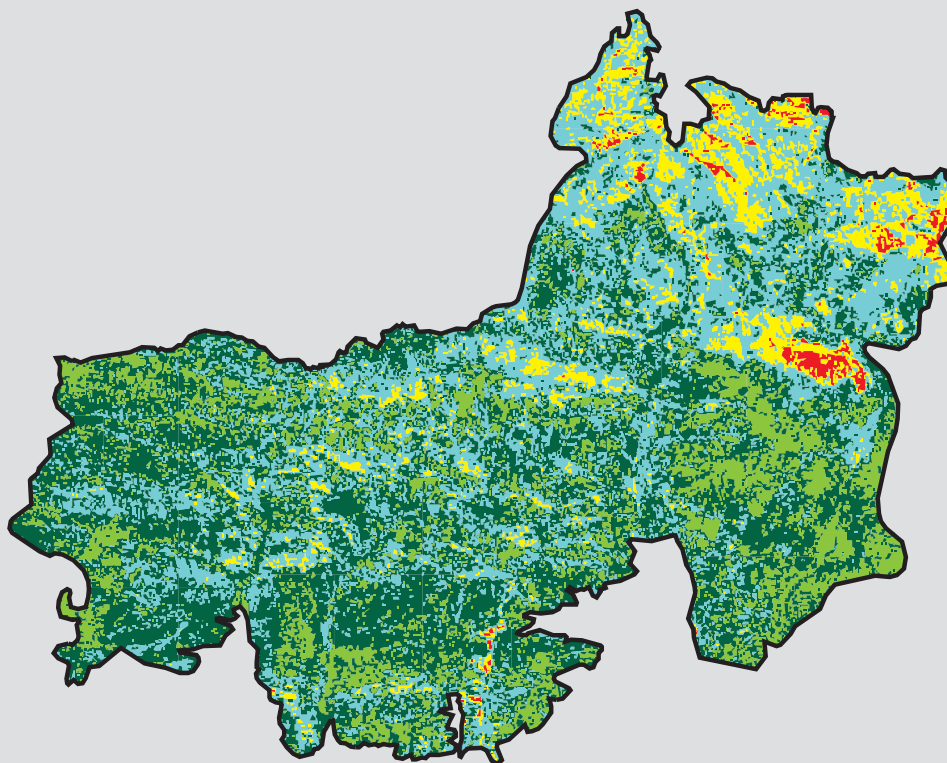
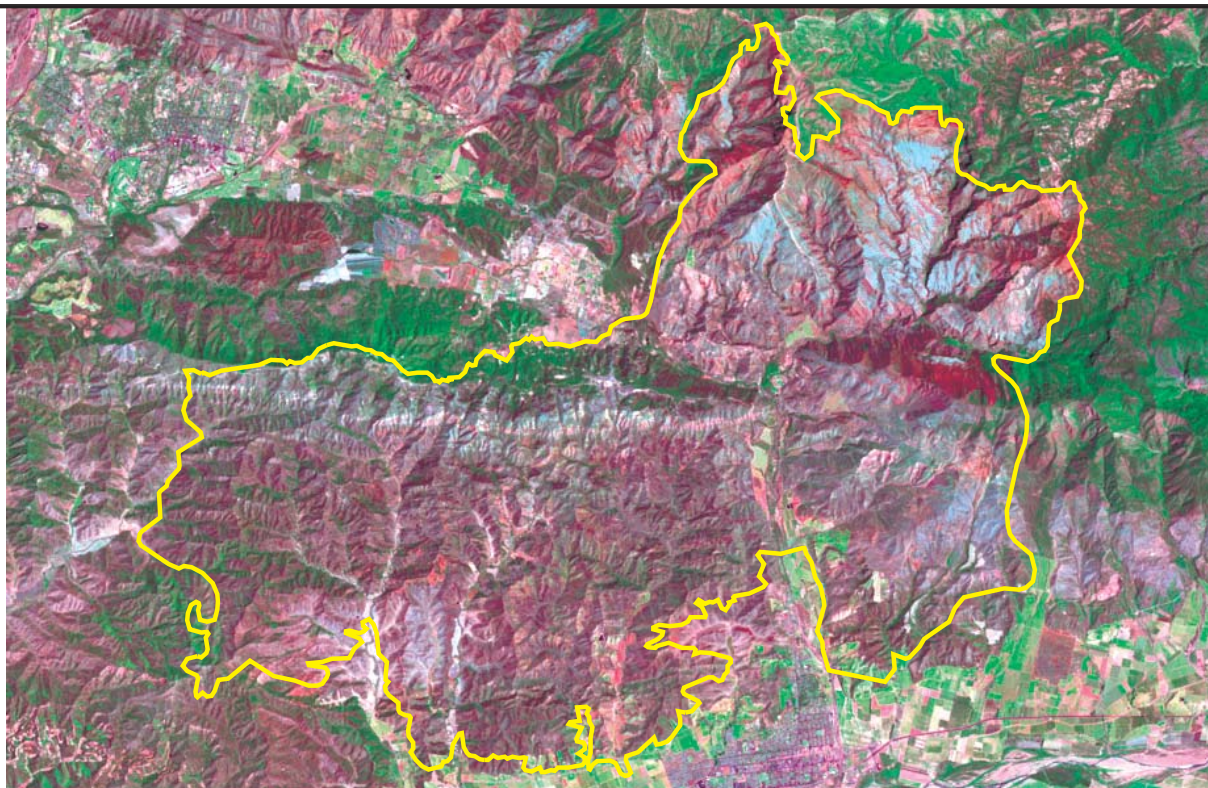
* - Areas in either the pre-fire or post-fire reflectance data containing clouds, snow, shadows, smoke, significantly sized water bodies or missing lines of data



Acreage of Burn Severity	
Burn Severity	Acres
Unburned to Low	562
Low	670
Moderate	2
High	0
Increased Greenness	14
Non-Processing Area Mask *	0
Total	1,248

1985 California: FERNDALE

(FS-0507-048-851014)



Latitude: 34° 24' 45.3" N
 Longitude: 119° 8' 55.5" W
 Fire Ignition Date: October 14, 1985
 Assessment Type: Extended
 Pre-Fire Image Date: June 30, 1984 (Landsat 5)
 Post-Fire Image Date: June 20, 1986 (Landsat 5)



Acreage of Burn Severity

Burn Severity	Acres
Unburned to Low	19,614
Low	14,786
Moderate	3,665
High	469
Increased Greenness	8,199
Non-Processing Area Mask *	0
Total	46,733

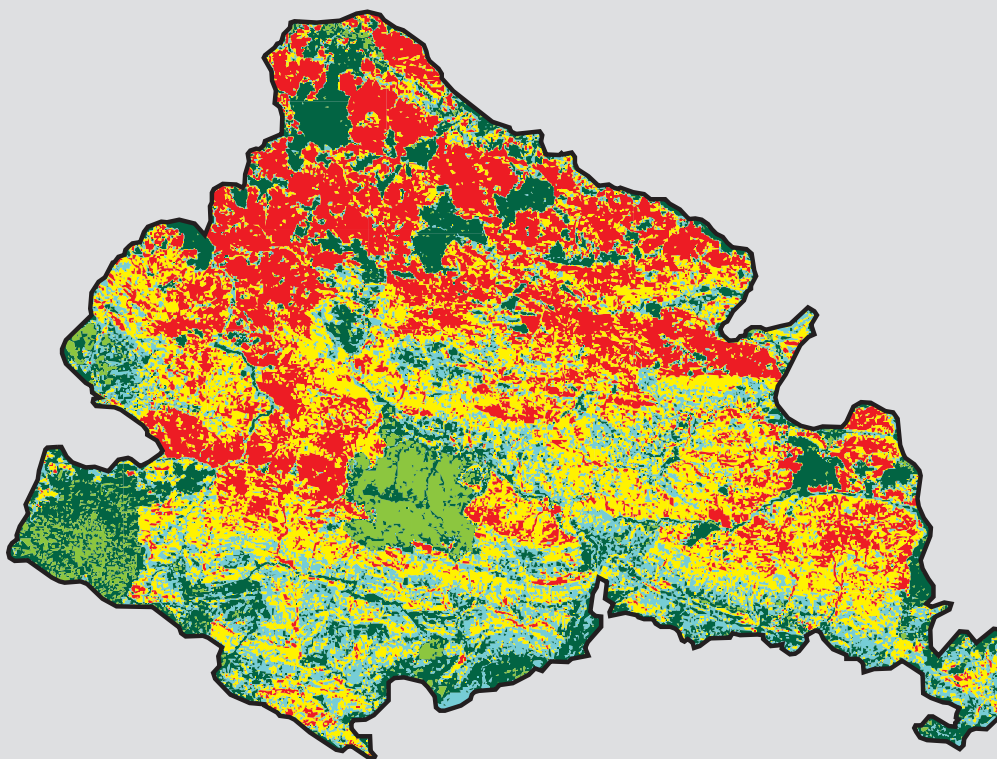
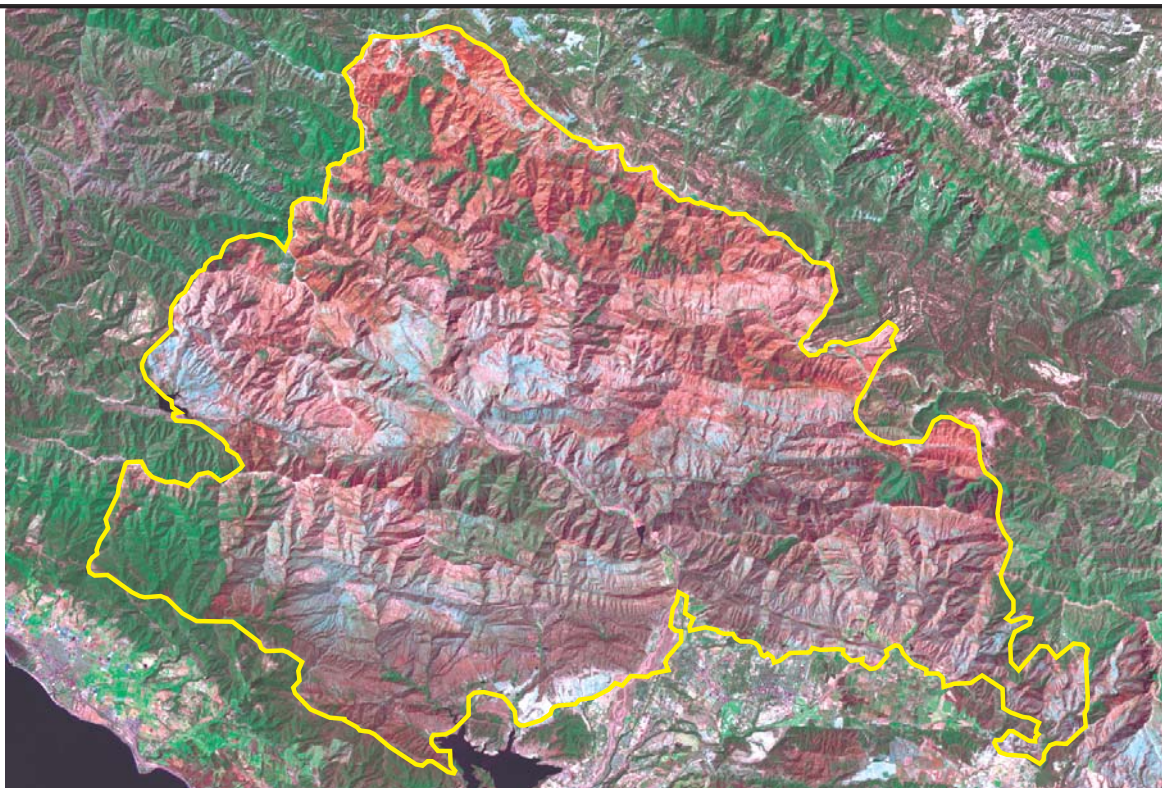
This map portrays fire severity for the fire specified in the map title and summarizes proportions of fire severity classes. These data are produced under the Monitoring Trends in Burn Severity (MTBS) project jointly implemented by the USGS EROS and the USFS RSAC. The MTBS project ascertains the locations of fires based on available fire occurrence information provided by federal and state agencies, and other reliable sources. The MTBS project reserves the right to correct, update or modify geospatial inputs to this map without notification.

* - Areas in either the pre-fire or post-fire reflectance data containing clouds, snow, shadows, smoke, significantly sized water bodies or missing lines of data



1985 California: WHEELER #2

(FS-0507-027-850701)



Latitude: 34° 30' 35.3" N
 Longitude: 119° 21' 15.4" W
 Fire Ignition Date: July 1, 1985
 Assessment Type: Extended
 Pre-Fire Image Date: July 07, 1984 (Landsat 5)
 Post-Fire Image Date: July 29, 1986 (Landsat 5)



Acreage of Burn Severity

Burn Severity	Acres
Unburned to Low	23,956
Low	24,202
Moderate	39,011
High	33,772
Increased Greenness	5,912
Non-Processing Area Mask *	0
Total	126,853

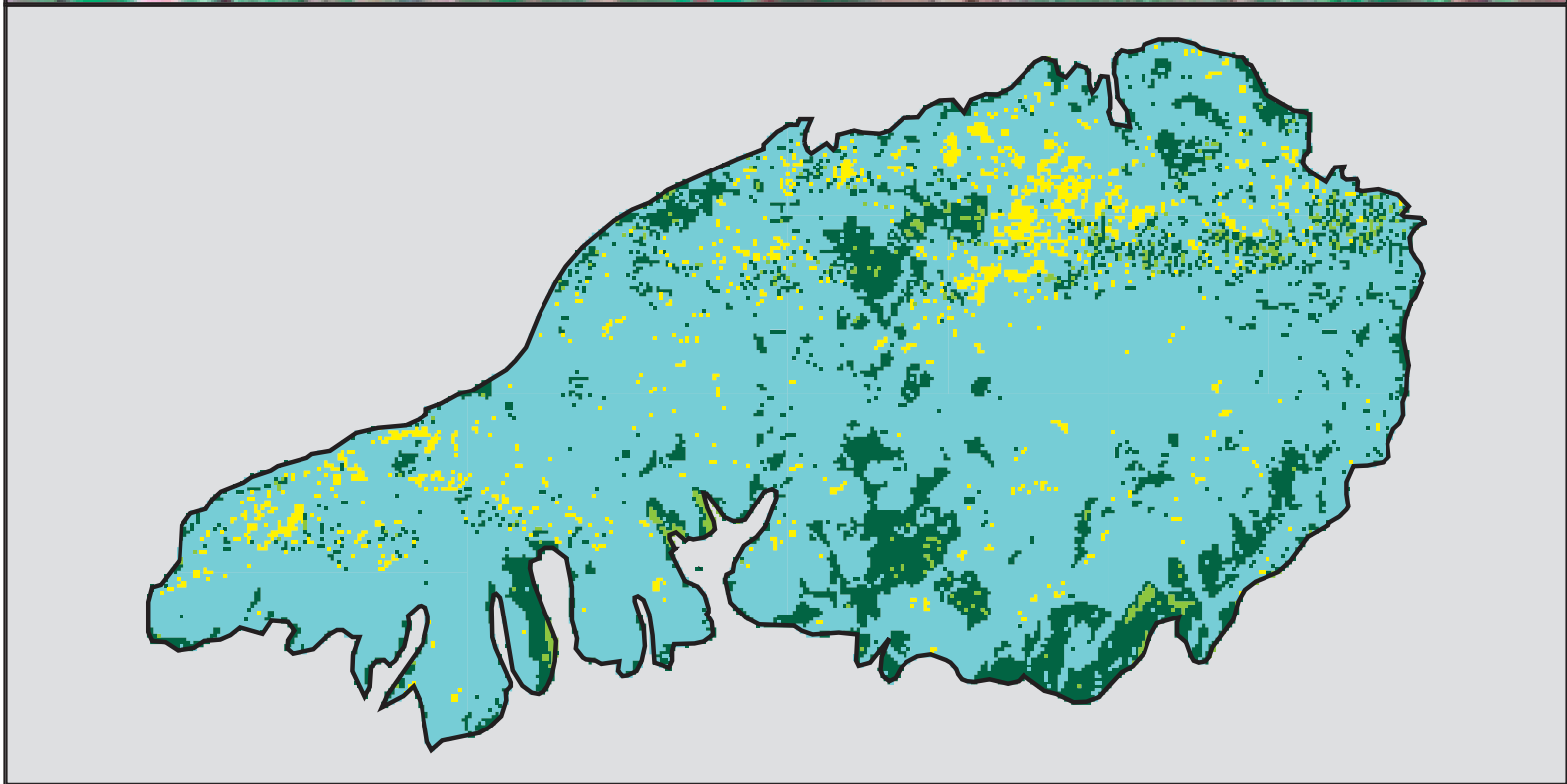
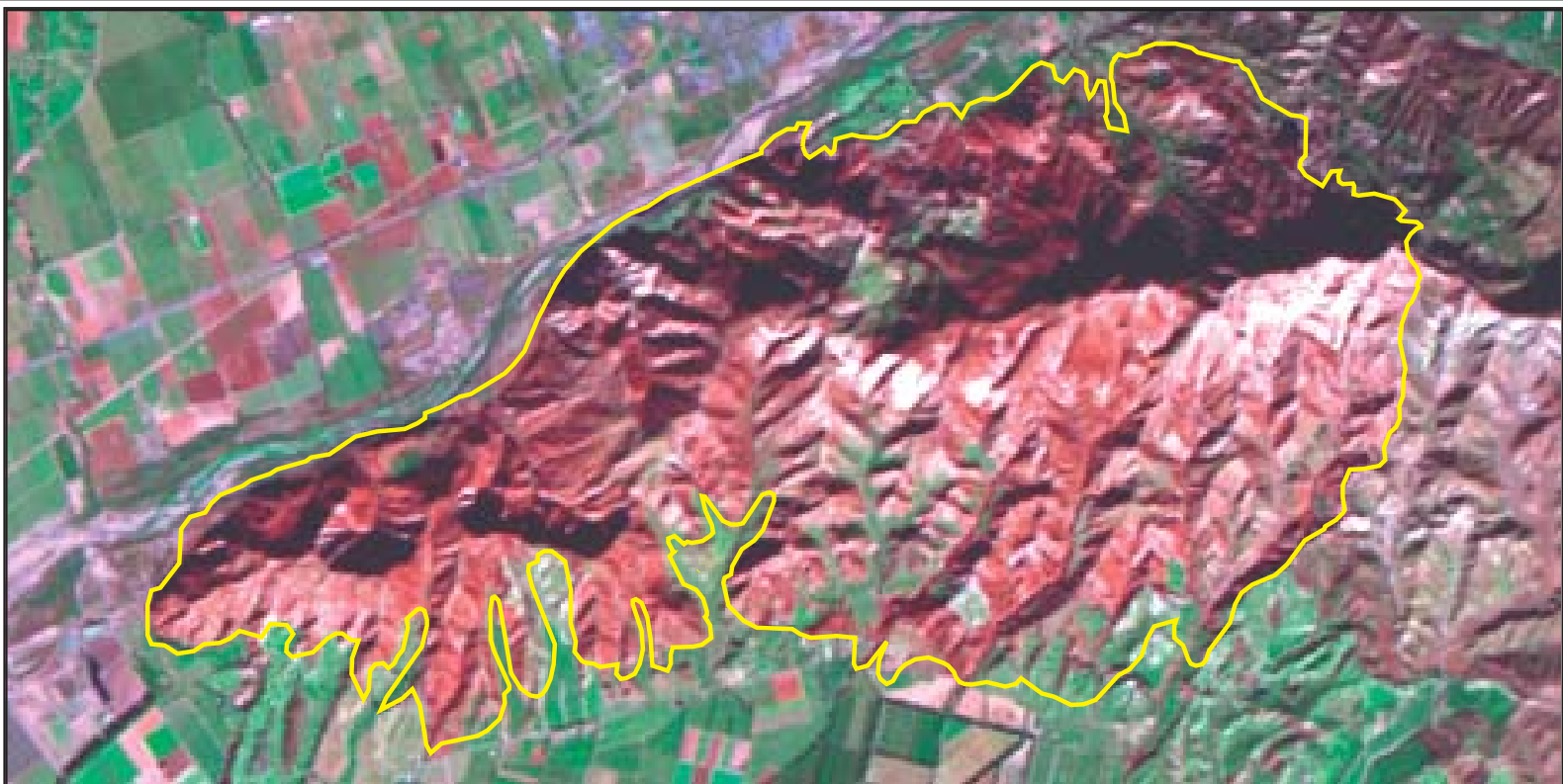
This map portrays fire severity for the fire specified in the map title and summarizes proportions of fire severity classes. These data are produced under the Monitoring Trends in Burn Severity (MTBS) project jointly implemented by the USGS EROS and the USFS RSAC. The MTBS project ascertains the locations of fires based on available fire occurrence information provided by federal and state agencies, and other reliable sources. The MTBS project reserves the right to correct, update or modify geospatial inputs to this map without notification.

* - Areas in either the pre-fire or post-fire reflectance data containing clouds, snow, shadows, smoke, significantly sized water bodies or missing lines of data



1986 California: BRADLEY

(CA-VNC-00000000-19861110)



Latitude: 34° 18' 15.5" N
 Longitude: 119° 3' 51.4" W
 Fire Ignition Date: November 10, 1986
 Assessment Type: Initial
 Pre-Fire Image Date: December 10, 1985 (Landsat 5)
 Post-Fire Image Date: November 27, 1986 (Landsat 5)

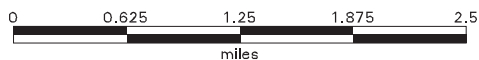


Acreage of Burn Severity

Burn Severity	Acres
Unburned to Low	1,481
Low	8,128
Moderate	377
High	0
Increased Greenness	117
Non-Processing Area Mask *	0
Total	10,103

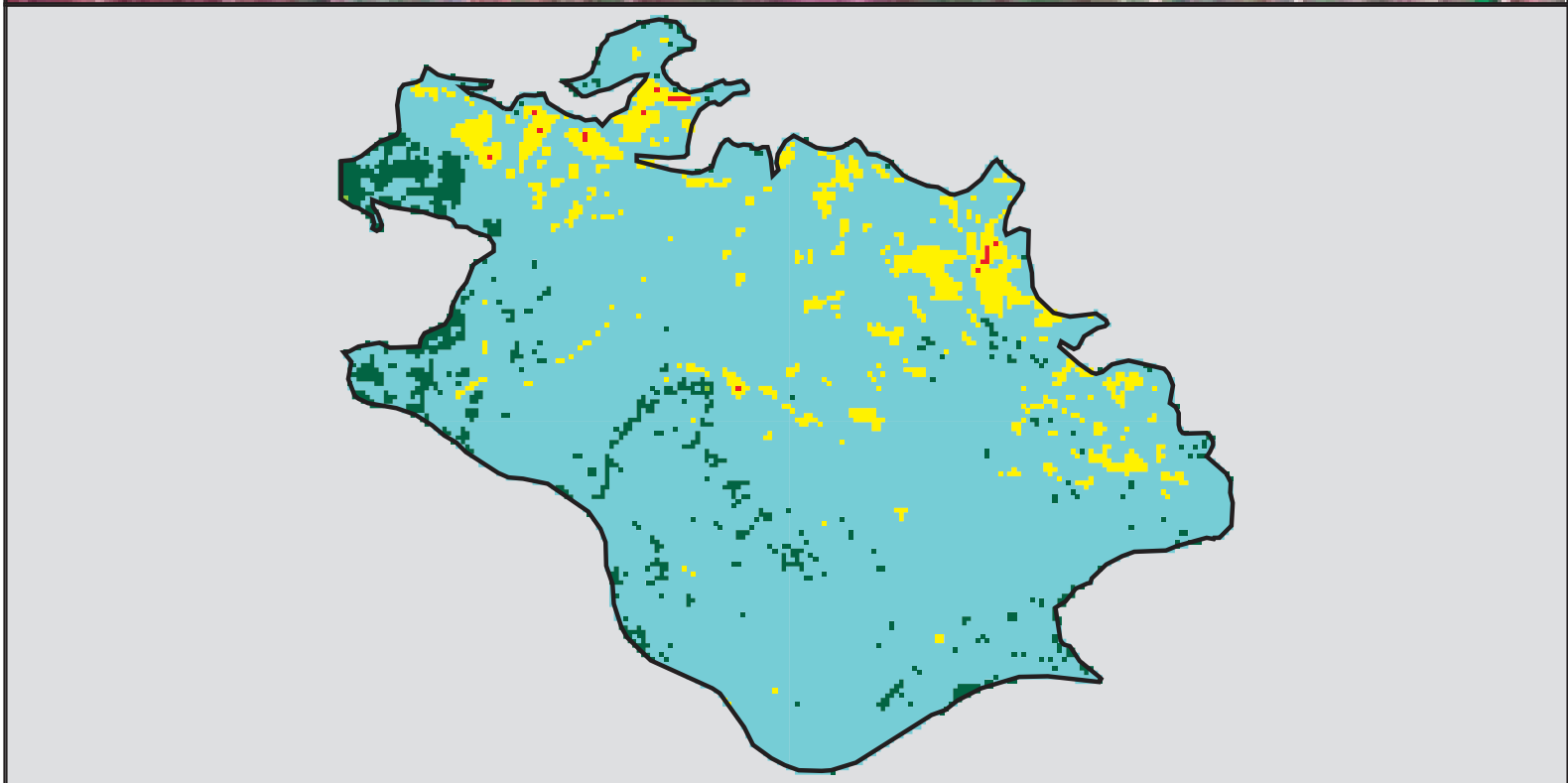
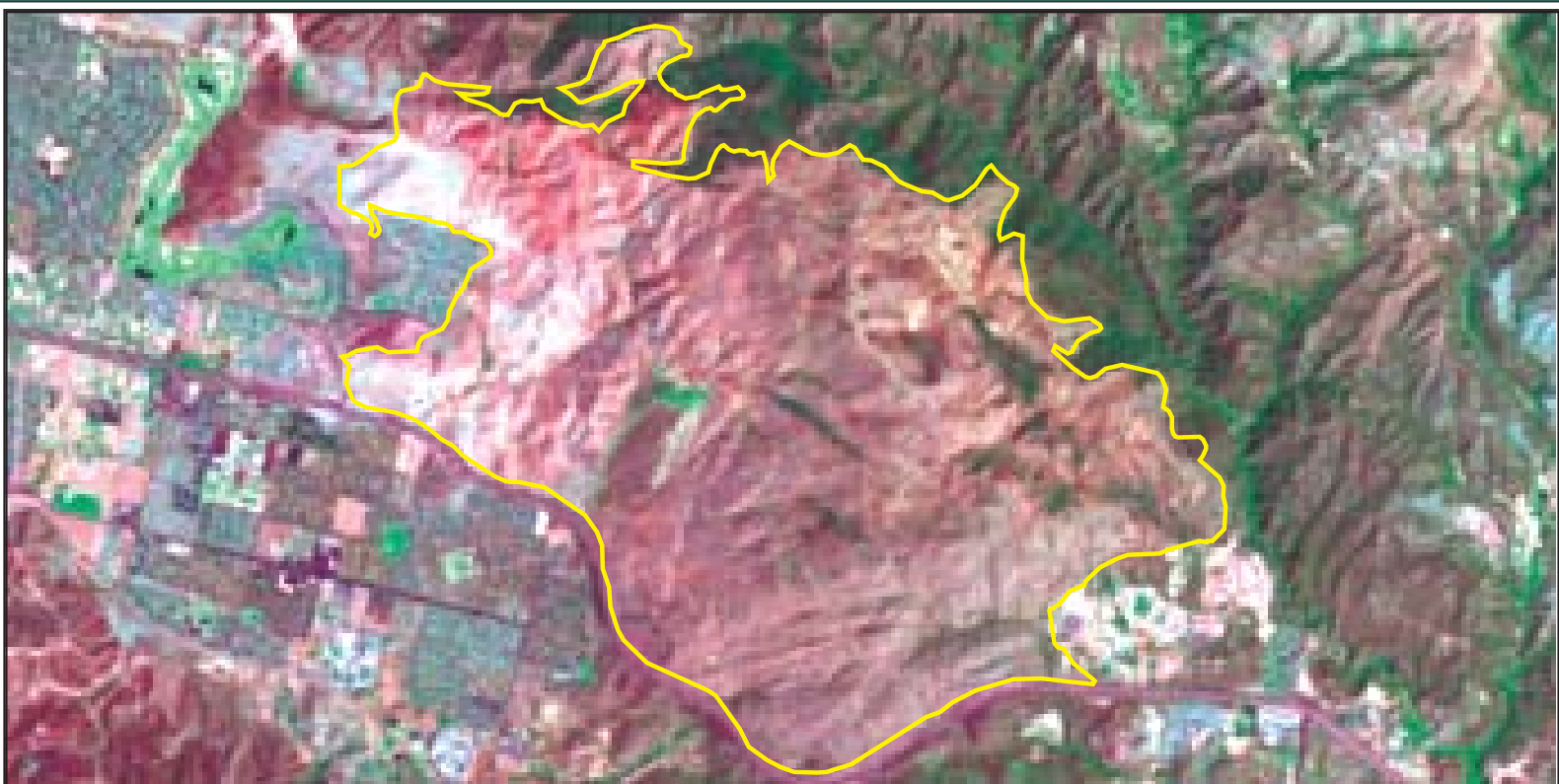
This map portrays fire severity for the fire specified in the map title and summarizes proportions of fire severity classes. These data are produced under the Monitoring Trends in Burn Severity (MTBS) project jointly implemented by the USGS EROS and the USFS RSAC. The MTBS project ascertains the locations of fires based on available fire occurrence information provided by federal and state agencies, and other reliable sources. The MTBS project reserves the right to correct, update or modify geospatial inputs to this map without notification.

* - Areas in either the pre-fire or post-fire reflectance data containing clouds, snow, shadows, smoke, significantly sized water bodies or missing lines of data



1988 California: KEUHNER FIRE

(CA-LAC-00000088-2-19880904)



Latitude: 34° 17' 16.8" N
 Longitude: 118° 38' 52.4" W
 Fire Ignition Date: September 4, 1988
 Assessment Type: Extended
 Pre-Fire Image Date: June 09, 1988 (Landsat 5)
 Post-Fire Image Date: May 27, 1989 (Landsat 5)



Acreage of Burn Severity

Burn Severity	Acres
Unburned to Low	200
Low	3,434
Moderate	262
High	4
Increased Greenness	0
Non-Processing Area Mask *	0
Total	3,900

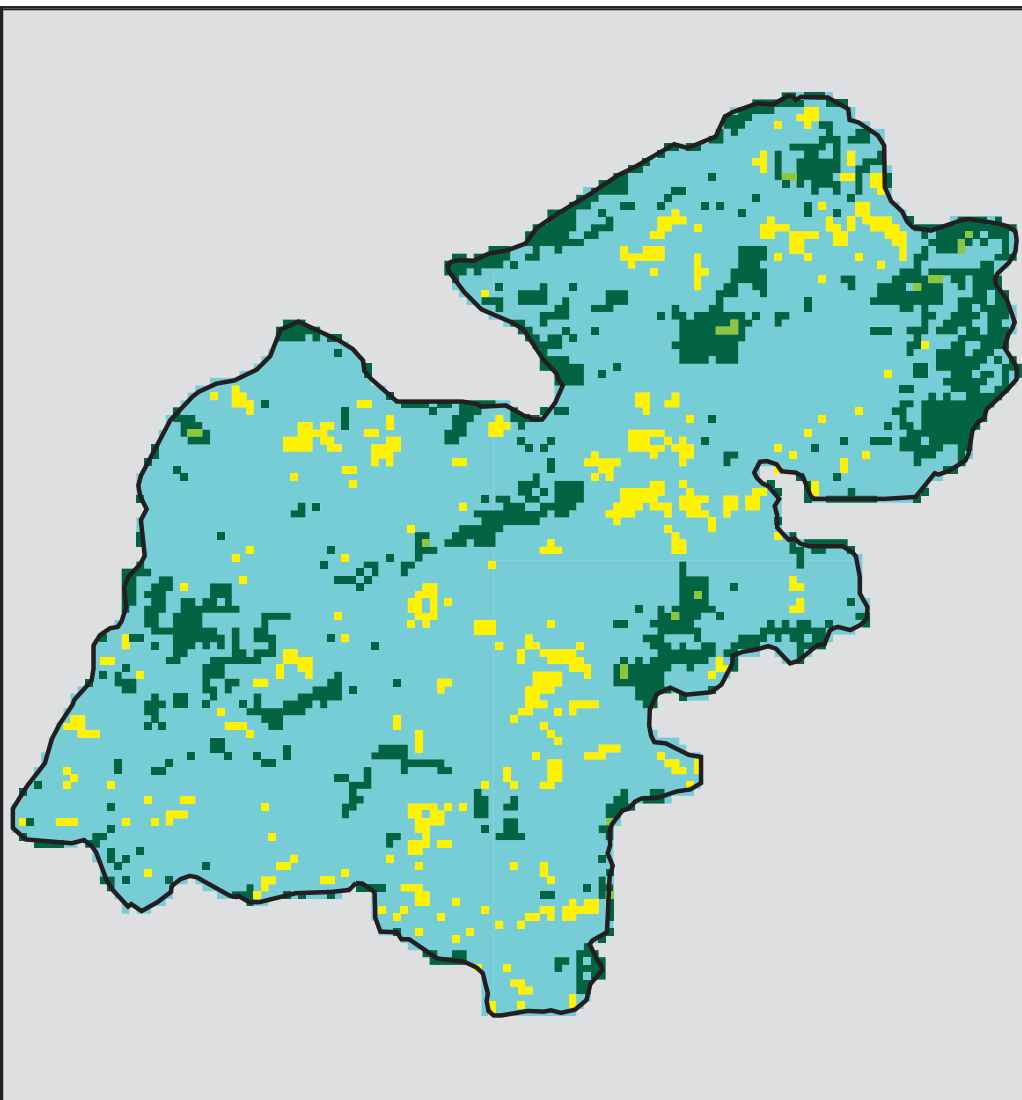
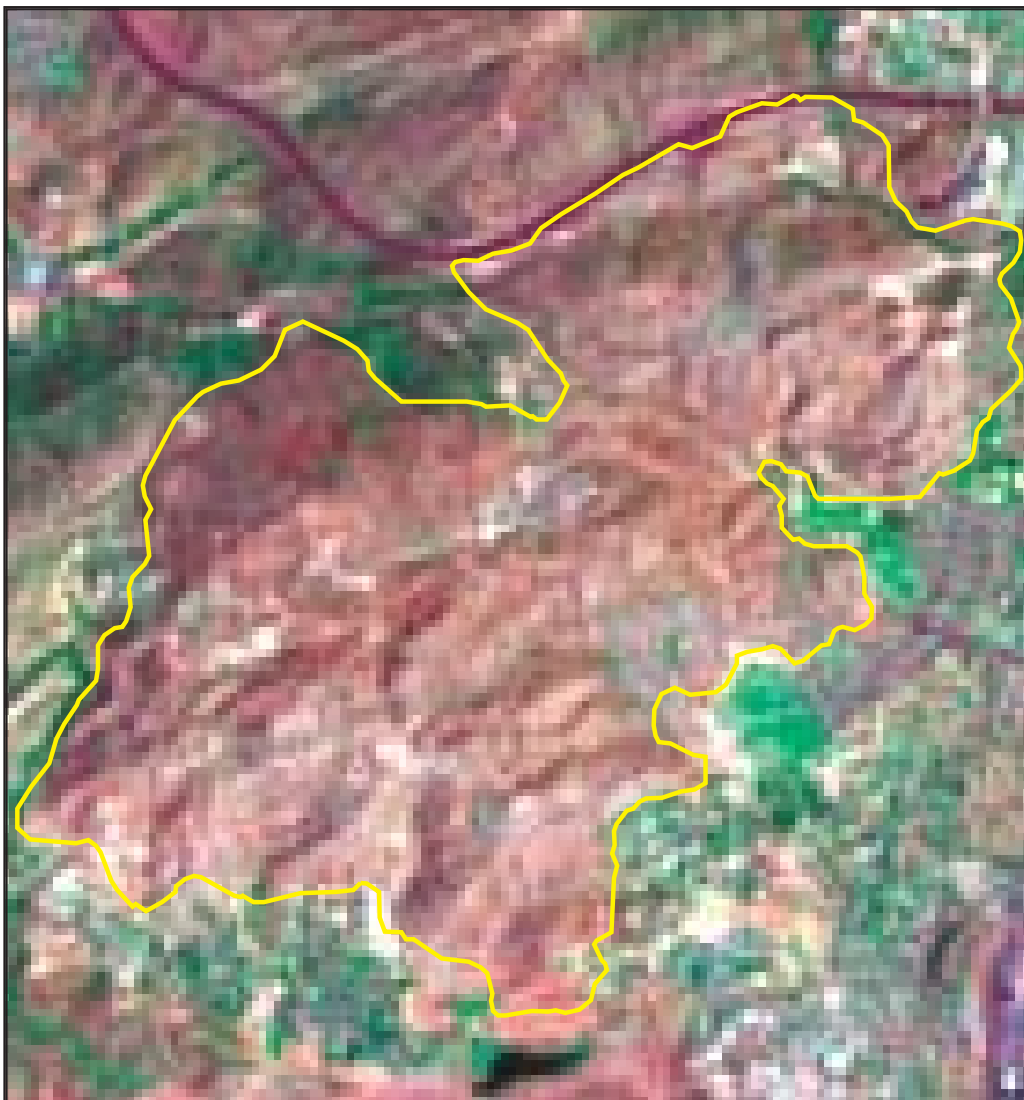
This map portrays fire severity for the fire specified in the map title and summarizes proportions of fire severity classes. These data are produced under the Monitoring Trends in Burn Severity (MTBS) project jointly implemented by the USGS EROS and the USFS RSAC. The MTBS project ascertains the locations of fires based on available fire occurrence information provided by federal and state agencies, and other reliable sources. The MTBS project reserves the right to correct, update or modify geospatial inputs to this map without notification.

* - Areas in either the pre-fire or post-fire reflectance data containing clouds, snow, shadows, smoke, significantly sized water bodies or missing lines of data



1993 California: CHATSWORTH FIRE

(CA-LAC-00000021-19931027)



Latitude: 34° 15' 24.3" N
 Longitude: 118° 37' 54.8" W
 Fire Ignition Date: October 27, 1993
 Assessment Type: Extended
 Pre-Fire Image Date: June 23, 1993 (Landsat 5)
 Post-Fire Image Date: June 26, 1994 (Landsat 5)

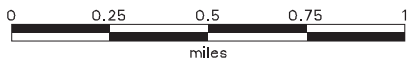


Acreage of Burn Severity

Burn Severity	Acres
Unburned to Low	281
Low	1,546
Moderate	119
High	0
Increased Greenness	4
Non-Processing Area Mask *	0
Total	1,950

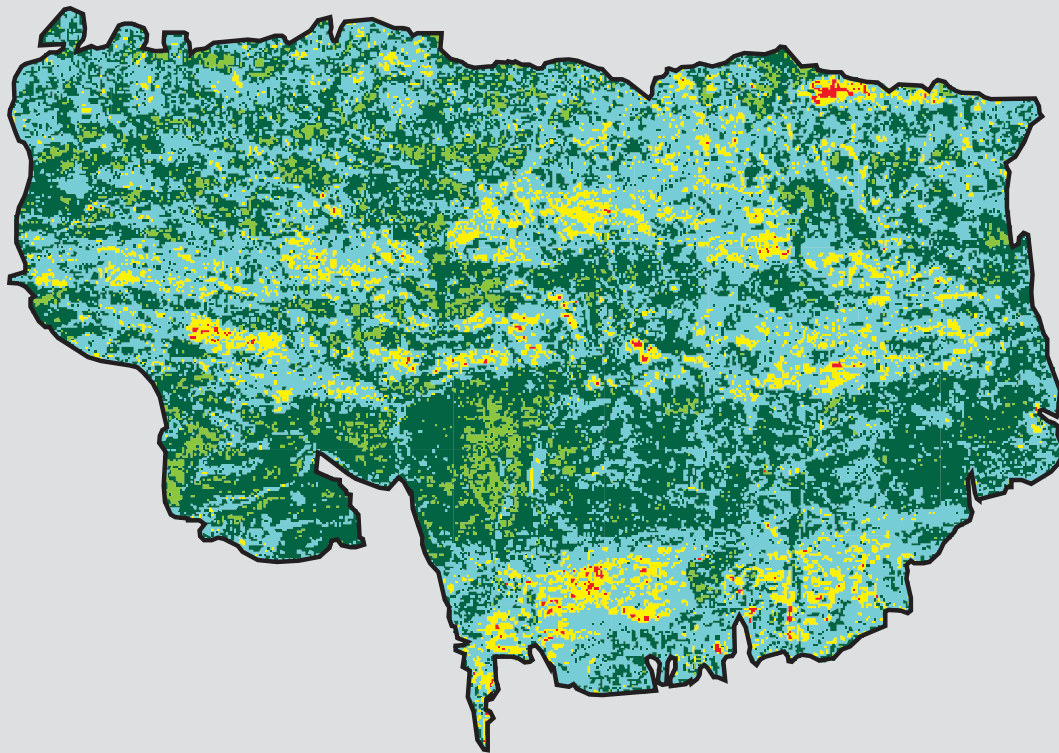
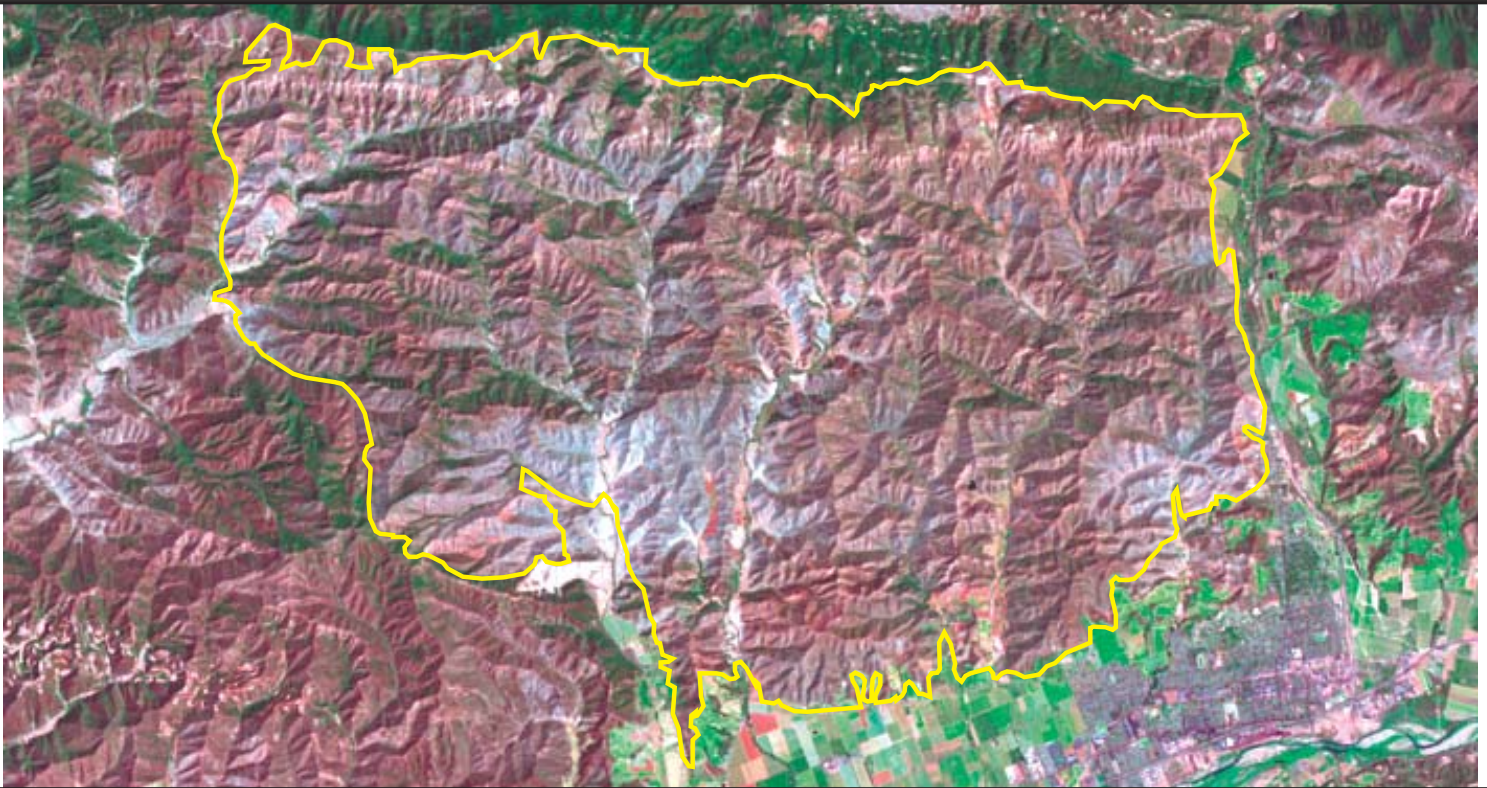
This map portrays fire severity for the fire specified in the map title and summarizes proportions of fire severity classes. These data are produced under the Monitoring Trends in Burn Severity (MTBS) project jointly implemented by the USGS EROS and the USFS RSAC. The MTBS project ascertains the locations of fires based on available fire occurrence information provided by federal and state agencies, and other reliable sources. The MTBS project reserves the right to correct, update or modify geospatial inputs to this map without notification.

* - Areas in either the pre-fire or post-fire reflectance data containing clouds, snow, shadows, smoke, significantly sized water bodies or missing lines of data



1993 California: STECKEL

(CA-VNC-00000000-19931027)



Latitude: 34° 22' 53.4" N
 Longitude: 119° 9' 9.1" W
 Fire Ignition Date: October 27, 1993
 Assessment Type: Extended
 Pre-Fire Image Date: August 01, 1993 (Landsat 5)
 Post-Fire Image Date: August 04, 1994 (Landsat 5)

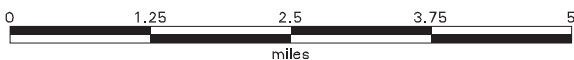


Acreage of Burn Severity

Burn Severity	Acres
Unburned to Low	10,841
Low	12,023
Moderate	2,040
High	88
Increased Greenness	1,206
Non-Processing Area Mask *	0
Total	26,198

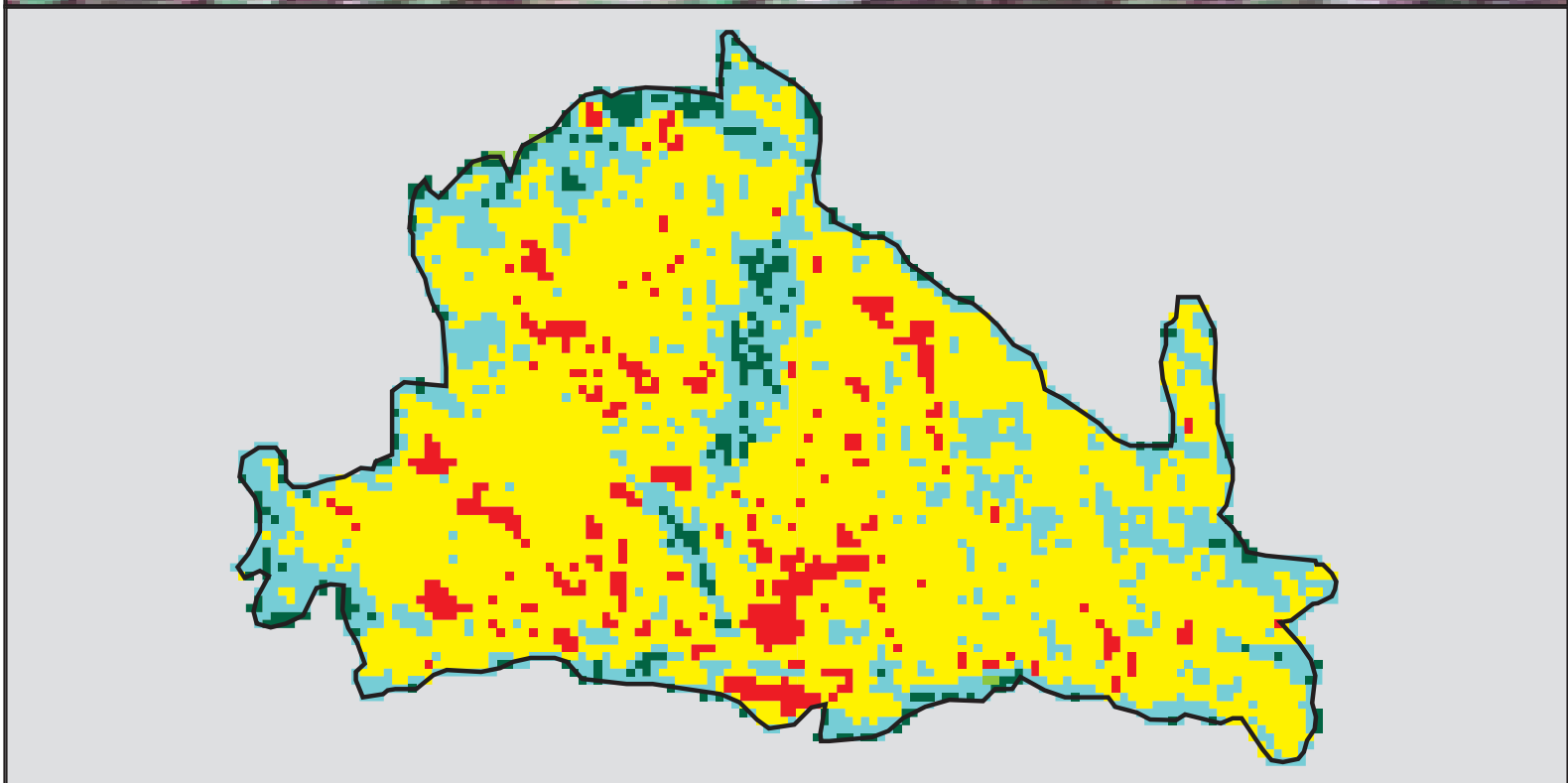
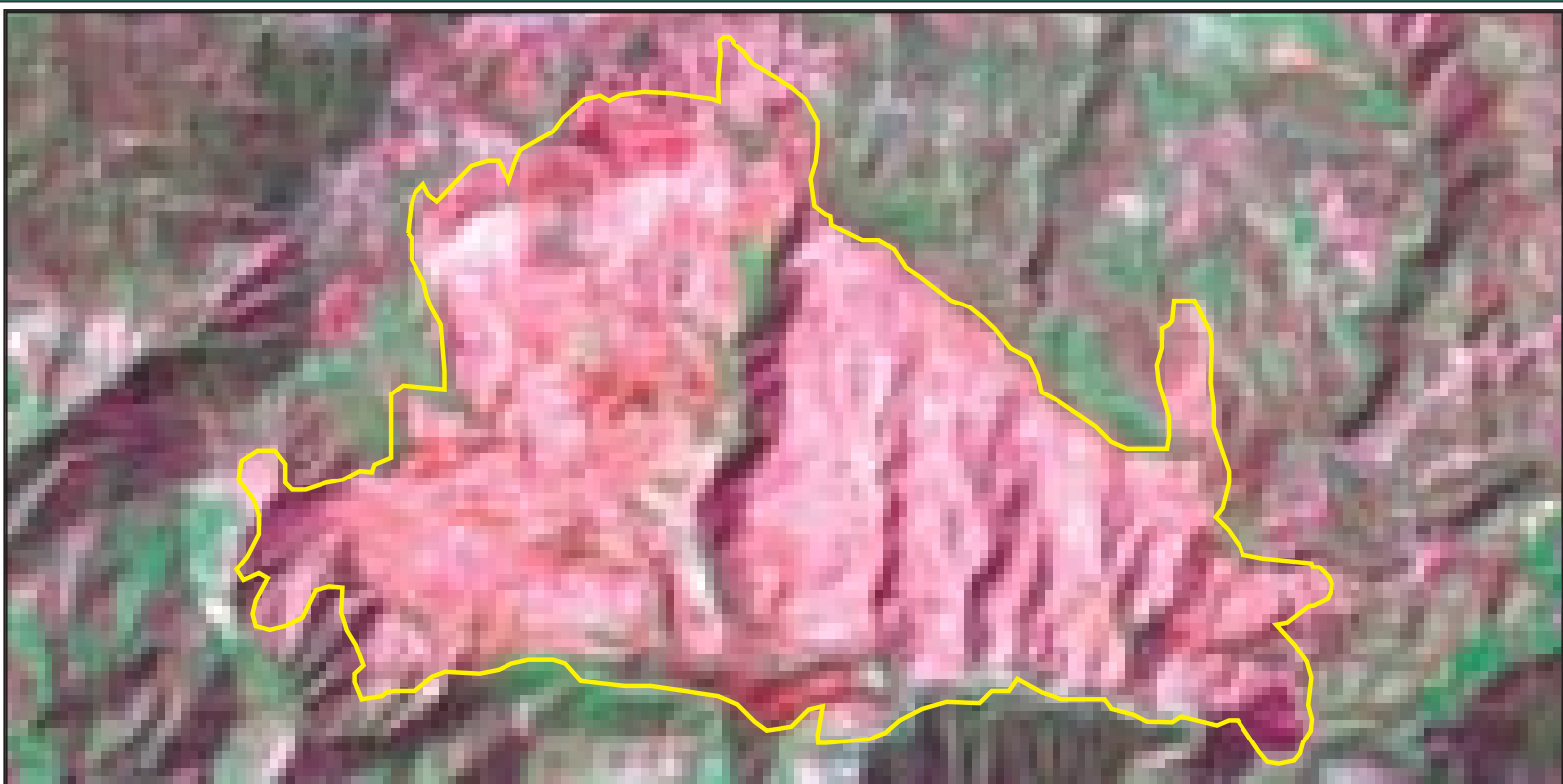
This map portrays fire severity for the fire specified in the map title and summarizes proportions of fire severity classes. These data are produced under the Monitoring Trends in Burn Severity (MTBS) project jointly implemented by the USGS EROS and the USFS RSAC. The MTBS project ascertains the locations of fires based on available fire occurrence information provided by federal and state agencies, and other reliable sources. The MTBS project reserves the right to correct, update or modify geospatial inputs to this map without notification.

* - Areas in either the pre-fire or post-fire reflectance data containing clouds, snow, shadows, smoke, significantly sized water bodies or missing lines of data



1993 California: WHEEL

(FS-0507-043-931027)

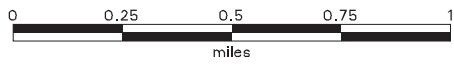


Latitude: 34° 30' 49.0" N
 Longitude: 119° 18' 13.7" W
 Fire Ignition Date: October 27, 1993
 Assessment Type: Extended
 Pre-Fire Image Date: August 01, 1993 (Landsat 5)
 Post-Fire Image Date: August 04, 1994 (Landsat 5)



This map portrays fire severity for the fire specified in the map title and summarizes proportions of fire severity classes. These data are produced under the Monitoring Trends in Burn Severity (MTBS) project jointly implemented by the USGS EROS and the USFS RSAC. The MTBS project ascertains the locations of fires based on available fire occurrence information provided by federal and state agencies, and other reliable sources. The MTBS project reserves the right to correct, update or modify geospatial inputs to this map without notification.

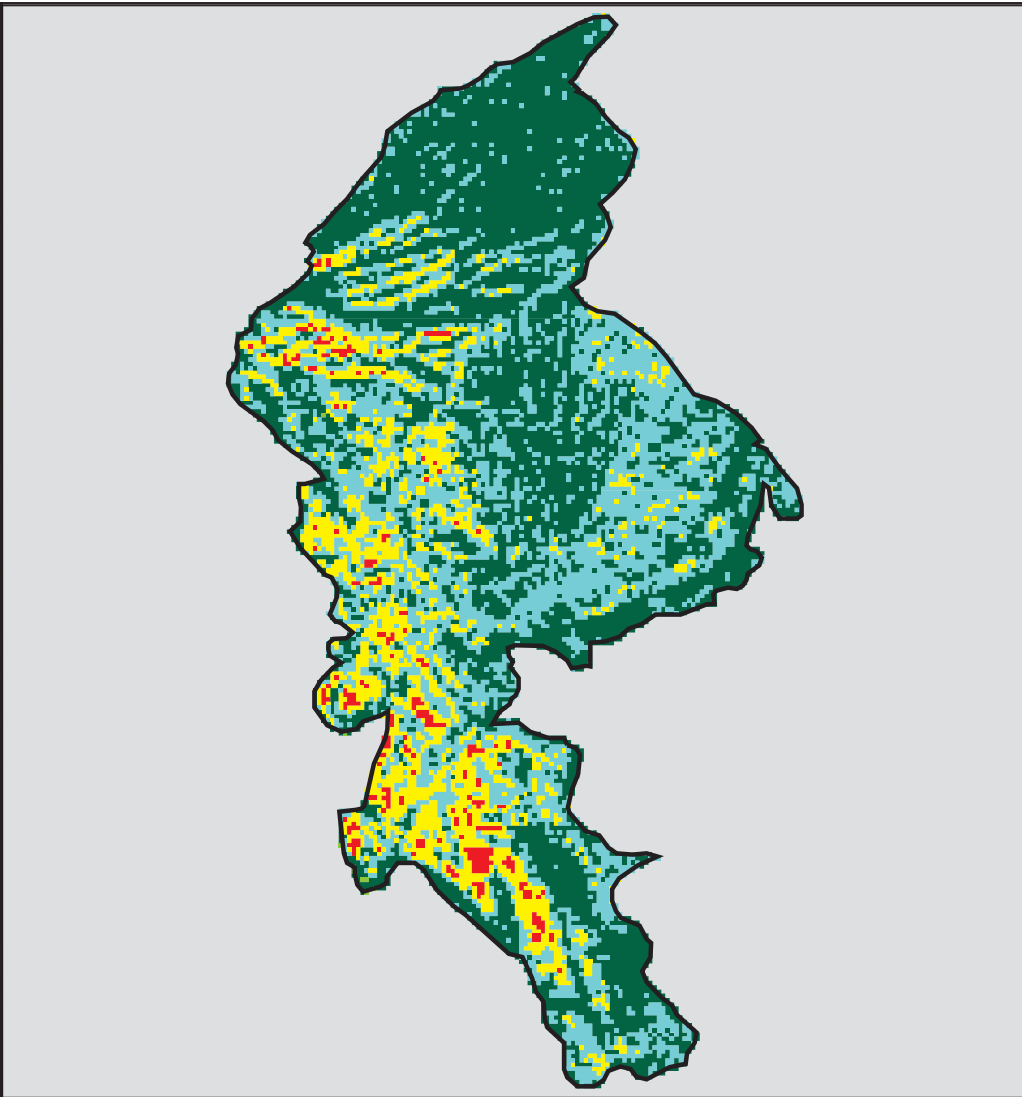
* - Areas in either the pre-fire or post-fire reflectance data containing clouds, snow, shadows, smoke, significantly sized water bodies or missing lines of data



Acreage of Burn Severity	
Burn Severity	Acres
Unburned to Low	55
Low	326
Moderate	977
High	102
Increased Greenness	1
Non-Processing Area Mask *	0
Total	1,461

1994 California: ALISO

(BLM-CABBD-D154-19940730)



Latitude: 34° 54' 32.5" N
 Longitude: 119° 43' 45.7" W
 Fire Ignition Date: July 30, 1994
 Assessment Type: Extended
 Pre-Fire Image Date: August 01, 1993 (Landsat 5)
 Post-Fire Image Date: July 22, 1995 (Landsat 5)



Acreage of Burn Severity

Burn Severity	Acres
Unburned to Low	1,618
Low	1,203
Moderate	518
High	66
Increased Greenness	1
Non-Processing Area Mask *	0
Total	3,406

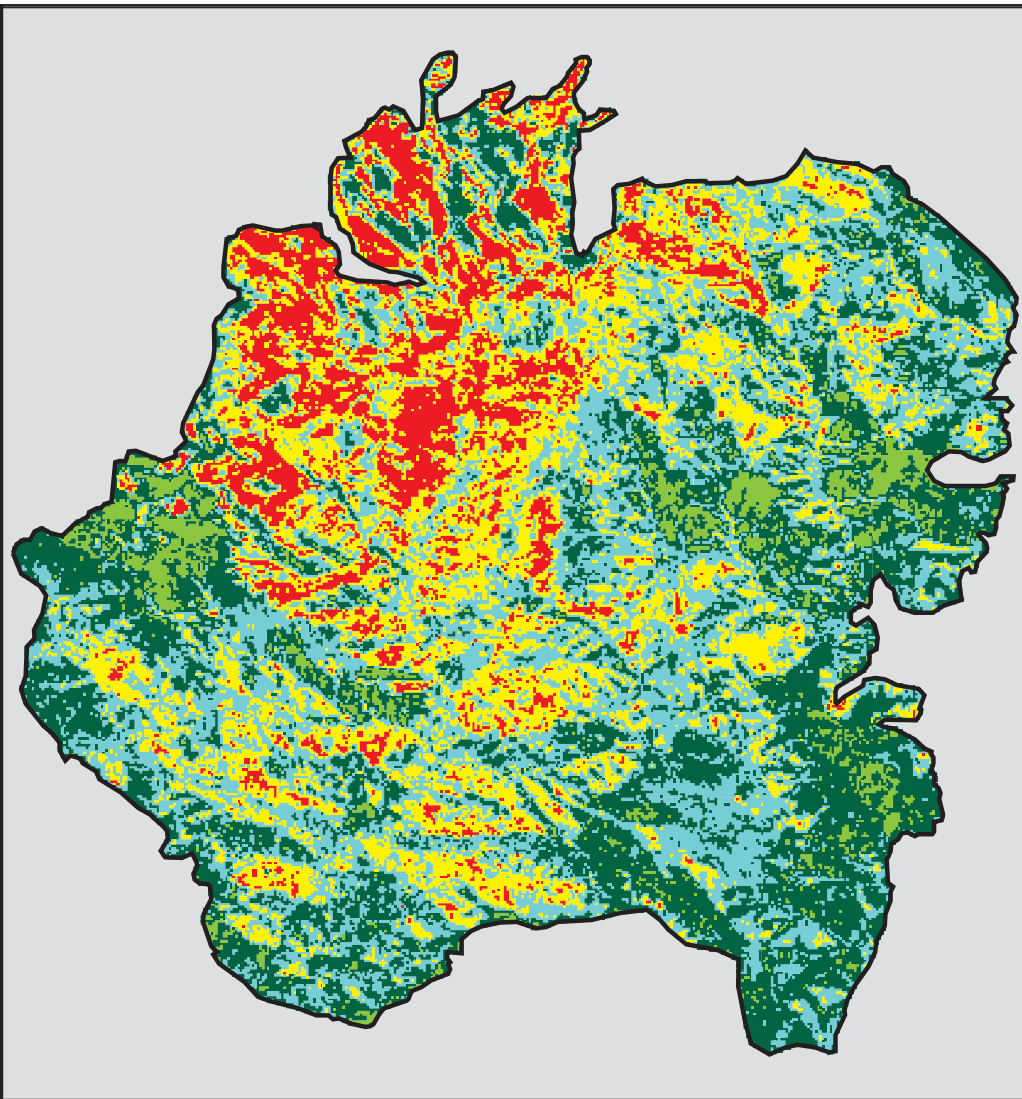
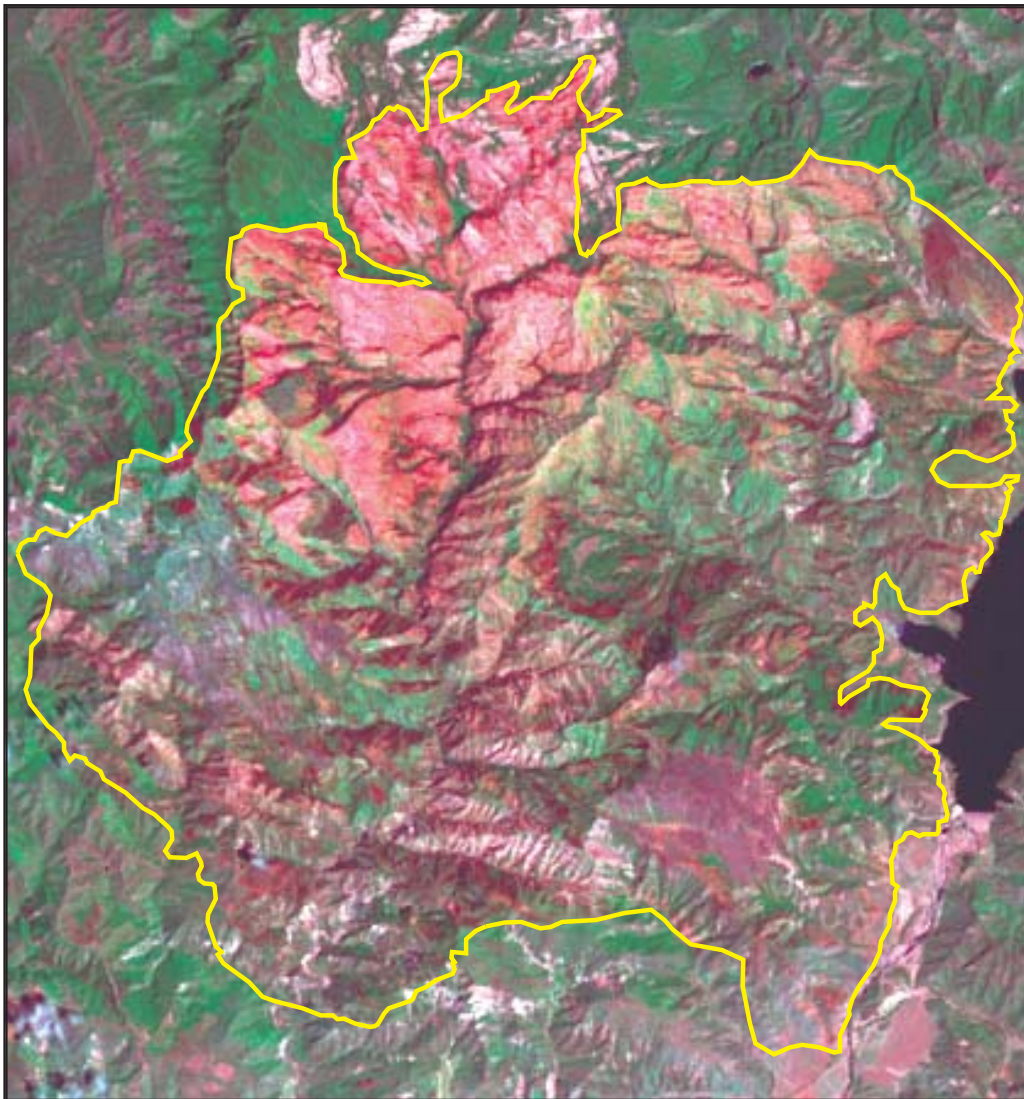
This map portrays fire severity for the fire specified in the map title and summarizes proportions of fire severity classes. These data are produced under the Monitoring Trends in Burn Severity (MTBS) project jointly implemented by the USGS EROS and the USFS RSAC. The MTBS project ascertains the locations of fires based on available fire occurrence information provided by federal and state agencies, and other reliable sources. The MTBS project reserves the right to correct, update or modify geospatial inputs to this map without notification.

* - Areas in either the pre-fire or post-fire reflectance data containing clouds, snow, shadows, smoke, significantly sized water bodies or missing lines of data



1997 California: HOPPER

(FS-0507-042-970805)



Latitude: 34° 28' 34.3" N
 Longitude: 118° 48' 57.9" W
 Fire Ignition Date: August 5, 1997
 Assessment Type: Extended
 Pre-Fire Image Date: May 01, 1997 (Landsat 5)
 Post-Fire Image Date: June 21, 1998 (Landsat 5)

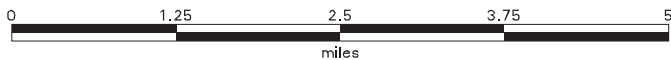


Acreage of Burn Severity

Burn Severity	Acres
Unburned to Low	6,872
Low	7,666
Moderate	5,896
High	2,585
Increased Greenness	1,057
Non-Processing Area Mask *	0
Total	24,076

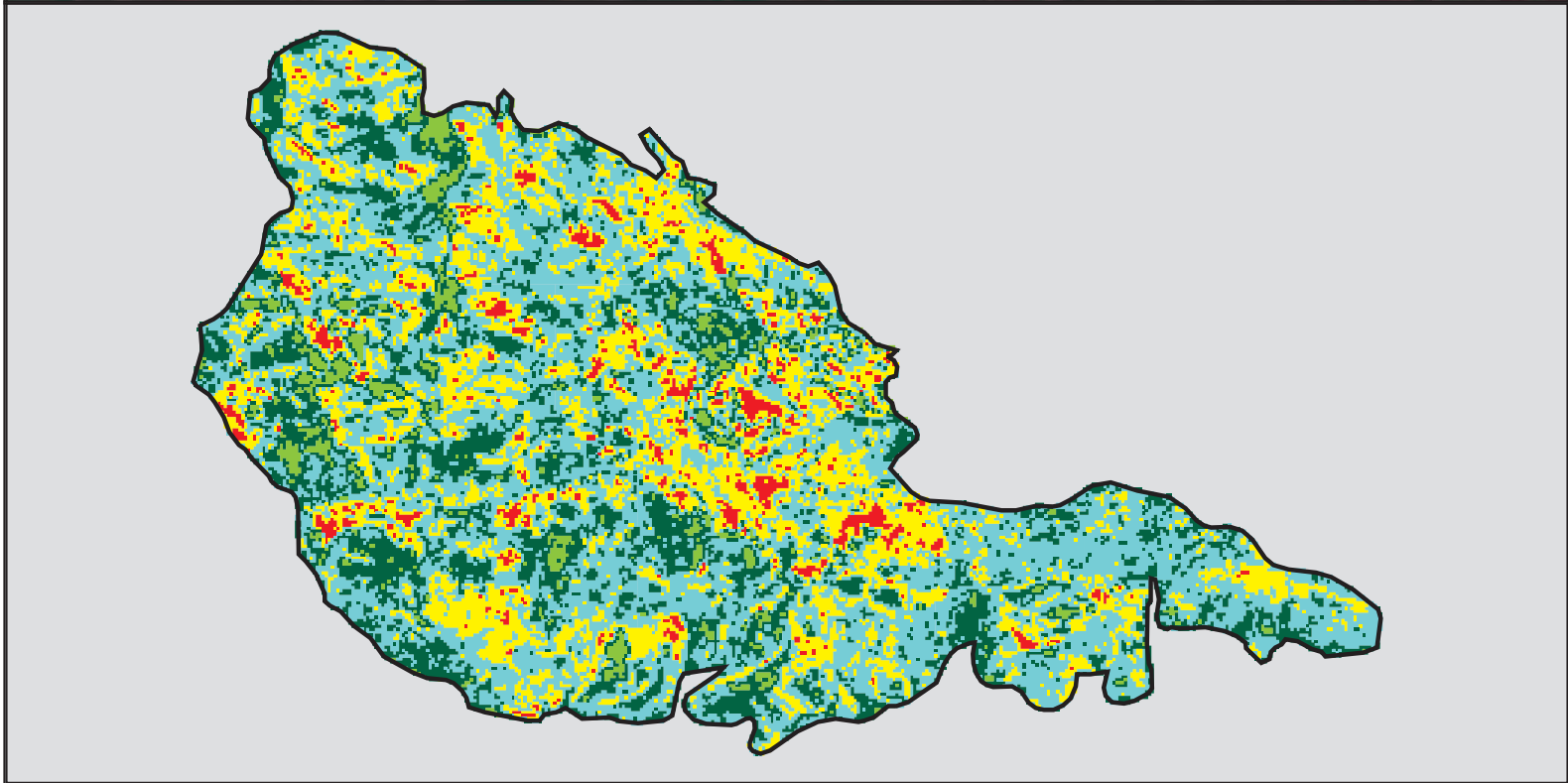
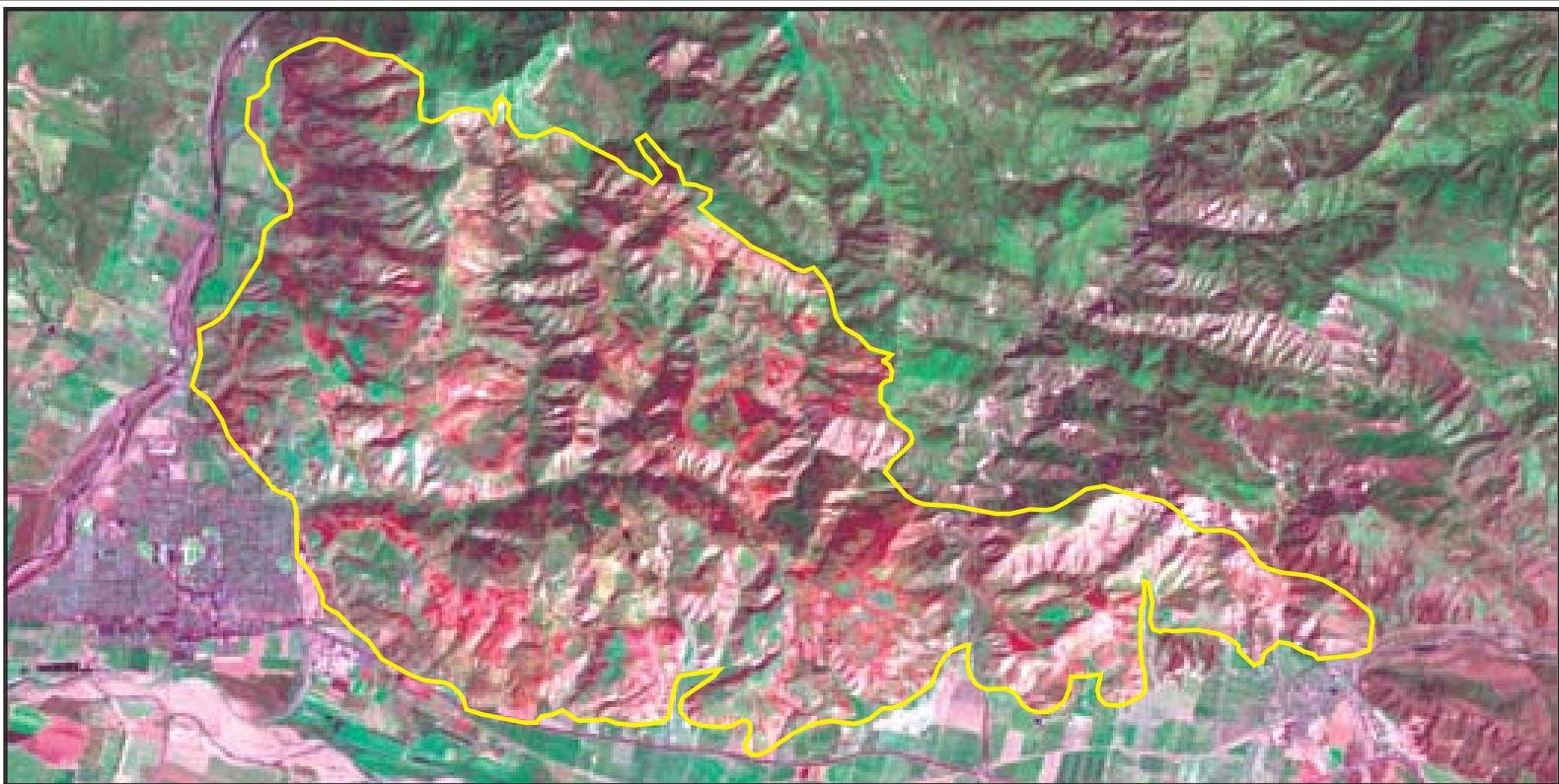
This map portrays fire severity for the fire specified in the map title and summarizes proportions of fire severity classes. These data are produced under the Monitoring Trends in Burn Severity (MTBS) project jointly implemented by the USGS EROS and the USFS RSAC. The MTBS project ascertains the locations of fires based on available fire occurrence information provided by federal and state agencies, and other reliable sources. The MTBS project reserves the right to correct, update or modify geospatial inputs to this map without notification.

* - Areas in either the pre-fire or post-fire reflectance data containing clouds, snow, shadows, smoke, significantly sized water bodies or missing lines of data



1998 California: PIRU

(CA-VNC-00000000-19981018)



Latitude: 34° 25' 20.3" N
 Longitude: 118° 52' 18.5" W
 Fire Ignition Date: October 18, 1998
 Assessment Type: Extended
 Pre-Fire Image Date: May 01, 1997 (Landsat 5)
 Post-Fire Image Date: May 07, 1999 (Landsat 5)

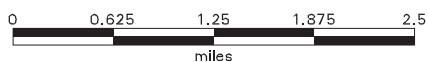


Acreage of Burn Severity

Burn Severity	Acres
Unburned to Low	2,324
Low	4,802
Moderate	2,531
High	379
Increased Greenness	377
Non-Processing Area Mask *	0
Total	10,413

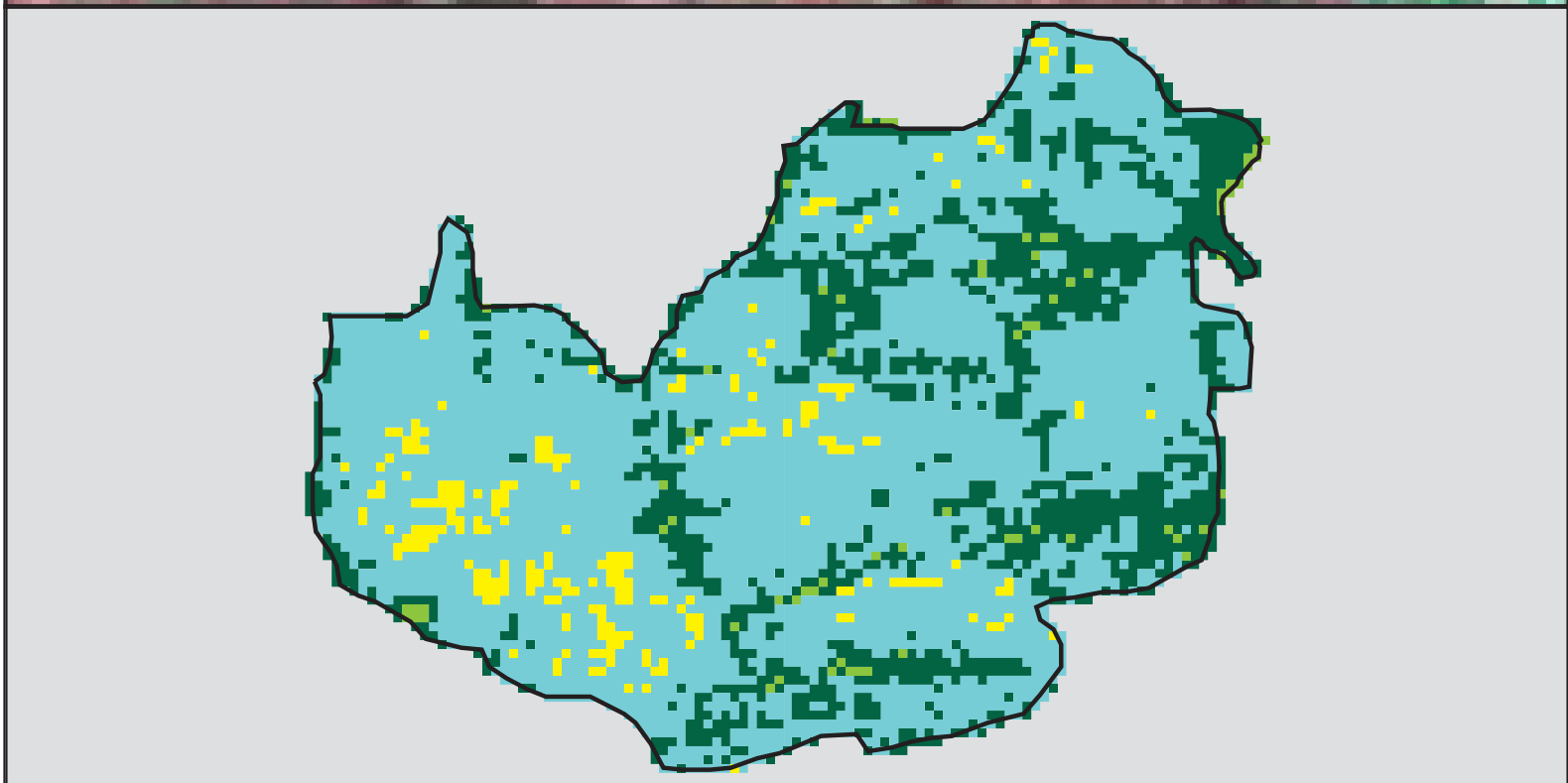
This map portrays fire severity for the fire specified in the map title and summarizes proportions of fire severity classes. These data are produced under the Monitoring Trends in Burn Severity (MTBS) project jointly implemented by the USGS EROS and the USFS RSAC. The MTBS project ascertains the locations of fires based on available fire occurrence information provided by federal and state agencies, and other reliable sources. The MTBS project reserves the right to correct, update or modify geospatial inputs to this map without notification.

* - Areas in either the pre-fire or post-fire reflectance data containing clouds, snow, shadows, smoke, significantly sized water bodies or missing lines of data



2003 California: ADAMS CANYON PHASE 1

(CA-RX-SOUTH-029-VNC-20030903)



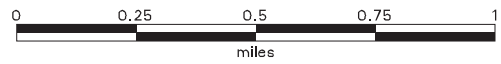
Latitude: 34° 24' 11.4" N
 Longitude: 119° 5' 59.4" W
 Fire Ignition Date: September 3, 2003
 Assessment Type: Initial
 Pre-Fire Image Date: September 20, 2002 (Landsat 5)
 Post-Fire Image Date: September 23, 2003 (Landsat 5)



Acreage of Burn Severity	
Burn Severity	Acres
Unburned to Low	286
Low	881
Moderate	54
High	0
Increased Greenness	14
Non-Processing Area Mask *	0
Total	1,235

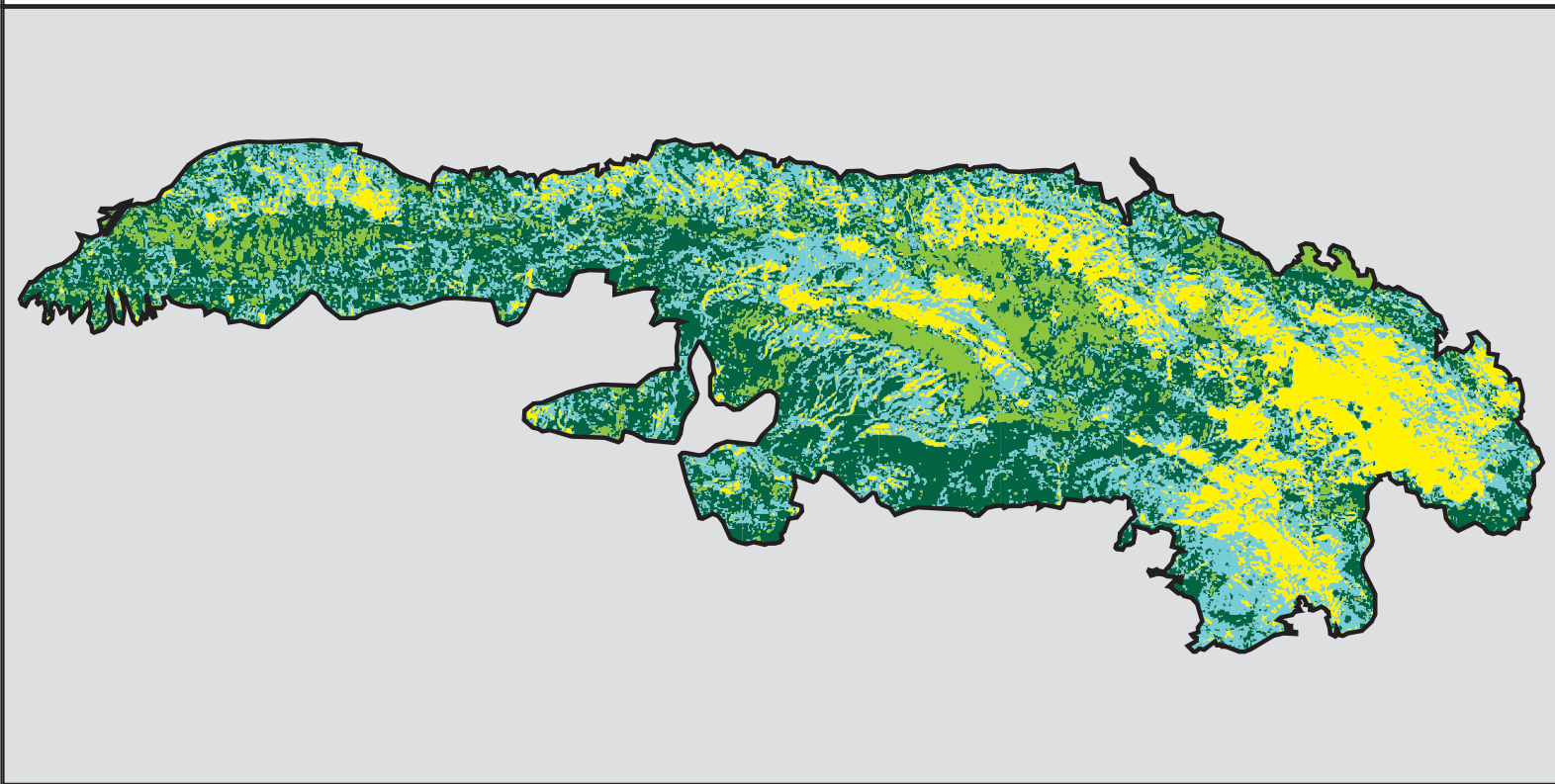
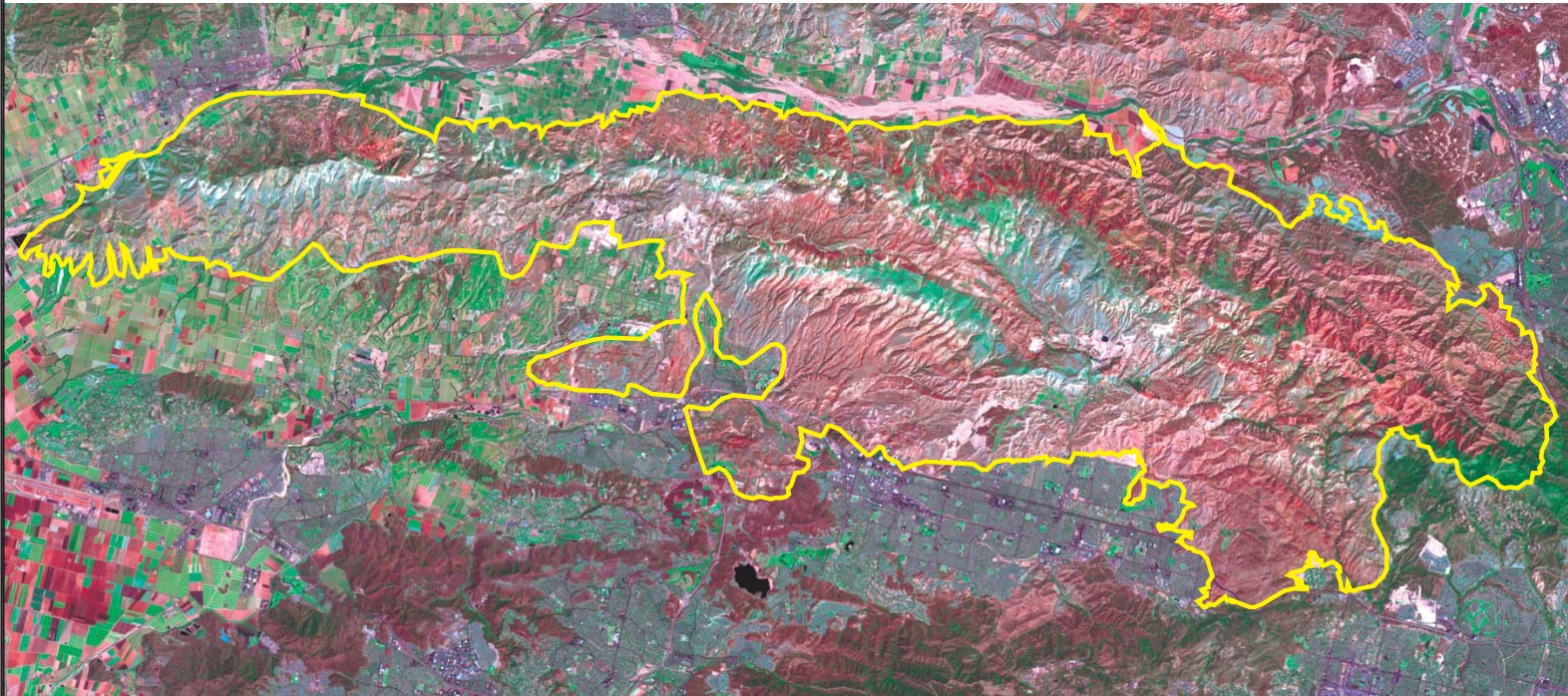
This map portrays fire severity for the fire specified in the map title and summarizes proportions of fire severity classes. These data are produced under the Monitoring Trends in Burn Severity (MTBS) project jointly implemented by the USGS EROS and the USFS RSAC. The MTBS project ascertains the locations of fires based on available fire occurrence information provided by federal and state agencies, and other reliable sources. The MTBS project reserves the right to correct, update or modify geospatial inputs to this map without notification.

* - Areas in either the pre-fire or post-fire reflectance data containing clouds, snow, shadows, smoke, significantly sized water bodies or missing lines of data



2003 California: SIMI

(CA-VNC-03080724-20031025)



Latitude: 34° 20' 7.1" N
 Longitude: 118° 47' 32.0" W
 Fire Ignition Date: October 25, 2003
 Assessment Type: Extended
 Pre-Fire Image Date: April 21, 2002 (Landsat 7)
 Post-Fire Image Date: May 04, 2004 (Landsat 5)



Acreage of Burn Severity

Burn Severity	Acres
Unburned to Low	43,283
Low	33,139
Moderate	20,502
High	0
Increased Greenness	10,830
Non-Processing Area Mask *	0
Total	107,754

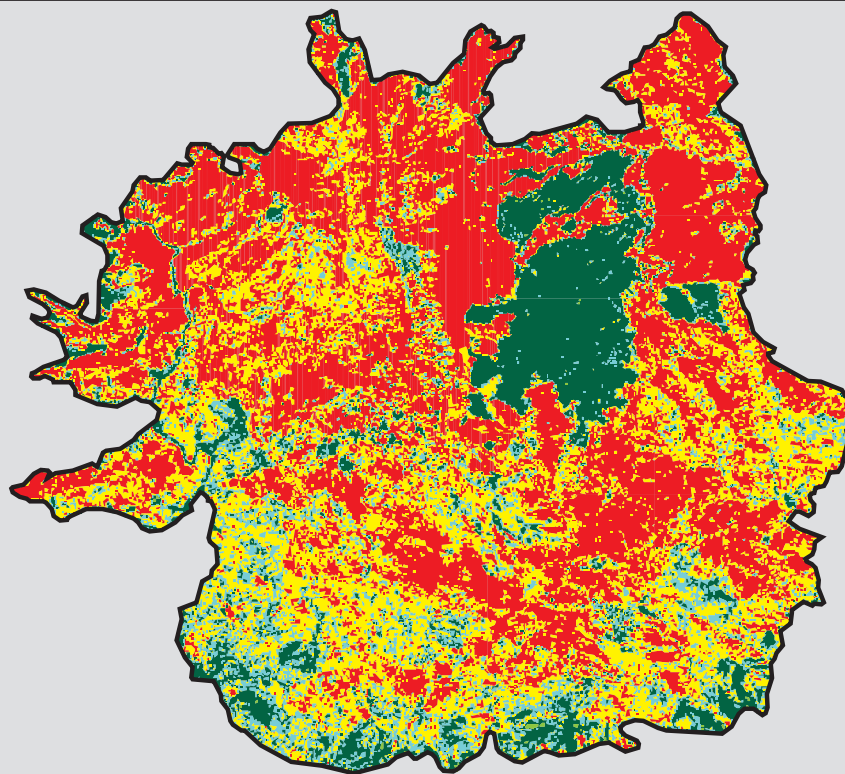
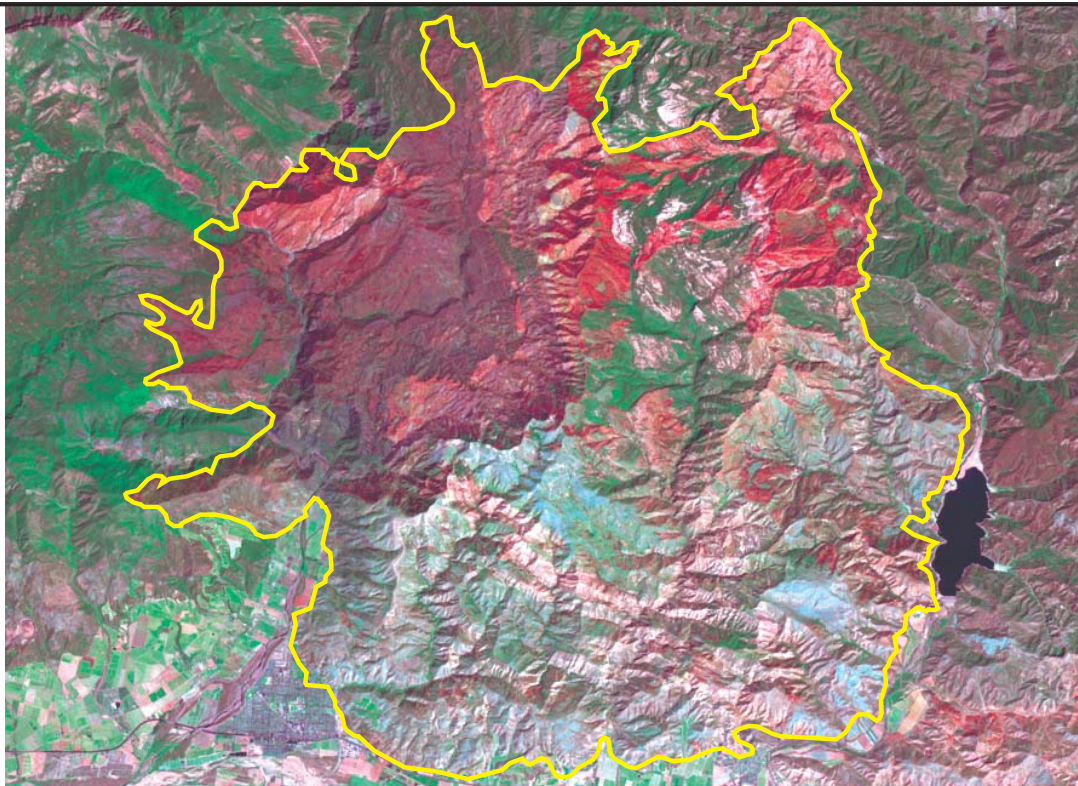
This map portrays fire severity for the fire specified in the map title and summarizes proportions of fire severity classes. These data are produced under the Monitoring Trends in Burn Severity (MTBS) project jointly implemented by the USGS EROS and the USFS RSAC. The MTBS project ascertains the locations of fires based on available fire occurrence information provided by federal and state agencies, and other reliable sources. The MTBS project reserves the right to correct, update or modify geospatial inputs to this map without notification.

* - Areas in either the pre-fire or post-fire reflectance data containing clouds, snow, shadows, smoke, significantly sized water bodies or missing lines of data



2003 California: PIRU

(CA-LPF-00000038-20031023)



Latitude: 34° 28' 46.9" N
 Longitude: 118° 51' 40.4" W
 Fire Ignition Date: October 23, 2003
 Assessment Type: Extended
 Pre-Fire Image Date: May 10, 2003 (Landsat 7)
 Post-Fire Image Date: May 04, 2004 (Landsat 5)



Acreage of Burn Severity

Burn Severity	Acres
Unburned to Low	9,380
Low	7,205
Moderate	20,095
High	27,180
Increased Greenness	61
Non-Processing Area Mask *	0
Total	63,921

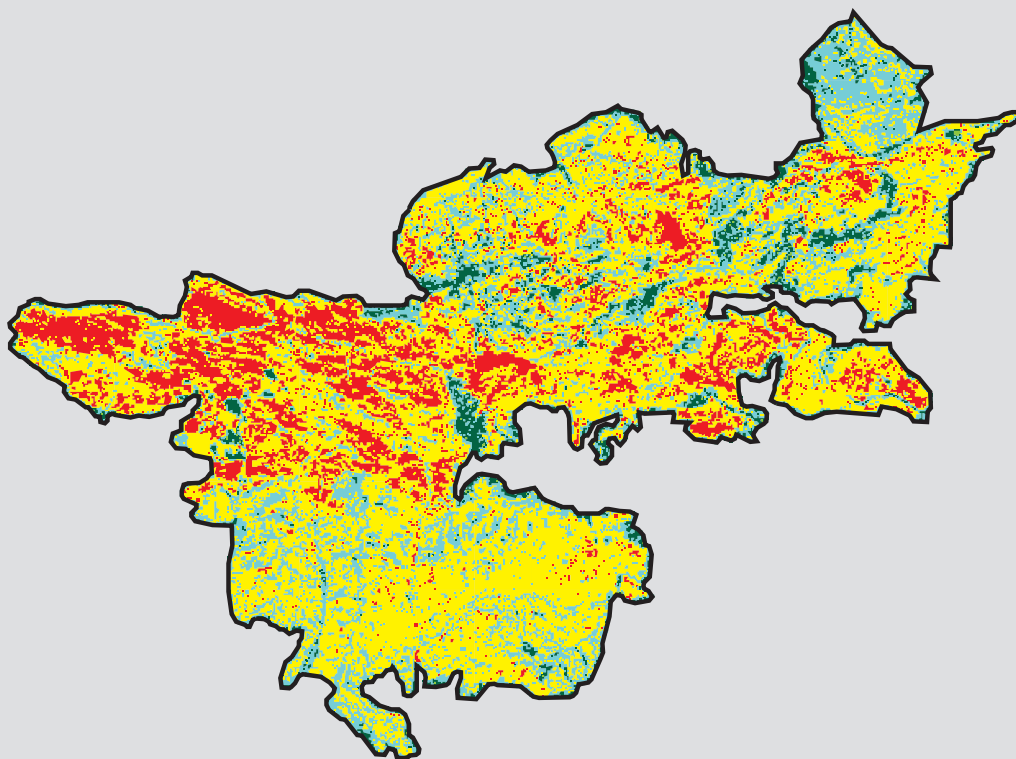
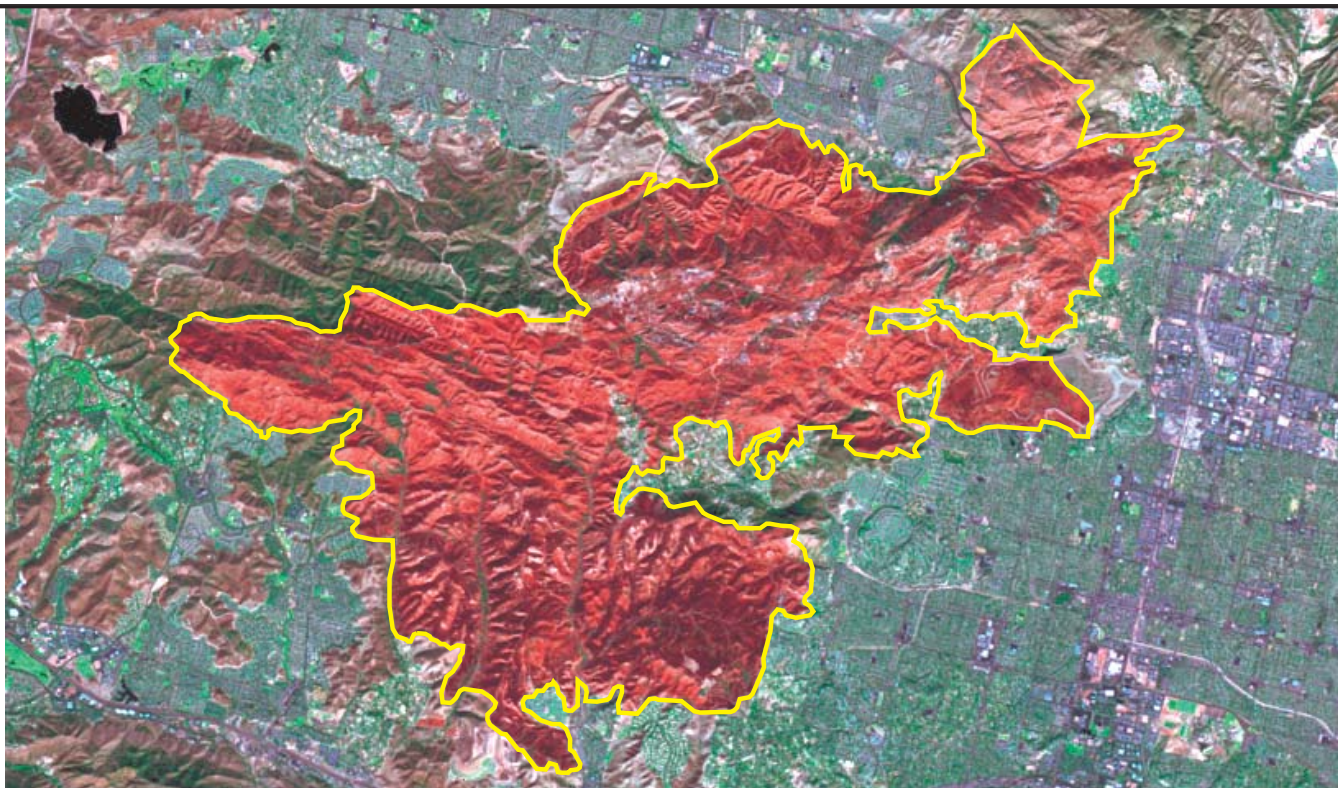
This map portrays fire severity for the fire specified in the map title and summarizes proportions of fire severity classes. These data are produced under the Monitoring Trends in Burn Severity (MTBS) project jointly implemented by the USGS EROS and the USFS RSAC. The MTBS project ascertains the locations of fires based on available fire occurrence information provided by federal and state agencies, and other reliable sources. The MTBS project reserves the right to correct, update or modify geospatial inputs to this map without notification.

* - Areas in either the pre-fire or post-fire reflectance data containing clouds, snow, shadows, smoke, significantly sized water bodies or missing lines of data



2005 California: TOPANGA

(CA-LAC-00000000-20050928)



Latitude: 34° 13' 4.9" N
 Longitude: 118° 41' 44.1" W
 Fire Ignition Date: September 28, 2005
 Assessment Type: Initial
 Pre-Fire Image Date: September 23, 2003 (Landsat 5)
 Post-Fire Image Date: October 14, 2005 (Landsat 5)



Acreage of Burn Severity

Burn Severity	Acres
Unburned to Low	1,568
Low	5,512
Moderate	13,328
High	3,680
Increased Greenness	42
Non-Processing Area Mask *	0
Total	24,130

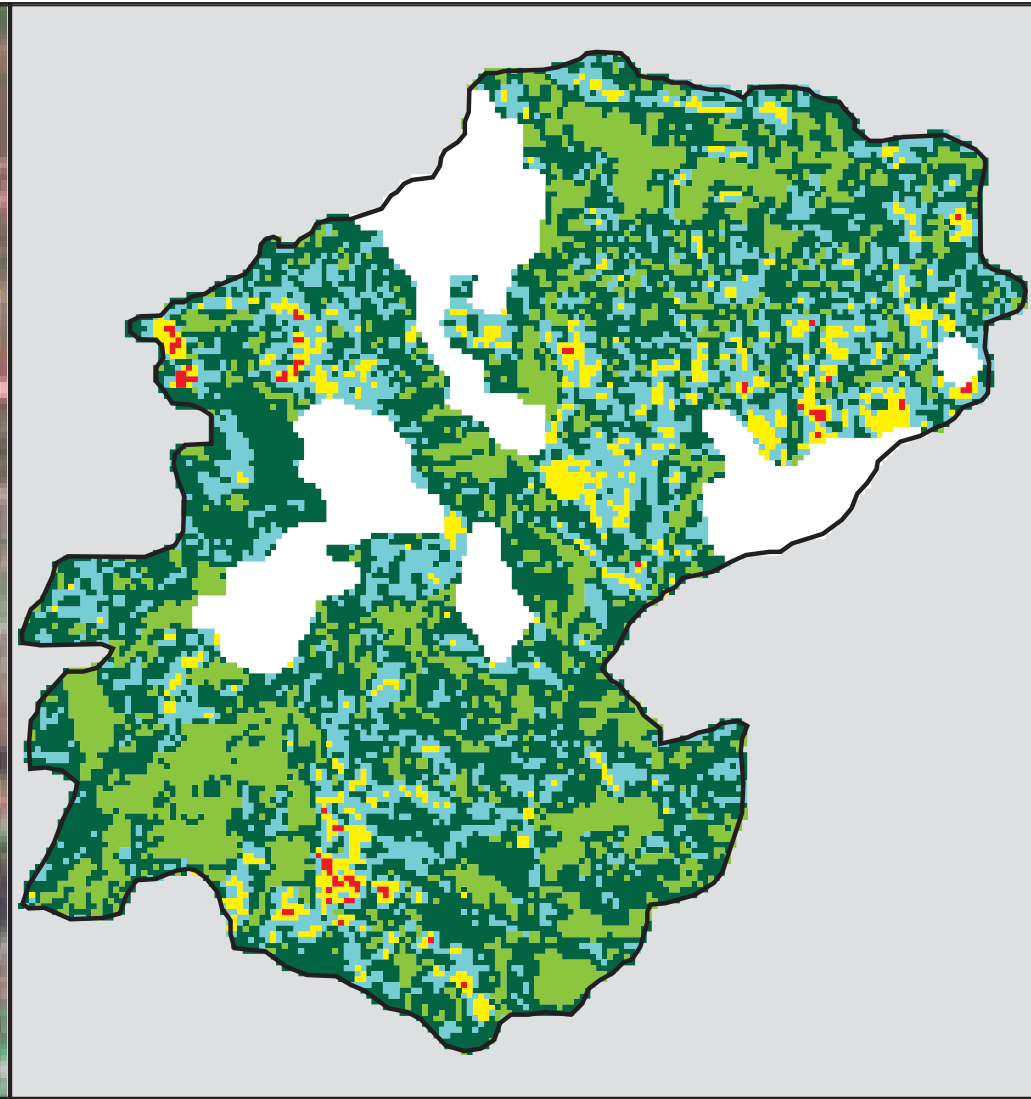
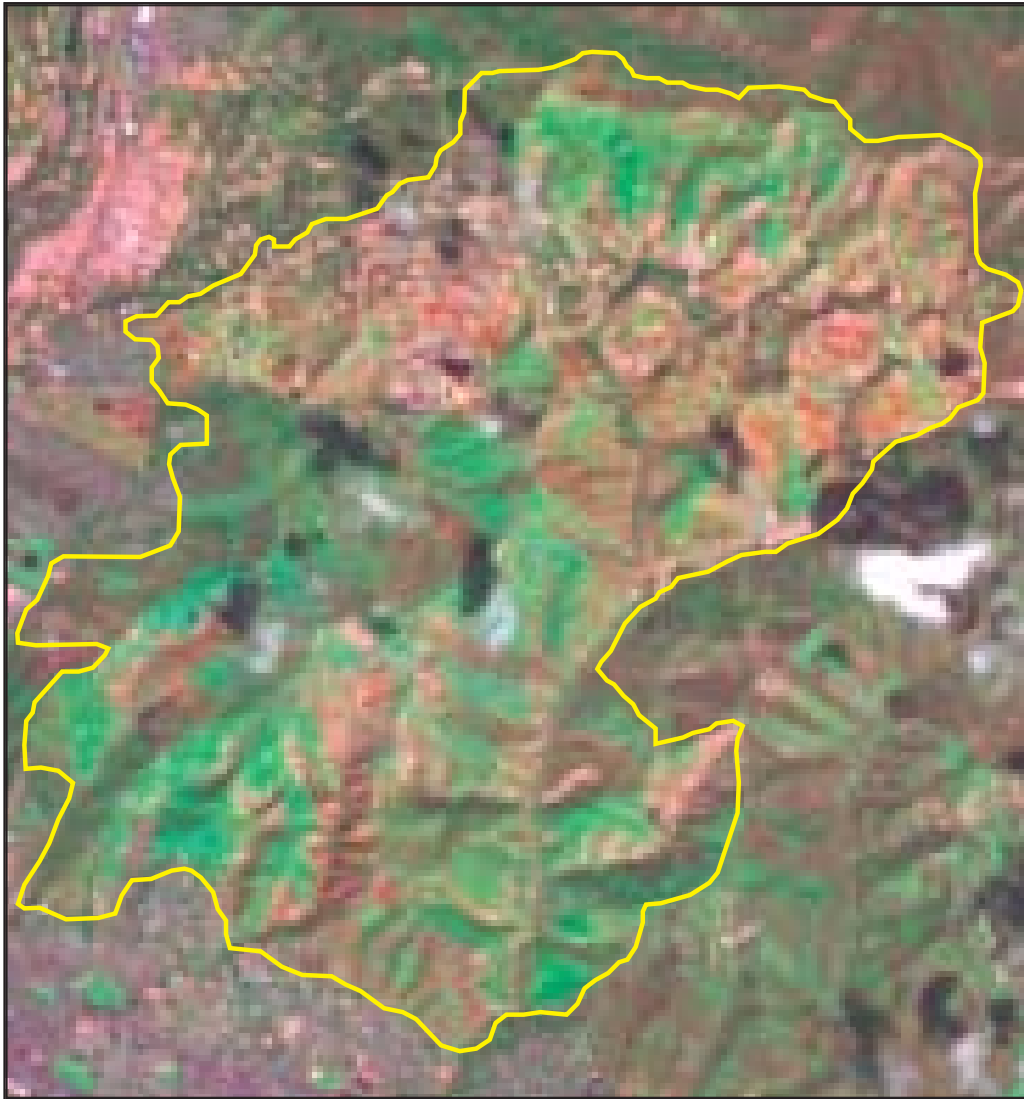
This map portrays fire severity for the fire specified in the map title and summarizes proportions of fire severity classes. These data are produced under the Monitoring Trends in Burn Severity (MTBS) project jointly implemented by the USGS EROS and the USFS RSAC. The MTBS project ascertains the locations of fires based on available fire occurrence information provided by federal and state agencies, and other reliable sources. The MTBS project reserves the right to correct, update or modify geospatial inputs to this map without notification.

* - Areas in either the pre-fire or post-fire reflectance data containing clouds, snow, shadows, smoke, significantly sized water bodies or missing lines of data



2005 California: SCHOOL INCIDENT

(CA-VNC-00000000-20051118)



Latitude: 34° 18' 25.6" N
 Longitude: 119° 15' 51.3" W
 Fire Ignition Date: November 18, 2005
 Assessment Type: Extended
 Pre-Fire Image Date: April 21, 2005 (Landsat 5)
 Post-Fire Image Date: April 24, 2006 (Landsat 5)



Acreage of Burn Severity

Burn Severity	Acres
Unburned to Low	1,717
Low	786
Moderate	220
High	17
Increased Greenness	776
Non-Processing Area Mask *	574
Total	4,090

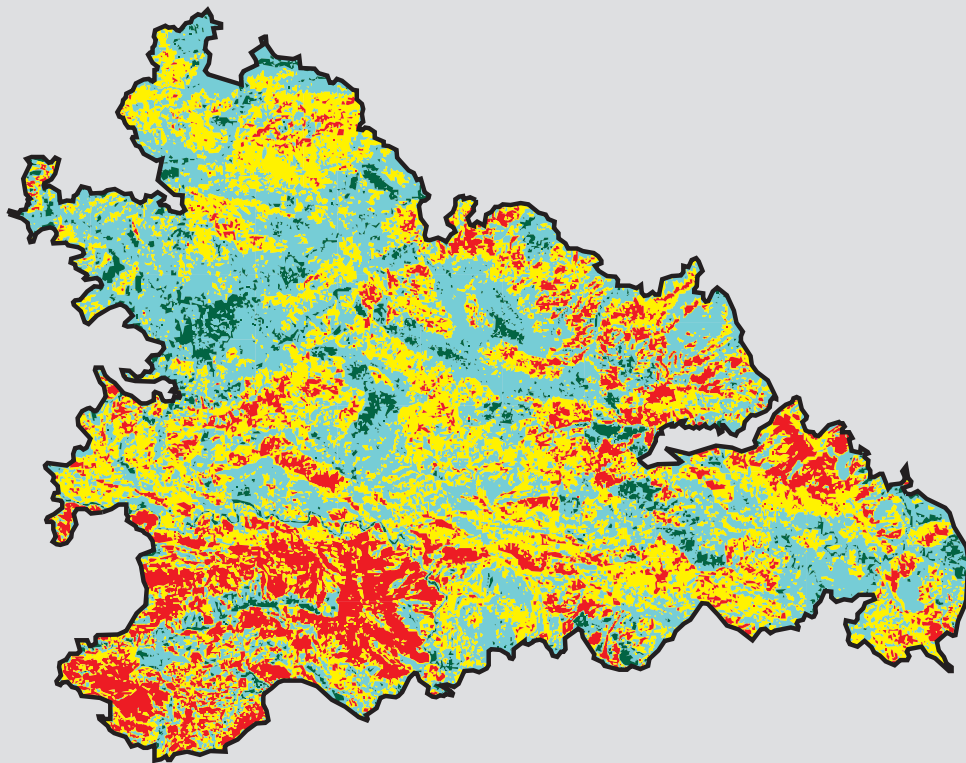
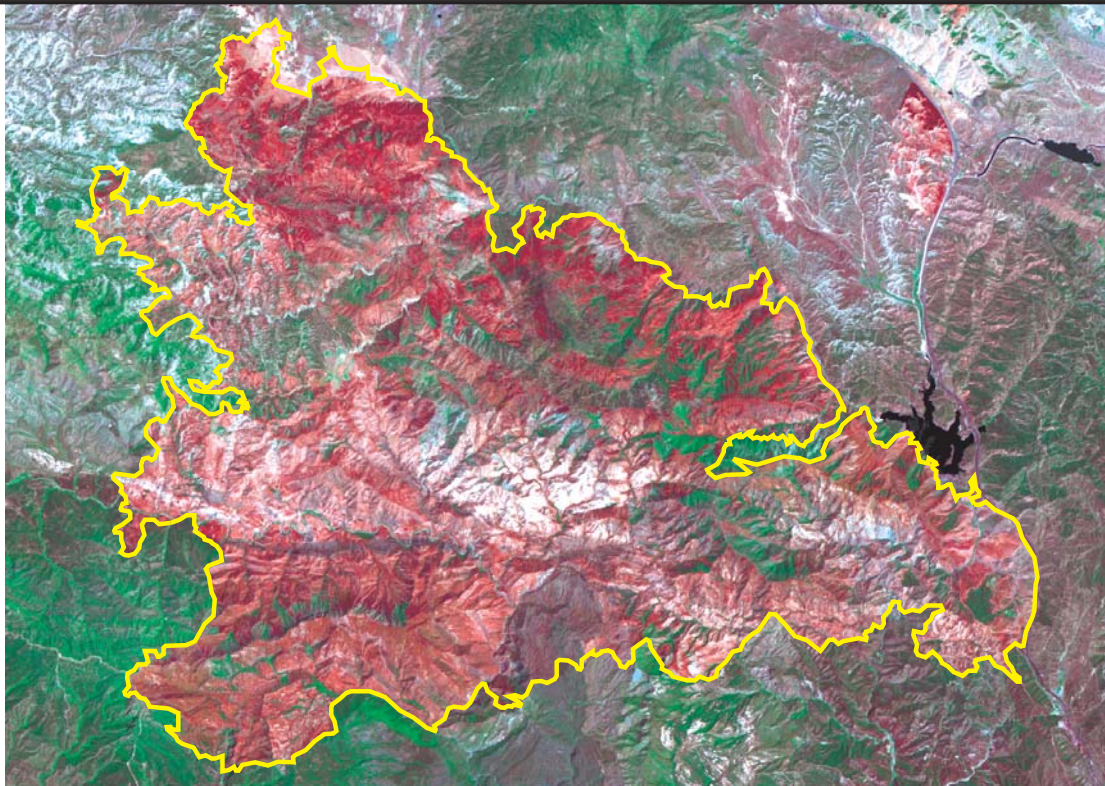
This map portrays fire severity for the fire specified in the map title and summarizes proportions of fire severity classes. These data are produced under the Monitoring Trends in Burn Severity (MTBS) project jointly implemented by the USGS EROS and the USFS RSAC. The MTBS project ascertains the locations of fires based on available fire occurrence information provided by federal and state agencies, and other reliable sources. The MTBS project reserves the right to correct, update or modify geospatial inputs to this map without notification.

* - Areas in either the pre-fire or post-fire reflectance data containing clouds, snow, shadows, smoke, significantly sized water bodies or missing lines of data



2006 California: DAY

(FS-0507-064-20060904)



Latitude: 34° 36' 53.7" N
 Longitude: 118° 58' 16.3" W
 Fire Ignition Date: September 4, 2006
 Assessment Type: Extended
 Pre-Fire Image Date: June 24, 2005 (Landsat 5)
 Post-Fire Image Date: June 14, 2007 (Landsat 5)



Acreage of Burn Severity

Burn Severity	Acres
Unburned to Low	9,602
Low	64,835
Moderate	58,215
High	27,053
Increased Greenness	2
Non-Processing Area Mask *	0
Total	159,707

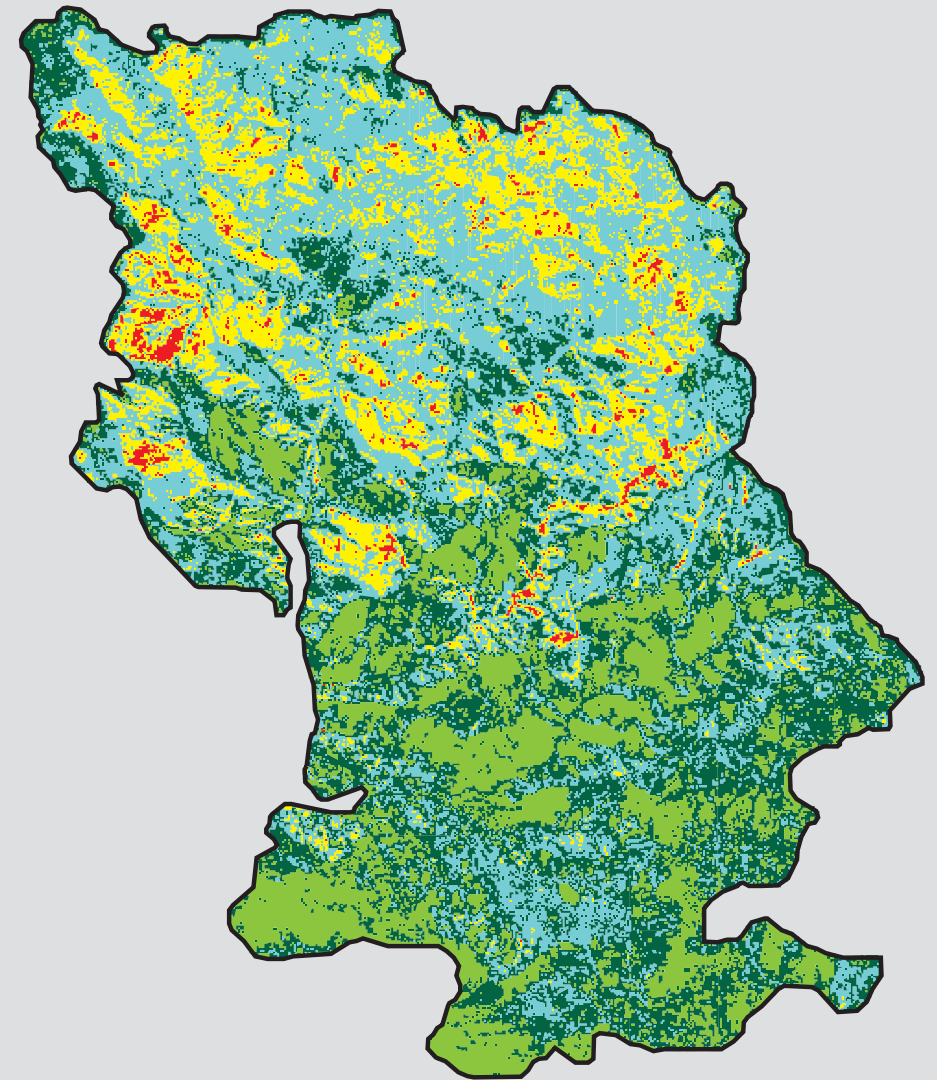
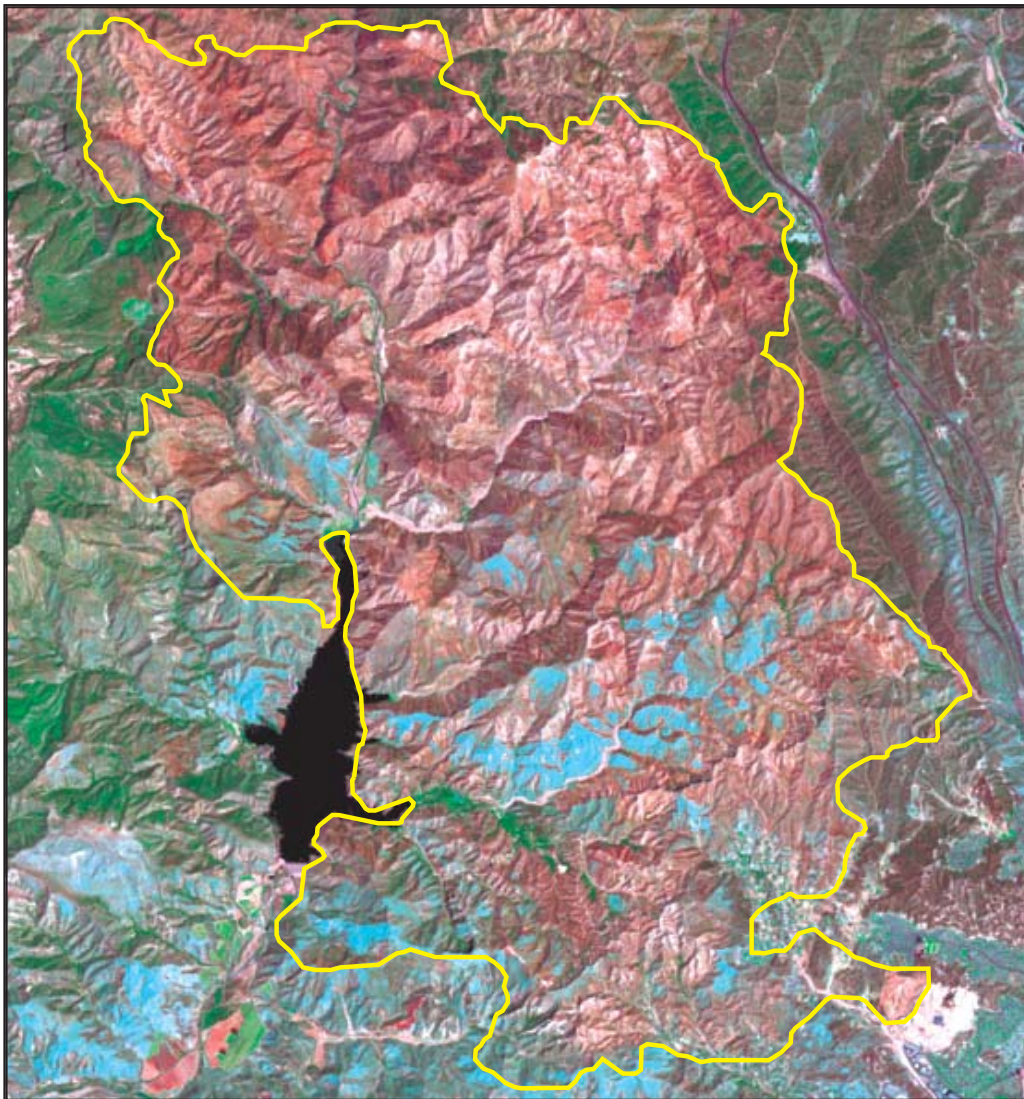
This map portrays fire severity for the fire specified in the map title and summarizes proportions of fire severity classes. These data are produced under the Monitoring Trends in Burn Severity (MTBS) project jointly implemented by the USGS EROS and the USFS RSAC. The MTBS project ascertains the locations of fires based on available fire occurrence information provided by federal and state agencies, and other reliable sources. The MTBS project reserves the right to correct, update or modify geospatial inputs to this map without notification.

* - Areas in either the pre-fire or post-fire reflectance data containing clouds, snow, shadows, smoke, significantly sized water bodies or missing lines of data



2007 California: RANCH

(FS-0501-166-20071020)



Latitude: 34° 30' 58.1" N
 Longitude: 118° 43' 37.0" W
 Fire Ignition Date: October 20, 2007
 Assessment Type: Extended
 Pre-Fire Image Date: June 14, 2007 (Landsat 5)
 Post-Fire Image Date: July 02, 2008 (Landsat 5)



Acreage of Burn Severity

Burn Severity	Acres
Unburned to Low	10,430
Low	13,600
Moderate	5,560
High	528
Increased Greenness	6,893
Non-Processing Area Mask *	0
Total	37,011

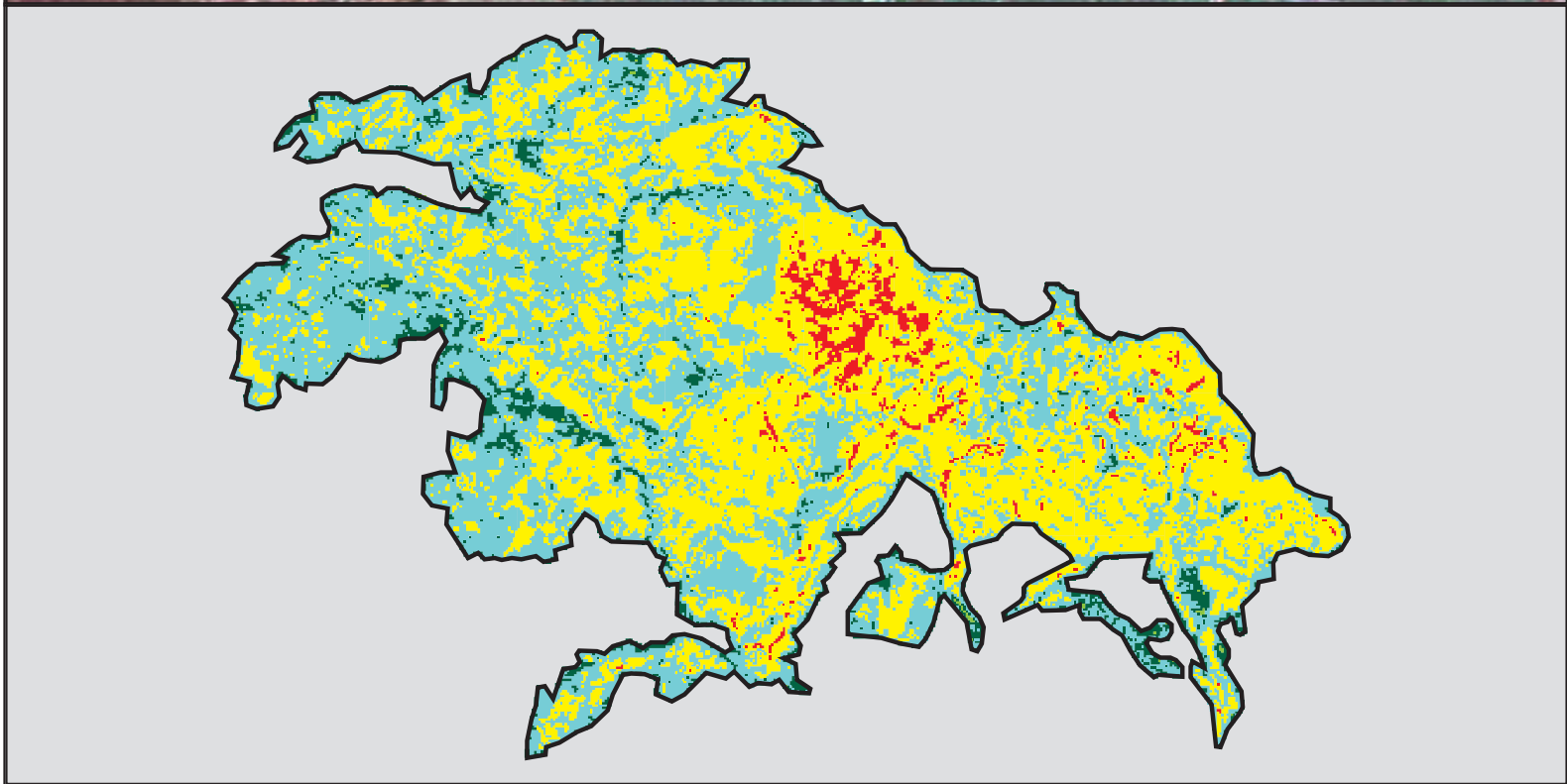
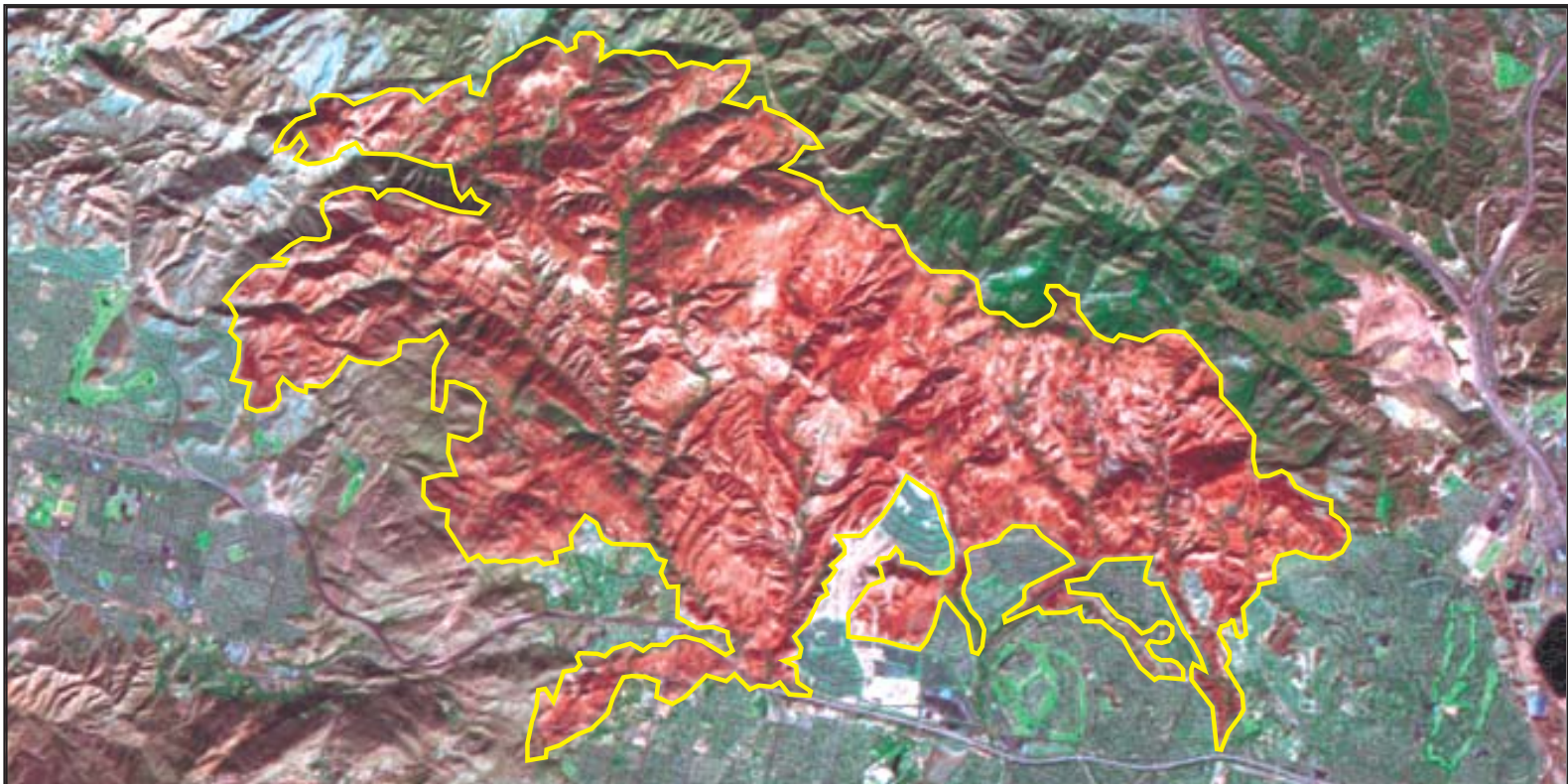
This map portrays fire severity for the fire specified in the map title and summarizes proportions of fire severity classes. These data are produced under the Monitoring Trends in Burn Severity (MTBS) project jointly implemented by the USGS EROS and the USFS RSAC. The MTBS project ascertains the locations of fires based on available fire occurrence information provided by federal and state agencies, and other reliable sources. The MTBS project reserves the right to correct, update or modify geospatial inputs to this map without notification.

* - Areas in either the pre-fire or post-fire reflectance data containing clouds, snow, shadows, smoke, significantly sized water bodies or missing lines of data



2008 California: SESNON

(BLM-CACDD-EM5Q-20081013)



Latitude: 34° 18' 26.1" N
 Longitude: 118° 36' 14.2" W
 Fire Ignition Date: October 13, 2008
 Assessment Type: Initial
 Pre-Fire Image Date: July 02, 2008 (Landsat 5)
 Post-Fire Image Date: October 22, 2008 (Landsat 5)

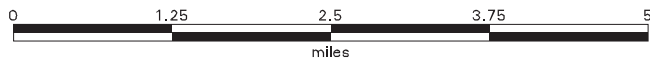


Acreage of Burn Severity

Burn Severity	Acres
Unburned to Low	910
Low	7,096
Moderate	6,817
High	389
Increased Greenness	16
Non-Processing Area Mask *	0
Total	15,228

This map portrays fire severity for the fire specified in the map title and summarizes proportions of fire severity classes. These data are produced under the Monitoring Trends in Burn Severity (MTBS) project jointly implemented by the USGS EROS and the USFS RSAC. The MTBS project ascertains the locations of fires based on available fire occurrence information provided by federal and state agencies, and other reliable sources. The MTBS project reserves the right to correct, update or modify geospatial inputs to this map without notification.

* - Areas in either the pre-fire or post-fire reflectance data containing clouds, snow, shadows, smoke, significantly sized water bodies or missing lines of data



APPENDIX C

EXAMPLE 1 – FACILITY DESIGN PROJECT

EXAMPLE 2 – EMERGENCY POST-FIRE PROJECT

EXAMPLE 1 – FACILITY DESIGN PROJECT

The following example demonstrates the application of the recommended burned and bulked flow policy for **design projects** related to critical infrastructure and/or downstream of known high sediment producing watersheds. Although the Pole Creek watershed boundary is used for the example, rainfall data and actual watershed area were taken from a watershed of similar size, geologic and climatic characteristics. The basin area is assumed to be undeveloped for the example. A map of the watershed limits and example project location is presented in Figure A-1.

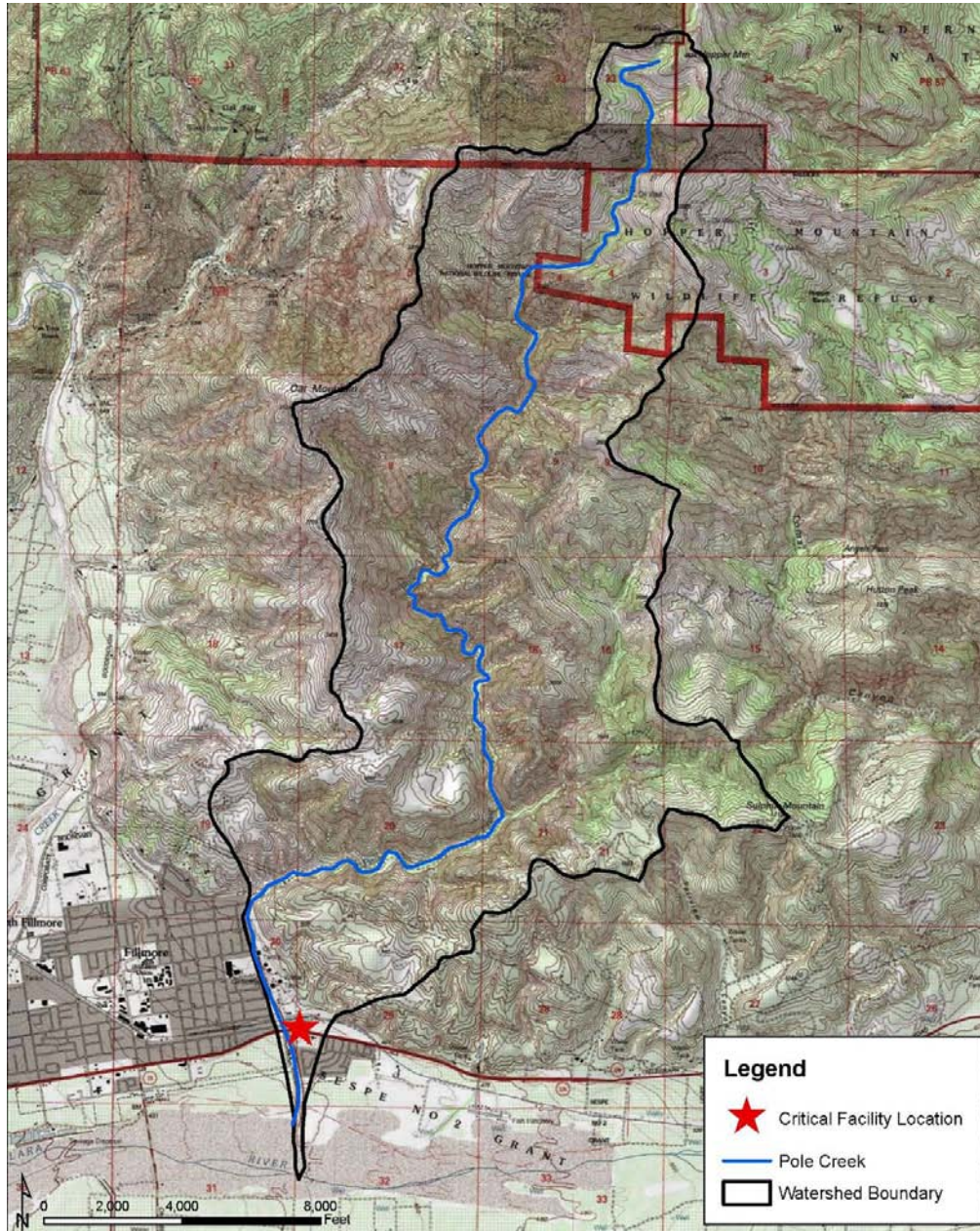


Figure A-1. Critical Facility Location in the Pole Creek Watershed

Any critical infrastructure developments placed within close proximity to a main channel, such as Pole Creek, require additional scrutiny and analysis to provide protection from loss of life and damage during design events. Because of the potential for high sediment production and susceptibility of the Pole Creek watershed to wildfires, the need for using a burn severity factor (BSF) and bulking factor (BF) is required for computation of design discharges. For the following example, the design of a concrete channel requires the design to be based on the 100-year design storm event and the assumption that at least 4.5 years (or approximately 77% vegetation regrowth recovery) has occurred since the last basin fire.

Further example details include:

Watershed area: 5,530 acres \approx 8.6 mi² (assume entire area is undeveloped)

Percent burn of watershed: \sim 100% or 5,530 acres

Project is not near or on an alluvial fan

Based on the scenario presented above and the flowchart presented in Figure 13-1 to Figure 13-3 of this report, the following steps are required to compute the post-fire burn peak flow (Q_{burn}) and bulked flow used to ensure that a critical facility will be built outside of the flood limits associated with the 100-year design event.

The following is a demonstration of applying these steps to this scenario:

Unburned Peak Flow ($Q_{unburned}$) Calculation (see Figure 13-1):

Step 1

Select the 100-year design storm for a project related to a critical facility

Step 2

Apply a BSF of 1.1 (See Section 11.3)

Step 3

Use the Modified Rational Method (MRM) to determine that $Q_{unburned} = 5,567$ cfs. Refer to Section 10.4 for selection of the appropriate hydrologic method.

(Note that the unburned peak flow ($Q_{unburned}$) and hydrograph is for example purposes only, and is not the actual hydrology for Pole Creek.)

Step 4

Apply the BSF from Step 2 directly to the $Q_{unburned}$ computed in Step 3 to obtain Q_{burn} :

$$Q_{burn} = BSF * Q_{unburned} = 1.1 * 5,567 \text{ cfs} = \boxed{6,124 \text{ cfs}}$$

Bulking Factor (BF) Calculation (see Figure 13-2):

Step 5

The BF can be calculated using either **Option 1** or **Option 2** described in Chapter 13, Figure 13-2. Both options are illustrated below.

Option 1 uses a conservative BF of 1.2 for a watershed area greater than 3 mi².

$$Q_{\text{design}} = Q_{\text{burn}} * \text{BF} = 6,124 \text{ cfs} \times 1.2 \approx 7,350 \text{ cfs}$$

Option 2 uses a bulking factor based on the SCOTSED debris production method described in Steps 6 and 7.

Step 6

SCOTSED is used to compute the debris production rate (yd³/mi²) for the Pole Creek watershed example. Primary input to the program includes the watershed area, fire factor (FF), percent burn, slope failure, and rainfall frequency data (see Section 5.2).

For a design project related to critical infrastructure, a FF equal to 20 is applied, which assumes 4.5 years or approximately 77% vegetation regrowth after a watershed has been completely burned. Figure A-2 is the SCOTSED output for the Pole Creek example.

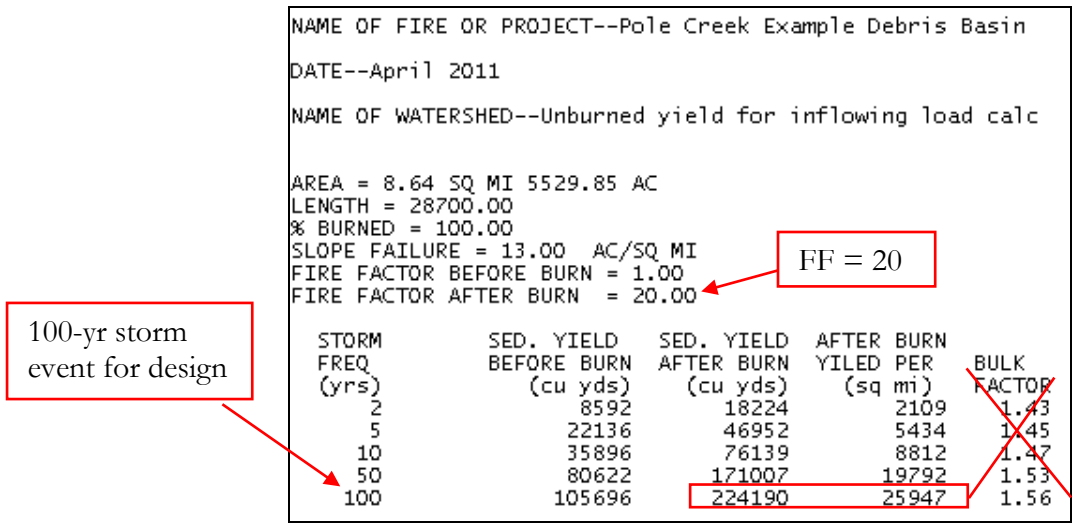


Figure A-2. SCOTSED Program Output for the Pole Creek Design Example

The bulking factor computed in the program has been crossed out in the figure because procedures in Step 7 were used instead to estimate the BF. Results from SCOTSED:

Post-fire sediment yield for the design 100-yr event = **224,190 yd³**

Post-fire debris production rate = **25,947 yd³/mi²**

Step 7

The Los Angeles County sediment distribution method was applied to compute the BF for the example using the debris production rate computed in Step 6.

The estimated debris production rate (25,947 yd³/mi²) is converted to a bulking factor using the post-burn hydrograph from Step 3. To distribute the total debris volume (224,190 yd³) throughout the flow hydrograph, the following equation is used:

$$Q_s = a Q_{burn}^n \quad (\text{computed for each time step} - \text{see spreadsheet example in Table A-1})$$

where:

Q_s = volumetric sediment discharge (cfs)

Q_{burn} = post-burn discharge (cfs) = 6,124 cfs

a and n = bulking constants (fixed throughout the hydrograph)

The value of n is set equal to 3 (Section 6.4). The coefficient a is determined by numerical integration of the squared 100-yr hydrograph ordinates as follows:

$$a = \frac{V_s}{\sum (\Delta t * Q_{burn}^{n-1})} = a = \frac{V_s}{\sum (\Delta t * Q_{burn}^2)} = \frac{139 \text{ ac-ft}}{3.2\text{E}+10 \text{ ac-ft}} = \boxed{4.3\text{E-}9} \quad (\text{see Table A-1})$$

where V_s is the total post-fire sediment yield and Δt is the computational time interval.

For the undeveloped watershed assumption where the entire area contributes debris, the bulked peak flow is expressed by:

$$Q_B = Q_{burn} + Q_s \quad (\text{computed for each time step of the hydrograph} - \text{Table A-1})$$

The BF is the ratio of the bulked discharge to the post-burn discharge for each time step of the hydrograph:

$$\text{BF} = \Sigma(Q_{burn} + Q_s)/Q_{burn} = \boxed{1.16} \quad (\text{computed using the example data} - \text{Table A-1})$$

Table A-1. Example Spreadsheet Set-up

Time (min)	Q_{burn}		Q_{burn}^3		$Q_s = a * Q_{burn}^3$		Bulked Q = $Q_s + Q_{burn}$		Time (min)
	Flow (cfs)	Volume (cf)	Flow (cfs)	Volume (cf)	Flow (cfs)	Volume, V_s (cf)	Flow (cfs)	Volume (cf)	
0.0	0.0	1.4E+05	0.0E+00	3.2E+08	0.00	1.36	0.0	1.4E+05	1.00
100	47	4.8E+05	1.1E+05	4.6E+09	0.00	20	47	4.8E+05	1.00
200	112	7.5E+05	1.4E+06	1.2E+10	0.01	51	112	7.5E+05	1.00
300	136	9.3E+05	2.5E+06	2.3E+10	0.01	99	136	9.3E+05	1.00
400	173	1.2E+06	5.2E+06	5.1E+10	0.02	220	173	1.2E+06	1.00
500	229	1.6E+06	1.2E+07	1.2E+11	0.05	518	229	1.6E+06	1.00
600	305	2.2E+06	2.8E+07	3.0E+11	0.12	1,289	305	2.2E+06	1.00
700	416	3.1E+06	7.2E+07	8.9E+11	0.31	3,807	416	3.1E+06	1.00
800	607	4.9E+06	2.2E+08	3.8E+12	0.96	16,354	608	4.9E+06	1.00
900	1,015	8.6E+06	1.0E+09	2.2E+13	4.49	96,315	1,020	8.7E+06	1.00



1,157	5,778	3.5E+05	1.9E+11	1.2E+13	828	50,355	6,606	4.0E+05	1.14
1,158	5,831	3.5E+05	2.0E+11	1.2E+13	851	51,712	6,682	4.0E+05	1.15
1,159	5,882	3.5E+05	2.0E+11	1.2E+13	873	53,244	6,755	4.1E+05	1.15
1,160	5,946	3.6E+05	2.1E+11	1.3E+13	902	54,513	6,847	4.1E+05	1.15
1,161	5,975	3.6E+05	2.1E+11	1.3E+13	915	55,439	6,891	4.2E+05	1.15
1,162	6,013	3.6E+05	2.2E+11	1.3E+13	933	56,468	6,945	4.2E+05	1.16
1,163	6,049	3.6E+05	2.2E+11	1.3E+13	950	57,321	6,999	4.2E+05	1.16
1,164	6,073	3.6E+05	2.2E+11	1.3E+13	961	57,868	7,034	4.2E+05	1.16



1,360	1,736	1.0E+06	5.2E+09	2.9E+12	22	12,422	1,758	1.0E+06	1.01
1,370	1,641	9.6E+05	4.4E+09	2.4E+12	19	10,483	1,660	9.7E+05	1.01
1,380	1,550	9.0E+05	3.7E+09	2.1E+12	16	8,841	1,566	9.1E+05	1.01
1,390	1,465	8.6E+05	3.1E+09	1.7E+12	13	7,484	1,479	8.6E+05	1.01
1,400	1,387	1.6E+06	2.7E+09	2.8E+12	11	11,894	1,399	1.6E+06	1.01
1,420	1,250	1.4E+06	2.0E+09	2.1E+12	8.4	8,800	1,258	1.4E+06	1.01
1,440	1,136	1.3E+06	1.5E+09	1.5E+12	6.3	6,650	1,143	1.3E+06	1.01
1,460	1,037	2.3E+06	1.1E+09	2.2E+12	4.8	9,229	1,042	2.3E+06	1.00
1,500	878	1.6E+06	6.8E+08	1.2E+12	2.9	5,224	881	1.6E+06	1.00
Unit Conversion	V (ac-ft)		$\sum (\Delta t * Q_{burn}^2)$		V_s (ac-ft)		V (ac-ft)	BF Max	
Totals:	2.6E+03		3.2E+10		139		2.7E+03	1.16	

*Note: Qburn was obtained from increasing the pre-burn peak runoff.

Step 8

The design discharge is computed using the Q_{burn} (6,124 cfs) from Step 4 and BF (1.16) from Step 7 as follows:

$$Q_{design} = Q_{burn} * BF = 6,124 \text{ cfs} * 1.16 = \boxed{7,104 \text{ cfs}}$$

EXAMPLE 2 - EMERGENCY POST-FIRE PROJECT

This example demonstrates the application of the recommended burned and bulked flow policy for **emergency post-fire projects** (e.g., design of a temporary sediment basin). The Pole Creek watershed limits and Piru Fire of 2003 burn severity maps are used in the example for illustration purposes only. For the example, it is assumed that the basin area is undeveloped. A map of the fire and watershed limits is presented in Figure A-3.

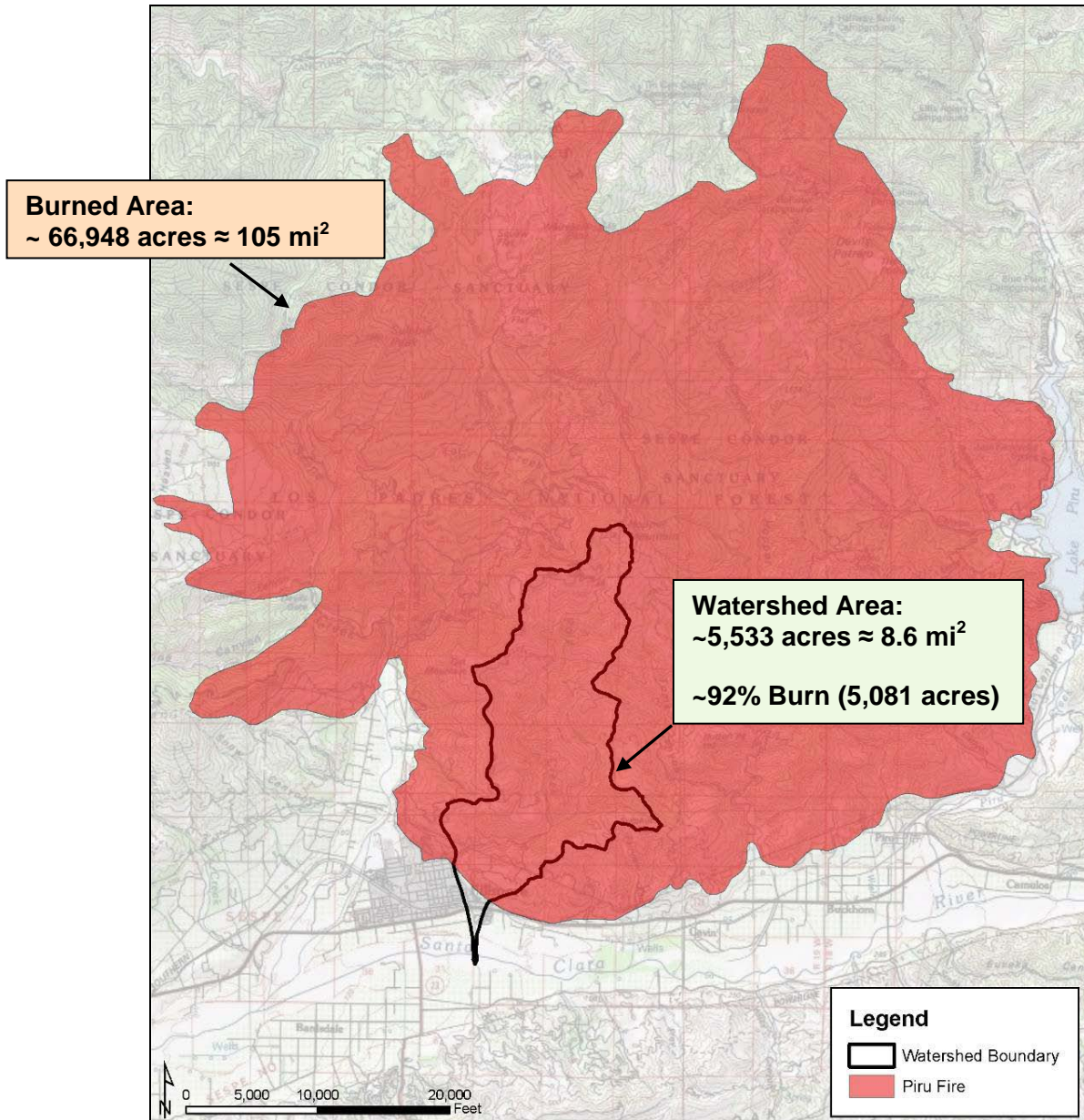


Figure A-3. Pole Creek Watershed and the 2003 Piru Fire

In this scenario, a recent wildfire (less than 6 months ago) has burned portions of the Pole Creek watershed leaving bare soil and a potential increase in slope failure and excessive erosion. The decision has been made to build an “emergency” temporary detention basin constructed to the 10-year design storm event to alleviate the potential for flooding and property damage within the watershed.

Watershed area: 5,533 acres \approx 8.6 mi² (assume entire area is undeveloped)

Piru fire burned area: 66,948 acres \approx 105 mi²

Percent burn of watershed: \sim 92% or 5,081 acres

Based on the scenario presented above and the flowchart presented in Figure 13-2 of the report, the following steps are required to compute the post-fire burn peak flow (Q_{burn}) and bulked discharge/volume used for the emergency detention facility design:

Unburned Peak Flow ($Q_{unburned}$) Calculation (see Figure 13-1):

Step 1

Use the 10-year design storm event.

Step 2

Obtain the burn severity map, e.g., the Burned Area Reflectance Classification (BARC) map, for the recent fire (Figure A-4)

Step 3

Compute the average weighted BSF based on the burn severity map and using the recommended BSFs described in Section 11 and presented in Table A-2.

Table A-2. Burn Severity Factors and Average Weighted BSF for the 2003 Piru Fire

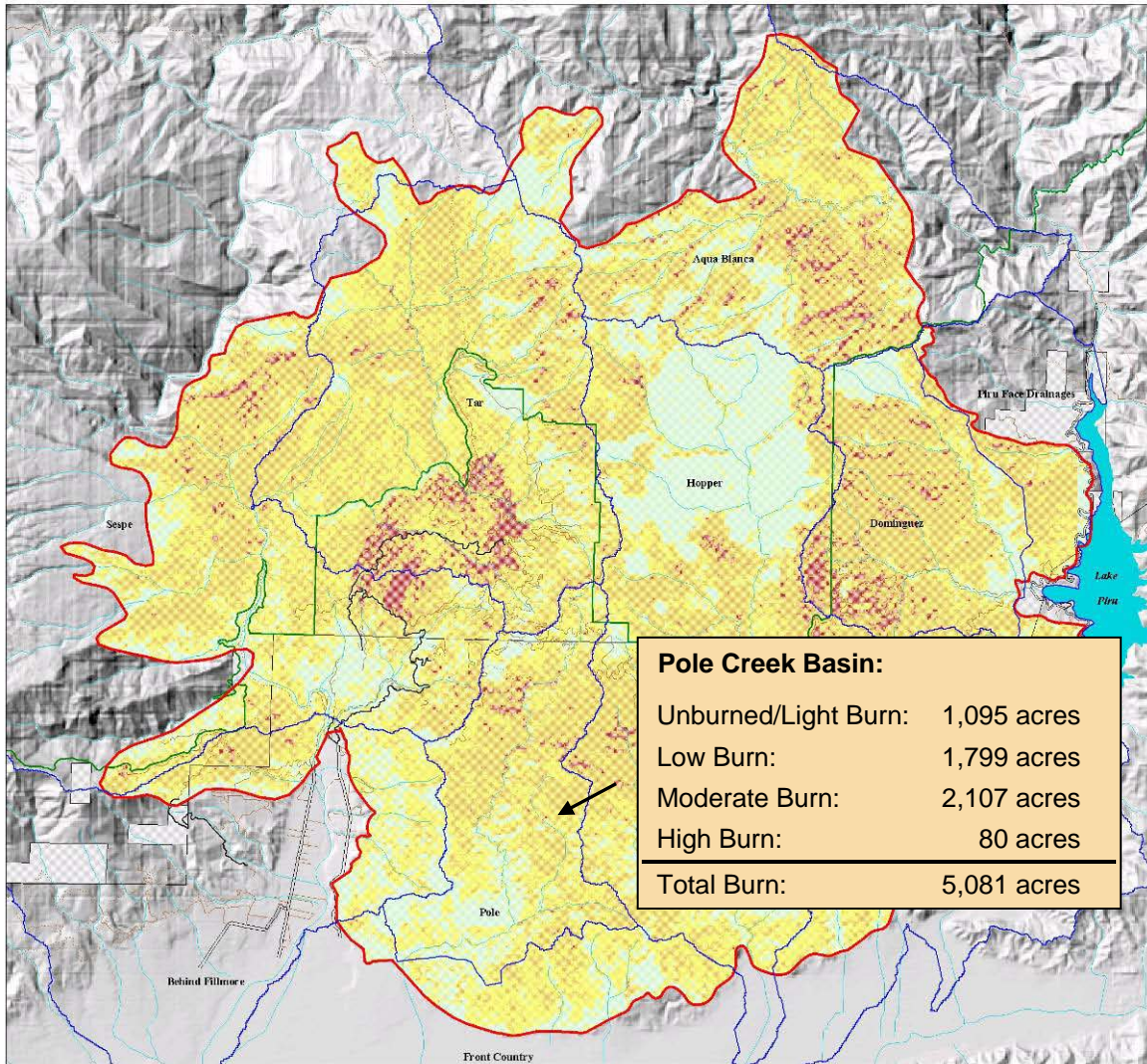
Burn Condition	BSF	Acres Burned	%Burned*	Average Weighted BSF**
Unburned to Very Low Burn	1.0	1,095	22	1.37
Low Burn	1.3	1,799	35	
Moderate Burn	1.6	2,107	41	
High Burn	2.0	80	2	
Total:		5,081	100	

*Note: The percent burn is computed from multiplying the area burned by the total area of the watershed. For the Pole Creek example the unburned to very low burn percentage was computed as follows: %Burned = acres burned/total watershed area = 1,095 ac/5,533 ac * 100 \approx 22% burned

**Average weighted BSF = (%burn*unburned to low burn)+(%burn*low burn)+(%burn*moderate burn)+(%burn*high burn)

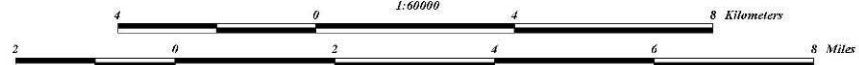
$$\text{Average weighted BSF} = (0.22 * 1.0) + (0.35 * 1.3) + (0.41 * 1.6) + (0.02 * 2.0) = \boxed{1.37}$$

Burned Area Reflectance Classification (BARC.) of the Piru Fire



Pole Creek Basin:

Unburned/Light Burn:	1,095 acres
Low Burn:	1,799 acres
Moderate Burn:	2,107 acres
High Burn:	80 acres
Total Burn:	5,081 acres



Watershed	Very Light / Unburned	Low	Moderate	High
Aqua Blanca	1450.813	1809.454	3426.153	355.838
Behind Fillmore	867.327	1045.101	609.585	13.054
Dominguez	625.164	651.805	3137.254	404.713
Front Country	1640.201	3283.655	2640.572	65.211
Hopper	4199.431	3518.168	7087.422	358.718
Piru Face Drainages	273.474	362.302	757.107	18.446
Pole	1095.39	1798.815	2106.911	79.974
Sespe	2072.574	3029.564	3998.279	290.301
Tar	1341.454	3739.822	5185.713	607.804

- Watersheds
- Piru Fire Perimeter
- Wilderness Boundary
- Lakes
- Streams
- County Lines
- Secondary Highway
- Improved Light Duty / Paved
- Gravel
- Unimproved Dirt
- Trail
- Administration
- National Forest Land
- Non-National Forest Land
- Outside Administrative Boundary

BARC Classification (Burn Severity)

- Very Low / Unburned
- Low
- Moderate
- High



Figure A-4. Burn Severity Map for the Piru Fire 2003
(<http://frap.cdf.ca.gov/socal03/baer/burnseverity-maps.html>)

Step 4

Apply the MRM unit-hydrograph developed for the unburned Pole Creek watershed to obtain the pre-burn or “unburned” peak discharge, $Q_{\text{unburned}} = 3,097 \text{ cfs}$.

(Note that the unburned peak flow (Q_{unburned}) and hydrograph is fictional is for this example only, and is not the actual hydrology for Pole Creek.)

Step 5

Apply the BSF from Step 3 directly to the Q_{unburned} computed in Step 4 to obtain Q_{burn} :

$$Q_{\text{burn}} = \text{BSF} * Q_{\text{unburned}} = 1.37 * 3,097 \text{ cfs} = \boxed{4,243 \text{ cfs}}$$

Bulking Factor (BF) Calculation (see Figure 13-2):

Step 6

The BF can be calculated using either **Option 1** or **Option 2** described in Chapter 13, Figure 13-3.

Option 1 uses a conservative **BF of 1.25** for a watershed area greater than 3 mi². This value was determined from the proposed bulking factor curve shown in Chapter 13, Figure 13-5.

$$Q_{\text{design}} = Q_{\text{burn}} \times 1.25 = 4,243 \text{ cfs} \times 1.25 \approx 5,300 \text{ cfs}$$

Option 2 the bulking factor is based on the SCOTSED debris production method and the proposed Ventura BF curve described in Steps 7 and 8:

Step 7

SCOTSED is used to compute the debris production rate (yd³/mi²) for the Pole Creek watershed example. Primary input to the program includes the watershed area, fire factor (FF), percent burn, slope failure, and rainfall frequency data (see Section 5.2).

For an emergency project, a FF equal to 88 is applied, which assumes six months of vegetation growth after a burn. Figure A-5 is the SCOTSED output for the Pole Creek example with 92% of the watershed burned.

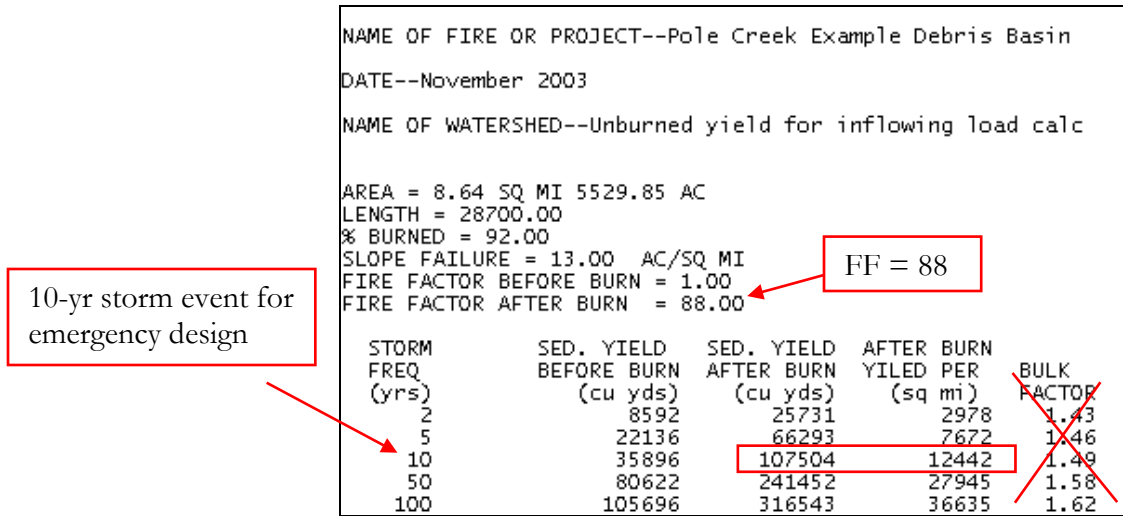


Figure A-5. SCOTSED Program Output for the Pole Creek Emergency Design Example

The bulking factor computed in the program has been crossed out in the figure. Instead, Figure A-6 was used to estimate a **BF = 1.25** with the computed debris production rate.

Post-fire sediment yield for the design 10-yr event = 107,504 yd³

Post-fire debris production rate = **12,442 yd³/mi²**

Step 8 The design discharge is computed using the Q_{burn} (4,243 cfs) from Step 5 and BF (1.25) from Step 7 as follows:

$$Q_{design} = Q_{burn} * BF = 4,243 \text{ cfs} * 1.25 = \mathbf{5,304 \text{ cfs}}$$

Please note that while Options 1 and 2 give the same design discharge in this example, this will not always be the case, and always never will be the case for small watersheds ($\leq 3 \text{ mi}^2$).

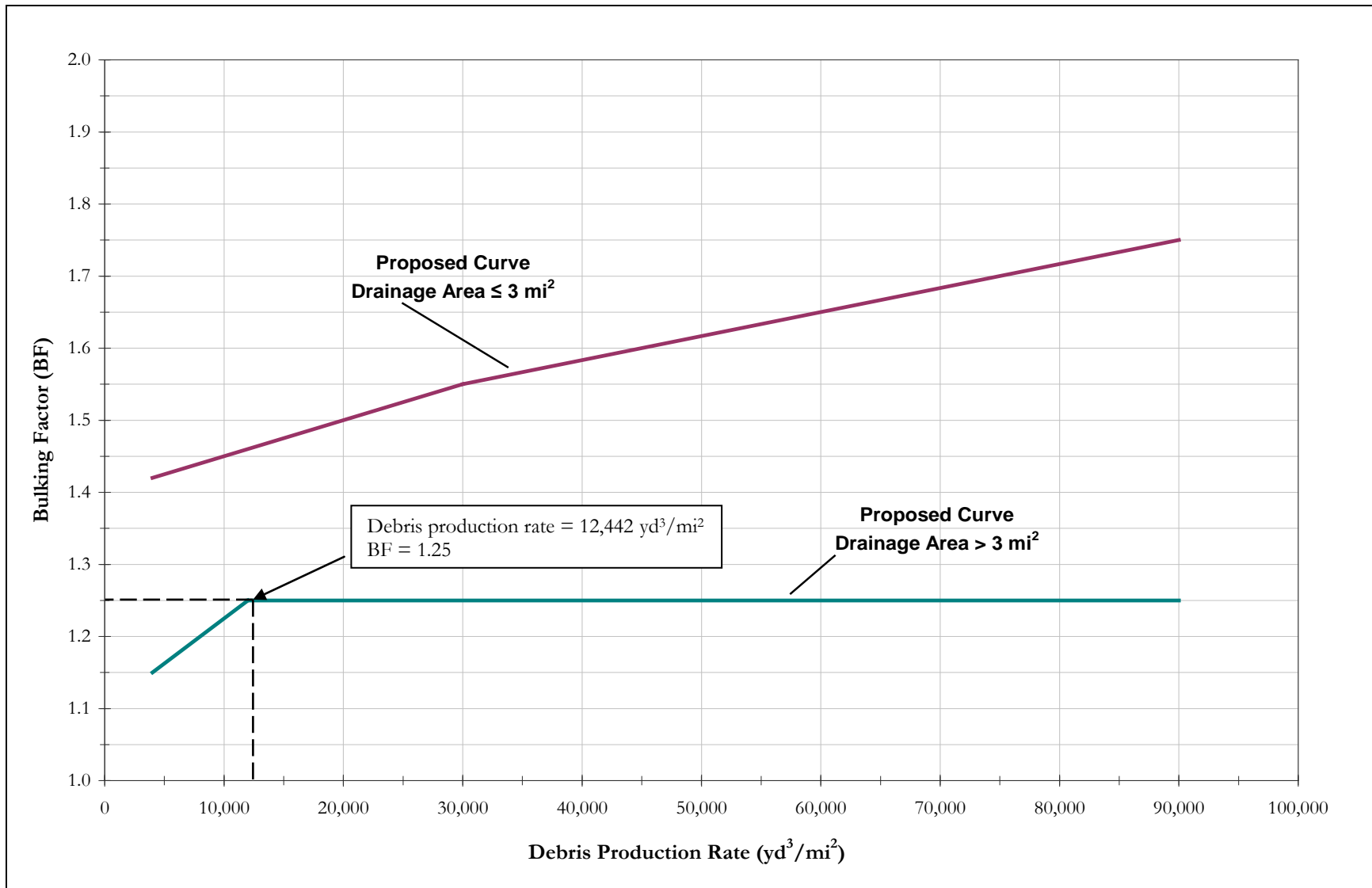


Figure A-6. Recommended Bulking Factor Curves – Emergency Projects (FF = 88)